

# Species dispersion from a closed Namaqualand metalliferous mine into water sources, South Africa

**IG Erdogan**

 [orcid.org/0000-0001-8754-0277](https://orcid.org/0000-0001-8754-0277)

Thesis accepted in fulfilment of the requirements for the degree *Doctor of Philosophy in Chemical Engineering* at the North-West University

Promoter: Prof E Fosso-Kankeu

Co-Promoter: Prof FB Waanders

Co-Promoter: Prof SK Ntwampe

Graduation: June 2021

Student number: 29645204

## DECLARATION

---

I, Innocentia Gugulethu Erdogan, hereby declare that the contents of this thesis represent my own unaided work and that the thesis has not previously been submitted for academic examination towards any qualification. Furthermore, it represents my own opinions and not necessarily that of the National Research Foundation of South Africa, North-West University or that of the Cape Peninsula University of Technology and their sponsors.

All intellectual concepts, theories, methodologies and mathematical derivations and model developments used in this thesis and published in various scientific journals (except those that were used for review articles) were derived solely by the candidate and first author of the published manuscripts. Where appropriate, intellectual property of others was acknowledged by using appropriate references. It should be noted that the styles of the referencing, equations, figures and tables of the journal articles and conference papers were altered from their original published format in order to adopt consistency for the full thesis submission. Furthermore, the contents of the manuscripts in this thesis were modified from submitted and or published versions to accommodate the examiners' comments.

The contribution of co-authors for conference and published manuscripts was in a training capacity: MEng student (Mr T. Moncho), Managing Director of the O'Kiep Copper Company Pty. Ltd. (Mr B. Fourie), GIS mapping (Mr A. Rand), Statistician (Mr T. Farrar) and software (Messrs D. Bent, K. Netshiongolwe and A. Mosai) and supervisory capacity (Prof. E Fosso-Kankeu, Prof. S.K.O. Ntwampe and Prof. F.B. Waanders) to meet the requirements for the doctoral degree award.

Signed: -----

Date: 22 February 2021-----

## DEDICATION

---

I dedicate this thesis to my late Father, **Mhlabuyajika Nichodimus Mkhize**, who throughout his lifetime etched in the walls of my heart the importance of education.

## ABSTRACT

---

South Africa is faced with challenges related to potable water quality, which has periodically deteriorated, coupled with inconsistent supply of tap water to households. On the other hand, South Africa is an important mining region, and nearly every province has remnants of active and closed metalliferous mining sites. Metalliferous mines produce a large quantity of metalliferous solid waste (MSW), which should be effectively managed to minimise the negative effects as it has the potential to produce acid rock drainage (ARD). The mobility of drainage alters the scarce water resources and aquatic species. These challenges are a primary concern to the community in the arid O’Kiep region, which is located in the Namaqualand district, South Africa, whereby the community has few alternatives to groundwater as a source of drinking water. The aim of this study was to assess species dispersion from a closed Namaqualand metalliferous mine into water sources in O’Kiep, Northern Cape province, South Africa.

This study aimed to determine the issues related to the deterioration of the surface water quality from the source to the point-of-use (POU) and contributing to the inadequate drinking water supply and shortages in O’Kiep. Quantitative and qualitative assessments of water quality parameters were taken; and the adverse human health outcomes experienced by the residents were surveyed. Furthermore, disease patterns were estimated based on administered questionnaires. Approximately 88% of community members indicated that the water supplied is often turbid, while a high number of people with teeth discolouration (72%) are living in the area and experience diarrhoea-like symptoms, which are likely associated with the ingestion of toxin-contaminated water. This was confirmed by some physicochemical parameters quantified from the drinking water supply system (DWSS), such as sulfate, that were not within the range prescribed for drinking water quality guidelines (SANS241-1, 2015; WHO, 2011). The statistical models did not suggest physicochemical properties as predictors of any of the health symptoms. However, regular monitoring and evaluation of the DWSS are essential for this vulnerable community. From this, it was recommended that a feasible way for water security in O’Kiep might be groundwater resources, as an alternative source to irregular surface water.

The hydrogeochemical parameters of groundwater assessed indicated that the continuous consumption of the groundwater without pre-treatment might result in possible human health risks as the groundwater quality index (GWQI) confirmed that the groundwater quality could be classified as being of moderate concern. Furthermore, the hydrogeochemical indices and cationic exchange values indicated that the aquifer is of inland origin, whereas the piper trilinear diagram revealed that the groundwater type in the area is categorised as saline, which was confirmed by sodium adsorption ratio (SAR). Similarly, the seasonal variation of the hydrogeochemical

characteristic changes of an open-pit groundwater (OPGW) near a closed metalliferous mine (CMM) were investigated against standards for drinking and irrigation usage. Based on the results, it was evident that the OPGW quality varied seasonally. The PHREEQC model indicated that cation exchanges played a significant role in the groundwater hydrogeochemical characteristic. Furthermore, the seasonal fluctuation in the groundwater quality was attributed to the water-table-level fluctuations, resulting in some instances in a lack of compliance to the drinking water quality guidelines (SANS241-1, 2015; WHO, 2011). Overall, the groundwater was slightly acidic with permissible levels for irrigation purposes. Therefore, excessive usage of the OPGW may have undesirable effects on plant growth. The groundwater hydrogeochemical characteristics of OPGW contamination suggested acid rock drainage formation potential (ARDP). The contamination of the groundwater by potentially toxic elements (PTEs) from soils and MSW in the study area was a matter of concern requiring further investigation.

Samples of the metalliferous soils and MSW were then evaluated for their ARDP using an integrated approach, combining geochemical characterisation, static tests and humidity cell tests (HCTs) assessing the balance between acidity potential (AP) and neutralisation potential (NP) of the slurry. Metalliferous soil leachates (MSL), stockpiled metalliferous waste leachates (SMWL) and metalliferous tailing leachates (MTL) were measured and quantified weekly for hydrogeochemical parameters. The static tests suggested that the metalliferous soils had a high acid-producing potential. This was confirmed by the results of the HCTs, which revealed signs of ARDP. Furthermore, the results also demonstrated weathering and production of ARD. The HCT results showed that the soils around the old mining town of O’Kiep are susceptible to ARDP and can release acid for elongated periods. Similarly, this study assessed ARDP from the stockpiled metalliferous waste (SMW) and metalliferous tailings (MTs) in O’Kiep. The static test results for the SMW were inconclusive, whereas the HCTs allowed the classification of the SMW as acid-producing material. In addition, the MTs were classified as acid-producing by the static tests and HCTs, with low mobility of PTEs when compared to SMW. Leaching of the SMW and MTs increases the risk of PTEs and acid contamination of surrounding soil and groundwater bodies in O’Kiep. Additionally, there are increasing concerns over significant potential environmental health effects of the SMW and MTs, including the mobility of PTEs.

Hydrogeochemical characteristic techniques and geochemical modelling were integrated to identify the significant factors governing groundwater hydrogeochemical evolution. The geochemical model PHREEQC suggested some geochemical reactions and mineral phases being responsible for the evolution of the groundwater chemistry. This indicates that the groundwater hydrogeochemical evolution is mainly controlled by carbonate mineral dissolutions, cation exchange, precipitation and weathering. The increase in sulfate concentration in 2019 in

the groundwater was most likely due to sulfide-mineral oxidation. Anthropogenic activities associated with the CMM and MSW may also contribute to the risk of PTE dispersion in the study area, leading to their increased level in groundwater in the long term. Exposure of the groundwater in O’Kiep to such contaminants has resulted in the progressive deterioration of water quality, with the significant increase of Na, Cl and SO<sub>4</sub> in particular. This information could contribute to risk assessments and evaluation of remediation strategies. It is therefore anticipated that the groundwater contamination will continue to persist in the study area for many years if mitigative strategies are not implemented. Although the SMW and MTs were disposed of years ago, they are inclined to ARDP for a long period unless phytoremedial solutions are taken into consideration for the rehabilitation of the mining site in the O’Kiep area. The accumulation of metalliferous soils and MSW within O’Kiep has culminated contamination of the groundwater, an alternative water source on which the community relies for various domestic needs. Unless robust interventions, including remediation, custodianship and conservation, are implemented, the community may face bigger challenges in the near future.

**Keywords:** Acid rock drainage, arid region, closed metalliferous mine, drinking water quality, groundwater, metalliferous soil and solid waste, O’Kiep.

## ACKNOWLEDGEMENTS

---

I wish to express my sincere appreciation to those who have contributed to this thesis and supported me in one way or the other during this amazing journey.

First and foremost, praises and thanks to God the Almighty for His showers of blessings throughout my research work to complete the research successfully.

Bayede kuMakhosi amakhulu akwaMkhize nawakwaKhumalo ngokungivumela ukuthi ngiphothule lezizifundo ngesikhathi ngithwasa. Ngibonge kakhulu nakuBaba Dr V.V.O. Mkhize ngokungamukela esigodlweni saseMlambomunye (Umsamo Institute – Home of African Ancestral Wisdom). Ngiyathokoza eMakhosini! To Dr L. Mekuto, Dr B. Godongwana and Mr A. Thole: words are not enough and thank you for your support while undergoing this spiritual journey.

I would like to express my sincere gratitude to my study leader, Prof. E. Fosso-Kankeu, for the continuous support, academic exposure related to research, his patience and motivation. He taught me the fundamentals of conducting scientific research and publishing.

I am indebted to my thesis co-promoter, Prof. S.K.O. Ntwampe, for his immense knowledge, motivation and patience, which gave me more energy and spirit to excel in the research.

I won't forget to express my gratitude to Prof. F.B. Waanders and Prof. N. Hoth for giving the encouragement and sharing insightful suggestions. I will forever be grateful for your guidance.

To Dr G. Gericke: thank you for being a good industrial mentor and for guiding me on the right path.

I am extremely grateful to Messrs T. Golela and A. Rand for their guidance and all the useful discussions and brainstorming sessions. Their deep insights helped me at various stages of this research.

I received generous support from Tendai Tawonezvi and Tlotlang Moncho (MEng students), and Maliqah Emandien, Avuziwe Mkefa and Khuselo Jadezweni (BTech students), who assisted with laboratory experiments.

My sincere gratitude is reserved for Dr L. Mekuto, my spiritual brother, for his invaluable insights and suggestions. His immense support actually guided me to rectify numerous things that could have created major challenges during this study. Words are not enough to describe my indebtedness to you.

To my spiritual father, Mr Myekeni Frederick Madondo, and my high school teacher. At a time when so many others turned away, you walked right into the storm with me. Thank you for being there for me. Ngithi unwele olude Mnquhe!

To my best friend, Aubrey Ntshabele, thank you for your support from the beginning to the end of this study.

I owe thanks to a very special person, My Bulldog, for his continued and unfailing love, support and understanding. You were always around at times I thought it impossible to continue and I deeply appreciate your belief in me.

I appreciate my beautiful daughter, Céline, for the patience and love you showed during this study. You have been a constant source of strength and inspiration. My message to you: never let anyone dull your flame. Never let the world harden you; touch the world with your gentle heart.

My appreciation to the O’Kiep Copper Company and Namakhoi Municipality for allowing me to conduct the research. And to the community of O’Kiep, thank you for making me feel at home while doing field sampling.

For the financial support, I would like to thank the following institutions: North-West University, Cape Peninsula University of Technology (University Research Grant No.: RY12 and Improvement of Qualification Programme Grant No.: PD-2019-000136), National Research Foundation (Thuthuka 2019: 117698) and Eskom Power Plant Engineering Institute (EPPEI).

## RESEARCH OUTPUT

---

The following research outputs represent the contributions by the candidate to scientific knowledge and development during her doctoral candidacy (2017-2020):

### **Published in journal articles**

**Erdogan, I.G.**, Fosso-Kankeu, E., Ntwampe, S.K.O., Waanders, F. and Hoth, N. 2020. Seasonal variation of hydrochemical characteristics of open-pit groundwater near a closed metalliferous mine in O’Kiep, Namaqualand region, South Africa. *Environmental Earth Sciences*, 79(5), 1-15. DOI: 10.1007/s12665-020-8863-2.

**Erdogan, I.G.**, Mekuto, L., Ntwampe, S.K., Fosso-Kankeu, E. and Waanders, F.B. 2019. Metagenomic profiling dataset of bacterial communities of a drinking water supply system (DWSS) in the arid Namaqualand region, South Africa: Source (lower Orange River) to point-of-use (O’Kiep). *Data in Brief*, 104135. DOI: 10.1016/j.dib.2019.104135.

**Erdogan, I.G.**, Fosso-Kankeu, E., Ntwampe, S.K.O., Waanders, F.B., Hoth, N. and Rand, A. 2019. Groundwater as an alternative source to irregular surface water in the O’Kiep area, Namaqualand, South Africa. *Physics and Chemistry of the Earth, Parts A/B/C*. DOI: 10.1016/j.pce.2019.09.003.

**Erdogan, I.G.**, Fosso-Kankeu, E., Ntwampe, S.K.O., Waanders, F.B., Hoth, N., Rand, A. and Farrar, T. 2019. Households water quality in O’Kiep-South Africa and community perception of related health risks. *Desalination and Water Treatment* [Manuscript ID: TDWT-2019-0184.R2]. DOI:10.5004/dwt.2019.24593.

### **Book chapter**

**Erdogan, I.G.**, Fosso-Kankeu, E., Ntwampe, S.K.O., Waanders, F.B. and Hoth, N. 2020. Management of Metalliferous Solid Waste and its Potential to Contaminate Groundwater: A Case Study of O’Kiep, Namaqualand South Africa. Recovery of By-products from Acid Mine Drainage Treatment, p.1. Wiley, 2020. ISBN: 9781119620075. DOI:10.1002/9781119620204.ch1.

## **Published conference proceedings**

**Erdogan, I.G.**, Netshiongolwe K., Mosai, A., Fosso-Kankeu, E., Ntwampe, S.K., Waanders, F.B., Hoth, N. 2020. Geochemical modelling data of groundwater in the O’Kiep, Namaqualand region, South Africa – 2013 to 2019: A case of evidenced contamination by historical mining activity. 18th International Conference on Science, Engineering, Technology and Waste Management (SETWM-20), Nov. 16-17, Johannesburg, South Africa.

Available: <https://doi.org/10.17758/EARES10.EAP1120218>

**Erdogan, I.G.**, Fosso-Kankeu, E., Ntwampe, S.K., Waanders, F.B., Hoth, N. and Rand, A. 2019. Static test-based acid rock drainage formation potential of metalliferous tailings from O’Kiep, South Africa. Nov. 18-19, Johannesburg, South Africa, 17th International Conference on Science, Engineering, Technology and Waste Management (SETWM-19).

Available: <https://doi.org/10.17758/EARES8.EAP1119262>

**Erdogan, I.G.**, Fosso-Kankeu, E., Ntwampe, S.K., Waanders, F.B., Hoth, N. and Rand, A. 2019. Acid rock drainage prediction of metalliferous soils from O’Kiep, Namaqualand, South Africa: A humidity cell test assessment. In IMWA 2019 Conference – Mine Water: Technological and Ecological Challenges, Perm, Russia.

Available: [https://www.imwa.info/docs/imwa\\_2019/IMWA2019\\_Erdogan\\_613.pdf](https://www.imwa.info/docs/imwa_2019/IMWA2019_Erdogan_613.pdf)

**Erdogan, I.G.**, Fosso-Kankeu, E., Ntwampe, S.K., Waanders, F.B., Hoth, N. and Rand, A. 2018. Potential toxic elements contamination of soils in O’Kiep, an arid region of Namaqualand, South Africa. In 10th International Conference on Advances in Science, Engineering, Technology and Healthcare ASETH-18), Nov. 19-20, Cape Town, South Africa.

Available: <https://doi.org/10.17758/EARES4.EAP1118238>

**Erdogan, I.G.**, Moncho, T., Fosso-Kankeu, E., Ntwampe, S.K.O., Waanders, F., Hoth, N., Rand, A. and Fourie, B. 2017. Hydrochemical characteristics of open-pit groundwater from a closed metalliferous mine in O’Kiep, Namaqualand region, South Africa. In 9th International Conference on Advances in Science, Engineering, Technology & Waste Management (ASETWM-17), Nov. 27-28, Parys, South Africa.

Available: <https://doi.org/10.17758/EARES.EAP1117022>

Moncho, T., **Erdogan, I.G.**, Emandien, M., Ntwampe, S.K.O., Fosso-Kankeu, E., Waanders, F., Rand, A. and Fourie, B. 2017. Prediction of metals bioavailability in the soils near mining areas in O’Kiep, South Africa. In 9th International Conference on Advances in Science, Engineering, Technology & Waste Management (ASETWM-17), Nov. 27-28, Parys, South Africa.

Available: <https://doi.org/10.17758/EARES.EAP1117023>

## LAYOUT OF THE THESIS

---

This study was conducted at the North-West University (Potchefstroom Campus) and Cape Peninsula University of Technology (Bioresource Engineering Research Group laboratory – Cape Town Campus), South Africa. The acid-base accounting (ABA) and HCTs were conducted at the commercial South African National Accredited Laboratory. The references listed at the end of the thesis were listed in accordance with the Harvard method of referencing.

**Chapter 1:** This chapter introduces the research background, briefly discusses the geology of the area, followed by a problem statement and a definition of the project objectives, motivation and significance of the study.

**Chapter 2:** The review chapter covers relevant literature pertaining to CMMs and their environmental challenges, including the description of different MSW as to their current disposal. Additionally, it discusses the rehabilitation and restoration of CMMs. Furthermore, fundamentals of ARD formation from different waste and its effects on groundwater are listed in this chapter.

**Chapter 3:** This chapter provides a description of drinking water quality challenges experienced by the community of O’Kiep. It also discusses community perceptions related to health risks associated with such water.

**Chapter 4:** This chapter discusses groundwater as an alternative source of potable water by means of discussing various hydrogeochemical parameters of the available groundwater. It further discusses chemical reactions and processes that govern groundwater chemistry.

**Chapter 5:** This chapter investigates the seasonal variation of the hydrogeochemical characteristics that affect the groundwater quality of an open pit near a CMM in O’Kiep, as the water was ground-sourced. It also discusses the mineral phases and chemical reactions using geochemical models.

**Chapters 6 and 7:** These chapters discuss the linkages between the mineralogy, geochemical characteristic of the mineralogy and geochemistry of the metalliferous soil and solid waste in O’Kiep. Prediction tools such as static and kinetic tests were used to predict and assess ARDP of different waste from the CMM with a potential to contaminate the groundwater in the area under study.

**Chapter 8:** The ultimate goal of this chapter was to report on the assessment of the hydrogeochemical changes of the groundwater using geochemical models to determine

geochemical processes and chemical reactions, even deterioration, controlling the groundwater chemistry in the study area over time. Moreover, the chapter aimed to investigate how the groundwater has been affected by the mining activities, and possibly the waste, in the area of study.

**Chapter 9:** This chapter lists conclusions and recommendations for future work from the overall research project, based on the results obtained thus far.

**Chapter 10:** This chapter contains the supplementary journals which form part of this thesis.

**Chapter 11:** This chapter is comprised of the list of consulted literature used in the form of in-text citations according to the North-West University Harvard referencing style.

**Chapter 12:** The annexures are covered in this chapter, comprising of letters of consent to residents of O’Kiep that were used for interviews and questionnaires.

## LIST OF SYMBOLS

---

<u>Symbol</u>	<u>Description</u>	
$Q_i$	Subindex of the water quality parameter	
$W_i$	Weight associated with the water quality parameter	
$\mu_i$	Actual mean value for $i^{\text{th}}$ treatment	
$H_A$	Alternative hypothesis	
$H_0$	Null hypothesis	
$j^{\text{th}}$	Index designating which of $n^i$ observations of sample $i$ is being considered	
$n$	Number of quality parameters	
$s_i$	The sample standard deviation	
		<u>Units</u>
AP	Acidity potential	kg/t
NP	Neutralisation potential	kg/t
DO	Dissolved oxygen	mg/L
DOC	Dissolved organic carbon	mg/L
EC	Electrical conductivity	mS/m
Eh / ORP/pe	Redox potential	mV
	Salinity	PPt
	Temperature	°C
	Turbidity	NTU
	Percentage	%
$S_{\text{total}}$	Total sulfur (LECO)	%

## GLOSSARY

---

### List of abbreviations used in this work

ABA	Acid-base accounting
ARD	Acid rock drainage
ARDP	Acid rock drainage formation potential
CMM	Closed metalliferous mine
DEFF	Department of Environment, Forestry and Fisheries
DNA	Deoxyribonucleic acid
DWA	Department of Water Affairs
DWSS	Drinking water supply system
GPS	Global positioning system
GWQI	Groundwater quality index
HCTs	Humidity cell tests
ICP-MS	Inductively coupled plasma mass spectrometry
ICP-OES	Inductively coupled plasma optical emission spectroscopy
MSW	Metalliferous solid waste
Mt	Metric tons
MTL	Metalliferous tailing leachates
MTs	Metalliferous tailings
MWR	Municipal water reservoir
NNP	Net neutralisation potential
NPR	Neutralising potential ratio
OCD	O’Kiep copper district
OPGW	Open-pit groundwater
PCR	Polymerase chain reaction
POU	Point-of-use
PSD	Particle size distribution
PTEs	Potentially toxic elements
RNA	Ribonucleic acid
SANS	South African National Standards
SAR	Sodium adsorption ratio
SI	Saturation index
SMW	Stockpiled metalliferous waste
SMWL	Stockpiled metalliferous waste leachates
SOM	Stockpiled overburden material

TDS	Total dissolved solids
TSF	Tailings storage facility
USEPA	United States Environmental Protection Agency
USGS	United States Geological Survey
WHO	World Health Organisation
XRD	X-ray powder diffraction
XRF	X-ray fluorescence

## TABLE OF CONTENTS

---

DECLARATION .....	II
DEDICATION.....	III
ABSTRACT .....	IV
ACKNOWLEDGEMENTS .....	VII
RESEARCH OUTPUT.....	IX
LAYOUT OF THE THESIS.....	XI
LIST OF SYMBOLS.....	XIII
GLOSSARY .....	XIV
CHAPTER 1: INTRODUCTION.....	1
1.1 Research background .....	2
1.2 Geological description of the O’Kiep closed metalliferous mine.....	3
1.3 Potentially toxic elements and their speciation .....	4
1.4 Motivation and rationale.....	5
1.5 Statement of the research problem .....	5
1.6 Aims and objectives .....	6
1.7 Research questions.....	6
1.8 Hypothesis .....	7
1.9 Significance of the research .....	7
1.10 Delineation of the study .....	7
CHAPTER 2: LITERATURE REVIEW .....	8
2.1 Management of metalliferous solid waste and its potential to contaminate groundwater: A case study of O’Kiep, Namaqualand South Africa .....	9
2.2 Introduction .....	9
2.3 Closed metalliferous mines: Overview and challenges .....	10
2.4 Metalliferous solid waste .....	11

2.4.1	Stockpiled overburden material .....	12
2.4.2	Stockpiled metalliferous waste.....	12
2.5	Metalliferous tailings .....	14
2.6	Environmental and social impact of closed metalliferous mines and metalliferous solid waste .....	16
2.7	Soil contamination.....	18
2.8	Groundwater contamination .....	19
2.9	Atmospheric contamination .....	19
2.10	Metalliferous solid waste management.....	19
2.11	Rehabilitation and restoration strategies .....	20
2.12	Characteristics of acidic rock drainage .....	21
2.13	Acid rock drainage formation and groundwater contamination .....	24
2.14	Overview of challenges associated with closed metalliferous mines .....	25
2.15	Summary .....	26
<b>CHAPTER 3: RESULTS AND DISCUSSION.....</b>		<b>27</b>
3.1	Households water quality in O’Kiep-South Africa and community perception of related health risks.....	28
3.2	Introduction .....	28
3.3	Objectives .....	29
3.4	Materials and methods.....	30
3.4.1	Study area and population.....	30
3.4.2	Background of drinking water supply system.....	30
3.4.3	Data collection methods .....	30
3.4.4	Water sampling and quality parameter quantification .....	32
3.4.5	Cyanobacterial toxin analysis .....	32
3.5	Results and discussion.....	33
3.6	Results .....	33
3.6.1	Statistical analyses.....	33
3.6.2	Logistic regression models .....	34

3.6.3	Questionnaire two-way frequency analysis.....	34
3.6.4	Cyanobacterial toxin analysis .....	37
3.7	Discussion .....	37
3.8	Summary .....	39
<b>CHAPTER 4: RESULTS AND DISCUSSION.....</b>		<b>41</b>
4.1	Groundwater as an alternative source to irregular surface water in the O’Kiep area, Namaqualand, South Africa .....	42
4.2	Objectives .....	43
4.3	Materials and methods.....	43
4.3.1	Geology and hydrogeology .....	43
4.3.2	Study area and data collection .....	44
4.3.3	Data treatment .....	45
4.3.4	Groundwater quality index.....	46
4.3.5	Classification of irrigation groundwater quality .....	46
4.4	Results and discussion.....	47
4.4.1	Hydrogeochemical characteristics of groundwater .....	48
4.4.2	Groundwater interactions and hydrogeochemical relations .....	50
4.4.3	Hydrogeochemical indices and cationic exchange values for groundwater.....	51
4.4.4	Geochemical classification of groundwater (trilinear piper plot).....	52
4.4.5	Groundwater for irrigation .....	54
4.5	Summary .....	54
<b>CHAPTER 5: RESULTS AND DISCUSSION.....</b>		<b>56</b>
5.1	Seasonal variation of hydrochemical characteristics of open-pit groundwater near a closed metalliferous mine in O’Kiep, Namaqualand region, South Africa .....	57
5.2	Introduction .....	57
5.3	Objectives .....	58
5.4	Materials and methods.....	59

5.4.1	Site description.....	59
5.4.2	Sample collection .....	59
5.4.3	Data analysis.....	61
5.4.3.1	The coefficient of variation and correlation analysis .....	61
5.4.3.2	Geochemical modelling .....	61
5.4.3.3	Sodium adsorption ratio .....	62
5.5	Results and discussion.....	62
5.5.1	Classification of the groundwater in O’Kiep.....	68
5.5.2	Evaluation of the ionic content of the groundwater in O’Kiep .....	71
5.5.3	The coefficient of variation and correlation analysis of the groundwater in O’Kiep .....	72
5.6	Summary .....	75
<b>CHAPTER 6: RESULTS AND DISCUSSION.....</b>		<b>76</b>
6.1	Acid rock drainage prediction of metalliferous soils from O’Kiep, an arid region of Namaqualand, South Africa: A humidity cell test assessment.....	77
6.2	Introduction .....	77
6.3	Objectives .....	80
6.4	Materials and methods.....	80
6.4.1	Sample collection .....	80
6.4.2	Acid-generation potential.....	81
6.4.3	Humidity cell tests.....	82
6.5	Results and discussion.....	83
6.5.1	Mineralogical composition of the metalliferous soil samples .....	83
6.5.2	Static test-based acid rock drainage formation potential of metalliferous soils .....	84
6.5.3	Weathering of metalliferous soils.....	85
6.5.4	Potentially toxic element mobility from metalliferous soils .....	90
6.6	Summary .....	91

<b>CHAPTER 7: RESULTS AND DISCUSSION.....</b>	<b>92</b>
7.1	<b>Acid rock drainage formation potential of metalliferous solid waste from O’Kiep, an arid region of Namaqualand, South Africa: A humidity cell test assessment..... 93</b>
7.2	<b>Introduction ..... 93</b>
7.3	<b>Objectives ..... 96</b>
7.4	<b>Materials and methods..... 96</b>
7.4.1	<b>Study area and sample collection ..... 96</b>
7.4.2	<b>Particle size distribution and porosity ..... 97</b>
7.4.3	<b>Static test predictions ..... 97</b>
7.4.4	<b>Humidity cell tests..... 98</b>
7.5	<b>Results and discussion..... 100</b>
7.6	<b>Results ..... 100</b>
7.6.1	<b>Particle size effects ..... 100</b>
7.6.2	<b>Mineralogy and geochemical characterisation..... 100</b>
7.6.3	<b>Static test predictions ..... 102</b>
7.6.4	<b>Humidity cell tests..... 102</b>
7.7	<b>Discussion ..... 111</b>
7.7.1	<b>Particles size distribution and porosity ..... 111</b>
7.7.2	<b>Mineralogical and geochemical characteristics ..... 111</b>
7.7.3	<b>Static test predictions ..... 112</b>
7.7.4	<b>Geochemical evaluation of the metalliferous solid waste leachate using humidity cell tests ..... 113</b>
7.7.5	<b>Mobility of sulfide-bound potentially toxic elements in the metalliferous solid waste ..... 117</b>
7.8	<b>Summary ..... 117</b>
<b>CHAPTER 8: RESULTS AND DISCUSSION.....</b>	<b>119</b>
8.1	<b>Geochemical modelling data of groundwater in the O’Kiep, Namaqualand region, South Africa – 2013 to 2019: A case of evidenced contamination by historical mining activity ..... 120</b>
8.2	<b>Introduction ..... 120</b>

8.3	Objectives .....	120
8.4	Materials and methods.....	121
8.4.1	Hydrogeochemical parameters.....	121
8.4.2	Geochemical modelling .....	121
8.4.3	Groundwater classification using the trilinear piper and Durov diagrams .....	122
8.5	Results and discussion.....	124
8.5.1	Hydrogeochemical characteristics.....	124
8.5.2	Groundwater classification.....	124
8.5.3	Geochemical modelling .....	125
8.6	Summary .....	126
<b>CHAPTER 9: CONCLUSION AND RECOMMENDATIONS .....</b>		<b>128</b>
9.1	Conclusion.....	129
9.2	Recommendations and future work .....	131
<b>CHAPTER 10: SUPPLEMENTARY FILES .....</b>		<b>134</b>
10.1	Supplementary files.....	135
10.1.1	S1: Supplementary data for Chapter 3 .....	135
10.1.2	S2: Supplementary data for Chapter 5 .....	149
10.1.3	Supplementary data for Chapter 8 .....	161
<b>CHAPTER 11: BIBLIOGRAPHY.....</b>		<b>174</b>
11.1	Bibliography.....	175
<b>CHAPTER 12: ANNEXURES.....</b>		<b>210</b>
12.1	Annexures for Chapter 3.....	211
12.1.1	Annexure A: Letter of consent (English language and Afrikaans language). .....	211
12.1.2	Annexure B: O’Kiep water supply and hygiene household questionnaires. ....	213
12.1.3	Annexure C: Frequencies from questionnaires. ....	219

## LIST OF TABLES

---

Table 1-1: Ore characteristics of east O’Kiep and west O’Kiep .....	4
Table 2-1: Metalliferous solid waste generation.....	15
Table 3-1: Chi-squared test $p$ -value: $8.389 \times 10^{-3}$ .....	34
Table 3-2: Chi-squared test $p$ -value: $2.885 \times 10^{-4}$ .....	35
Table 3-3: Chi-squared test $p$ -value: $8.389 \times 10^{-3}$ .....	35
Table 3-4: Physicochemical determinants compared to drinking water quality guidelines .....	36
Table 4-1: Groundwater quality index guidelines .....	46
Table 4-2: Statistical summary of the hydrogeochemical parameters compared to drinking groundwater standard .....	48
Table 4-3: Ionic ratios and cationic exchange values for groundwater.....	52
Table 5-1: Physicochemical characteristics of open-pit groundwater compared to water quality guidelines.....	63
Table 5-2: Ionic ratios of the open-pit groundwater.....	71
Table 5-3: Correlation coefficient for different parameters during dry season in the open-pit groundwater in O’Kiep.....	73
Table 5-4: Correlation coefficient for different parameters during wet season in the open-pit groundwater in O’Kiep.....	74
Table 6-1: Averaged mineralogical composition of metalliferous soils from the O’Kiep area.....	83
Table 6-2: Paste pH and acid-base accounting of metalliferous soils from the O’Kiep area .....	85
Table 6-3: The maximum metalliferous soil leachate quality compared to drinking water guidelines.....	90
Table 7-1: Static tests for metalliferous solid waste from the O’Kiep area .....	102
Table 7-2: Maximum metalliferous solid waste leachate quality compared to drinking water permissible limits.....	110
Table 8-1: Comparison of hydrogeochemical parameters in groundwater (periods 2013 and 2019) .....	121
Table 10-1: Bacterial community composition of the Orange River as identified by 16S rDNA amplicon gene sequencing.....	137
Table 10-2: Bacterial community composition of the treated water board agency reservoir as identified by 16S rDNA amplicon gene sequencing .....	138

<b>Table 10-3: Bacterial community composition of the O’Kiep municipal reservoir as identified by 16S rDNA amplicon gene sequencing .....</b>	<b>139</b>
<b>Table 10-4: Bacterial community composition of the O’Kiep municipal reservoir as identified by 16S rDNA amplicon gene sequencing .....</b>	<b>140</b>
<b>Table 10-5: Bacterial community composition of the O’Kiep municipal reservoir as identified by 16S rDNA amplicon gene sequencing .....</b>	<b>142</b>
<b>Table 10-6: Bacterial community composition of the O’Kiep municipal reservoir as identified by 16S rDNA amplicon gene sequencing .....</b>	<b>143</b>
<b>Table 10-7: Bacterial community composition of the household as identified by 16S rDNA amplicon gene sequencing .....</b>	<b>144</b>
<b>Table 10-8: Bacterial community composition of the household as identified by 16S rDNA amplicon gene sequencing .....</b>	<b>145</b>
<b>Table 10-9: Bacterial community composition of the household as identified by 16S rDNA amplicon gene sequencing .....</b>	<b>146</b>
<b>Table 10-10: Bacterial community composition of the household as identified by 16S rDNA amplicon gene sequencing .....</b>	<b>147</b>
<b>Table 10-11: Statistical summary of saturation indices of minerals in O’Kiep groundwater using PHREEQC .....</b>	<b>152</b>
<b>Table 10-12: A presentation of major ions from boreholes in the Namaqualand region, O’Kiep .....</b>	<b>164</b>
<b>Table 10-13: Saturation index of minerals in O’Kiep groundwater .....</b>	<b>165</b>

## LIST OF FIGURES

---

Figure 2-1: Contaminated overburden material from a partially closed metalliferous mine in O’Kiep.....	12
Figure 2-2: Stockpiled metalliferous wastes and contaminated soil .....	13
Figure 2-3: Open-pit in O’Kiep.....	14
Figure 2-4: Aerial view of the tailings storage facility in O’Kiep.....	15
Figure 2-5: Metalliferous solid waste generation .....	16
Figure 2-6: Contaminated soils of O’Kiep.....	18
Figure 2-7: Leachates from metalliferous storage facility in O’Kiep .....	24
Figure 2-8: Overview of challenges associated with closed metalliferous mining.....	25
Figure 3-1: Study area and sampling points .....	31
Figure 3-2: Dipsticks for screening of microcystins.....	37
Figure 4-1: Study area and sampling points.....	44
Figure 4-2 A and B: The Gibbs diagrams classification of groundwater samples of the aquifer of the study area .....	51
Figure 4-3: Trilinear piper diagram for groundwater classification in the area.....	53
Figure 4-4: Classification of irrigation waters .....	54
Figure 5-1: Study area, sampling points including possible sources of contaminants ...	60
Figure 5-2: Trilinear piper plot for both dry and wet seasons.....	69
Figure 5-3: The graph represents the mineral phases that could potentially precipitate during the mixing of the dry and we season .....	71
Figure 6-1: Location of study area and sampling points.....	81
Figure 6-2: Schematic diagram of humidity cell tests .....	82
Figure 6-3: Major oxides of metalliferous soil samples from O’Kiep.....	84
Figure 6-4: Major potentially toxic element characterisation of metalliferous soil samples compared to soil screening values.....	84
Figure 6-5: Electrical conductivity correlation to total dissolved solids and sulfate .....	86
Figure 6-6: Concentrations profile of potentially toxic elements in the metalliferous soil leachates .....	87
Figure 6-7: Oxidative-neutralising curve for the metalliferous soil leachates .....	88

<b>Figure 6-8: Relationship between anions for the metalliferous soil leachates .....</b>	<b>89</b>
<b>Figure 7-1: Location of study area and sampling points.....</b>	<b>97</b>
<b>Figure 7-2: Schematic diagram of the humidity cell test assessment of the metalliferous solid waste.....</b>	<b>99</b>
<b>Figure 7-3: Averaged mineralogical composition of metalliferous solid waste from the O’Kiep area.....</b>	<b>101</b>
<b>Figure 7-4: Major oxides of the metalliferous solid waste by X-ray fluorescence .....</b>	<b>101</b>
<b>Figure 7-5: Potentially toxic element characterisation by X-ray fluorescence.....</b>	<b>102</b>
<b>Figure 7-6: Evaluation of pH, electrical conductivity and total dissolved solids from metalliferous solid waste leachates.....</b>	<b>104</b>
<b>Figure 7-7: Oxidative-neutralising curve for metalliferous solid waste leachates.....</b>	<b>105</b>
<b>Figure 7-8: Calcium, magnesium and sulfate release rates of the metalliferous solid waste leachates.....</b>	<b>106</b>
<b>Figure 7-9: Geochemical parameters of stockpiled metalliferous waste leachates .....</b>	<b>108</b>
<b>Figure 8-1: Trilinear piper and Durov diagrams of the hydrogeochemical facies for groundwater classification.....</b>	<b>123</b>
<b>Figure 8-2: Saturation index of mineral phases in Namaqualand for the 2013 and 2019 periods .....</b>	<b>126</b>

## CHAPTER 1: INTRODUCTION

---

## 1.1 Research background

It is projected that approximately five billion people, out of a total population of around eight billion, will be living in countries experiencing water stress, utilising more than 20% of the available resources by 2025 (Root *et al.*, 2015). The Constitution of the Republic of South Africa of 1996 (Act 108 of 1996) states that individuals have the right to water, an environment that is not harmful to their health and welfare, and to have the environment protected for the benefit of present and future generations (Prasad and Shih, 2016). South Africa is a country where water shortages are becoming persistent, making water a scarce resource that is essential for the sustenance of its populace (Kwon *et al.*, 2015).

Closed metalliferous mines (CMMs), including metalliferous solid waste (MSW), pose a significant health risk to ecosystems and neighbouring communities due to mine-contaminant dispersion, which culminates in environmental degradation by potentially toxic elements (PTEs) such as Al, As, Cu, Cd, Fe, Hg, Pb and Zn (Kirillov *et al.*, 2016; Huang *et al.*, 2016; Sima *et al.*, 2011). MSW comprising of unrecovered beneficial minerals may also become the source of mineralisation which will result in contamination (Prasad and Shih, 2016; Kwon *et al.*, 2015; Sheoran and Sheoran, 2006). CMMs are reported to be sources of contamination as oxidation of sulfides exposed to free oxygen leads to the formation of acid rock drainage (ARD), a microbial-mediated process of sulfidic-matter oxidation (Sany, 2016; Navarro *et al.*, 2008; Tordoff *et al.*, 2000). Such constituents are often a major source of PTE contamination in the regional environment by leaching of minerals into nearby waterways and dust blowing (Saha and Sinha, 2016). The mobility and/or transportation of such contaminants are due to heavy periodic rainfall and associated events that are facilitated by climate change, which further play a contributory role facilitating the dispersion of PTEs in semi-arid regions with minimal vegetative growth (Naidoo, 2014). The driving force behind the formation of ARD is pH, metal ions and complex anion dispersion and migration (Hobbs and Cobbing, 2007). The untreated ARD poses a threat to the environment as it contaminates the surface as well as underground water reservoirs (Clifford and Barton, 2012).

The South African government has the responsibility to address such environmental contamination and associated challenges caused by mining activities as highlighted in the Constitution of the Republic of South Africa of 1996 (Act 108 of 1996). South Africa is facing numerous challenges concerning ARD due to previous and current mining practices (Eglington, 2006). Although several CMMs exist globally, limited information on these derelict mines as a source of environmental contamination is consolidated in the literature reviewed. In particular, not much has been reported about the area selected for this study, namely a CMM in O'Kiep,

Namaqualand, South Africa. Overall, minimal research has been conducted on the impact that the CMM has on environmental health and local communities.

## **1.2 Geological description of the O’Kiep closed metalliferous mine**

The major mineral mined underground at the O’Kiep CMM was Cu ore comprising Al, Cd, Mn, Ni, Sr and Zn, with limited water resources available for mining (Raith and Meisel, 2001). The O’Kiep terrain is characterised by rich base metal deposits (Clifford and Barton, 2012; Raith and Meisel, 2001), with rocks not older than 1250 Ma consisting of orthogneisses, granites and mafic intrusions (Raith and Meisel, 2001). The O’Kiep copper district (OCD) geology also comprises intrusive rocks dominated by granitic characteristics up to 1210 Ma, consisting of a thick sheet of granite and small bodies up to 1500 m (Raith and Meisel, 2001). In the study of granulite facies transition in the OCD by Raith and Meisel (2001), two types of metabasites were determined to arise along the granulite amphibolite facies. The southern granulite facies of O’Kiep includes Mg-rich ol-normative forms and low-MgO ores. Central and northern O’Kiep domains consist of a group of dark-coloured granulite facies. A display of mineralised composites consists of SiO<sub>2</sub> and MgO up to 50.9 wt. % and 19.7 wt. %, respectively. This was observed with low TiO<sub>2</sub> content ranging between 4 wt. % to 1.5 wt. %. Copper-sulfide (Cu<sub>2</sub>S) mineral is a group of mafic bodies that intrudes the meta-volcano sediment, which was largely dominated by mineralisation and has been mined. The eastern parts of O’Kiep with Cu-bearing mafic bodies were also found in the west part of O’Kiep and consist of Cu ranging from 1.75% to 14% (Raith and Meisel, 2001). Overall, O’Kiep is mainly dominated by Cu-rich sulfide minerals such as chalcopyrite and bornite, with Cu and Ni ratios reaching up to 100 (Raith and Meisel, 2001; Rozendaal and Horn, 2013). Conversely, Maier *et al.* (2012) discovered irregularly shaped body layers or bodies of biotite and Cu-rich granulite characterised by the presence of platinum-group elements and PTEs in a leuconorite rock type from the OCD, scattered within the O’Kiep belt as listed in Table 1-1.

**Table 1-1: Ore characteristics of east O’Kiep and west O’Kiep (Maier, 2000)**

	Sample No.	Ba	Sr	Y	Cr	Ni	V	Cu	S	Ru	Rh	Pd	Ir	Au	Pt
		mg/kg													
East O’Kiep	e02	992	699	23	34	172	216	10 225	1	2.5	-	5.9	0.1	0.9	-
	e03	867	746	17	45	100	227	9990	1	3.5	-		0.1	21.4	-
	e06	242	629	35	38	83	248	12 264	1	3.4	-	5.4	<0.05	23.2	9.0
	e08	256	650	31	29	83	210	13 294	1	-	-	7.0	<0.05	27.5	-
West O’Kiep	w02	293	626	50	324	396	711	41 663	1	-	1.0	-	0.1	177.8	-
	w04	251	667	37	436	434	572	42 628	1	6.7	4.9	-	1.6	157.4	-
	w06	252	644	54	371	209	863	9140	0	2.1	-	2.5	<0.05	21.4	6.4

However, geological data on the OCD show that the source of these mineral deposits remains unknown (Maier and Barnes, 1999). Samples of calcite, chalcocite, chalcopyrite, fluorite, and gypsum have been collected from other mines in the district, such as NababEEP West, by Maier and Barnes (1999).

### 1.3 Potentially toxic elements and their speciation

Rain- and groundwater are the major transporting agents for ions and by-products resulting from weathered rocks. The weathered or crushed rocks as a result of mining activity are influenced by biological, physical, and chemical factors (Cairncross, 2004; Maier and Barnes, 1999). These factors can transform the PTEs into various ionic and anionic forms. The ionic forms are likely to be mobile with and within the water bodies. Mobility is closely related to the tendency of a mineral to be stable in a water-soluble (ionic) form and thus with the ability to be transformed by biological factors. Mobile PTEs include soluble salts, hydrogen [H<sup>+</sup>] and hydroxyl [OH<sup>-</sup>] ions influenced by the formation of colloidal solutions (Maret, 2016). Ionic concentration of H<sup>+</sup>/OH<sup>-</sup> is responsible for pH changes and influences redox oxidation potential, which is responsible for many chemical and precipitation reactions forming various metal hydroxyl complexes (Tikhomirov, 2016). Since some of these stable soluble forms of mineral colloids have colour, they sometimes reveal themselves in groundwater as orange, yellowish to brown for ferric ion complexes, and greenish for ferrous iron complexes (Barnes *et al.*, 2016; Tikhomirov, 2016). Colloidal suspended particles can float in water bodies for elongated periods and cannot be treated. Cationic trace elements form a large number of complexes with common ligands such as Cl<sup>-</sup>, OH<sup>-</sup>, CO<sub>3</sub><sup>2-</sup>, SO<sub>4</sub><sup>2-</sup>, HCO<sub>3</sub><sup>-</sup>, HPO<sub>4</sub><sup>2-</sup>, and H<sub>2</sub>PO<sub>4</sub><sup>-</sup>. The result is that the total chemical analysis of any element in solution includes both free ion and its speciated forms. The speciation of ions becomes increasingly important as the salinity of the solution increases. Soluble trace cationic complexes should be considered with free ion concentrations when chemical equilibria in slurry and surface waters are considered. The trace-

element cations that form inorganic ligand complexes in semi-arid soils include  $Zn^{2+}$ ,  $Cu^{2+}$ ,  $Ni^{2+}$ ,  $Mn^{2+}$ ,  $Cd^{2+}$ ,  $Pb^{2+}$  and  $Hg^{2+}$  (Barnes *et al.*, 2016). Irregularities also occur as some PTEs are transported by animals, ice, frost, groundwater, soil, and surface water. These transporting agents contribute to a characteristic dispersal pattern similar to those seen in the weathering by-products of ore deposits (Fitzpatrick and Shand, 2008).

#### **1.4 Motivation and rationale**

The South African government's wastewater management regulations are important in contributing to and managing ARD (Jurinak and Tanji, 1993). This matter has featured significantly both in national and international scientific reports (Govett, 2013). In South Africa, ARD was observed in 2002 when the West Rand Basin was flooded with twenty million litres of contaminated water. It was projected that 90% of the ARD originated from closed mines that were operational decades ago, with approximately 6000 closed mines being the main source of the ARD (Cobbing, 2008). In a study on ARD by Feris and Kotzé (2014), it was reported that ARD is not only found in South Africa but in a number of countries such as Australia, Canada, Germany and the USA. South Africa has experienced contamination problems attributed to ARD nationwide in 1) Mpumalanga and KwaZulu-Natal coal fields, 2) Witwatersrand goldfields and 3) O'Kiep copper fields. Furthermore, conventional wastewater treatment methods using chemical agents were determined not to be appropriate for ARD treatment (Naidoo, 2017; Funke and Jacobs, 2011; Ramontja *et al.*, 2011; DWAF, 2008). Research studies have also reported that active and closed metalliferous mines contribute to the ARD problem. Ongoing research activities are associated with ARD from Cu mining (Coetzee *et al.*, 2010; Strydom *et al.*, 2010). The OCD has been identified by the Inter-Ministerial Committee (Ramontja *et al.*, 2011) on mine water management as a lower priority area, but further assessment and monitoring is required. Few studies have focused on the O'Kiep area and this has culminated in not many research reports being published on the subject. No research studies conducted on the impact of ARD as a result of the CMM in O'Kiep have been reported. Therefore, it is necessary to focus on O'Kiep and assess the impact of the CMM to the community that stays closer to this CMM.

#### **1.5 Statement of the research problem**

The potentially hazardous contaminants from the CCM, including their dispersion, can pose a threat to human and environmental health, including groundwater contamination. O'Kiep is affected by MSW that were left without rehabilitation. Different risks associated with such mining activity include ARD, contamination of the water table and secondary mineral sedimentation (García-Giménez and Jiménez-Ballesta, 2017; Coetzee *et al.*, 2010). High concentrations of PTEs from the nearby CMM represent a continuing human health challenge and environmental

hazard as the MSW, including by-products, can leach into soil and groundwater (Martín-Moreno *et al.*, 2016; You *et al.*, 2015). Such contaminants can lead to outbreak of disease in humans through water consumption and contaminated agricultural produce (Abreu *et al.*, 2008). The problem can be escalated when contaminated water in the form of ARD reaches the river basin system, thus contaminating the valuable groundwater resource, which will significantly impact the growth of the community that will depend on groundwater in the near future (Lee *et al.*, 2009).

## **1.6 Aims and objectives**

- To determine the quality of drinking water supplied to the community and to identify possible related human health risks.
- To assess the quality of groundwater and to determine its suitability for domestic and irrigation purposes.
- To assess the seasonal variation of the open-pit groundwater (OPGW) quality and determine its fitness for the purpose of drinking and irrigation.
- To predict ARD potential and weathering rates of the metalliferous soils.
- To develop a better understanding of the main MSW constituents and reliable predictions of the ARD risks in a disposal scenario.
- To determine hydrogeochemical evolution and mineral phases using geochemical modelling.

## **1.7 Research questions**

- What are the types of water sources and their availability?
- Is the surface water and groundwater suitable for drinking and irrigation purposes?
- Does the seasonal variation of groundwater have an effect on drinking water quality and agricultural water quality?
- What are the sources of soil and groundwater contamination?
- What is the impact of the CMM on soil and groundwater quality?
- Do the metalliferous soils and solid waste have the potential to generate or neutralise acid?
- Has groundwater deteriorated over time and what are the mineral phases responsible for groundwater evolution?
- Have any noticeable groundwater hydrogeochemistry changes occurred over time?
- Which processes are the primary drivers of changes in groundwater hydrogeochemistry?
- What are the primary sources that pose significant effects on groundwater quality?

## **1.8 Hypothesis**

Dispersion of species is affected by the physical, chemical, and biological factors which result in pollutant formation due to changes in redox and pH environmental factors, thus facilitating the chemical process at the water-sediment interface due to periodic leaching. It was hypothesised that species dispersion from the CMM does influence and contribute to the groundwater-source deterioration in O’Kiep, Namaqualand, South Africa.

## **1.9 Significance of the research**

This research provides information on the contributory role of the CMM in the contamination of limited water sources in O’Kiep and surrounding areas. Conducting the research was important as the CMM is within the O’Kiep town, which is a local population centre for the populace. The outcome of this research highlights that the CMM has possible human health and environmental risks towards the local community. Land rehabilitation is often hampered by minimum research that has been conducted and identification of the degree of contamination. The information as presented in this thesis can also be valuable to the Department of Mineral Resources for rehabilitation purposes and the Department of Water and Sanitation since it is strategically aligned to functions of these departments in the South African government.

## **1.10 Delineation of the study**

The following were not assessed in this study:

- The variation in hydrochemical facies.
- Only laboratory-scale tests were conducted for this study, without correlation to field-scale environments.
- No kinetic modelling was conducted during this study.
- The use of other kinetic tests such as the bio-kinetic test for prediction of ARD.
- Treatment of ARD.
- The recovery of rich PTEs in groundwater.

## CHAPTER 2: LITERATURE REVIEW

---

Published as:

**Erdogan, I.G.**, Fosso-Kankeu, E., Ntwampe, S.K.O., Waanders, F.B. and Hoth, N. 2020. Management of Metalliferous Solid Waste and its Potential to Contaminate Groundwater: A Case Study of O’Kiep, Namaqualand South Africa. Recovery of By-products from Acid Mine Drainage Treatment, p.1. Wiley, 2020. ISBN: 9781119620075.

DOI:10.1002/9781119620204.ch1.

# **Management of metalliferous solid waste and its potential to contaminate groundwater: A case study of O’Kiep, Namaqualand South Africa**

## **2.2 Introduction**

Mining and mineral processing industries have been the critical focus of research in many countries due to increasingly stringent regulatory conditions as sustainability concerns increase and the effect of global warming and environmental degradation in general (Naidoo, 2015). Several non-metalliferous and metalliferous mines globally are situated in arid and semi-arid regions and are operated through both surface and underground mining methods (Farjana *et al.*, 2019). They have been an important industry in many countries worldwide (Preite *et al.*, 2019), including South Africa, where metalliferous deposits containing Au, Pt, Zn and Cu have played and some continue to play a vital role (Palumbo-Roe and Colman, 2010).

The economic benefits of metalliferous mines have often surpassed the major challenges posed to the environment in which they are operated as they provide employment to vulnerable communities; albeit, enormous quantities of MSW are generated. A number of these challenges include the dust, groundwater and surface water contamination and an incapability to use the land for developmental purposes during post-mining operations (Bell *et al.*, 2002). The CMM and MSW generated, pose a serious health risk to ecosystems and neighbouring communities due to contaminant dispersion, particularly in the form of PTEs with special emphasis on Sb, Al, Cr, Cu, Fe, Pb, Mn, Ni, Ag, Zn and sulfide-bearing minerals (Gitari *et al.*, 2018). Additionally, MSW are reported to be sources of PTEs containing leachates, as oxidation of (di-) sulfides leads to the formation of ARD, a process microbially-mediated (Prasad and Shih, 2016), and the creation of secondary contaminants such as PTE via dissolution of MSW (Komnitsas *et al.*, 1995). Changing climatic patterns, especially in arid regions, further play a contributory role by facilitating the dispersion and mobility of PTEs contributing to minimal vegetation growth (Kwon *et al.*, 2015) which appears to be the case in O’Kiep, Namaqualand, South Africa.

O’Kiep is a former copper mining area with ore mineralisation being dominated by Cu-rich sulfidic ores, namely bornite and chalcopyrite, which are the most abundant copper-bearing minerals in the area. Some of these constituents undergo oxidation. The CMM which ceased production in 2004 produced a large number of metalliferous tailings (MTs) with approximately 5.8 Mt of material. MSW from the CMMs were deposited in the vicinity of the community of O’Kiep (Rozendaal *et al.*, 2017; Amponsah-Dacosta and Reid, 2014; Navarro *et al.*, 2008).

The potential formation of ARD poses a threat to the environment resulting in the contamination of surface as well as groundwater reservoirs, which became evident in the hydrochemical

characteristics of OPGW of O’Kiep. Therefore, such environmental contamination and associated challenges attributed to problems caused by mining activities need to be addressed, as highlighted in the Constitution of the Republic of South Africa, 1996 (Act 108 of 1996). Generally, South Africa has numerous challenges concerning ARD formation due to previous and current mining practices Constitution of the Republic South Africa, Act 108 of 1996 (Prasad and Shih, 2016).

O’Kiep is affected by MSW which is a potential cause of diseases in humans (Naidoo, 2014). These challenges can be escalated when contaminated water reaches the aquifer, the only valuable groundwater resource especially in areas that have no peripheral rivers. This is also the case for O’Kiep, with the lower Orange River being the only perennial river located approximately 150 km from the town. It is a major source of piped potable water for agricultural, domestic and industrial use (Lee *et al.*, 2009). As the lower Orange River is running dry due to climatic changes and minimal rainfall, this community will soon have to rely on groundwater. Because minimal research has been conducted on environment health and the local community of O’Kiep, this chapter discusses these effects of CMM and MSW and the potential formation of ARD.

### **2.3 Closed metalliferous mines: Overview and challenges**

The number of CMMs globally is in the hundreds of thousands, and all are capable of generating ARD, increasing PTE solubility; thus mobility, culminating in the degradation of the environment (Pehoiu *et al.*, 2019). For example, CMM in Romania known to produce Cu and U is a potential danger to the health of the communities of Anina, Ciudanovița, Lavrion, Lișava, Moldova Nouă and Năvodari as well as to the surrounding environment (Ippolito *et al.*, 2019; Komnitsas *et al.*, 1998). Similarly, a CMM located in Malaysia yielded 2.47 Mt of concentrate comprising of approximately 600 Mt of Cu, 45 t of Au and 294 t of Ag, produced approximately 250 Mt of stockpiled overburden material (SOM) and MTs of approximately 150 Mt (Kontopoulos *et al.*, 1995). Another CMM located in Bulgaria producing Cu concentrates, created environmental risks for the region, especially for the local aquifer, whereby rainfall fills the pit, forming a water body containing high concentrations of PTE. It was determined that the PTEs were highly mobilised during the wet season, with many reported cases of contamination by PTEs close to the mine (Van der Ent and Edraki, 2018). Similarly, a CMM in Alaska with MSW comprising of Cu, Fe, Pb and Zn sulfide minerals which were exposed to biochemical weathering culminated in CMM and remnant MSW extending into the coastal zone of Prince William Sound with field investigations revealing that the oxidation of sulfidic MSW at these sites will generate ARD with subsequent transportation of PTEs into the marine environment (Nikolov and Borisova, 2012). Thousands of CMMs with MSW containing PTEs from Au, Cu, Pb, and Zn mining in the USA, have been reported (Koski and Munk, 2007). These mines once reflected the historical development of the

American continents, yet they represent a possible threat to human health with local environments being the repository for the contaminants they generated (Venkateswarlu *et al.*, 2016). CMMs often contain unmined SOM, stockpiled metalliferous waste (SMW) and MTs that weather and leach to the surrounding environment. Several of these CMMs are located on or adjacent to public land. To mitigate such effects, governments need to provide a wide range of scientific expertise to assist and collaborate with the local municipalities whereby environmental strategies to mitigate adverse environmental effects can culminate in effective remediation of CMMs. In Cyprus, CMMs caused severe off-site ecological challenges and health hazards for the local residents (Antivachis *et al.*, 2017). Groundwater sources were affected by the leaching of PTEs, surface water was contaminated due to water erosion, and harmful dust comprising of PTEs spread because of wind erosion. In addition to the ecological hazards associated with the CMMs, several of these locations are aesthetically unpleasant, and remain a financial liability to investors and the community in general, due to the downgrading of nearby areas, non-development and therefore, loss of income. These factors are essential for countries such as Cyprus, whereby tourism is a noteworthy source of revenue for local residents (Antivachis *et al.*, 2017). Similarly, the O’Kiep region is known for its seasonal flowers; however, these flowers, plants and wild animals have been diminishing with the environment being damaged due to mining activities (Cowling, 2015).

#### **2.4 Metalliferous solid waste**

The MSW is the high-volume material estimated at thousand million tons generated annually that originates from the excavation and further chemical and physical processing of a varied range of non-metalliferous and metalliferous minerals by both surface and underground methods (Cowling, 2015). These mines are generally essential for profitability of low-grade ore bodies, and consequently, volumes of MSW are generated. It is produced during the process of beneficiation, extraction and mineral processing and can be divided into: 1) coarse-grained waste rock material generated during mining, 2) SOM, 3) SMW that are usually stored in heaps and 4) fine-grained MTs, usually stored in hydraulic-fill structures. Additionally, the oxidation of MSW can generate leachates and gaseous by-products during MSW oxidation (Preite *et al.*, 2019; Vallero and Blight, 2019). Approximately one-half of the MSW generated is SMW and one-third is MT, with 61% of the MSW originating from copper-bearing waste (Xtract, 2015).

The SOMs, SMW and MTs do contain PTEs that are a source of environmental contamination from mining activity. They might pose human health hazards and agricultural produce contamination through contaminated surface or groundwater usage for irrigation purposes, culminating in the uptake of PTEs by vegetation in which animals graze thus further bioaccumulating in the food chain (Szczepańska and Twardowska, 2004). Both SOMs and SMW generally have reduced water holding capacity, low organic matter content; albeit, with elevated

levels of PTEs (Chaturvedi *et al.*, 2012). Interaction of pyrite-rich SMW and groundwater bodies at CMMs is an environmental concern globally (Galanopoulos *et al.*, 2019). When the SMW is rich in sulfidic constituents, potentiality of ARD formation and the release of dissolved metals under aerobic conditions can ensue (Campbell and Beardall, 2019).

#### **2.4.1 Stockpiled overburden material**

The SOMs are site-specific and differ from one mine to another due to different geological settings and characteristics of the ore being mined. In mining, SOM lies above an area that lends itself to economic exploitation, and SOMs are distinct from MTs, as SOMs are typically not contaminated with high concentrations of PTEs. The mining industry has to handle and dispose of the overburden material (Priya and Kumar, 2018). SOMs may also be used to restore and rehabilitate an exhausted mining site to its original condition (Shanmuga and Kumar, 2015). Though attempts have been made to use the overburden material in O’Kiep, these SOMs lie above a partially rehabilitated CMM and have consequently been contaminated over time (Figure 2-1).



**Figure 2-1: Contaminated overburden material from a partially closed metalliferous mine in O’Kiep**

#### **2.4.2 Stockpiled metalliferous waste**

Metalliferous mining operations of some ores produce large quantities of waste known as MTs and SMW (Kogel *et al.*, 2006). SMW are made of coarse-grained rock, crushed from larger rocks to fine particles which are heterogeneous and are stored nearby the mining site (Tayebi-Khorami *et al.*, 2019). The structure of the SMW has a serious effect on the groundwater because of the oxidation of metal sulfides present and because it often occupies large areas, which might result

in environmental concerns (Tayebi-Khorami *et al.*, 2019). Occasionally, SMW are stored within a tailings storage facility (TSF) to prevent ARD formation, as most SMW contain PTEs, sulfides and radioactive minerals (Likus-Cieřlik *et al.*, 2017). SMW can also be a resource of metals and minerals or have other applications at the mine site, such as backfilling of underground mines or for capping of TSF (Beauford, 2012). The chemical and physical characteristics of SMW vary depending on the geological setting, geochemistry and mineralogy of the ore being mined, and the type of process used to beneficiate that ore (Tayebi-Khorami *et al.*, 2019). In the case of O’Kiep, the SMW is mixed with slag (Figure 2-2), with a depth of approximately 8 m as the mine generated an estimated 5 Mt of slag. During the mine’s life, attempts to recover Cu from the slag by flotation were unsuccessful resulting in slags or SMW heaps. Rehabilitation of a mine site can be possible to limit the disposal of the slag, with reinvestigations into the possibility of reprocessing of slag as a Cu resource using advance methods (Yucel and Baba, 2016).



**Figure 2-2: Stockpiled metalliferous wastes and contaminated soil**

Also, in Japan MTs containing pyrite ( $\text{FeS}_2$ ) and substantial quantities of Cu and Zn were reported in a study by Tabelin *et al.* (2019). For O’Kiep, MSW severely contaminated nearby soils and acidified the soils, thus increasing the mobility of PTEs (Moncho *et al.*, 2017), to areas in the vicinity of the houses (Figure 2-1). These SMW have become problematic (Figure 2-3).



**Figure 2-3: Open-pit in O'Kiep**

Similar findings were reported by Křibek *et al.* (2019), which revealed that the SMW in Zambia were highly contaminated with PTEs, which could pose hazards to human health and contaminate groundwater. Namaqualand (South Africa) is well known for its widespread distribution of small mines and has an extensive mining history; currently, it has been listed as a highly contaminated region with major environmental damage (Hohne and Hansen, 2008). Most SMW in the region was characterised by Cr, Pb and P which are high-risk PTEs for the local ecosystem and inhabitants of the area. Overall, the wind-blown dust from the SMW and TSF has also been considered a health problem in O'Kiep and could result in respiratory diseases (Figure 2-4). However, rehabilitation of the SMW and TSF remains a part of the challenges for the local population, which must be earmarked for future rehabilitation; albeit, such an undertaking has not materialised yet.

## **2.5 Metalliferous tailings**

South Africa holds approximately 400 TSF covering an estimated 400 km<sup>2</sup> (Hohne and Hansen, 2008). In Witwatersrand basin alone, 270 TSFs can be found and most of them are unlined and produce SMW leachate. According to Gauteng's Department of Agriculture and Rural Development these mine residues cover an area of 321 km<sup>2</sup> (Rozendaal *et al.*, 2017). Biototoxicity of MTs is primarily due to its low pH leachate and the high concentrations of PTEs contained within the waste. Figure 2-4 present the aerial view of the TSF of O'Kiep.



**Figure 2-4: Aerial view of the tailings storage facility in O’Kiep, Namaqualand Region South Africa (made with CapeFarmMapper version 2.3.2.5 <https://gis.elsenburg.com/apps/cfm>.)**

Additionally, MTs produced by low grade, high tonnage operations are progressively increasing their environmental footprint across Southern Africa (Fosso-Kankeu *et al.*, 2015) (Table 2-1).

**Table 2-1: Metalliferous solid waste generation**

Minerals mined	Stockpiled metalliferous waste (Mt)	Metalliferous Tailings (Mt)	Potential risk	References
Antimony	-	420-525	-	(Amponsah-Dacosta and Reid, 2014)
Copper	0.2-124	0.1-791	Massive release of PTEs and Groundwater acidification	(García-Giménez and Jiménez-Ballesta, 2017, Titshall <i>et al.</i> , 2013)
Iron	102	75		(Derkics, 1985)
Lead	2	9	PTEs in groundwater contamination	(Beauford, 2012)
Silver	20	6		(Gitari <i>et al.</i> , 2018)
Zinc	1	6-50 000	-	(Xtract, 2015, Godfrey <i>et al.</i> , 2007)

Approximately one-half of the MSW generated by the segments of concern is SMW and one-third is MT. Most of the MSW is from copper-bearing (61%) waste. The quantities of MSW generated by each metalliferous mining sector of concern are presented in Figure 2-5.

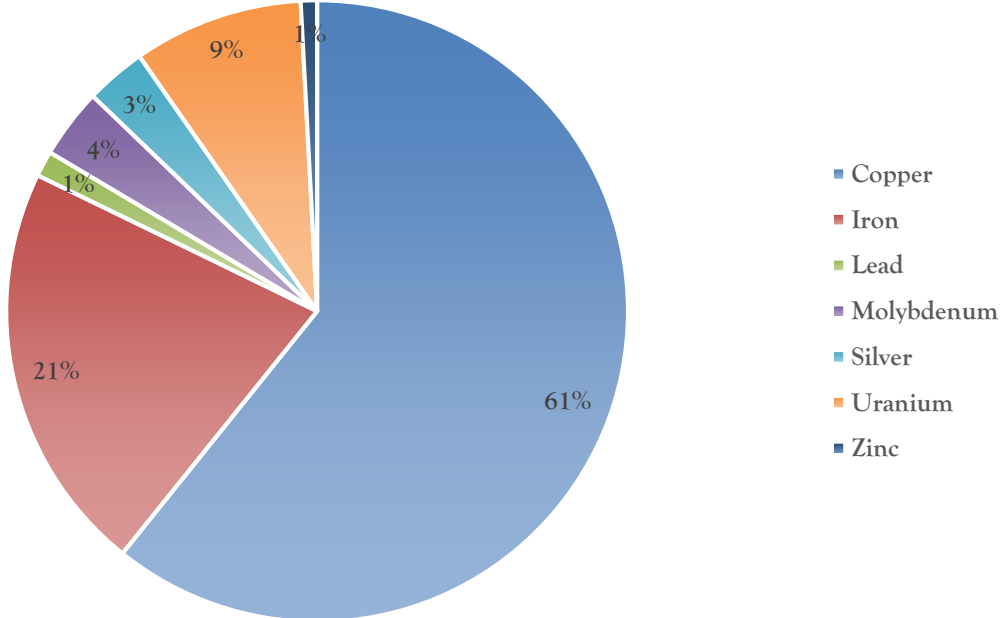


**Figure 2-5: Metalliferous solid waste generation (EPA, 1985)**

MTs often lead to high bulk densities and low infiltration rates and have low organic matter (Earthworks, 2004). Similar to SMW, the PTEs in the TSF can pose a severe threat to the environment and human health (Derkics, 1985). MTs are often fine-grained and silt-sized particles with high PTE concentrations. Upon oxidation, MT with high pyritic contents and PTEs are associated with reduced plant productivity, environmental contamination, and human health concerns (Derkics, 1985). It is well known that a high concentration of PTEs could lead to numerous clinical outcomes of the population who live on these contaminated sites (Figure 2-4). MTs are usually placed in impoundment areas exposed to precipitation and water runoff, which can allow PTEs to be leached (Derkics, 1985). Some MTs such as those in Limpopo province (South Africa) were investigated and reported to have an average pH of 8.0 indicating an alkaline medium; albeit, with the concentration of PTEs, namely As, Cd and Cr, which strongly bind to the smaller fractions in mining waste. Results show a high concentration and easily extractable Cu in the MTs, which indicated bioavailability thus environmental and human exposure risks (Derkics, 1985).

**2.6 Environmental and social impact of closed metalliferous mines and metalliferous solid waste**

As has been shown above, CMMs are potential sources of environmental contamination and may pose a health risk to local populations (Oyourou *et al.*, 2019). A primary environmental concern

associated with active and CMMs is the production of ARD from the oxidation of disposed sulfidic waste material when exposed to moisture and oxygen in the air, especially in the presence of iron- and sulfur-oxidising bacteria (EPA, 1985). Although several CMMs and MSW exist in South Africa, information on their potential negative effects has not been consolidated in the literature reviewed especially for O’Kiep. After the closure of the mine, MSW was abandoned, resulting in degraded soils near the mining sites, that is areas which were pristine, a phenomenon often causing major geotechnical instability of the waste resulting in further PTE mobility (Mehta *et al.*, 2019).

Additionally, communities after mine closure tend to experience adverse environmental and other social impact phenomena. In the case of O’Kiep, the OPGW has been characterised as having a low pH and elevated concentrations of PTEs. Additionally, measures were not in place to ensure that the CMM in O’Kiep was rehabilitated effectively. This resulted in the negative effects of CMM and MSW not being addressed thus a lack of accountability.

Generally, unrehabilitated CMMs can generate ARD, increasing PTE solubility, and the degradation of the environment, including local water sources. CMMs can also result in vast vegetation reduction attributed to changes in the soil quality and structure (Zawadzki *et al.*, 2016). On the other hand, the presence of carbonates and other caustic type gangue minerals can lead to reactions to reduce the ARD formation potential; albeit, this can still result in poor-quality drainage with high concentrations of sulfate and PTEs (Tayebi-Khorami *et al.*, 2019). One of the challenging issues associated with soil contamination is PTE mobility which is initiated by MSW weathering by wind action which is highly likely in O’Kiep since the MSW has resulted in soil degradation (Moncho *et al.*, 2017), and possible groundwater contamination. The possible effects of the MSW near local communities are the high concentrations of PTEs and low soil organic matter availability due to the arid nature of the area which makes PTE mobility easier.

Currently, mining industries are consistently under intense scrutiny from the general public and governments due to some improper disposal methods of MSW after mine closure. Contaminant containing MSW in South Africa is currently a challenge of higher concern both for the mining industry and the government. This includes several TSF that have been abandoned and never been rehabilitated. Subsequent analysis by Wapwera *et al.* (2015) showed that there are radioactive substances in CMM operations which can exceed the international guidelines; therefore, they can result in observable consequences on the health of the local population, who reside in the vicinity of such mines. Generally, Cu mining waste make-up the largest percentage of metal mining and processing wastes generated globally. There is a broad range of naturally occurring radioactive materials that have been concentrated or exposed in MSW, and as a result, animal and human exposure becomes unavoidable.

Mining and extraction of Cu by surface or underground methods can concentrate and expose radionuclides in the SMW and MTs (Vearrier *et al.*, 2009). Nkosi *et al.* (2015), reported that there is increasing evidence that environmental factors such as air contamination by volatile constituents from SMW resulted in an increased risk of chronic respiratory symptoms of individuals in communities located near SMW in South Africa. Additionally, long-term aerosols containing Cu constituents can irritate human respiratory mucous membranes, causing headaches, dizziness and nausea (Paredes, 2016). Similarly, drinking water containing excessive quantities of Cu can lead to nausea, vomiting, diarrhoea, and if taken intentionally, can cause liver and kidney damage including death. Since the highest chance of ingesting excess Cu is via drinking water in the form of groundwater, it is essential to monitor Cu release to aquifers such as that of O’Kiep (Ippolito *et al.*, 2019).

**2.7 Soil contamination**

The CMM and MSW in O’Kiep has contaminated nearby soils (Figure 2-6) with elevated concentration of S, Cu, F, Ba, Mn and Cl (Moncho *et al.*, 2017). Lee *et al.* (2016), comprehended spatial variation of PTEs in the soil to identify adequate measures to preventing pristine soil contamination at closed metalliferous mining areas, whereby the spatial distribution of Cu and Pb was monitored. This is mainly done to develop rehabilitation strategies to mitigate environmental contaminant mobility, that is PTE distribution to contaminant free areas, or into other natural resources including groundwater.



**Figure 2-6: Contaminated soils of O’Kiep**

## **2.8 Groundwater contamination**

Several factors are associated with MSW and CMMs that affect groundwater, with one being ARD seepage (Likus-Cieślík *et al.*, 2017). Furthermore, PTEs stored in MTs, soils and MSW have become potential secondary groundwater contaminants (Qin *et al.*, 2019). Open pits are formed during surface mining operations and are thereafter filled with water, either through groundwater recharge or surface run-off. Generally, the success in closing open pit mines has varied tremendously (Vandenberg *et al.*, 2015) and the groundwater from these open pits end up being contaminated by ARD. CMMs can present challenges for environmental restoration due to the presence of a high concentration of sulfidic constituents in the MSW, with rainfall further exacerbated the problem as it would result in large volumes of contaminated groundwater recharges and surface run-off open pit water (Van der Ent and Edraki, 2018). There are well known examples of legacy sites requiring perpetual treatment of their water such as open-pits, with O’Kiep being an example; albeit, some other open pit water had achieved various beneficial traits for end-users such as agricultural use (Villain *et al.*, 2015). Static tests suggested that the soils of O’Kiep had a high acid-producing potential, which was confirmed by humidity cell tests (HCTs), with the likelihood of weathering, of either rock, soil or MSW under moisturous conditions leading to acidification of any stagnant water.

## **2.9 Atmospheric contamination**

Metalliferous mine dust associated with PTEs containing aerosols released into the atmosphere through the dust and other gases from the MSW is one such environmental contamination challenge related to the cause of adverse health effects in humans and vegetation (Rozendaal *et al.*, 2017; Entwistle *et al.*, 2019; Mark, 2006). Despite occupational health improvements within the mining industry, the release of metalliferous dust into the atmosphere remains a human health challenge, especially in regions with poorly developed regulatory standards and whereby historic mining has left a legacy of exposed MSW. The global challenge associated with unrehabilitated MTs is blowing dust under desertification conditions attributed to changes in climatic patterns which could further be entrenched in arid regions (Hattingh and Van Deventer, 2004). Dust generation is a problem in drier climates and typically where the TFs are exposed.

## **2.10 Metalliferous solid waste management**

The MSW should be subjected to extensive testing such as mineralogy and geology characterisation and hydrogeological modelling. The suite of tests performed should include static tests such as acid-base accounting (ABA) (Yucel and Baba, 2016) and kinetic testing, such as

HCTs. All these tests have been used in various scientific exercises and MSW management planning Decision 2009/337/EC (European Commission, 2009).

### **2.11 Rehabilitation and restoration strategies**

Mining industries in many countries are required to follow environmental and rehabilitation standards to ensure the area mined is rehabilitated closely to its original state. This is due to cumulative quantities of MSW produced annually. Environmental and communal issues associated with the disposal of such waste on pristine land, mining companies are in search of alternative techniques of MSW disposal even for repurposing (Hudson-Edwards and Dold, 2015). The restoration efforts of the CMM, however, remains mostly ineffective since vegetation that was planted could not withstand post-mining activities due to the severely deteriorated hydrogeochemical soil qualities. However, it is anticipated that enhanced knowledge on growing conditions and selection of suitable plant species could contribute to the improvement of a phytoremediation rehabilitation strategy for a low-cost and maintainable restoration programme of the CMMs (Helsen *et al.*, 2009). Furthermore, this will have a direct usefulness to the areas such as O’Kiep that are similarly affected by the existence of PTEs in the environment. This indicates that rehabilitation and treatment might be costly in the long term as further and localised environmental deterioration advances itself when rehabilitation is neglected.

As a result, the recent two decades have witnessed a global surge in research on post-mining landscape restoration, yielding a suite of techniques, including phytoremediation (Festin *et al.*, 2019). The rehabilitation schemes proposed are required for the restoration of ecological indicators of mine sites and to reduce human health exposure to minimise risks (Ali *et al.*, 2019). Such remediation strategies would thus reduce acid-producing constituents in MSW (Tayebi-Khorami *et al.*, 2019). However, restoration of MSW and contaminated soil through vegetation growth is a favourable, eco-friendly and cost-effective technology for long term directed site rehabilitation (Petrisor *et al.*, 2004).

The rehabilitation of mine sites can be very complex due to a variety of PTEs and soil quality which might influence the remediation scheme (Bruneel *et al.*, 2019). Other studies propose microorganisms which can play a role in the biogeochemical phases of the soil in order to control PTE behaviour in contaminated environments. However, certain microorganisms can accelerate the oxidation and dissolution of (di-)sulfide minerals, leading to the formation of ARD (Bruneel *et al.*, 2019). Generally, different biological strategies have been explored for the elimination of PTEs and remediation systems even for ARD. These include the use of algae, fungi, bacteria and wild yeast in passive treatment technologies (Ali *et al.*, 2019). According to Bruneel *et al.* (2019), few studies reporting on CMMs have been conducted in sub-Saharan African countries including

South Africa. However, no remediation studies have been conducted in O’Kiep to address even the microbiological treatment of the open pit groundwater let alone the surrounding environment.

Mine waste storage areas need to be constructed and protected in such a way that their adverse effects on human health and the natural environment are minimised in the long-term (Vallero and Blight, 2019). Only a few studies have been reported in South Africa that explore the restoration, remediation and rehabilitation practices areas after mining disturbance. According to Claveria *et al.* (2019), high concentrations of As and Cu, and their cumulative behaviour in nature could be considered as a reason enough for site remediation of metalliferous soils to reduce these PTEs influence on the mine site, using suitable post-mining rehabilitation schemes. The TSF in O’Kiep could be safely cordoned off, and an ARD canal could be erected around the TSF with a settling pond which can be interlinked to a passive treatment system. Furthermore, the place should be enclosed in order to prevent children and people of the nearby community from entering the site which is not the case currently. A similar remediation strategy was recommended by Křibek *et al.* (2019) in the study of environmental impacts and remediation measures in Zambia’s Kabwe Pb-Zn smelter. MTs have been re-used and recycled as backfill post, extraction of minerals repurposed and used in the production of bricks (Kuhn and Meima, 2019).

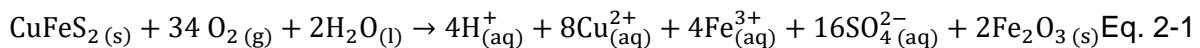
Within the last decade, research into challenges of revegetation of TSF has expanded considerably especially in CMM; therefore, reducing environmental damage including landscape modification with the vegetation regrowing and the burden of contamination on the food chain being reduced, will result in a reduced threat to human health. Where plants are to be used for restoration and rehabilitation of CMM’s, the plants can be genetically adapted to metal-enriched soils (Bini *et al.*, 2014), either through directed evolution and the use of advanced molecular biology techniques.

## **2.12 Characteristics of acidic rock drainage**

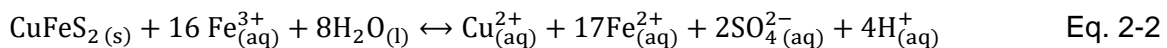
The oxidation of sulfide minerals usually causes ARD and it is generally defined as the flow of contaminated water usually from CMMs and MSW. This may include runoff at the surface, sometimes in considerable quantities (Cobbing, 2008; Adler and Rascher, 2007). The impact of ARD has been identified in the study area by the Council of Geoscience of South Africa during an investigation and the inspection of closed mines in the OCD as reported by the expert team of the Inter-Ministerial Committee, namely Ramontja *et al.* (2011) and Coetzee *et al.* (2010). These mines appear to have an impact on the local communities and surrounding areas, although possible long-term effects are unknown. Several mining countries such as Australia, Canada and the USA have encountered similar ecological and environmental challenges (Naidoo, 2017). ARD remediation is costly and poses a significant risk to natural resources due to its environmental impact (Ochieng *et al.*, 2010). The effects are noticeable in groundwater, including surface water

resources long after mining activities ceased (Naidoo, 2017; Coetzee *et al.*, 2010; Younger and Robins, 2002).

The significant indicator of ARD is the manifestation of sulfide gas and minerals that are in air and water. The formation of sulfide minerals is catalysed by microbial activity under satisfactory conditions such as excess of O<sub>2</sub>, pH, and nutrient availability. The main processes facilitating drainage chemistry from sulfide geological material are oxidation of sulfide-mineral deposits and subsequent transportation of PTEs by leaching. Oxidation changes Cu, Fe and S into ions such as Cu<sup>2+</sup>, Fe<sup>3+</sup>, and SO<sub>4</sub><sup>2-</sup>; sulfidic mineral such as chalcopyrite (CuFeS<sub>2</sub>); iron hydroxide (Fe(OH)<sub>3</sub>) and secondary minerals copper carbonate malachite (Cu<sub>2</sub>CO<sub>3</sub>(OH)<sub>2</sub>) (Price, 2009). Water soluble minerals can be transported to groundwater thus contaminating surface water whereby the water table is high, discharging toxic by-products and metals including the production of acid. Increasing acidity and lower pH raises the solubility of numerous PTEs of interest, including Cu (Price, 2009). Factors affecting the oxidation of CuFeS<sub>2</sub> are not as well investigated and reported compared to Fe sulfides, although high concentrations of Cu are potentially threatening to the overall health of the environment (Lottermoser, 2016). Acid produced from CuFeS<sub>2</sub> oxidation, Fe<sup>3+</sup> hydrolysis, and Fe<sup>2+</sup> oxidation is illustrated in Eq. 2-1.

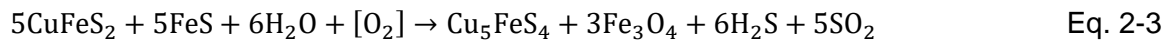


Anaerobic oxidation of CuFeS<sub>2</sub> to Fe<sup>3+</sup> also results in the reduction of pH as described in a reversible reaction. Thus oxygen consumption (Eq. 2-1), can also affect aquatic life due to oxygen depletion and microorganisms, Eq. 2-2 (Thurston *et al.*, 2010).



Under aerobic environment, microbial influences upon oxidation-reduction were investigated and evaluated by Thurston *et al.* (2010); whereby the reduction in pH was noticed immediately in the presence of *Acidithiobacillus ferrooxidans* when compared to abiotic controls cultures. CuFeS<sub>2</sub> dissolution is also exploited by high oxidant concentrations, high temperatures, and strong oxidants. In environmental trials, minerals were observed to react by forming product layers of jarosite and sulfur. The density and thickness of these layers can act as barriers that cause the dissolution rate to be controlled by the rate of diffusive transport of reactants to or away from the chalcopyrite surface (Kimball *et al.*, 2010). The factors affecting the sulfide oxidation of arsenopyrite, pyrite, and pyrrhotite have been well studied and investigated. However, the factors influencing the oxidation of chalcopyrite are not well characterised (Lottermoser, 2016).

O’Kiep ores have been studied, and none have been completely and satisfactorily described in terms of characteristics based on the rare sulfide assemblage (Maier *et al.*, 2012). Recommendations were made that the ores formed by metamorphic oxidation and desulfurisation of a primary magmatic sulfide assemblage are derived from mantle basalt dominated by pyrrhotite and chalcopyrite, in comparison to an assemblage consisting of bornite which is dominated by chalcopyrite and pure magnetite; for such ores the dominant reaction is as shown in Eq. 2-3.



The reaction explains as to what processes might occur in the CMM where the abundance of bornite and magnetite is prevalent as is in most Cu-rich ores. Similarly, Cu-rich ores in other metamorphic terrains are also characterised by rich bornite and magnetite (Maier and Barnes, 1999). However, according to Maier *et al.* (2012), the oxidation of  $\text{CuFeS}_2$  provides no clarification for the high Cu and Ni ratios of the O’Kiep ores. Therefore, an additional or alternative mechanism is required to describe the oxidation of ores in the selected study area.

Cu occurs naturally in a diversity of mineral deposits, of which chalcopyrite (sulfide) is the most common (Dudka and Adriano, 1997). Cu deposits are mostly excavated in open pits; these operations tend to produce massive quantities of MTs and SMW. Open-pit Cu mines are seldom rehabilitated after mine closure. Cu-sulfide tailings from ore beneficiation amount to approximately 98% of the ore volume and are disposed of in SMW (Barney, 1980). In the study of environmental management of dredged material and MTs, Salomons and Forstner (2012), identified four categories of beneficiation and mining process waste streams are ARD, dump heap leach, MTs, and SMW. Modern mines are rehabilitated to meet the legislative requirements of most countries with the treatment of MSW being the main focus of such rehabilitation. However, open-pit Cu mines are not often re-graded and revegetated; and these mines are rich in metals that are a source of ARD. Dudka and Adriano (1997), also concluded that Cu mining has a negative impact on the environment as it produces significantly large quantities of MSW. Locally, ARD is largely associated with coal and gold mining operations which currently affects the water quality of the Olifants and Vaal River systems (McCarthy, 2011). However, these cannot be the only areas in the country affected by ARD, with local conditions being hypothesised to facilitate ARD associated with the Cu bearing mineral deposits. The impact of ARD is reliant on local conditions such as climate, geomorphology, and transportation of the ARD. To appreciate the effect of ARD in South Africa, it is therefore essential to consider these factors (McCarthy, 2011).

### 2.13 Acid rock drainage formation and groundwater contamination

South African government's wastewater management regulations are essential in contributing to the management of ARD in the mining industry. This challenge of ARD formation has featured substantially both in national and international scientific reports (Feris and Kotzé, 2014). In South Africa, ARD became a matter of concern in 2002, when the West Rand Basin was flooded with 20 million litres of ARD (DWAF, 2008). In a recent ARD study, Naidoo (2017) reported that ARD is also a concern in countries such as Australia, Canada, the USA and Germany. South Africa's ARD contamination challenges were observed nationwide in: 1) Mpumalanga and KwaZulu-Natal's coal fields, 2) Witwatersrand goldfields, and 3) the O'Kiep copper fields (Rozendaal and Horn, 2013), but natural attenuation increased the pH values to circumneutral in several areas. One main environmental and health concern was the initially vast production of ARD, in the city of Johannesburg, which the Department of Water Affairs (DWA) estimating that at up to 92 million litres per day are produced. ARD mobilises PTEs in the environment and contaminates surface water supplies (Olalde, 2016). ARD can represent a complex challenge due to the MSW oxidation state (Elghali *et al.*, 2019). The TSF in O'Kiep also has a potential of generating ARD during the wet season (Figure 2-7), which can leach into soils with secondary potential groundwater contamination.



**Figure 2-7: Leachates from metalliferous storage facility in O'Kiep**

Furthermore, conventional wastewater treatment methods using chemical agents were determined not to be appropriate for all cases of ARD treatment. There are on-going research activities associated with ARD from Cu mining. Although O'Kiep was identified by the Inter-Ministerial Committee on mine water management in South Africa as a lower priority area, further assessment and monitoring is required at this stage as evidenced by leachates from the TSF.

## 2.14 Overview of challenges associated with closed metalliferous mines

The chronology of challenges associated with CMMs are illustrated in Figure 2-8. There is still a concern with both the detrimental health effects and environmental impacts of suboptimal management of waste and increasing contamination in O’Kiep.

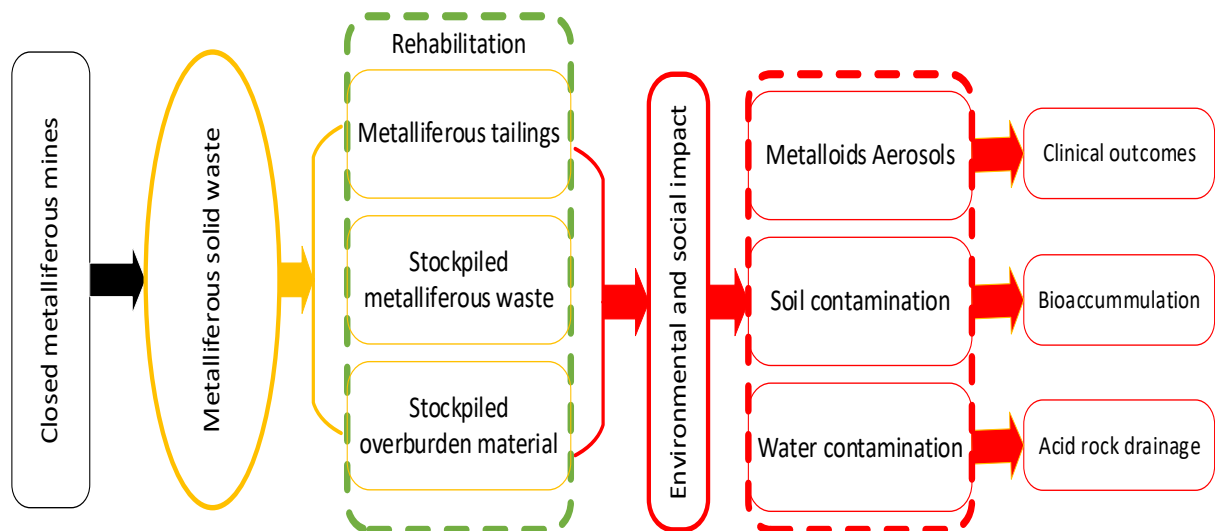


**Figure 2-8: Overview of challenges associated with closed metalliferous mining**

CMMs generate a large quantity of waste in the form of aerosols, liquids and solids. Numerous of these wastes are potentially hazardous to the environment and are dangerous to living organisms, including human beings. The MSW generated comprises of PTEs, and only 0.4% is discharged with ARD, and 0.007% of mining waste takes the form of air emissions; referred to as aerosols (Makgae, 2011). Cases of inadequate mine waste management practice are amongst the most noticeable features of the world-wide CMMs. Mining waste in the form of SOM, SMW, MTs, from unrehabilitated CMMs under suitable circumstances can result in direct discharges into waterways that can result in long-term environmental and social consequences. There is enough evidence that improper disposal of these wastes may cause contamination of air, groundwater, surface water, soils and bioaccumulation in the wildlife. There is a need for comprehensive long-term strategies for transforming the area of O’Kiep to move toward a zero-contaminant environmental footprint. As PTEs are persistent in the environment (Makgae, 2011). In line with international standards, local authorities and society are encouraged to seek rehabilitation strategies whereby MSW can be recycled and reduced. According to Adler *et al.* (2007) negative externalities associated with CMMs were not internationalised; as a result, the mining industry failed to prepare for closure adequately and to dispose of MSW in a manner that is in line with current global best practice. In particular, cumulative harm to the population within the vicinity of the mine, resulted in modified water tables during the rainy season, culminating in contaminated groundwater sources, ARD formation and aquifer instability. All these challenges must be

addressed before they cause even more devastating socio-economic and environmental consequences.

### **2.15 Summary**

The CMMs and MSW in general, need environmental health and safety assessments. Additionally, MSW are potential sources of PTEs and were identified as a greater threat to the communities surrounding mining sites. Accumulation of high concentrations of PTEs in areas associated with Cu mining can cause human health risks and environmental challenges. It is essential to determine the firmness of MSW heaps as well as their potential failure during the wet season to ensure implementation of mitigation strategies to minimise contamination. To reduce the mining footprint and effects as well as to limit population exposure to harmful MSW, access to MSW may be advisable with its redistribution to environmentally acceptable sites while other treatment strategies plans are being developed to resolve the present contamination. This strategy can provide an immediate relief in rehabilitation challenges in sites such as O’Kiep. Also, SMW treatment is needed to prevent additional oxidation of sulfide minerals by air and moisture contact which could further result in the release of PTEs into groundwater bodies and their deposition as aerosols in pristine areas further away from the mining site. Therefore, there is a need for appropriate remedial procedures to initially determine the properties of all waste generating metalliferous dust in order to also reduce its negative effects, with further environmental assessments and clinical outcomes being monitored on individuals living in the vicinity of the CMM and MSW being of paramount importance.

## CHAPTER 3: RESULTS AND DISCUSSION

---

Published as:

- 1]. **Erdogan, I.G.**, Fosso-Kankeu, E., Ntwampe, S.K.O., Waanders, F.B., Hoth, N., Rand, A. and Farrar, T.J., 2019. Households water quality in O’Kiep-South Africa and community perception of related health risks. *Desalination and Water Treatment*, 167,145-155.

DOI: 10.5004/dwt.2019.24576.

Data article (supplementary data of the above-mentioned article)

- 2]. **Erdogan, I.G.**, Mekuto, L., Ntwampe, S.K., Fosso-Kankeu, E. and Waanders, F.B., 2019. Metagenomic profiling dataset of bacterial communities of a drinking water supply system (DWSS) in the arid Namaqualand region, South Africa: Source (lower Orange River) to point-of-use (O’Kiep). *Data in Brief*, 25,104135.

DOI: 10.1016/j.dib.2019.104135 (Supplementary file: S1).

---

### **3.1 Households water quality in O’Kiep-South Africa and community perception of related health risks**

#### **3.2 Introduction**

Drinking water supply and use in some areas of South Africa is generally unsustainable, with a multitude of communities without access to consistent water supply for drinking purposes (Swartz, 2009). Access to adequate water is a human basic right (Constitution of the Republic South Africa, Act 108 of 1996). The National Water Act 36 of 1998 identifies drinking water as a scarce and an unequally supplied resource nationally that must be made available to all communities of the republic (Weaver *et al.*, 2017). Currently, there is a multitude of communities in the country without access to consistent water supply for drinking purposes (Swartz, 2009), including O’Kiep.

Generally in South Africa, drinking water from surface water is collected and distributed through a public drinking water supply system (DWSS) that may be supplemented by commercial bottled water and/or water tankers in the event of worsening water quality and/or water shortages for communities with poor infrastructure (Constantine *et al.*, 2017; WHO and UNICEF, 2006). However, water supply through the DWSS remains problematic in some areas (Rietveld *et al.*, 2009). The maintenance of the DWSS varies from urban systems where maintenance is of good quality, but services a minor portion of the population. In O’Kiep infrastructure is inadequate, with people having to rely on other sources such as bottled/purchased and water from tankers of drinking water. There are many problems associated with such DWSS, which are often related to microbial and inadequate treatment methods (Regan *et al.*, 2003). Biofilm growth (Camper, 2004) and microbially mediated corrosion (Beech and Sunner, 2004), and the proliferation of cyanobacteria in reservoirs are identified as contributing to contamination and disease outbreaks (Walls *et al.*, 2018). Therefore, adequate control measures for contaminants within the local DWSS are often achieved through disinfectants to limit waterborne diseases (Berry *et al.*, 2006). The production of drinkable water which meets defined quality guidelines (SANS241-1, 2015; WHO, 2011); does not guarantee suitable drinking water quality for the end-user due to maintenance problems and interruptions in the DWSS (Niquette *et al.*, 2001). Overall, the majority of water health related problems are associated with microbial contamination (WHO, 2004), with bacterial and algal contamination contributing largely to the degradation of drinking water quality even in the presence of a disinfectant (Zhou *et al.*, 2017). According to the WHO (2011), some of the important parameters to be monitored within the DWSS are pH, turbidity and toxins. It is essential for water utilities to provide aesthetically satisfactory drinking water as end-users always initially judge the quality of the water by its odour, colour and taste. The confidence in the quality

of a community's drinking water supply has in fact dropped by 8% since 2012 in South Africa (Rademeyer, 2013), an indication of numerous problems associated with the supply of drinking water to households (Galaiti *et al.*, 2016).

In South Africa, the monitoring and management of drinking water quality is governed by legislation and by-laws based on international standards and best practice. Municipalities or water service authorities and agencies are therefore required to periodically submit information concerning water quality status and to implement management strategies. Additionally, one of the critical aspects of water management is the monitoring of microbial prevalence in drinking water. Programmes such as the Green Drop Certification Programme, which is a National Water Quality Monitoring system especially for the management of sewage water treatment plants and the Blue Drop Certification Programmes for drinking water quality monitoring were introduced by the DWA to encourage best practices (Adeleke and Bezuidenhout, 2011; Rivett *et al.*, 2013). Also, concerns grew about the quality of drinking water supplied to the residents of the Northern Cape Region (Ayoob and Gupta, 2006). According to a report (DWA, 2012), the Northern Cape provincial blue drop score (BDS) was 68.2%, as a result of inadequate measures for water safety planning. Furthermore, the Namakhoi Municipality BDS was reported as 63.47% in 2012 (DWA, 2012). The municipalities in the region were thus certified non-compliant, with a provincial average green drop score (GDS) of 33%. As a result, these municipalities were placed under regulatory surveillance, in accordance to the Water Services Act (108 Of 1997) Sections 62 and 63 (DWA, 2013).

O'Kiep is vulnerable due to its arid environmental conditions such as high temperatures in summer (37°C), and the population relying only in groundwater as an alternative water source for future use. Furthermore, a lack of adequate DWSS has either hindered or increased the burden on other basic services such as health services in O'Kiep, with water related diseases being identified as possible human health threat due to an infrequent and possibly contaminated water supply. Other infrastructural irregularities include, but are not limited to burst pipes, an indication of poor maintenance of the drinking water supply in this community. The O'Kiep area was therefore selected for this study because of its arid environmental conditions, water scarcity, infrastructural inadequacies and population density.

### **3.3 Objectives**

The objectives for this part of the study were:

- to determine the quality of drinking water supplied to the community of O'Kiep;
- to identify possible related human health risks; and
- to use statistical models for prediction of health symptoms.

### **3.4 Materials and methods**

#### **3.4.1 Study area and population**

O’Kiep is located in the Northern Cape, South Africa [29°35’45”S 17°52’51”E], and has a geographical coverage of 38.63 km<sup>2</sup> (see Figure 3-1). Copper deposits were discovered in O’Kiep as early as 1862 and in the 1870s it was ranked the richest copper mining district in the world (Erasmus, 2004). According to the Nama Khoi local Municipality integrated work plan (2018/2019), the population size of O’Kiep was around 6300 at the time of the 2011 census and has remained stagnant or even decreased slightly since then. Applying the average South African household size of 3.3 persons per household (ArcGIS, 2017), a sampled population size of roughly N = 1900 households was established.

#### **3.4.2 Background of drinking water supply system**

A Local Water Board Agent (LWBA) supplies O’Kiep with drinking water sourced from the lower Orange River. Subsequent to its treatment and supply to various towns via a DWSS to households, and also to agricultural and industrial areas, the water is chlorinated, which is the preferred disinfection method prior to distribution (DWA, 2009). In the unpublished report by the LWBA, the 419 mm steel pipeline with coupon lining was replaced in sections in 2005. The mortar lining pipeline needs replacement as in many places it has come loose and/ or water seeps between the mortar and the pipe wall causing corrosion. The pipeline has deteriorated to such a state that frequent pipe burst occur and the supply to nearby towns is constantly interrupted, including O’Kiep.

#### **3.4.3 Data collection methods**

This research study was designed during April 2017 and samples collected from Tuesday to Friday as per the availability of the personnel. During this period, drinking water samples were collected from the source (n = 3), namely lower Orange River, a Local Water Supply Agency reservoir (LWSA) and a Municipal Reservoir (MWR). For point-of-use (POU) (n = 50): households (questionnaires) and water samples were collected from household taps. A total of fifty-three (n = 53) water samples were collected from source to POU (tap water) in each household when identified as the primary source of drinking water by at least one individual. Figure 3-1 shows the location of the study area and sampling points.

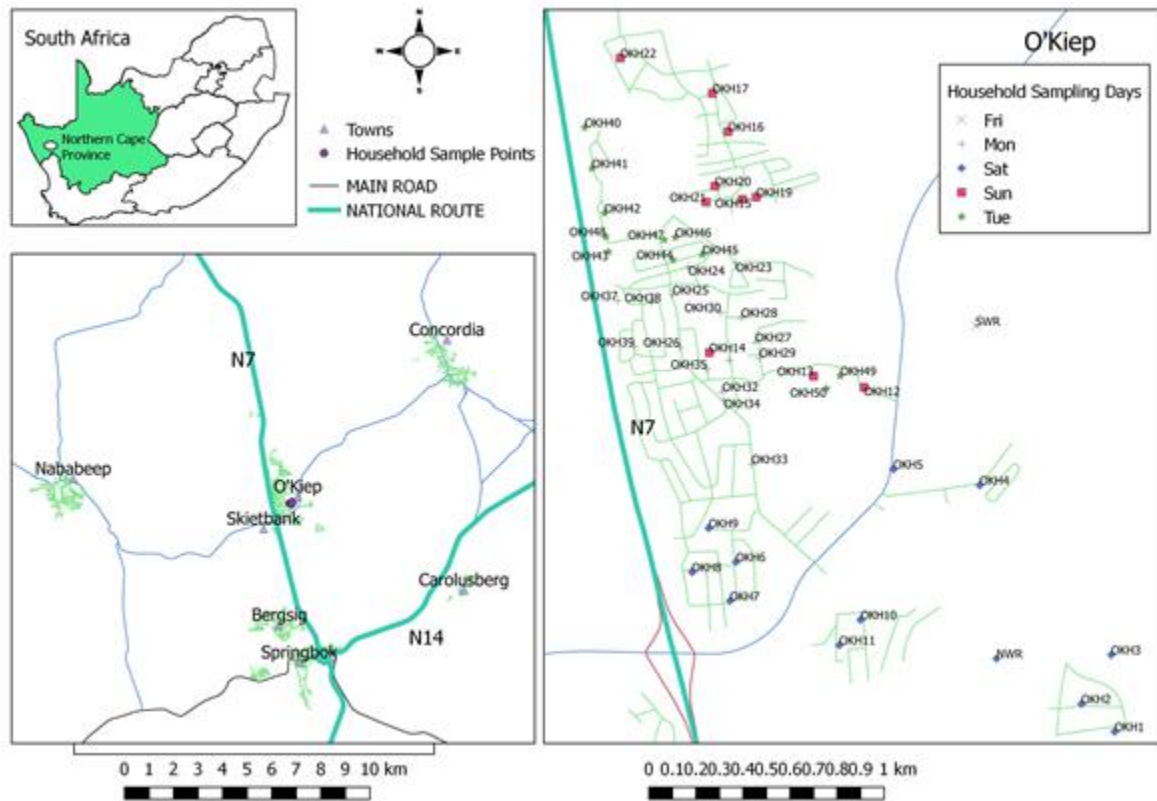


**Figure 3-1: Study area and sampling points: Geological maps were generated using Quantum GIS software (v. 2.18.11) and data from National Geo-Spatial Information (NGI), a component of the Department of Rural Development and Land Reform, South Africa**

Prior to the administration of the questionnaire discussed below, and the collection of drinking water samples, permission was sought and granted by the Nama Khoi Municipality. Invasive human procedures such as medical examinations were not considered as part of the study. A structured questionnaire was used, consisting of both closed and open-ended questions. It had four sections: demographic information, drinking water, health-related questions, and water exposure history. The questionnaire was based on WHO and UNICEF (2006) water hygiene guidelines. A skilled local interpreter, with considerable fluency in the various languages (Afrikaans, Xhosa and English) mainly used by the community, administered the questionnaires by means of face-to-face interviews. Individuals in each household were selected to respond to the questionnaire, with some households identifying a proxy to do so on their behalf. A sample size of  $n = 50$  households was used. Purposive sampling was adopted from Saladi and Salehe (2017) used due to the low response rate: numerous people when approached at their household declined to participate in the study. The refusal by some households to participate in the study, made a pure probability sampling approach unfeasible. The interviewees selected were  $>55$  yrs of age, generally people responsible for the management of drinking water in each household. Participants ( $n = 50$ ) agreed to undertake the survey with a household response rate of 100%. The majority of the respondents (66%) had lived in O'Kiep for a lifetime. The number of males

(56%) was slightly higher than females (44%). The ethnicity distribution of the sample roughly fit the demographic profile of O’Kiep from the 2011 census, although self-identifying persons of colour were underrepresented in the sample (74% vs. 95% in the population).

#### **3.4.4 Water sampling and quality parameter quantification**

In the questionnaire, drinking water was defined as water obtained from the tap without additional treatment. All instruments were calibrated prior to sampling, as advocated by Gibs and Wilde (2020). Polypropylene sample bottles (500 mL) were thoroughly washed using soapy water and rinsed with dilute hydrochloric acid (0.5 M), followed by a final rinse with sterilised deionised water. The bottles were dried and stored with the caps on to prevent contamination prior to sample collection. The bottles were also rinsed with sample water before sampling and immediately after sampling, and the following physical determinants were quantified in the morning between 7am and 11am: dissolved oxygen (DO), pH, temperature, electrical conductivity (EC), salinity, redox potential (Eh), and total dissolved solids (TDS). Most of these determinants were measured on-site using an EXSTIK II® EC500 probe, while the DO was measured using an EXSTIK II® CA895 probe, both instruments were supplied by Extech Instruments, U.S.A. To ensure consistency, these probes were calibrated daily using appropriate standards while a 1413 mS standard was used to verify the calibration for EC. The DO readings were taken first for every sampling point to avoid atmospheric influences (Sundaram *et al.*, 2009; Weaver *et al.*, 2007). All samples were handled according to the guidelines used for drinking water quality quantification (WHO, 2011). Immediately after field analyses, samples were placed in an insulated box filled with ice and then transported to the laboratory where there were further analysed for turbidity, anions, cations and dissolved organic carbon. Analyses were performed using an inductively coupled plasma instrument coupled either with an optical emission spectrometer (ICP-OES), or a mass spectrometer (ICP-MS) (Agilent Technologies, USA), high-performance liquid chromatography (HPLC) Thermo Fisher Scientific, USA). and a UV-Vis spectrophotometer (Thermo Fisher Scientific, USA). Subsequently, with confirmatory analyses being conducted at an external laboratory accredited by the South African National Accreditation System (SANAS).

#### **3.4.5 Cyanobacterial toxin analysis**

Samples were further screened for algal toxins on-site using ABRA-520017 test strips which are used for finished drinking water, with a lower detection limit of 0.5 µg/L (WHO, 1998). This method is used for monitoring and quantification of algal toxins in drinking water in South Africa (Swanepoel *et al.*, 2008), and is also used by the City of Cape Town as a primary screening test for finished drinking water.

### 3.5 Results and discussion

#### 3.6 Results

The frequencies of the results obtained from the questionnaire are evident in Supplementary Table (Annexure C). The identified primary sources of drinkable water were household taps (90%) while a minute proportion (10%) was attributed to purchase bottled water, which is indicative of the reliance on tap water. Some respondents indicated that they were dependent on water tankers as a source of water during interruptions. All the participants reported water shortages at least once a week, with an average water shortage period between 1 and 2 days (20%). Furthermore, participants (86%) reported an unpleasant smell emanating from the tap water, with a salty taste (100%) being identified as one of the predominant problems associated with the water. The majority of the participants (88%) stated that the perceived quality of the tap water was indicative of its unsuitability for drinking and concerned that they might become ill from consuming water directly from the tap without additional treatment, a problem mitigated by either boiling (64%) or adding bleach (36%) prior to storage. Participants (81%) were convinced that the quality of the water could affect their health status. Furthermore, respondents reported diarrhoea-like effects subsequent to drinking the tap water, attributing the effects directly to the quality of the water supplied, with 72% reporting periodic discolouration of their teeth over a lifetime and the (POU) tap water measured  $F^-$  concentration was up to 0.17 mg/L.

##### 3.6.1 Statistical analyses

Basic statistical hypothesis tests such as  $t$ -tests and Wilcoxon signed-rank test, adopted from Luby *et al.* (2018) and Lothrop *et al.* (2018), were used to determine the relationship between the household questionnaires and drinking water physicochemical parameters. For each physicochemical determinant for which a (SANS241-1, 2015) upper limit was available ( $F^-$ ,  $Na^+$ ,  $Mg$ ,  $Cl^-$ ,  $SO_4^{2-}$ ,  $Zn$ , turbidity, EC), a one-sample  $t$ -test was used to test the null hypothesis that the mean household value is below the (SANS241-1, 2015) upper limit (i.e., for the  $j$ th parameter,  $H_0: \mu_j \leq s_j$ ) against the alternative that the mean household value is above the (SANS241-1, 2015) upper limit (i.e., for the  $j$ th parameter,  $H_A: \mu_j > s_j$ ). The  $t$ -test could not be used for two parameters ( $Al^{3+}$  and  $Cu$ ) for which the data contained interval-censored values that were below the minimum detectable amount of the equipment ( $< 0.05$  for  $Al^{3+}$  and  $< 0.01$  for  $Cu$ ). For these two elements, the Wilcoxon signed-rank test—a nonparametric method—was implemented with the interval-censored values considered to be tied at the lowest rank. Among all the parameters that were tested, there were two cases for which the null hypothesis was rejected at 5% significance level:  $SO_4^{2-}$  ( $p$ -value =  $2.870 \times 10^{-3}$ ) and EC ( $p$ -value =  $8.395 \times 10^{-133}$ ). This indicates that the average level of  $SO_4^{2-}$ , and average EC level in POU water in O’Kiep households is above the recommended upper limit of (SANS241-1, 2015).

**3.6.2 Logistic regression models**

Logistic regression model adopted from Cox and Snell (1989) was used to assess possible relationships between health and other indicators from the household questionnaire, on the one hand, and chemical and physical properties of household water samples, on the other. The indicators fit to logistic regression models as the binary dependent variable were, respectively, “Does anyone in the family suffer from pain or tiredness?” (Yes/No), “Have you been sick from the water you drank?” (Yes/No), “How does the water smell?” (Unpleasant Smell/No Smell), “When you brush your teeth have you noticed bleeding gums?” (Yes/No), and “Have you noticed discolouration of your teeth in the past?” (Yes/No). The logistic regression model did suggest a statistically significant relationship between two physical parameters and the smell of the water. For every unit increase in DO, the odds of an unpleasant smell being reported by that household increased by a factor of 12.391 (significance *p*-value: 0.0186). For every unit increase in pH, the odds of an unpleasant smell being reported by that household increased by a factor of 260.083 (significance *p*-value: 0.0266). It is difficult to say whether this empirical relationship is spurious or real.

**3.6.3 Questionnaire two-way frequency analysis**

A few statistically significant relationships between categorical variables from the questionnaire were identified using the Pearson chi-squared test (De Miranda *et al.*, 2018) of independence (see Tables 3-1 to 3-3).

**Table 3-1: Chi-squared test *p*-value: 8.389x10<sup>-3</sup>**

Use of tankers for water during Interruptions		
Bleaching	No	Yes
No	5	27
Yes	10	8

Interpretation: Those who do not use water from tankers during interruptions in water service are more likely to use bleaching to improve water quality than those who do use water from tankers during water service interruptions.

**Table 3-2: Chi-squared test  $p$ -value:  $2.885 \times 10^{-4}$**

Use of storage tanks for water during Interruptions		
Bleaching	No	Yes
No	28	4
Yes	6	12

Interpretation: Those who *do* use water from storage tanks during interruptions in water service are more likely to use bleaching to improve water quality than those who do *not* use water from storage tanks during water service interruptions.

**Table 3-3: Chi-squared test  $p$ -value:  $8.389 \times 10^{-3}$**

Purchase of water during interruptions		
Bleaching	No	Yes
No	27	5
Yes	8	10

Interpretation: Those who *do* purchase water during interruptions in water service are more likely to use bleaching to improve water quality than those who do *not* purchase water during water service interruptions.

Table 3-4 provides detailed information on the physicochemical water quality parameters quantified for each of the sampling points used in this study from the source to the POU (i.e. TW), the results of the analysis were further compared to drinking water guidelines (SANS241-1, 2015, WHO, 2011).

**Table 3-4: Physicochemical determinants compared to drinking water quality guidelines**

Determinants	Units	Source			POU: Tap Water			POU (Tap Water)	Drinking water quality guidelines	
		LOR	LWS A	MWR	Min	Max	Average	% of Households Above (SANS241-1, 2015)	(SANS241-1, 2015)	(WHO, 2011)
Colour	Pt-Co-true	<10	<10	2.9	<10	<10	<10	-	<15	-
Dissolved Oxygen (DO)	mg/L	2.3	3.4	581	0.5	2.9	2.0	-	-	5
Electrical Conductivity (EC)	mS/m	574	578	8.0	570	660	595	100%	≤170	100
pH	-	8.3	8.0	-40,8	7.6	8.9	8.3	0%	5-9,7	6,5-9,5
Redox	mV	-13,3	-26,8	288	-	-11.4	-45.5	-	-	-
Salinity	mg/L	284	288	25.0	277	326	293	-	-	-
Temperature	°C	28	29.3	405	21	35	28	-	-	-
Total Dissolved Solids (TDS)	mg/L	401	407	0.3	396	459	414	0%	≤1200	500
Turbidity	NTU	18.1	0.4	0.15	0.15	7.8	0.45	2%	≤5	-
Fluoride (F)	mg/L	0.16	0.15	38	0.12	0.17	0.15	0%	≤1,5	1.5
Calcium (Ca)	mg/L	38.3	38.5	191	36.9	40.9	38.2	-	-	-
Sodium (Na)	mg/L	158	136	18.5	99.5	228	159	14%	≤200	100
Magnesium (Mg)	mg/L	18.9	19.1	11.4	18.0	19.6	18.7	0%	400	-
Potassium (K)	mg/L	10.4	8.91	48	8.3	11.0	9.1	-	-	-
Chloride (Cl)	mg/L	43.6	49.4	679	42.4	51.4	47.1	0%	≤300	5
Sulfate (SO <sub>4</sub> <sup>2-</sup> )	mg/L	528	449	<0.16	314	867	557	64%	≤500	200
Ammonia (NH <sub>3</sub> )	mg/L	<0.16	<0.16	<1.1	<0.1	<0.16	<0.16	0%	≤1,5	-
Nitrate (N)	mg/L	<1.1	<1.1	<1.7	<1.1	<1.1	<1.1	-	-	-
Ortho-Phosphate (P)	mg/L	<1.7	<1.7	0.17	<1.7	<1.7	<1.7	-	-	0.4
Zinc (Zn)	mg/L	0.05	0.15	0.07	0.06	0.97	0.16	0%	≤5	2
Aluminium (Al <sup>3+</sup> )	mg/L	0.06	0.06	<0.01	0.05	0.12	0.06	0%	≤0,3	-
Arsenic (As)	mg/L	<0.01	<0.01	<0.01	<0.0	<0.01	<0.01	0%	≤0,01	0.01
Copper (Cu)	mg/L	<0.01	<0.01	<0.05	0.01	0.21	0.02	0%	≤2	1
Iron (Fe)	mg/L	<0.05	<0.05	<0.01	<0.0	<0.05	<0.05	0%	≤2	0.3
Manganese (Mn)	mg/L	<0.01	<0.01	4.0	<0.0	<0.01	<0.01	0%	≤0,4	0.05
Dissolved Organic Carbon	mg/L	6.1	3.6	4.0	2.0	5.0	3.7	-	-	-

### 3.6.4 Cyanobacterial toxin analysis

The results of toxin screening test strips for microcystins indicated the presence of toxins from the water source to the POU as indicated in Figure 3-2; (WHO, 1998) guidelines restrict cyanobacterial toxin level in drinking water to 1 µg/L for microcystin-LR. Furthermore, this was confirmed by various microorganisms present in the DWSS (see S1: Supplementary data). Therefore, long-term toxin exposure of the community in O’Kiep needs to be considered with regard to implementing appropriate remedial action. Currently, cyanobacterial toxins, especially microcystins, are treated with the addition of free chlorine for toxin oxidation, thus deactivation (Swanepoel *et al.*, 2008), while the O’Kiep community use bleach as a mitigation strategy for such toxins. The occurrence of microcystin in drinking water is generally unacceptable; most of the respondents criticised the quality and treatment processes used for the water.

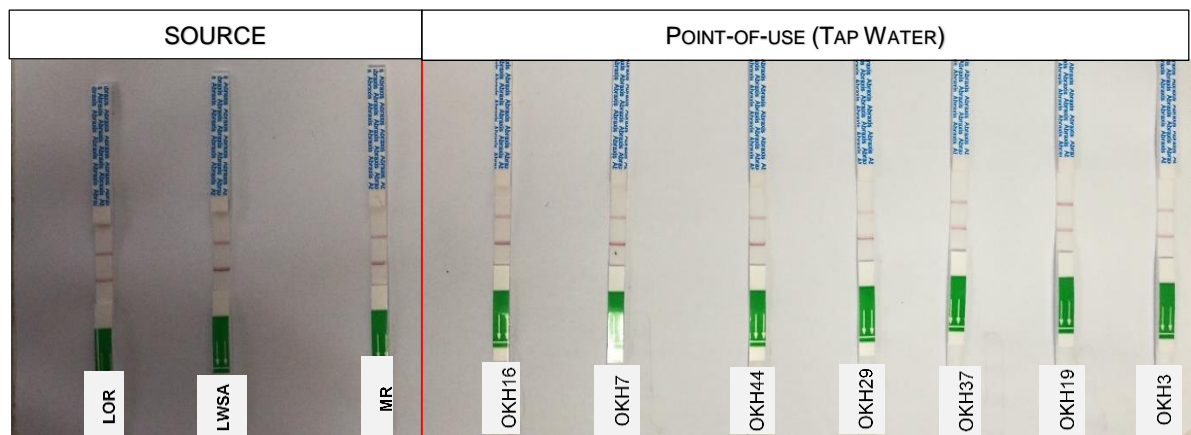


Figure 3-2: Dipsticks for screening of microcystins

### 3.7 Discussion

The physicochemical properties of drinking water from the DWSS in O’Kiep were assessed using pH, oxidation-reduction potential, aqueous ions, toxin screening and turbidity as the primary water quality parameters quantified, because they directly affect water quality. The lower Orange River samples’ quality was characterised by low Eh (-13.3 mV) and DO (2.3 mg/L) with a high average EC (574 mS/m) including  $\text{SO}_4^{2-}$  (528 mg/L), values deemed not within the drinking water guidelines set out in WHO (2011) and SANS241-1 (2015), while  $\text{Na}^+$ ,  $\text{Cl}^-$  and  $\text{PO}_4^{3-}$  were all within the drinking water guidelines set by the WHO (2011) averaging 158, 43.6, and 1.7 mg/L respectively. The turbidity (18.1 NTU) of the tap water was not within the SANS241-1 (2015) drinking water guidelines, as expected. It was observed that both  $\text{Na}^+$  and  $\text{Cl}^-$  increased when the water was stored in the municipal reservoir, with concentrations of 191 and 48 mg/L being observed respectively, while the Eh decreased to -40,8 mV (see Table 3-3). An increase in  $\text{Cl}^-$  was attributed to water chlorination prior to distribution to households. The source of  $\text{Na}^+$  is presumably contributed to the salty taste of the tap water. For observed increases in salinity,

DWSS corrosion scales can be triggered by sudden water chemistry changes, resulting in a bad taste of water which is deemed drinkable and as such the water might become odorous, which often leads to non-compliant water quality (Imran *et al.*, 2006). All the other determinants for the source water were within the drinking water standards recommended by both WHO (2011) and SANS241-1 (2015). The effect of source water quality on the deterioration of water quality parameters post treatment and within the DWSS is complex, with the mechanisms involved being especially unclear in O’Kiep.

The temperature of the tap water samples ranged from 21.2 to 35.4°C with the water temperature within the DWSS being affected by environmental temperature changes throughout the day. Thus, the DWSS might exhibit different corrosion behaviour in the morning when compared to the afternoon (McNeill and Edwards, 2002). The dissolved organic carbon (DOC) quantified as 3.7 mg/L in this study and a reduced redox potential (-11.4 to -69.5 mV) are related to the quantity of oxidisable constituents or trace elements in the water (Delpla *et al.*, 2009). The pH values (7.6 to 8.9) were not within the permissible limit set by SANS241-1 (2015) and WHO (2011), with the EC and salinity being in the range between 570 to 660 mS/m and 277 to 326 mg/L, respectively, as EC is largely influenced by salinity (Rotiroti *et al.*, 2017) and TDS (Ukpong *et al.*, 2017). The maximum TDS observed within the DWSS reached a maximum of 459 mg/L, which is within the prescribed drinking water guidelines by SANS241-1 (2015) and WHO (2011). However, the DO averaged 2.0 mg/L, which is lower than that required for drinking water (WHO, 2011). At higher temperatures, reduced DO suggests that microbial proliferation within DWSS is prevalent (McNeill and Edwards, 2002). Furthermore, the low DO could also be an indication of a high concentration of dissolved minerals in the water, as the salinity averaged 293 mg/L, conditions suitable for excessive algal growth in drinking water. Some researchers ascribe this to the chemical instability of Fe<sup>2+</sup> released from corroded iron pipes (Sarin *et al.*, 2004). However, quantified metals and their ions, namely Al, As, Cu, Fe, Mn, F, Mg and Zn, were all determined to be within SANS241-1 (2015) and WHO (2011) drinking water guidelines.

Although F<sup>-</sup> in the sampled drinking water was low, 72% of the respondents indicated discolouration of teeth. This was hypothesised to be due to a lifetime exposure to fluorine. According to WHO (2011), the optimum fluoride levels in drinking water should not exceed 1.5 mg/L, with higher concentrations being associated with human health complications, including teeth discoloration, decay, and neurological problems in severe cases (Chandrawat *et al.*, 2005; Das *et al.*, 2005; Ahmad *et al.*, 2005). Additionally, treated tap water should have a positive Eh (200 to 400 mV), depending on the locality of the source water and the treatment method being used (Goncharuk *et al.*, 2010). Samples from this research showed Eh of -11.4 to -69.5 mV with an average of -45.4 mV. The redox conditions within DWSS can widely vary under anoxic

conditions, particularly for disinfected drinking water, due to the existence of redox reactions; while tap water is largely a weak pro-oxidant, particularly where  $\text{Cl}^-$  concentrations are below an average of 47.1 mg/L (James *et al.*, 2004).

Characteristically, the anions also play an important role in the quality of drinking water, particularly when anions such as  $\text{SO}_4^{2-}$  are high (549 to 679 mg/L) at the POU. The intake of elevated concentrations of  $\text{SO}_4^{2-}$  through drinking contaminated water may cause health effects such as diarrhoea particularly to consumers not accustomed to drinking water with a high concentration of sulfates (WHO and UNICEF, 2015; Schutte, 2001). A large proportion of the respondents complained about diarrhoea subsequent to ingestion of tap water supplied, which might contain bacteria and this was confirmed by the presence of cyanobacteria in the DWSS (see S1). Generally, elevated concentrations of  $\text{SO}_4^{2-}$  are common in water in mining areas (Schutte, 2001), including when air exposed reservoirs are utilised for treated water storage. For water quality assessments, numerous standards for drinking water can be used, and most are categorised into two classifications, that is primary and secondary standards. Primary standards are based on health concerns and are intended to safeguard individuals from pathogens, radioactive elements and toxic pollutants including chemicals. Secondary standards are based on staining properties, taste, smell, colour and corrosivity, of which sulfates must not exceed a maximum of 250 mg/L (EPA, 2003), with higher concentrations being associated with microbial growth (Yang *et al.*, 2014) which further exacerbates water colour problems in a DWSS, such as the O’Kiep DWSS studied. Biofilms in the DWSS can also be influenced by water temperature, chlorine levels, organic compound concentrations and compositional characteristics of storage, and by DWSS pipe materials (Niquette *et al.*, 2001). *Thiobacteria* and sulfate-reducing bacteria (SRB) are also the main indicators of sulfurous compounds in DWSS with mycobacteria being associated with an earthy and musty odour (Zhou *et al.*, 2017; Dickschat *et al.*, 2007). Similarly, the DOC (3.7 mg/L) can have adverse aesthetic implications including water colour, odour and taste, although, concentrations up to 5 mg/L have minimal effects on human health in chlorinated water (SANS241-1, 2015). However, long-term high DOC exposure can have deleterious effects on human health; the supplied water in O’Kiep was reported in this study to have green (28%), brown (28%) and white (26%) tints.

### **3.8 Summary**

To address concerns such as diarrhoea-like symptoms and taste and colour associated to the drinking water supplied to O’Kiep by the local DWSS, it is paramount that effective treatment systems and distribution infrastructure are in place. Although, most of the drinking water quality indicators were deemed to be within the required quality guidelines as indicated by WHO (2011) and SANS241-1 (2015) some parameters were out of specification, in particular, DO, which was

below the recommended levels in all samples analysed. Temperature, DO, DOC, Eh, EC, TDS, Na, Cl<sup>-</sup>, and SO<sub>4</sub><sup>2-</sup> were the parameters contributing to low water quality in the study area. These factors are responsible for aesthetic qualities of the drinking water when out of specification, due to a lack of appropriate treatment systems. Further, contaminant seepage into the DWSS and an irregular water supply can contribute to the negative perception of the water quality supplied. The drinking water of the study area should thus be boiled or disinfected using bleach prior to consumption, as is currently the norm. There is also a need to develop cost-effective water testing capabilities within the region for daily monitoring of water quality, focusing on Eh, which must be measured at regular intervals as an indication of the effectiveness of the dose of chlorine used within the O’Kiep DWSS. None of the statistical models suggested physicochemical properties as predictors of any of the health symptoms. However, it must be remembered that each water sample represents a single point in time; one would need to assess the long-term water quality at the respective households to be able to identify relationships with health indicators. It is reasonable to conclude that DWSS vulnerability plays some role on POU drinking water quality, and that methods for improvement should be studied. The study has further revealed high concentration of EC, salinity, TDS and SO<sub>4</sub><sup>2-</sup> from source to POU. This means that it will be likely in future to better understand the sources of these elements in the DWSS for the betterment of drinking water quality. The long-term exposure of the community to microcystins must be considered with regard to implementing appropriate remedial action. Furthermore, biofilm growth and microbially mediated corrosion and the proliferation of cyanobacteria in the DWSS studied needs further investigation in O’Kiep. From this, it was deduced that a feasible way for water security in O’Kiep might be groundwater resources, as an alternative source to irregular surface water in the O’Kiep area – see Chapter 4.

## CHAPTER 4: RESULTS AND DISCUSSION

---

Published as:

**Erdogan, I.G.**, Fosso-Kankeu, E., Ntwampe, S.K.O., Waanders, F.B., Hoth, N. and Rand, A., 2019. Groundwater as an alternative source to irregular surface water in the O'Kiep area, Namaqualand, South Africa. *Physics and Chemistry of the Earth, Parts A/B/C*, 114, 102801.  
DOI: 0.1016/j.pce.2019.09.0.

#### **4.1 Groundwater as an alternative source to irregular surface water in the O’Kiep area, Namaqualand, South Africa**

Groundwater is often the preferred source for drinking water since it is acceptable to various communities as it is often free from odour. It is often considered to be the best alternative to tap water due to its natural protection from contamination when compared to surface water. It is perceived to be low in contamination due to its low turbidity (Edokpayi *et al.*, 2018). Despite the perceived safety associated with groundwater consumption, several researchers have shown that groundwater can also be susceptible to contamination (Chakraborti *et al.*, 2016; Indelicato *et al.*, 2017). Several factors that influence the groundwater quality index (GWQI) include the climate, geology of the aquifer and anthropogenic activities such as mining in the locality of the aquifer (Aslam *et al.*, 2018, Lee *et al.*, 2017). In the peri-urban and rural areas, most of the groundwater is usually untreated. It has been reported that it is difficult for groundwater to purify itself to acceptable standards and is very expensive to treat (Edokpayi *et al.*, 2018).

Several studies have been published in Namaqualand regarding the area’s groundwater quality, with a high fluoride concentration being reported by Abiye *et al.* (2018) and Abiye and Leshomo (2013). These studies investigated the groundwater flow, its radioactivity and metal enrichment, which is contaminated with ARD. Additionally, ARD can persist more than 10 km from its source and might have an impact on groundwater bodies of neighbouring areas (Naicker *et al.*, 2003), further contributing to the challenges as it contains various types of PTEs such as Cd, Cu, Cr, Pb, Ni, F, As and Zn. These PTEs may accumulate in water bodies and could form critical long-term hazards for groundwater.

Négrei *et al.* (2007), indicated that the mixture of contaminant transference into groundwater up to the depth of 50 m underneath the surface, is feasible. A study conducted by Giri *et al.* (2017) also justified that 50% of the groundwater is highly contaminated with respect to PTEs such as Cu, Ni, Co, Cr, Mn and Pb in the vicinity of a copper mining area, which suggests a possible way for human exposure (Singh *et al.*, 2018), particularly whereby groundwater is an alternative source of drinking water. As a result, the use of groundwater sources of unknown quality puts the consumers at risk to possible waterborne diseases (Edokpayi *et al.*, 2018). These contaminants can enter the human body through various pathways such as inhalation and through skin absorption. Once they enter the human body, a majority of PTEs are adsorbed and bioaccumulate in the human body, culminating in the development of a range of illnesses due to long-term exposure (Avigliano and Schenone, 2015). O’Kiep is located in the Namaqualand area, which is characterised as being an arid environment whereby groundwater is the only alternative source of water supply for the community living there. Also, this former copper mining town has challenges with chronic water shortages. Therefore, groundwater resources offer an opportunity

to improve resilience against recurring droughts due to inadequate potable water supply and to mitigate general drinking water insecurity. Extensive mining of Cu-ore has left a legacy of contaminated mine waste heaps and mine tailings distributed throughout the copper mineral belt in the O’Kiep area. The hazards caused by MSW, especially the deterioration of groundwater quality in this area, can culminate in negative human health clinical outcomes.

## **4.2 Objectives**

The objectives for this part of the study were:

- to assess the quality of groundwater in O’Kiep; and
- to determine its suitability for domestic and irrigation purposes.

## **4.3 Materials and methods**

### **4.3.1 Geology and hydrogeology**

The primary copper bearing minerals are chalcopyrite ( $\text{CuFeS}_2$ ), chalcocite ( $\text{Cu}_2\text{S}$ ), bornite ( $\text{Cu}_5\text{FeS}_4$ ) and other minerals including biotite, plagioclase, quartz, and magnetite. The copper content of the Koperberg Suite in O’Kiep, is erratic, with embedded PTEs (Wulfse and Holdsworth, 1994; Stumpfl *et al.*, 1976). The geology of O’Kiep has also been described as comprising of intrusive rocks, consisting of a thick sheet of granite (Abiye and Leshomo, 2013; Clifford and Barton, 2012). In the study of granulite facies transition in the O’Kiep area by Raith and Meisel (2001), two types of metabasites were determined to be arising along the granulite amphibolite facies. The southern granulite facies of the O’Kiep includes Mg-rich ol-normative forms and low-MgO ores. The O’Kiep area is characterised by an arid to semi-arid climate which has direct impact on the effective recharge (Abiye and Leshomo, 2013), with groundwater occurring from a fractured, crystalline basement and an alluvial aquifer, which is efficiently recharged during the rainy season. The climate is further influenced by an altitude, topography and distance from the sea (Xu and Beekman, 2019; Adams *et al.*, 2004). The aquifer extent and distribution in the area is largely controlled by the tectonics, fracture frequency, distribution of alluvial sediments and weathering zones (Abiye and Leshomo, 2013). The thickness and characteristics of the composite aquifer varies from one site to another, particularly in relation to its petrographic composition of respective rocks, their type, including their tectonic deformations due to weathering effects and changing climatic conditions (Adams *et al.*, 2004).

### 4.3.2 Study area and data collection

Groundwater samples (n = 8) were collected in June 2018 during the winter season with minimal rainfall of approximately 2mm and with ambient temperatures averaging 6 °C (Accuweather, 2018). GPS coordinates were used to demarcate sampling sites as presented in Figure 4-1.

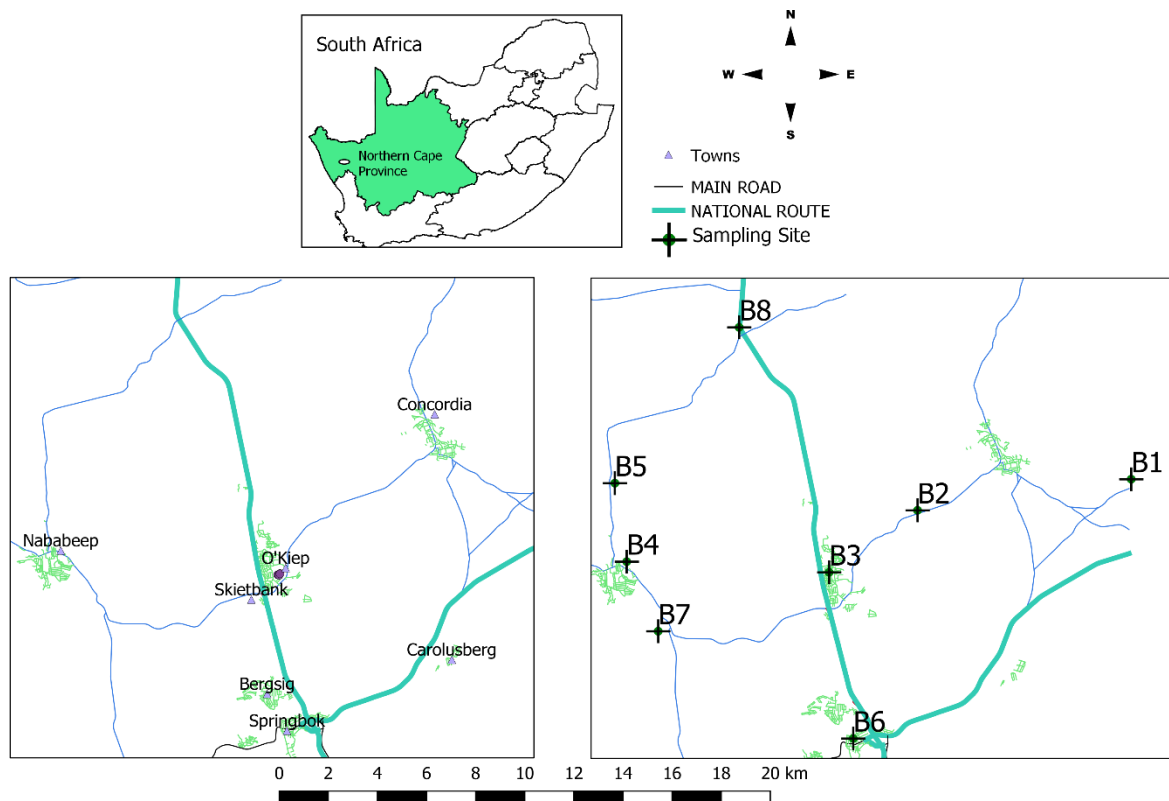


**Figure 4-1: Study area and sampling points: Geological maps were generated using Quantum GIS software (v. 2.18.11) and data from National Geo-Spatial Information (NGI), a component of the Department of Rural Development and Land Reform, South Africa**

Groundwater samples were collected according to the groundwater sampling guidelines as described by Nielsen and Nielsen (2006). The groundwater samples were collected near the well head of each of the boreholes. The boreholes in this study ranged from 30 to 150 mbgl in depth and pumping rate of approximately 0.5 L/s, which was also confirmed by Titus *et al.* (2002), with boreholes B1, B2, B3, B6 and B8 ranging between 13 and 25 km apart, while B5, B4 and B7 between 6 and 8 km apart. Moreover, B3 is the only borehole water situated at the school. Students and teachers use this borehole water during the infrequent supply of tap water, as highlighted in Chapter 3. The samples were collected after 15 min of pumping and a maximum of three samples were collected into sterile 1L schott Duran bottles per visit to minimise possible sample deterioration, which might affect the sampled groundwater chemistry. Multi-parameter instruments and sensors were calibrated prior to field measurements used according to national

field water measurement standards (Li and Migliaccio, 2010). Bottles were also rinsed with sample water prior to sampling.

During sampling, the following physical parameters were quantified on-site, namely temperature, pH, EC, redox potential and totally dissolved solids, using an EXSTIK II® EC500 to minimise atmospheric variations (Sundaram *et al.*, 2009; Weaver *et al.*, 2007). Samples were also filtered through a 0.45-µm pore-size cellulose membrane using a hand-vacuum pump into 1L Schott Duran bottles (APHA, 2005). The unfiltered samples were digested with technical grade nitric acid (0.2 M) at pH < 2. Unless otherwise stated, all reagents used were of analytical grade standard, while standardised analysis methods were used (APHA, 2005). All samples were stored in cooler boxes with ice to ensure their preservation during transportation to the laboratory where further analyses were performed. All samples were analysed without dilution. Analyses were performed to measure the concentrations of anions, cations, trace elements and chemical oxygen demand, using a UV-Vis spectrophotometer (Thermo Fisher Scientific, USA), an inductively coupled plasma either attached to a mass spectrometer (ICP-MS) or an optical emission spectrometer (ICP-OES) (Agilent Technologies, USA) and a high-performance liquid chromatography (Thermo Fisher Scientific, USA). Subsequently, confirmatory analyses being conducted at an external laboratory accredited by the South African National Accreditation System (SANAS).

#### 4.3.3 Data treatment

Multivariate statistical analyses were used for the assessment of the groundwater quality and flow. The most commonly used methods and software used in the analyses included MSOffice Excel2016®, Cation and Anion Balance (CAB) and Cationic Exchange Values (CEV), GWQI, Sodium adsorption ratio (SAR) and a trilinear piper plot.

Analysed groundwater samples showed that the value of computed CAB error (Eq. 4-1) adopted from Domenico and Schwartz (1998), was 2.4% which was within the acceptable limit of ±5%.

$$\text{Cation and Anion Balance (CAB)} = \frac{\text{TC}-\text{TA}}{\text{TC}+\text{TA}} \times 100 \quad (4-1)$$

where, TC = total cations and TA = total anions.

The CEV of the groundwater as described by Nwankwoala and Ememu (2018) and Abadom and Nwankwoala (2018) were calculated using Eq. 4-2:

$$\text{Cationic Exchange Values (CEV)} = \frac{\text{Cl}-(\text{Na}+\text{K})}{\text{Cl}} \times \frac{\text{Mg}}{\text{Ca}} \quad (4-2)$$

#### 4.3.4 Groundwater quality index

Assessment of groundwater quality status was done by using the GWQI method, which is an effective tool to assess spatial and temporal changes in groundwater quality. GWQI was calculated according to the mathematical expression for National Sanitation Foundation as reported in the study of Rickwood and Carr (2007) and Tyagi *et al.* (2013) (see Eq. 4-3).

$$GWQI = \sum_{i=1}^n Q_i W_i \quad (4-3)$$

where:

$Q_i$  = sub index of the water quality parameter

$W_i$  = weight associated with the water quality parameter

$n$  = number of quality parameters

The parameters used were pH, temperature, turbidity, total phosphorus and nitrates (number of quality parameters used was five,  $n = 5$ ). The index generates a number between 1 and 100, with one (1) being the poorest and hundred (100) indicating excellent water quality. The ratings were defined according to Tyagi *et al.* (2013) and Rickwood and Carr (2007) using the following categories as presented in Table 4-1:

**Table 4-1: Groundwater quality index guidelines**

Category of Groundwater Quality	Groundwater Quality index
Excellent groundwater quality	91-100
Good groundwater quality	71-90
Medium groundwater quality	51-70
Bad groundwater quality	26-50
Very bad groundwater quality	0-25

#### 4.3.5 Classification of irrigation groundwater quality

In this part of the study, the groundwater quality with respect to irrigation was assessed by the following methods: The SAR and Mg hazard. Hence, to consider the groundwater suitability for irrigation the assessment of sodium concentration was essential. The sodium or alkali hazard in the use of water for irrigation was determined by the absolute and relative concentration of the cations in the groundwater. The relative activity of sodium ion in the exchange reaction with soil was expressed in terms of SAR. The SAR, which indicated the effect of relative cation concentration on  $Na^+$  accumulation in the soil, was used for evaluating the sodicity of irrigation water. The sodicity hazard of water is generally described by the SAR (Adimalla and Venkatayogi, 2018) as shown in Eq. 4-4.

$$\text{Sodium Adsorption Ratio (SAR)} = \frac{\text{Na}}{\sqrt{\text{Ca}+\text{Mg}/2}} \quad (4-4)$$

Classification of irrigation groundwater quality, with respect to salinity hazard and sodium hazard was according to method reported in (Richards, 1954).

#### **4.4 Results and discussion**

The hydrogeochemical results of the groundwater are presented in Table 4-2, including a comparison with the standard guideline values as recommended by the WHO (2011) and SANS241-1 (2015), for drinking and public health which was undertaken in order to have an overview of the groundwater quality of O’Kiep.

**Table 4-2: Statistical summary of the hydrogeochemical parameters compared to drinking groundwater standard**

Parameters	Units	Min.	Max.	Av.	SANS241-1 (2015)	WHO (2011)
Chemical Oxygen Demand (COD)	mg/L	14.6	18.0	15.0	-	20
Alkalinity (CaCO <sub>3</sub> )	mg/L	51.4	333	134	-	-
pH	-	7.41	9.55	8.1	5 ≤ 9.7	6.5-9.5
Temperature	°C	14.20	16.1	15.0	-	-
Electrical conductivity (EC)	mS/cm	43.3	476	241	≤170	100
Turbidity	NTU	0.2	196	27	≤5	-
Redox Potential (Eh)	mV	-87.2	-34.1	-57	-	-
Total Dissolved Solids (TDS)	mg/L	303	3874	1793	≤1200	500
Calcium (Ca)	mg/L	31.3	384	184	-	-
Sodium (Na)	mg/L	27.6	501	243	≤200	100
Magnesium (Mg)	mg/L	12.4	142	67.3	-	-
Potassium (K)	mg/L	2.1	44.4	15.3	-	-
Chlorine (Cl)	mg/L	23.0	1255	470	≤300	5
Fluoride (F)	mg/L	0.10	2.03	1.33	≤1.5	1.5
Sulfate (SO <sub>4</sub> )	mg/L	43.4	1210	455	≤500	200
Ammonia (NH <sub>3</sub> )	mg/L	0.16	0.16	0.16	≤1.5	-
Nitrate (NO <sub>3</sub> )	mg/L	0.10	7.80	2.16	≤11	-
Phosphate (P)	mg/L	0.50	0.50	0.50	-	0.4
Aluminium (Al)	mg/L	0.05	0.05	0.05	≤0.3	-
Antimony (S)	mg/L	0.02	0.02	0.02	≤0.02	-
Arsenic (As)	mg/L	0.01	0.01	0.01	≤0.01	0.001
Cadium (Cd)	mg/L	0.003	0.003	0.003	≤0.003	-
Chromium (Cr)	mg/L	0.01	0.01	0.01	≤0.05	-
Cobalt (Co)	mg/L	0.01	0.01	0.01	≤0.5	-
Copper (Cu)	mg/L	0.01	0.13	0.03	≤2	1
Iron (Fe)	mg/L	0.05	0.23	0.07	≤2	0.3
Manganese (Mn)	mg/L	0.01	0.12	0.02	≤0.4	0.05
Mercury (Hg)	mg/L	0.01	0.01	0.01	≤0.006	-
Nickel (Ni)	mg/L	0.02	0.02	0.02	≤0.07	-
Selenium (Se)	mg/L	0.04	0.13	0.06	≤0.04	-
Vanadium (V)	mg/L	0.01	0.01	0.01	≤0.2	-
Zinc (Zn)	mg/L	0.00	0.01	0.00	≤5	2
Cyanide (CN)	mg/L	0.00	0.01	0.01	≤0.2	-

#### 4.4.1 Hydrogeochemical characteristics of groundwater

The groundwater quality challenges usually result from a high composition of anions and cations with elevated concentrations of PTEs being a concern, which renders the groundwater unsafe for numerous anthropogenic purposes, in particular, drinking. The groundwater was alkaline with a median pH value of 8.1 and was within the acceptable guidelines stipulated by SANS241-1 (2015) and WHO (2011). The CaCO<sub>3</sub> in samples was classified as of low alkalinity to moderately hard (Sawyer and McCarty, 1967), with its range being 51.4 to 333 mg/L, a profile attributed to the

groundwaters' flow through the surface and subsurface of carbonate layers in the aquifer (Abboud, 2018; Rao *et al.*, 2012). This is an indication of brackish and hard groundwater (Zhang *et al.*, 2018). Similarly, the EC concentration values for B1, B2, B3, B5, B7 and B8 ranged between 178 and 476 mS/cm, which were above SANS241-1 (2015) guidelines for drinking water. However, these high EC values may not be an indication of the presence of toxic dissolved metalloids in the groundwater as locally elevated ECs are common in any hydrogeological settings (Tessema *et al.*, 2014).

The alkaline pH and high EC values are well documented in the Namaqualand region (Nell and Van Huyssteen, 2014). Another important indicator of groundwater quality is TDS, with its fluctuation being attributed to the dissolution of minerals in the rock of the aquifer. TDS concentrations above the (SANS241-1, 2015) were observed for samples from B1, B2, B3, B5, B7 and B8 with TDS ranging between 1248 and 3874 mg/L; while B4 and B6 had EC and TDS concentrations that were within the guidelines stipulated by both the SANS241-1 (2015) and WHO (2011). Abboud (2018) indicated that TDS greater than 1000 mg/L in groundwater is a characteristics of brackish type water. Generally, TDS and EC are dependent on the characteristics of the aquifers' geological formation (Tessema *et al.*, 2014) with higher EC and TDS in the study area being an indication of a salt-enriched environment with the leaching of salts from soils and the rocks into groundwater being prevalent (Prasanth *et al.*, 2012), an indication that the groundwater is not suitable for drinking.

Similarly, Eh values of -34.1 to -87.2 mV were indicative of geochemical conditions being predominantly reductive (Soldatova *et al.*, 2017, Pirajno, 2012). The crucial consequence of the decrease of Eh could be a shift in a balance of nitrogen species in the groundwater of the study area (Sun *et al.*, 2014). The Eh and pH are also important parameters which control the mobility of elements in geological systems (Pirajno, 2012). Furthermore, turbidity values of B2 and B6 were 196 and 18.8 NTU, respectively, which were determined not to be within the guidelines of (SANS241-1, 2015) and (WHO, 2011). High turbidity is a common phenomenon in shallow-water environments that experience periodic alteration of ecological interactions and weathering conditions (Niu *et al.*, 2018). The COD of groundwater ranged between 14.6 and 18.0 mg/L averaging 15.0 mg/L, which was indicative of a restoration of the dissolved oxygen in the groundwater systems (Jayalakshmi *et al.*, 2011). According to (WHO, 2011), desirable limit of COD is 20 mg/L. The concentration of COD at all sampling sites were shown to be within the limit of the WHO (2011), standards.

The most abundant cations were  $\text{Ca}^{2+}$ ,  $\text{Mg}^{2+}$ ,  $\text{Na}^+$  and  $\text{K}^+$ .  $\text{Ca}^{2+}$  with  $\text{Mg}^{2+}$  concentration values of 31.3 to 384 mg/L and  $\text{Mg}^{2+}$  being from 12.4 to 142 mg/L. These were expected as a high  $\text{Mg}^{2+}$  concentration could also be due to the geology of the study area, with southern granulite facies

including Mg-rich forms and a low-MgO structure display of mineralised composites consisting of MgO up to 19.7 wt. % (Maier *et al.*, 2012; Maier, 2000), with an average of 67.3 mg/L. According to Afolabi Olubukola *et al.* (2018),  $Mg^{2+}$  occurs in natural water, but its concentration is always lower than that of  $Ca^{2+}$ , which seems to be the case in the study area. The principal sources of  $Ca^{2+}$  and  $Mg^{2+}$  in groundwater samples are detrital minerals such as plagioclase amphibole, feldspar, garnet and pyroxene (Srinivas *et al.*, 2017). Clarke *et al.* (2014), Lombaard *et al.* (1986) and Schoch and Conradie (1990) reported that the source of  $Mg^{2+}$  could be due to the mafic nature of the ore body, which consist of pyroxenitic and noritic variations of the Koperberg Suite. The  $Na^{2+}$  concentrations for B1, B2, B3, B5, B7 and B8 ranged from 134 to 501 mg/L and were not within the permissible concentration values for drinking water as indicated by SANS241-1 (2015) and WHO (2011). Additionally, the  $Na^+$  and  $K^+$  can be attributed to a contribution from geogenic activities such as the weathering of ferromagnesian minerals, namely feldspars and mica (Srinivas *et al.*, 2017).

The most abundant anions in B1, B2, B3, B4, B5, B7 and B8 samples were  $Cl^-$  (23.0 and 1255 mg/L) and  $SO_4^{2-}$  (213 to 1210 mg/L) with these anions being above the permissible drinking water guidelines recommended by SANS241-1 (2015) and WHO (2011). A high concentration of both  $SO_4^{2-}$  and  $Cl^-$ , can be attributed to the oxidation of sulfidic minerals taking place due to dominant sulfidic ores being present in the area. The concentration values for B2, B3, B4, B5, B7 and B8 for  $NO_3^-$  (1.1 to 7.8 mg/L) were shown not to be within the limit of the WHO standards and no geological origin for  $NO_3^-$  exists in the area as reported by Adams *et al.* (2004). The concentration values of  $F^-$  (1.33) from all samples were within the drinking water guidelines recommended by SANS241-1 (2015) and WHO (2011). However, lifetime exposure to  $F^-$  can results in dental fluorosis as previously reported by Abiye *et al.* (2018) and Pietersen *et al.* (2009), as this anion tend to occur where fluorine-bearing minerals are abundant in the fractured rock aquifers, which is the case in Namaqualand as reported by Pietersen *et al.* (2009). Additionally, all the PTEs such as Al, S, As, Cd, Cr, Co, Cu, Fe, Mn, Hg, Ni, Se, V, Zn and CN were all below 0.2 mg/L, which were within the standardised drinking groundwater guidelines. The GWQI of 52 indicated that the groundwater quality of the study area was a moderate concern (Tyagi *et al.*, 2013).

#### **4.4.2 Groundwater interactions and hydrogeochemical relations**

The Gibbs diagram suggested by Gibbs (1970) is used to differentiate the dilution, evaporation and rock weathering as hydrogeological processes affecting the groundwater of the aquifer. Gibbs' diagram (Figures 4-2 A and B) for chemical data combines evaporation and chemical weathering as interlinked phenomena. This suggests evaporation means concentration by dissolution that occurs in case of no dilution, because the concentration process is reasonably more effective in groundwater. Similar results were also obtained in a study by Awadh *et al.* (2016)

since the aquifer in the study area is mainly controlled by weathering reactions. Gibbs' diagram displayed a minimal dilution process which reflects a lack of precipitation in the recharge area that feeds the aquifer. The  $\text{Na}/(\text{Na} + \text{Ca})$  ratios ranged between 0.5 and 0.6, which is an indication that carbonate minerals do dominate since groundwater chemistry tends to be driven to lower  $\text{Na}/(\text{Na} + \text{Ca})$  ratios (Marandi and Shand, 2018)

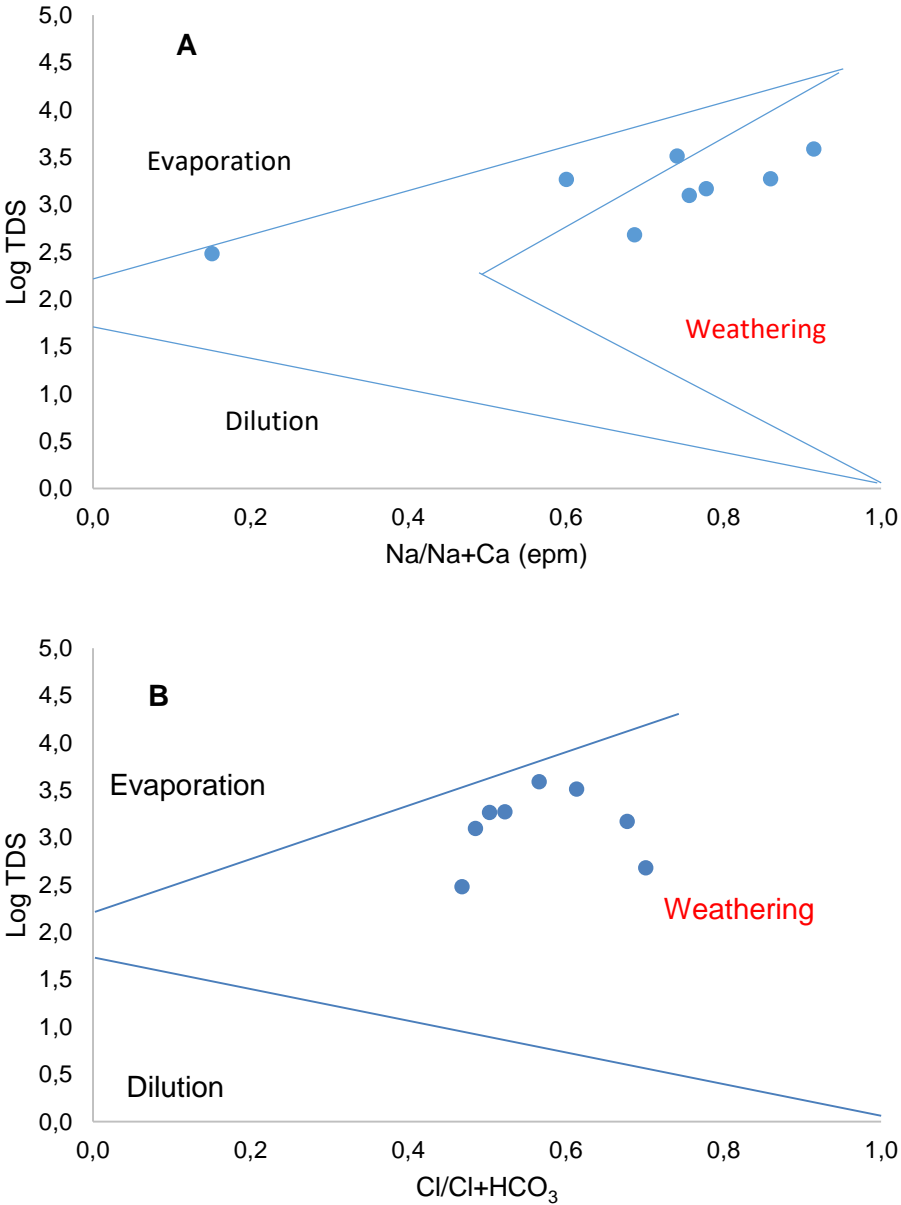


**Figure 4-2 A and B: The Gibbs diagrams classification of groundwater samples of the aquifer of the study area**

**4.4.3 Hydrogeochemical indices and cationic exchange values for groundwater**

Table 4-3: Hydrogeochemical indices and CEVs for the groundwater. The hydrogeochemical index values of  $\text{Cl}/\text{CaCO}_3$  (0.2 to 11) indicated that inland groundwater values between 0.1 and

5 are attributed to inland-based water sources, while sea water ranges between 20 and 50 (Nwankwoala and Udom, 2011). Values of CEV specified for inland waters are close to zero and, for seawater, are +1.2 to +1.3 (Al-Mashakbeh, 2017). Additionally, the CEV values in the study area were below 1.0, ranging from -0.2 and 0 indicating that the groundwater in the study area appeared to be of an inland origin, because waters under marine influence would have CEV's of around 5 (Nwankwoala and Udom, 2011). On the other hand, Mg/Ca values of 0.2 to 1.0 indicated a complexity between Mg<sup>2+</sup> and Ca<sup>2+</sup> due to their interactions with rocks (Naseem *et al.*, 2010) and the arid climate in the study area. As such, the hydrogeochemical indices (CaCO<sub>3</sub>/Cl and Mg/Ca) and CEV's indicated that the groundwater chemistry was due to the rock weathering of minerals, as the aquifer of the area is comprised of more fractured and higher permeability rock with exposure to loamy sand soils (Musekiwa and Majola, 2013).

**Table 4-3: Ionic ratios and cationic exchange values for groundwater**

Sample No	B1	B2	B3	B4	B5	B6	B7	B8
CaCO <sub>3</sub> / Cl	0.3	0.3	0.2	4.6	0.7	0.5	0.3	0.1
Na/Ca	0.9	2.1	1.1	0.9	1.0	2.4	1.6	1.3
Ca/Cl	0.4	0.3	0.6	1.4	1.2	0.3	0.3	0.3
Mg/Cl	0.1	0.1	0.1	0.6	0.7	0.1	0.1	0.1
K/Cl	0.004	0.003	0.005	0.004	0.010	0.002	0.002	0.001
SO <sub>4</sub> /Cl	0.5	0.7	1.9	1.9	6.5	0.8	0.5	0.4
Mg/Ca	0.3	0.5	0.2	0.5	0.6	0.4	0.5	0.2
Ca/SO <sub>4</sub>	0.7	0.4	0.3	0.7	0.2	0.3	0.6	0.8
CEV	0.2	0.2	0.0	-0.2	-0.2	0.1	0.3	0.1

#### 4.4.4 Geochemical classification of groundwater (trilinear piper plot)

The hydrogeochemical facies interpretation is a tool for determining the flow pattern and the origin of chemical species of groundwater (Back, 1960), which reflects the effect of chemical processes

occurring between the minerals within the subsurface rock units and the groundwater as presented in Figure 4-3.

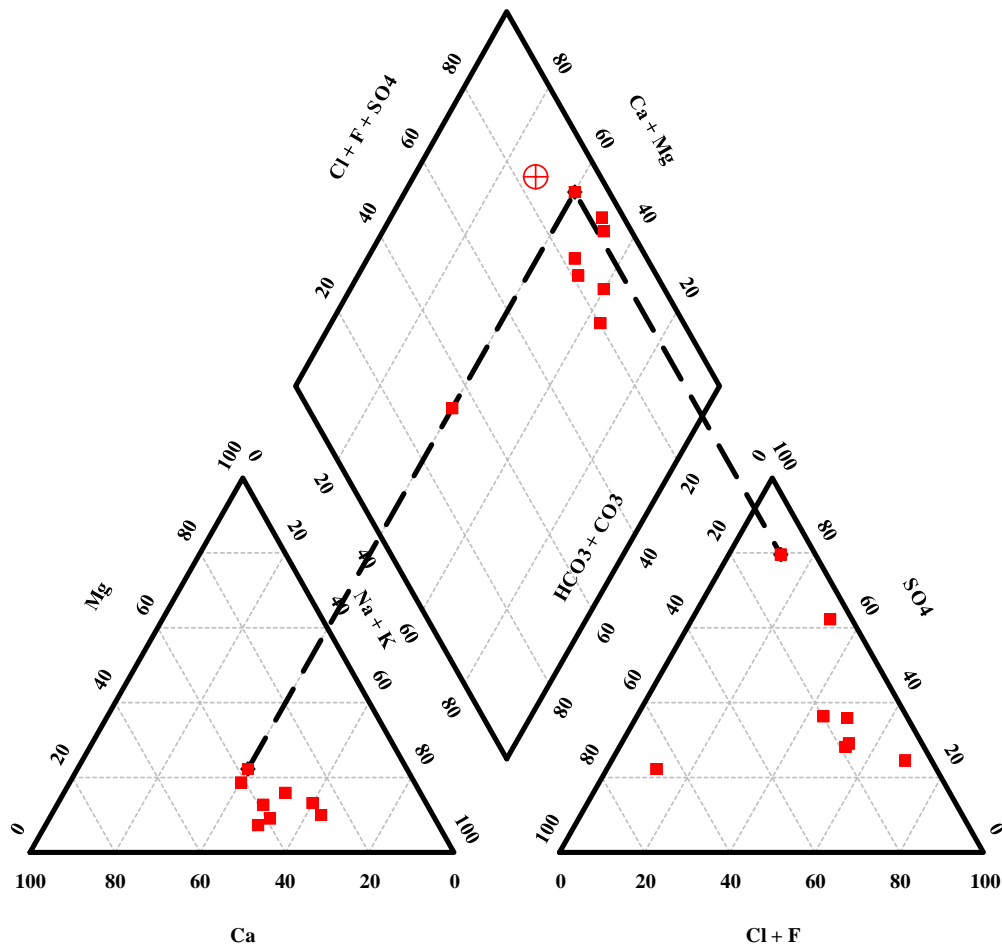


**Figure 4-3: Trilinear piper diagram for groundwater classification in the area**

The representation of chemical results on a trilinear piper diagram (Figure 4-3) shows that the groundwater evolves towards  $\text{SO}_4^{2-}$  since O’Kiep mainly comprises Cu-rich sulfide minerals dominated by chalcopyrite and bornite (Maier, 2000, Maier *et al.*, 2012). The study area shows that there is a mixture of three types of groundwater with variable concentrations of major ions. These are based on major ion data, the chemical composition of the groundwater sampled with three major groups in the region of B1, B2, B3, B5, B7 and B8; Na–K–Cl– $\text{SO}_4$  water type, while B4 falls within  $\text{CaCO}_3$ –Cl– $\text{SO}_4$  water type. Furthermore, the presence of carbonate in this factor indicates localized recharge as  $\text{HCO}_3$  is primarily derived from the dissolution of carbonate minerals by slightly acidic rainwater (Adams *et al.*, 2004). However, Abiye *et al.* (2018) reported that the groundwater in the Namaqualand falls within Na–Cl water type. The diamond also confirmed a water type of Na–Cl origin, which was attributed to preferential dissolution and leaching of the more evaporitic salts during infiltration (Adams *et al.*, 2004).

#### 4.4.5 Groundwater for irrigation

The groundwater quality with respect to irrigation is presented in Figure 4-4. The groundwater for B1–B4 was classified as a low salinity hazard, with B7–B8 samples being of a medium salinity hazard. The alkalinity hazard for B1, B2, B4, B5 and B6 was less than 10; whereas, for B7–B8 samples, medium alkalinity hazard was allocated as the classification was above 10. Additionally, SAR values for B1, B2, B3, B4, B5 and B6, that is 2.0 to 9.2, classified the samples as of low salinity, whereas for B7 and B8, the classification of medium salinity was assigned; although, the groundwater in the study area can be classified as of medium to low alkalinity. Excess usage may have an undesirable effect on plant growth.

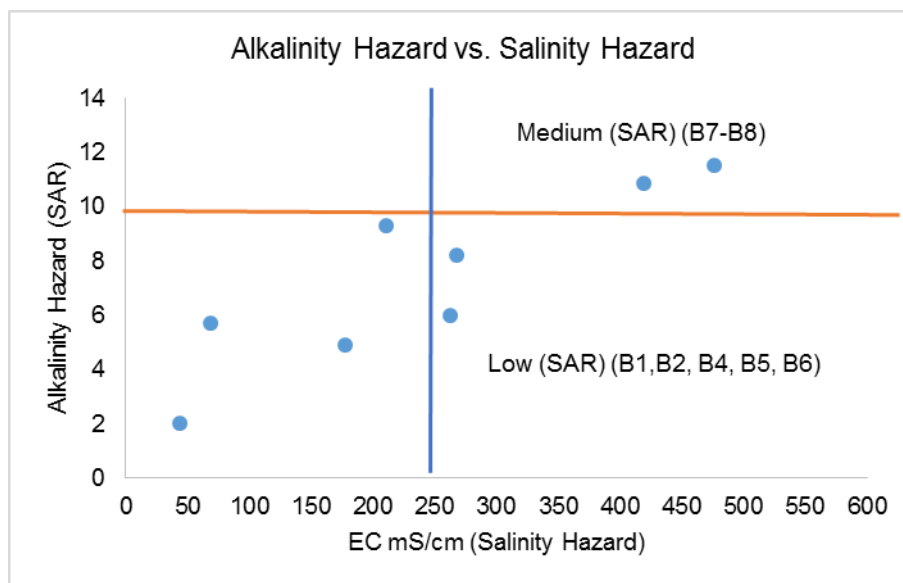


Figure 4-4: Classification of irrigation waters

#### 4.5 Summary

The groundwater quality data indicated that the following PTEs, namely; Al, S, As, Cd, Cr, Co, Cu, Fe, Mn, Hg, Ni, Se, V, Zn and CN, were within the acceptable range for drinking groundwater standards set-out by the SANS241-1 (2015) and WHO (2011). The groundwater was classified as being of a low to medium alkalinity as well as having low to high hardness due to the  $\text{CaCO}_3$  concentration in samples, indicating that the groundwater is brackish. The TDS, EC,  $\text{Cl}^-$ ,  $\text{SO}_4^{2-}$ ,  $\text{Na}^+$ ,  $\text{Ca}^{2+}$  and  $\text{Mg}^{2+}$  were not within the drinking groundwater guidelines. TDS and EC, which depend on the characteristics of the geological formation in the study area, were higher, indicating leaching of salts into the groundwater, with the lowest Eh values being indicative of a reducing environment. The crucial consequence of the decrease of redox potential could be a shift in a balance of nitrogen species in the groundwater of the study area. The most abundant anions and cations in the study area were  $\text{Cl}^-$ ,  $\text{SO}_4^{2-}$ ,  $\text{NO}_3^{2-}$  and  $\text{F}^-$  and  $\text{Na}^+$ ,  $\text{Ca}^{2+}$ ,  $\text{Mg}^{2+}$  and  $\text{K}^+$  with a GWQI classification indicating that the groundwater contamination was of moderate concern. Former

mining activities were therefore assumed to have moderately contributed to O’Kieps’ groundwater contamination and its quality.

The aquifer in this study area was determined to be controlled by weathering reactions, with minimal dilution processes, which reflects lack of precipitation in the recharge area that feeds the aquifer. Also, the Mg/Ca ratios indicated the complexity between  $Mg^{2+}$  and  $Ca^{2+}$ , an interaction generally observed in arid regions. The groundwater type in the area was categorised as Na–K–Cl– $SO_4$ ,  $CaCO_3$ –Cl– $SO_4$  and Na–Cl groundwater type, with the water further being classified as being of low to medium salinity and therefore, an alkalinity hazard. However, excess usage for irrigation purposes may have an undesirable effect on plant growth. Further water quality problems arise as a result of the contamination of groundwater from anthropogenic activities such as mining. Furthermore, the high TDS, EC, Cl,  $SO_4^{2+}$ ,  $Na^+$ ,  $Ca^{2+}$  and  $Mg^{2+}$ , suggested that strategies and appropriate remediation and rehabilitation protocols are required to improve the current challenges in the study area. This would include the implementation of in-situ groundwater monitoring, remediation and desalination technologies, if the groundwater is to be used for drinking and agricultural purposes. Lastly, improved management of groundwater resources in O’Kiep will lead to a more reliable and maintainable resource. Therefore, this part of the study suggests regular monitoring of boreholes in the area. However, there is a need to ascertain any seasonal variation of the characteristics of the groundwater in order to determine seasonal contamination patterns from the CMM in O’Kiep, as reported in Chapter 5.

## CHAPTER 5: RESULTS AND DISCUSSION

---

Published as:

- 1]. **Erdogan, I.G.**, Fosso-Kankeu, E., Ntwampe, S.K.O., Waanders, F. and Hoth, N., 2020. Seasonal variation of hydrochemical characteristics of open-pit groundwater near a closed metalliferous mine in O’Kiep, Namaqualand Region, South Africa. *Environmental Earth Sciences*, 79(5), 1-15.  
DOI: 10.1007/s12665-020-8863.
- 2]. **Erdogan, I.G.**, Moncho, T., Fosso-Kankeu, E., Ntwampe, S.K.O., Waanders, F., Hoth, N., Rand, A. and Fourie, B. 2017. Hydrochemical characteristics of open-pit groundwater from a closed metalliferous mine in O’Kiep, Namaqualand region, South Africa. In 9th International Conference on Advances in Science, Engineering, Technology and Waste Management (ASETWM-17), Nov. 27-28, Parys, South Africa.  
Available: <https://doi.org/10.17758/EARES.EAP1117022>

Dataset of the above-mentioned articles

- 3]. **Erdogan, I.G.**, Bent, D., Ntwampe, S.K.O., Fosso-Kankeu, E. and Waanders, F.B. 2019. Geochemical modelling and seasonal hydrogeochemical processes of the open-pit groundwater at O’Kiep, Namaqualand, South Africa.  
DOI: 10.25381/cput.9746537.v1. (Supplementary file: S2).

## **5.1 Seasonal variation of hydrochemical characteristics of open-pit groundwater near a closed metalliferous mine in O’Kiep, Namaqualand region, South Africa**

### **5.2 Introduction**

In South Africa, the vicinity of operating mines to water sources culminates in the contamination of such sources including groundwater due to the exposure of different geochemical profiles of underground aquifers by elements mined. The variance in the hydrochemical profile of groundwater differs for each location, thus depends on climatic and seasonal changes including the geological profile of the area (Jonch-Clausen, 2004; DWA, 2004). Mining activity can also change the hydrochemical profile of groundwater. Contaminated groundwater has been one of the challenges being faced by communities in South Africa as groundwater is considered as one of the primary water resources for developmental activities, with its quality being adversely affected or degraded as a result of anthropogenic activities that introduce contaminants into the groundwater. Overall, groundwater contamination is usually irreversible (Rajendran *et al.*, 2019; Abdelgawad, 2015).

Environmental challenges arising from mining activities are receiving increasing attention in South Africa. Generally; however, less so in small former copper mining areas such as O’Kiep, which was considered in the eighteenth century to be the richest copper mining area in the world (Cairncross, 2004). Currently, this town is experiencing various challenges such as poor drinking water quality. In O’Kiep, the mining of copper left a legacy of metalliferous waste such as tailings, waste rock and contaminated soils within the vicinity of this town. Generally, such mining activities are known to contaminate both the immediate environment and ground and/or surface water resources. This can culminate in water shortages, even if water is available from various sources (Singh and Kamal, 2015) it might be contaminated.

Groundwater is a key component of the water resources of South Africa. As such, it can provide much of the water required for households, especially since the country’s surface water resources are unevenly distributed and cannot cope with growing demand (Bredenhann and Braune, 2000). In a report of surface and groundwater assessment in Namaqualand, an area which includes O’Kiep, the quality of the groundwater from some boreholes were determined to be higher than the SANS Class II drinking water limits and therefore the water was not suitable for human consumption (DWAF, 1996, Holmes, 1995). Additionally, the analysis also indicated that, the groundwater quality exceeded the recommended values for livestock use, as set out in South African water quality guidelines for agricultural use and livestock (Holmes, 1995), with mining activity suspected to be a source of the contamination.

The geochemistry of the minerals mined in the O’Kiep area is such that sulfidic ores are the dominant minerals in the copper-rich ore body of the area (Faris *et al.*, 2017). Copper sulfide ores that are common in the O’Kiep area are bornite ( $\text{Cu}_5\text{FeS}_4$ ), chalcopyrite ( $\text{CuFeS}_2$ ), chalcocite ( $\text{Cu}_2\text{S}$ ), digenite ( $\text{Cu}_9\text{S}_5$ ), enargite ( $\text{Cu}_3\text{AsS}_4$ ) and pyrite ( $\text{FeS}_2$ ) (Hangone *et al.*, 2005). These are the primary constituents in the ore body that facilitate ARD, sulfide geological material oxidation and the transportation of PTEs by leaching (Fosso-Kankeu *et al.*, 2017, Munyai *et al.*, 2016, Fosso-Kankeu *et al.*, 2015). Dissolved minerals in the surface water can be transported and thus contaminate groundwater when the water table is high. Sulfide containing ores—are known to produce acid with exposure to oxygen and water (Plumlee, 1999). The oxidation of pyrite and copper sulfide ores in tailings and mine dumps is due to weathering as described by Antonijević *et al.* (2008). Generally, such weathering—can enhance the mobility of PTE species which can contaminate groundwater.

The national state on water resources report by the DWA (2011–2012) on climatic conditions, indicated a reduction in rainfall and an increase in evaporation due to higher temperatures that impacted on the SA’s scarce water resources. Additionally, the groundwater in O’Kiep is highly susceptible to high evaporation rates. Natural factors that could influence changes in the quality of the groundwater in O’Kiep include the host rock, precipitation, evapotranspiration and ARD formation (Van Dyk *et al.*, 2008). Under excessive evaporative conditions, groundwater salinity displays a cumulative tendency to increase (Abiye and Leshomo, 2013). Furthermore, groundwater arid and semi-arid environments is subjected to periodic salinisation due to high evaporation rates and low rainfall (Nakwafila, 2015). The understanding of groundwater hydrochemical characteristics is a vital factor in determining its safety for use in domestic and agricultural activities. Therefore, it was necessary to investigate the seasonal variation in the quality of an OPGW near a CMM. Earlier studies carried out in this area, evaluated the hydrochemical characteristics of the OPGW quality. However, these studies did not attempt to assess the seasonal variation in the OPGW quality.

### **5.3 Objectives**

The objectives of this part of the study were:

- to assess the seasonal variation of the OPGW quality; and
- to determine its suitability for drinking and irrigation purposes.

## 5.4 Materials and methods

### 5.4.1 Site description

O’Kiep is situated in Namaqualand, Northern Cape Province of South Africa (Cairncross, 2004) with coordinates [29°35’45”S 17°52’51”E]. This town is 38.63 km<sup>2</sup> in size with a reported population of approximately 6300 people in 2011 and is approximately 570 km from Cape Town. O’Kiep is characterised by an arid climate, with no perennial river systems. The lower Orange River is the only perennial river, located some 150 km east of O’Kiep and it is a major source of piped drinking water supply for agricultural, domestic and industrial use for the town. The geometry of the aquifer systems in O’Kiep has been largely influenced by the underlying geology of metamorphic rocks such as granites (Pietersen *et al.*, 2009). The groundwater in the so-called Namaqualand aquifer occurs in the alluvial and crystalline basement rocks (Adams *et al.*, 2004), with the Spektakel aquifer previously having supplied water to O’Kiep, Nababeep and Springbok. However, this was replaced by the water supply scheme from the lower Orange River (Nuclear, 2006) due to suspected contamination of the aquifer attributed to long-term copper mining and poor groundwater management practices. The hydrochemistry of groundwater in the Namaqualand aquifer indicates dissimilar composition due to the ensuing complex geochemical processes as the chemistry is being controlled primarily by dissolution, redox reactions and mixing (Abiye and Leshomo, 2013). A further source of water is an open-pit situated 1.1 km downstream from the closed O’Kiep metalliferous mine, which is filled with water.

### 5.4.2 Sample collection

Prior to sample collection, permission was granted by the O’Kiep Copper Company and Nama Khoi municipality for the purposes of this study. Samples (n = 10) in duplicate were collected from the open-pit [29°35’55.1”S 17°52’47.6”E] (144 m width, 10 m depth), on the 5<sup>th</sup> of April 2017, a dry season (average temperature of 37°C) and on the 8<sup>th</sup> of August 2017, a wet season (average temperature of 16°C) with a minimal rainfall occurring in the area on the day of sampling (Accuweather, 2017). The samples were collected between 7am and 11am for both seasons. The sampling points were randomly selected due to soil erosion and restricted access to the open-pit. Multi-parameter instruments were calibrated prior to field measurement usage according to the national field water measurement standards (Gibs and Wilde, 2007; Wilde and Radtke, 1998), with polypropylene sample bottles (500 mL) being used for sample collection. The sampling bottles were thoroughly cleaned and rinsed in dilute 0.5 M HCL, prior to rinsing with sterile deionised water. The bottles were airdried and stored closed to prevent pollution prior to sample collection. Samples were collected around the open-pit in duplicate at depths between 1 and 9.5 m (dry season) and 1 and 11 m (wet season) using a HydraSleeve™ "No-Purge" groundwater sampler according to the method described by Trick *et al.* (2008), with GPS coordinates being

recorded at the sampling points as shown in Figure 5-1, which indicates the sampling area, and potential sources of contaminants such as stockpiled mine waste and the TSF.

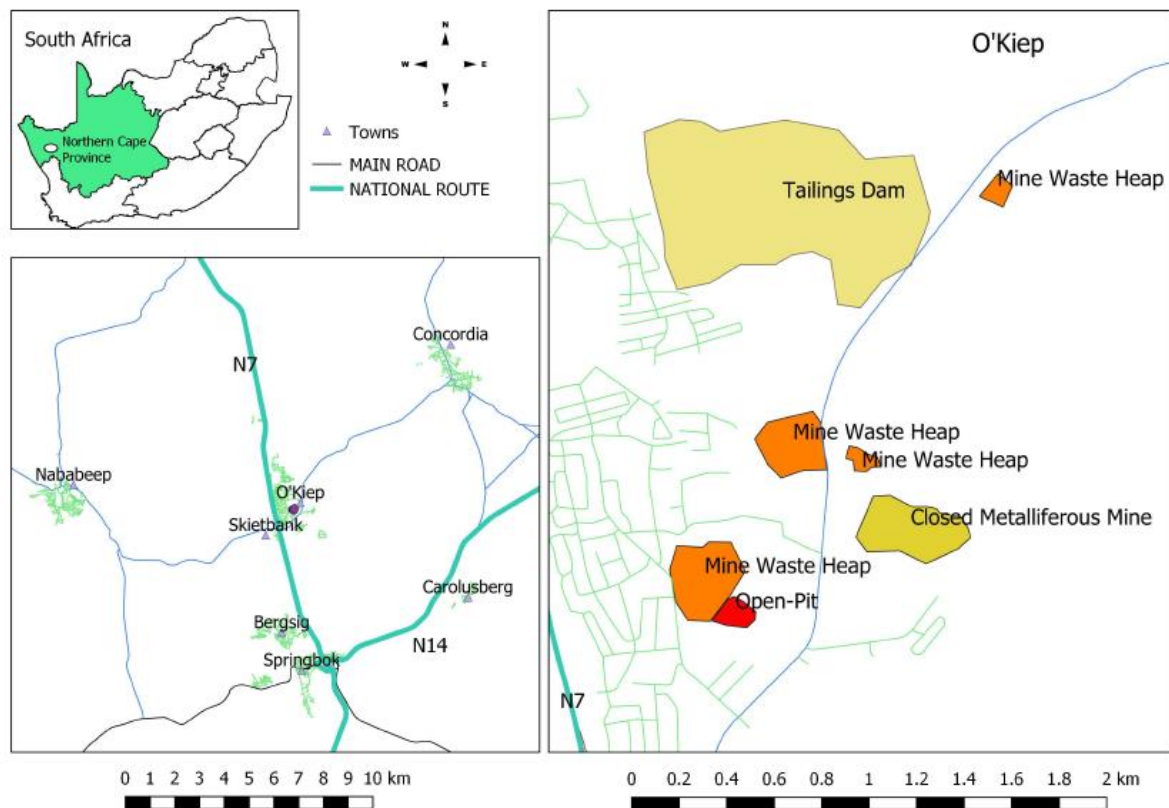


**Figure 5-1: Study area, sampling points including possible sources of contaminants: Geological maps were generated using Quantum GIS software (v. 2.18.11) and data from National Geo-Spatial Information**

During sampling, the following physical parameters were quantified on-site, using an EXSTIK II® EC500 and an EXSTIK II® CA895, for dissolved oxygen (DO): pH, temperature, EC, redox potential (ORP), salinity and TDS. The instruments were calibrated prior to sampling using standard procedures as described by Shah and Mjalli (2014). The temperature was measured in-situ to minimise atmospheric variations according to the method described by Weaver *et al.* (2007). Samples were also filtered through a 0.45 µm cellulose membrane filter, using a hand-vacuum pump, into polypropylene sampling bottles (APHA, 2005, Ball *et al.*, 1999). The unfiltered 100 mL per sample were digested with technical grade nitric acid (0.2 M). Unless otherwise stated, all reagents used, were of analytical grade, while standardised methods of analysis were used (APHA, 2005).

All samples were stored in cooler boxes with ice to ensure preservation during transportation to the laboratory whereby further analyses were performed. All samples were analysed without dilution. Analyses performed included quantification of anions, cations, PTEs, and chemical oxygen demand, using UV-Vis spectrophotometer, high-performance liquid chromatography,

inductively coupled plasma coupled with either a mass spectrometer (ICP-MS) or an optical emission spectrometer (ICP-OES) at an external SANAS-accredited laboratory.

### 5.4.3 Data analysis

Multivariate statistical analysis using Microsoft Office Excel 2016<sup>®</sup>, was used for the assessment of the OPGW quality focusing on the coefficient of variation (Stanković *et al.*, 2015), correlation analysis and the trilinear piper plot.

#### 5.4.3.1 The coefficient of variation and correlation analysis

The quality variability of the OPGW can be measured by determining fluctuations in the water table and can be expressed as a coefficient of variation (Stanković *et al.*, 2015). The contributing aquifer can have a dynamic range of groundwater levels as they discharge and recharge seasonally (Quevauviller *et al.*, 2009). The CV was determined using Eq. 5-1 (Abdi, 2010):

$$CV = \frac{\text{Standard Deviation}}{\text{Mean}} \times 100 \quad (5-1)$$

The first step prior to the multivariate statistical analyses is to reduce data sizes by eliminating the variables that do not provide important information of groundwater quality. Therefore, parameters indicating a < 5% CV, were considered almost constant and thus excluded from the statistical analyses (Pacheco Castro *et al.*, 2018; Güler *et al.*, 2002). A correlation analysis is a bivariate technique used to define the degree of relation between two hydrochemical parameters. Correlation analysis has been broadly used as an unbiased method for drawing meaningful information in the analysis of water quality variation (Singh *et al.*, 2005; Selvakumar *et al.*, 2017).

#### 5.4.3.2 Geochemical modelling

A thermodynamic model with a mathematical programme was applied to determine ion interactions (Konikow and Glynn, 2013). Dissolution–precipitation processes, saturation indices (SI) of some mineral phases were calculated with PHREEQC Version 3 software (US Geological Survey) that elucidate speciation and reaction mechanisms (Zhu and Anderson, 2002; Parkhurst and Appelo, 1999). Furthermore, speciation, solubility, reaction and inverse mass balance modelling were activated to complete the process. The MINTEQ.V4.DAT database was used for the ion interaction approach. The redox potential (pe) value was determined using a portable ORP instrument (Hi 98190). The Ag/AgCl electrode reference was used as a comparison with the hydrogen scale (Nordstrom and Wilde, 2005). Additionally, a PHREEQC batch reaction model was used to perform irreversible and equilibrium reactions (see Eqs. 5-2 and 5-3).

$$Eh = ORP + E\theta \quad (5-2)$$

$$pe = Eh (mv)/59.2 mV \quad (5-3)$$

#### 5.4.3.3 Sodium adsorption ratio

The SAR is a measure of the suitability of water for irrigation purpose. The formula for calculating the SAR is presented in Eq. (5-4) (Manoj *et al.*, 2017).

$$SAR = \frac{Na^+}{1/2[Ca^{2+}+Mg^{2+}]} \quad (5-4)$$

### 5.5 Results and discussion

Table 5-1 present the seasonal variation of the OPGW. The OPGW temperature showed a wide range of variation from an average of 23.0°C (dry season) to 14.4°C (wet season), which reflected a seasonal change in atmospheric air temperature. The pH values of OPGW samples during dry and wet season were slightly acidic, at pH 4.5 to 5.2 and 3.7 to 3.8, respectively. The pH values for the water sampled in both seasons were not within the permissible limit for drinking water according to by SANS241-1 (2015) and WHO (2011). This includes the low average DO concentrations in both dry (0.9 mg/L) and wet season (0.1 mg/L) samples, indicative of the anaerobic conditions of the OPGW. A decrease in COD ranging from 53 to 15 mg/L for both seasons indicated low organic matter in the OPGW thus an insignificant organic matter contamination; albeit, COD can also be reduced due to chemically induced chelatin during thermal oxidation in slight acidic water (Osborne *et al.*, 2009). Overall, the CODs were greater than the (WHO, 2011) water quality guideline value of 4.0 mg/L.

**Table 5-1: Physicochemical characteristics of open-pit groundwater compared to water quality guidelines**

Parameters	Units	Dry Season (n = 5)					Wet Season (n = 5)					Water Quality Guidelines (SANS241-1, (WHO, 2011).	
		Min	Max	STDV.	Averag	CV	Min	Max	STDV.P	Averag	CV		
Chemical Oxygen Demand	mg/L	14.6	88	28.2	53	53%	14.6	15	0.0	14.6	0%	-	4
Alkalinity (CaCO <sub>3</sub> )	mg/L	10.0	10.0	0.0	10.0	0%	10.0	10.0	0.0	10.0	0%	-	-
Colour	Pt-Co-true	10.0	23	5.2	12.6	41%		10.0	0.0	10	0%	<15	-
Turbidity	NTU	502	400	1504	1396	108	14.9	148	57	50	113	≤5	5
pH at 25°C	-	4.5	5.2	0.2	4.9	4%	3.7	3.8	0.1	3.7	2%	5-9.7	6.5-8.5
Temperature	°C	19.2	24.7	2.0	23.0	9%	14.1	14.3	0.1	14.2	1%	-	-
Electrical Conductivity (EC)	m\$/m	738	900	527	8202	6%	6065	7005	399	6756	6%	≤170	-
Total Dissolved Solids (TDS)	mg/L	514	628	370	5717	6%	3435	3640	81.4	3501	2%	≤1200	500
Dissolved Oxygen (DO)	mg/L	0.4	1.2	0.3	0.9	30%	0.1	0.1	0.0	0.1	0%	-	5
Salinity	PPt	3.7	4.5	0.3	4.1	6%	4.8	5.1	0.1	4.9	2%	-	-
Redox (ORP)	mV	110	130	7.0	123	6%	159	167	3.1	164	2%	-	-
Calcium (Ca)	mg/L	544	631	29.6	600	5%	533	541	3.1	536	1%	-	-
Sodium (Na)	mg/L	420	559	50.1	492.8	10%	477	572	40.0	503	8%	≤200	100
Magnesium (Mg)	mg/L	434	683	85.1	544	16%	475	505	12.6	483	3%	400	-
Potassium (K)	mg/L	29.2	42.8	4.5	34.9	13%	31.3	33	0.4	31.9	1%	-	-
Fluoride (F <sup>-</sup> )	mg/L	5.41	9.6	1.4	6.8	21%	1.0	4.0	1.2	2.7	43%	≤1.5	1.5
Chloride (Cl <sup>-</sup> )	mg/L	607	759	60.1	686.8	9%	960	1080	45.6	1035	4%	≤300	250
Sulfate (SO <sub>4</sub> <sup>2-</sup> )	mg/L	402	602	665	4830	14%	4240	4450	85.8	4303	2%	≤500	200
Ammonia (NH <sub>3</sub> )	mg/L	0.18	2.4	0.9	1.0	93%	0.47	0.5	0.0	0.5	2%	≤1.5	-
Nitrate (N)	mg/L	10.0	10.0	0.0	10.0	0%	0.5	0.5	0.0	0.5	0%	≤0.9	45
Ortho-Phosphate (P)	mg/L	3.51	3.77	0.1	3.6	2%	0.5	0.5	0.0	0.5	0%	-	0.4
Aluminium (Al)	mg/L	8.4	76.7	24.5	38.8	63%	7.5	8.0	0.19	7.7	3%	≤300	-
Antimony (Sb)	mg/L	0.02	0.02	0.0	0.02	0%	0.01	0.02	0.004	0.018	25%	≤20	-
Arsenic (As)	mg/L	0.01	0.01	0.0	0.01	0%	0.01	0.02	0.004	0.013	35%	≤20	0.01
Cadmium (Cd)	mg/L	0.06	0.08	0.01	0.07	10%	0.0	0.1	0.01	0.0	41%	≤3	0.003
Chromium (Cr)	mg/L	0.04	0.16	0.05	0.08	57%	0.0	0.0	0.01	0.0	33%	≤50	-
Cobalt (Co)	mg/L	1.43	1.64	0.07	1.54	5%	1.8	1.8	0.02	1.8	1%	-	-
Copper (Cu)	mg/L	464	113	252	628	40%	440	453	5.2	447	1%	≤2000	1.0

Iron (Fe)	mg/L	28.8	214	77.8	79.5	98%	0.4	0.8	0.1	0.6	18%	≤2000	0.3
Manganese (Mn)	mg/L	36.5	40.5	1.5	39.0	4%	31.4	32.0	0.2	31.8	1%	≤400	0.05
Mercury (Hg)	mg/L	6.0	6.0	0.0	6.0	0%	0.01	0.0	0.0	0.01	0%	≤6	-
Nickel (Ni)	mg/L	9.29	11.4	0.7	9.9	8%	9.21	9.3	0.0	9.3	0%	≤70	70
Selenium (Se)	mg/L	0.04	0.04	0.0	0.04	0%	0.04	0.04	0.0	0.04	0%	≤40	40
Vanadium (V)	mg/L	0.01	0.15	0.06	0.06	98%	0.01	0.01	0.0	0.01	0%	≤200	-
Zinc (Zn)	mg/L	0.01	0.03	0.01	0.02	52%	0.005	0.00	0.0	0.005	1%	≤0.005	2
Cyanide (CN <sup>-</sup> )	mg/L	0.14	0.39	0.08	0.30	28%	0.034	0.08	0.02	0.049	41%	≤200	-

Generally, DO has a significant effect upon groundwater quality since it regulates the solubility of many trace metals and limits the bacterial metabolism of organic compounds, by aerobic bacteria. Some bacteria use DO as part of their metabolism in certain cases, facilitating the oxidation of ammonia, hydrogen sulfide, organic carbon and other reductants (Weaver *et al.*, 2007). The DO content also indicated changes in the redox state and microbial activity of the water samples (Pretorius *et al.*, 2008) as ORP increased from 123.1 mV (dry season) to 164 mV (wet season).

The OPGW salinity was noticed to increase from 4.1 g/L (dry season) to 4.9 g/L (wet season) with a standard deviation of  $\pm 0.6$ . The OPGW salinity is a significant groundwater quality indicator, which is controlled by many factors such as aquifer mineralogy, and topography even mobility of PTEs into the water from the surface of the contaminated area as a result of mining activity (Praveena *et al.*, 2011). Rabbani *et al.* (2010) also reported that saline water starts to infiltrate inland during the wet season, with Yan *et al.* (2015) concluding that groundwater salinity varies with the fluctuation of groundwater level. According to Northern Cape Department of Environmental Affairs and Nature Conservation Goegap Nature Reserve report (2018), most of the rainfall in O’Kiep varies between 100 and 300mm per year; however, during sampling in August 2017, only 2mm of rain was recorded.-Furthermore, the TDS and EC slightly decreased from 5717 mg/L and 8202 mS/m (dry season) to 3501 mg/L and 6756 mS/m (wet season), respectively. EC of the OPGW is a direct function of its TDS and indicates concentration of soluble salts in the groundwater (Harilal *et al.*, 2004, Purandara *et al.*, 2003). These values were not within the allowable limits by SANS241-1 (2015) and (WHO, 2011). The OPGW contained high dissolved solids content which may be caused by human activity (Ramakrishnaiah *et al.*, 2009).

For different seasons, the groundwater turbidity varied from a maximum of 4000 NTU (dry season) to a minimum of 148 NTU (wet season). High turbidity values during the dry season were due to clay and silt-sized particles found at the edges of the open-pit. The turbidity values for both seasons were above the drinking water quality limit stipulated by SANS241-1 (2015). The causes of water turbidity are diverse and in most cases the suspended and dissolved solid particles contribute to high turbidity, with some particles being pneumatically transported into receiving water especially during the dry season. However, turbidity can also indicate the presence of dissolved hazardous PTEs and the proliferation of microbial contaminants. The less turbid water (NTU 148) obtained during wet season could be an indication of aquifer recharge (Mativenga and Marnewick, 2018). The CV for turbidity increases were from 108% (dry season) to 113% (wet season) with both seasons having a CV greater than 100%, an indication of variability (Ma *et al.*, 2011). This was an indication that environmental alterations might critically affect the OPGW in this arid area. Similarly, an alkalinity of 10 mg/L for both seasons was observed, with sulfate reduction being hypothesised as contributory factor (Whitworth *et al.*, 2014), which is also an

indication of sustained microbial activity and slow weathering of noncarbonated rocks such as the igneous granite and gneiss (Pretorius *et al.*, 2008).

The ions concentration in the OPGW samples varied in both seasons. The most abundant cation and anions were  $\text{Ca}^{2+}$  and  $\text{SO}_4^{2-}$ . The high level of  $\text{Ca}^{2+}$ ,  $\text{Mg}^{2+}$  and  $\text{SO}_4^{2-}$  concentration was associated with the oxidation and weathering of sulfide minerals, which may be due to dissolution of gypsum and calcium-bearing minerals (Selvakumar *et al.*, 2017). Similar results were obtained in a study of Abiye *et al.* (2018) whereby hydrogeochemical parameters of the groundwater system in the Namaqualand region were studied. The relative ionic species abundance in the OPGW showed species concentration in the following sequence  $\text{Ca}^{2+} > \text{Na}^+ > \text{K}^+ > \text{NH}_3$  and  $\text{SO}_4^{2-} > \text{Cl}^- > \text{NO}_3^- > \text{F}^- > \text{PO}_4^{3-}$  for anions. An increase in  $\text{Na}^+$ ,  $\text{Cl}^-$ ,  $\text{Ca}^{2+}$ , and  $\text{SO}_4^{2-}$  was an indication of the dissolution of quaternary sand, scree rubble and sandy soil deposits in which minerals such as anhydrite, halite and gypsum occur.

The CV of the abundant  $\text{Cl}^-$  and  $\text{SO}_4^{2-}$  anions decreased during the wet season from 9 to 4% and from 14 to 2%, respectively. On the other hand,  $\text{F}^-$  had a lower variation in the dry season (21%) albeit higher in the wet season (43%). Fluoride is a major component of fluorite ( $\text{CaF}_2$ ), a mineral in granites. Dissolution of such minerals can constitute a major source of  $\text{F}^-$  in groundwater (Reddy *et al.*, 2010; Edmunds and Shand, 2009). Additionally, many people in nearby areas in Namaqualand suffer from tooth decay, and decolouration assumed to be due to exposure to high concentration of  $\text{F}^-$  in groundwater used for drinking. The high  $\text{F}^-$  concentration is typical for groundwater in granitic aquifers (Abiye *et al.*, 2018).

Al, Cr, Cd, Cu, Fe and Zn all decreased from dry season to wet season from 63 to 3%, 57 to 33%, 5 to 1%, 40 to 1%, 98 to 1% and 52 to 1%, respectively. However, the Sb, As, Cd, and  $\text{CN}^-$  increased to 15, 35, 41 and 41%, respectively. This was attributed to natural seasonal groundwater table fluctuations (Rijal *et al.*, 2010). When the OPGW pH is low, the higher the mobility of Sb, As, Cd, and  $\text{CN}^-$ . This mobilisation in the groundwater is a phenomena linked to the geological profile of the study area, which is further influenced by the MSW, which contaminates the immediate environment (Moncho *et al.*, 2017; Amponsah-Dacosta and Reid, 2014; Rozendaal and Horn, 2013). Aquifers in the Northern Cape, Namaqualand, are mostly assumed to be affected by natural conditions with only seasonal trends responsible for water level fluctuations. The aquifer type including rainfall, can have a more significant influence on the groundwater quality (Van Dyk *et al.*, 2008; Adams *et al.*, 2004). Some aquifers are susceptible to contamination from surface sources. Fractured aquifers also allow rapid migration of contaminants via a preferred pathway, culminating in the potential to contaminate vast areas along the fracture network (Adams *et al.*, 2004). The topography in this region is defined as a flat terrain with isolated mountains and hills. The observed hydraulic head and elevation data

gathered from the hydro-census indicate that the groundwater level in Namaqualand is related to its topography (Roets, 2008; Ferreira *et al.*, 2015). During the raining season, water can flow along the hydraulic gradient from the North-West to the South-East (Ferreira *et al.*, 2015).

The vegetation and flowers in this area bloom during the wet season, having adapted to this habitat with its alternating periods of exposure and inundation. From the results, it is observed that the maximum SAR value for the dry season was 22, while for the wet season was 25. These values are within permissible levels for water intended for irrigation. However, as this groundwater is mildly acidic (pH = 3.7-5.2) with a high salinity index and Na<sup>+</sup> concentration levels, determined to be influenced by weathering of overburden in this mining area, thus continuous use of such water may cause an impoverished physical soil environment. A high amount of Na<sup>+</sup> concentration in irrigation water can adjust the osmotic pressure in the root zone of some plants, which can result in limiting the amount of water taken in by the plant which will consequently hinder plant growth (Ouyang *et al.*, 2014; Selvakumar *et al.*, 2017).

Similarly, the OPGW had a high sulfate concentration of 4830 mg/L for the dry season and 4303 mg/L for the wet season. Also, there were elevated concentrations of dissolved trace elements in the dry season, in particular, Cu > Fe > Al > Mn. It was also noted that the higher the water table would rise due to seasonal fluctuation during the wet season, the lower the values of trace elements (Cu > Fe > Al > Mn), and turbidity (Rao, 2006). However, PTEs such as Al, Sb, As, Cd, Cr, Co, Cu, Fe, Mn, Hg, N, Se, V, Zn and CN were all within ≤20 mg/L, a water quality guideline as stipulated by the SANS241-1 (2015), while As, Cu, Fe, Mn were above 0.01 mg/L and not being within limits as indicated. The presence of As and Fe is an indication of oxidation of arsenic sulfides such as arsenopyrite (FeAsS) and pyrite (FeS<sub>2</sub>) in the groundwater (Zheng *et al.*, 2004) and As also mobilises under anaerobic conditions as it is influenced by low DO concentrations (Tomlinson *et al.*, 2017) as observed for the OPGW. However, it can be seen in Table 5-1 that As was (0.01 mg/L); albeit, the nitrate concentration was 10 mg/L with DO of 0.9 mg/L (dry season) and 0.1 mg/L (wet season) being observed. Additionally, in the study of Leshomo (2011), As was rarely detected in the groundwater of Namaqualand area. Similarly, no Uranium was detected in the OPGW for both seasons which could be due to the geology of the O’Kiep (Clifford and Barton, 2012). Moreover, Uranium concentrations in groundwater in granite geological formations results in spatial distributions which are preferentially localised (Cho and Choo, 2019). Similar result were also observed in a Jurassic granite in Korea with low concentration of Uranium (Cho and Choo, 2019). Lowest Uranium concentrations were also observed in groundwater characterised by iron and sulfate reducing conditions (Riedel and Kübeck, 2018). These observation are further supported by the fact that the O’Kiep geology consists of a thick sheet of granite gneiss up to 1500 m thick (Clifford and Barton, 2012). Some physical parameters, cations, anions and trace

elements such as pH, TDS, Na<sup>+</sup>, Mg<sup>2+</sup>, K<sup>+</sup>, F<sup>-</sup>, Cl<sup>-</sup>, SO<sub>4</sub><sup>2-</sup>, NO<sub>3</sub><sup>-</sup>, PO<sub>4</sub><sup>3-</sup>, Al, Cu, Fe, Mn, and Zn would be much higher than those of natural groundwater associated geological formations, with the physical parameters being hypothesised to be due to leaching of elements from the surrounding MSW.

Further studies are however needed to better understand the mobility mechanism and sources of these PTEs occurring in various concentrations in the OPGW (Larkins *et al.*, 2018). The chloride observed is a broadly distributed component in all types and forms of rocks (Pretorius *et al.*, 2008). It's affinity towards sodium is high, with Na<sup>+</sup> and Cl<sup>-</sup> concentrations increasing during the wet season from an average of 493 to 503 mg/L and from 687 to 1035 mg/L, respectively. According to Jeevanandam *et al.* (2007), the active dissolution of the halite in the OPGW was assumed to be the main cause of the high Na<sup>+</sup> and Cl<sup>-</sup> during the wet season. Soil permeability and porosity also has a key role in chloride concentration development (Ramakrishnaiah *et al.*, 2009).

#### **5.5.1 Classification of the groundwater in O’Kiep**

The trilinear piper diagrams of the OPGW samples for both seasons are shown in Figure 5- 2. Groundwater in granitic rock is normally classified as Na–(Ca)–Cl water-type and it is possibly controlled by mixing processes occurring between higher salinity groundwater Na–(Ca)–Cl water-type and low salinity groundwater (Na–(Ca)–HCO<sub>3</sub> water-type in the sedimentary rocks (Iwatsuki *et al.*, 2005). Namaqualand experiences excessive evaporative conditions due to its aridity. As such the hydrochemical parameters increased, with the overall salinity being observed to be elevated. These changes in the groundwater quality might be primarily through parent rock weathering, dissolution and anthropogenic sources. It was presumed that natural geological sources could be the cause for the groundwater quality deterioration in the area, which is further driven by climatic changes (Abiye and Leshomo, 2013).

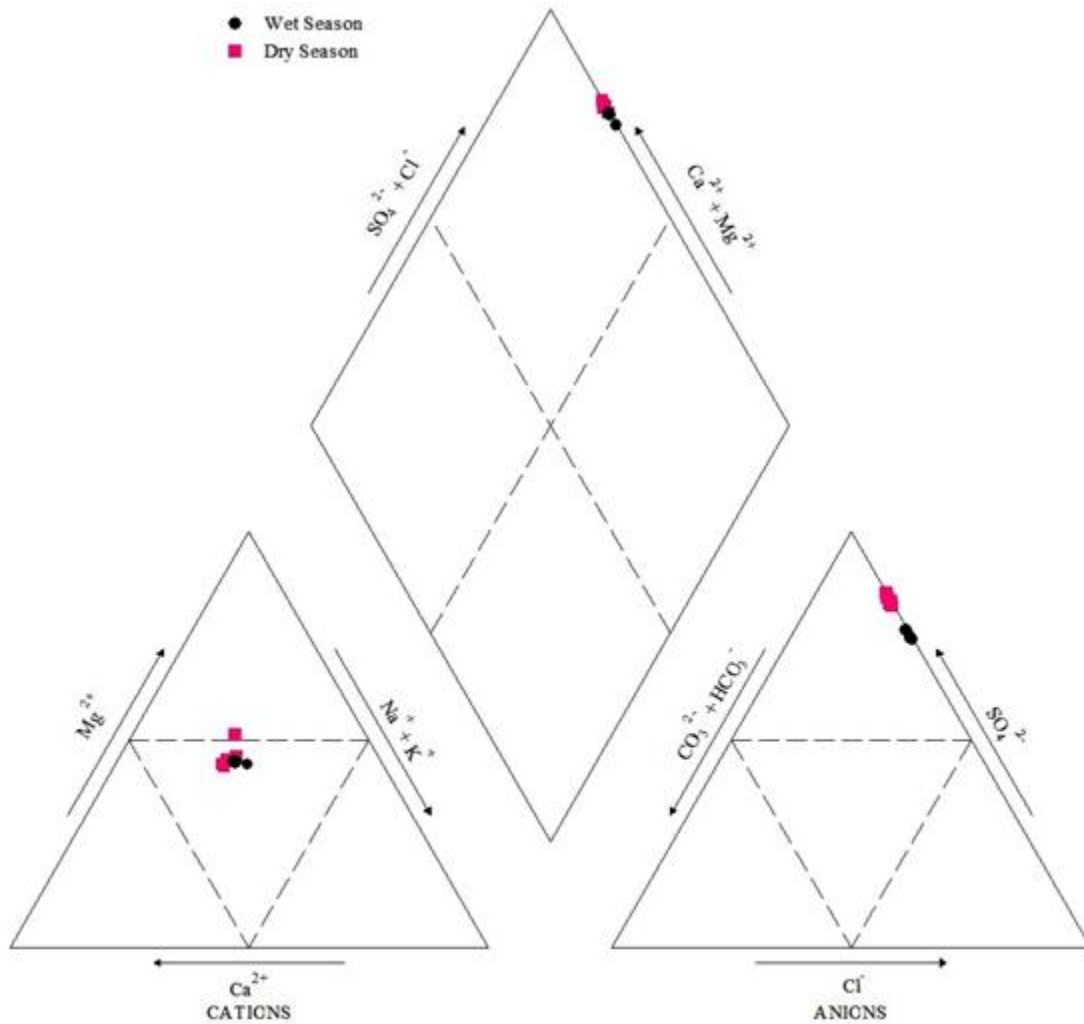


**Figure 5-2: Trilinear piper plot for both dry and wet seasons**

For the dry and wet season, all samples show  $\text{SO}_4^{2-}$  contents making up to 80% of the total anion load, indicating mixed water, without  $\text{Ca}^{2+}$  and  $\text{Mg}^{2+}$  cations exceeding 50% concentrations. When the concentrations of the ions were evaluated, it was observed that the OPGW was relatively rich in  $\text{SO}_4^{2-} > \text{Cl}^- > \text{Mg}^{2+} > \text{Ca}^{2+} > \text{Na}^+ > \text{K}^+$  during the dry season. Additionally, an increase of  $\text{Na}^+$  is likely to be attributed to silicate weathering (Brindha *et al.*, 2017). An increase in  $\text{Cl}^-$  concentrations indicated an anthropogenic effect or flow of water into a nearby aquifer (Kumar *et al.*, 2006).

Overall, the groundwater has a distinct Na-Cl character, mainly due to the geochemical composition of the crystalline rocks and alluvium from the Namaqua Metamorphic Complex (Titus, 2002; Van Wyk *et al.*, 2012; Braune and Xu, 2010; Xu and Braune, 2009) which primarily hosts groundwater in the study area. The chemical composition of the OPGW indicated the dominance of the  $\text{Na}^+$  and  $\text{Cl}^-$  ions resulting in a Na-Cl water type, results similar to those obtained by Nakwafila (2015). The Na-Cl dominant rainfall, dissolution and leaching of evaporates can further augment the salinity of the groundwater (Van Wyk *et al.*, 2012). The hydrochemistry of the area

indicates dissimilar groundwater composition due to complex geochemical processes whereby groundwater flow takes place and its chemistry is controlled primarily by redox reactions, dissolution and mixing processes. Under excessive evaporative conditions due to climatic aridity, groundwater salinity is observed to increase (Abiye and Leshomo, 2013). Anions such as  $\text{Cl}^-$  and  $\text{SO}_4^{2-}$  dominated the OPGW composition, a phenomena attributable to gypsum and pyrite oxidation including halite dissolution which was reported by Raith *et al.* (2003) in this area. These processes might contribute to the ion enrichment facilitated by dissolution, redox reactions and evaporation, which will promote consistent dissolution due to water–rock interactions. Geogenic sources of chemical constituents especially PTEs (Abiye and Leshomo, 2013) might contribute to the poor water quality in the region. The OPGW was mostly classified into three types:  $\text{Ca}^{2+}\text{--Mg}^{2+}\text{--Cl}^- \text{--SO}_4^{2-}$ ;  $\text{Ca}^{2+}\text{--Mg}^{2+}\text{--F}^-$  and  $\text{Ca}^{2+}\text{--Mg}^{2+}\text{--SO}_4^{2-}$ . The presence of these waters was attributed to the geology of O’Kiep with its rock forming feldspars comprising of anorthosite, and amphibole (Ca-bearing) (Clifford and Barton, 2012). The  $\text{Ca}^{2+}\text{--Mg}^{2+}\text{--SO}_4^{2-}$  water type represents effects of ARD and sulfide-mineral dissolution (Lee *et al.*, 2005).

The geochemical modelling performed with PHREEQC indicated that the cation exchange plays a significant role in controlling the OPGW chemistry. Additionally, the data generated suggested that a number of geochemical factors are influential; namely temperature and pH. Figure 5-3 lists minerals that are partially in equilibrium and which are likely to precipitate during contact between species. Chalcocite,  $\text{CuSe}$ , Anilite and  $\text{Cu}_3\text{Se}_2$  appeared to be the minerals with the greatest chance of precipitation followed by  $\text{Mn}_2\text{Sb}$  and  $\text{AlSb}$ , respectively.  $\text{Cu}_3\text{Se}_2$ ,  $\text{FeSe}_2$  and  $\text{HgSb}$  had values greater than 10 while gypsum was likely to remain in equilibrium. Furthermore,  $\text{Cu}_3\text{Se}_2$  was identified as the most saturated and most likely to precipitate.  $\text{MnHPO}_4$  is labelled as the least saturated and has a minute chance to precipitate than the others. Chalcocite is known to contain the highest copper content (Beale, 1985), which translates to high copper concentrations according to the model; albeit, high values do not always ensure precipitation and are highly dependent on the reaction of the mineral in solution (Bosire *et al.*, 2018). Several other minerals such as halite were determined to remain in a dissolution state (see S2).

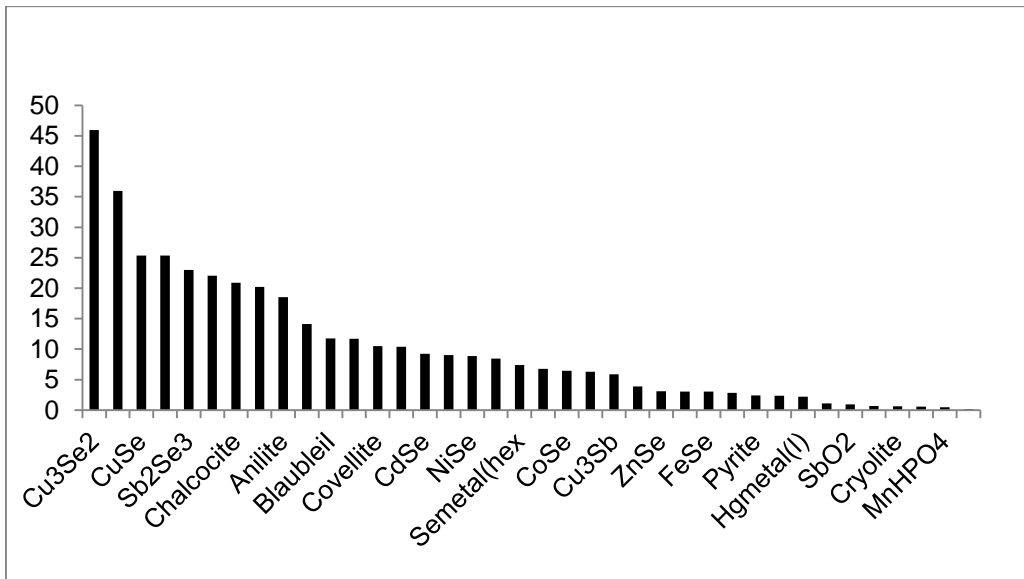


**Figure 5-3: The graph represents the mineral phases that could potentially precipitate during the mixing of the dry and wet season**

The temporal variations in the hydrochemical characteristics of the OPGW corresponded well with fluctuations in sampling locations. Interestingly, the OPGW sampling was conducted at <10 m whereby the chemical evolution would be driven in part by biogeochemical reactions, evapoconcentration, and rock-water interactions (Mladenov *et al.*, 2014). Sample depth showed no significant seasonal variation during the monitoring period, implying that temporal variations in hydrochemical characteristics in the OPGW were affected by either or internal sources surface contributions (Shen *et al.*, 2019). The hydrochemical characteristics of the samples in both seasons (<10 m) showed insignificant seasonal variation, and any change in the hydrochemical characteristics of the OPGW was inferred as being associated with local anthropogenic activities.

### 5.5.2 Evaluation of the ionic content of the groundwater in O’Kiep

Ionic ratios of the OPGW are presented in Table 5-2. Hydrochemical indices assessed the salinity and origin of the groundwater in the study area.

**Table 5-2: Ionic ratios of the open-pit groundwater**

Units	Dry Season (n = 5)			Wet Season (n = 5)		
	Min	Max	Average	Min	Max	Average
CaCO <sub>3</sub> /Cl	0.02	0.01	0.01	0.01	0.01	0.01
Mg/Ca	0.80	1.08	0.91	0.89	0.93	0.90
Na/Ca	0.77	0.89	0.82	0.89	1.06	0.94
Na/Cl	0.69	0.74	0.72	0.50	0.53	0.49
Ca/Cl	0.90	0.83	0.87	0.56	0.50	0.52
K/Cl	0.05	0.06	0.05	0.03	0.03	0.03
Ca/SO <sub>4</sub>	0.14	0.10	0.12	0.13	0.12	0.12

Generally, composition relations among dissolved species can reveal the source of solutes and the processes that generated the observed groundwater composition. Since Na, Ca, Cl, K, Mg, SO<sub>4</sub> were predominant ions in the OPGW, an analysis was made of stoichiometric relations that could account for the relative concentrations of these ions. The average Na/Cl ratios for both dry and wet seasons were approximately 0.7 and 0.5, respectively, which is an indication of an alluvial aquifer since the ratio is less than 1 (Fisher, 1997). Overall, Mg/Ca, Na/Ca, Ca/Cl, K/Cl and Ca/SO<sub>4</sub> ratios were all less than 2.0.

According to the interpretation of these indices, the groundwater in the study appears to be slightly of inland origin, because groundwater under marine influence would have ratio values of approximately 5 (Morrel *et al.*, 1986). An exception whereby other processes such as cationic exchange with localised waste materials would then contribute to increased ratio values up to 4 (Nwankwoala and Udom, 2011). Ratios of Na/Ca, indicating cation exchange reaction can show some mixed behaviour but would mostly decrease with decreasing TDS during the wet season while an increase would be observed during the dry season. This is a good indicator of salinisation processes in an aquifer (Nwankwoala and Udom, 2011; Edet and Okereke, 2002).

### **5.5.3 The coefficient of variation and correlation analysis of the groundwater in O’Kiep**

The variation among various OPGW quality parameters were calculated and the values are given in Tables 5-3 and 5-4. The resultant correlation analysis illustrated that COD showed a good negative correlation (-1.0) with pH and temperature, and a positive correlation (+1.0) with EC, DO and ORP. The COD also showed a medium to weak correlation with turbidity, TDS and salinity. A significant positive correlation of SO<sub>4</sub><sup>2-</sup> was noticed with Na<sup>+</sup>, Mg<sup>2+</sup> and K<sup>+</sup>; although, EC and TDS had a good correlation between salinity and DO in the dry season. The good correlation of Ca<sup>2+</sup>, Mg<sup>2+</sup>, Cl<sup>-</sup> and PTEs (except Fe) with SO<sub>4</sub><sup>2-</sup> indicated that most of the ions were involved in hydrochemical reactions and seasonal changes of groundwater in O’Kiep, which indicated a common origin for these ions (Sahraei Parizi and Samani, 2013). The groundwater mineralisation is predominantly related to these components (Shorieh *et al.*, 2015). Such a correlation was obvious as EC is normally a function of dissolved ionic species in groundwater (Appelo and Postma, 2004). The COD and DO did not show any significant relationship with any of the tested parameters during the wet season. The Cl<sup>-</sup> also showed a significant positive relationship with Na<sup>+</sup>, Mg<sup>2+</sup> and K<sup>+</sup>. The turbidity had a positive correlation with pH, TDS, salinity and ORP during the wet season.

**Table 5-3: Correlation coefficient for different parameters during dry season in the open-pit groundwater in O’Kiep**

Chemistry Parameters	COD	Colour	Turbidity	pH	Temperature	EC	TDS	DO	Salinity	ORP
COD	1									
Colour	0,6	1								
Turbidity	0,6	0,6	1							
pH at 25°C	-1,0	-0,2	-0,8	1						
Temperature	-1,0	0,1	-0,7	<b>0,9</b>	1					
EC	<b>1,0</b>	0,2	-0,5	0,4	0,7	1				
TDS	0,3	0,2	-0,5	0,4	0,7	<b>1,0</b>	1			
DO	<b>1,0</b>	0,4	-0,5	0,6	<b>0,9</b>	0,8	0,8	1		
Salinity	0,4	0,2	-0,5	0,4	0,7	<b>1,0</b>	<b>1,0</b>	0,7	1	
Redox (ORP)	<b>1,0</b>	0,5	-0,5	-0,8	-0,5	-0,2	-0,2	-0,1	<b>1,0</b>	1
Cation & Anion Parameters	Ca <sup>+</sup>	Na <sup>+</sup>	Mg <sup>2+</sup>	K <sup>+</sup>	F <sup>-</sup>	Cl <sup>-</sup>	SO <sub>4</sub> <sup>2-</sup>	NH <sub>3</sub>	P	
Calcium (Ca)	1									
Sodium (Na)	0,7	1								
Magnesium (Mg)	0,5	<b>1,0</b>	1							
Potassium (K)	0,5	0,7	1,0	1						
Fluoride (F <sup>-</sup> )	0,3	-0,2	-0,2	-0,1	1					
Chloride (Cl <sup>-</sup> )	0,6	<b>0,9</b>	<b>0,9</b>	0,8	-0,1	1				
Sulfate (SO <sub>4</sub> <sup>2-</sup> )	0,5	0,7	<b>1,0</b>	<b>1,0</b>	-0,1	0,8	1			
Ammonia (NH <sub>3</sub> )	0,1	0,0	0,5	0,6	0,4	0,3	0,6	1		
Ortho-Phosphate (P)	-0,1	0,5	0,4	0,4	-0,2	0,7	0,3	0,2	1	
Elemental Parameters	Al	Cd	Cr	Co	Cu	Fe	Mn	Ni	Zn	CN
Aluminium (Al)	1									
Cadium (Cd)	<b>0,9</b>	1								
Chromium (Cr)	<b>1,0</b>	<b>1,0</b>	1							
Cobalt (Co)	0,6	0,5	0,2	1						
Copper (Cu)	0,8	<b>1,0</b>	<b>1,0</b>	0,3	1					
Iron (Fe)	<b>1,0</b>	<b>1,0</b>	-0,2	0,2	<b>1,0</b>	1				
Manganese (Mn)	0,8	-0,1	0,5	<b>1,0</b>	0,5	0,6	1			
Nickel (Ni)	<b>1,0</b>	<b>1,0</b>	<b>1,0</b>	0,4	<b>1,0</b>	<b>1,0</b>	0,6	1		
Zinc (Zn)	<b>1,0</b>	0,0	-0,1	0,0	-0,2	-0,3	0,0	-0,1	1	
Cyanide (CN)	<b>0,9</b>	0,4	0,4	0,2	0,6	0,6	0,3	0,5	-0,9	1

**Table 5-4: Correlation coefficient for different parameters during wet season in the open-pit groundwater in O’Kiep**

Chemistry Parameters	Turbidity	pH	Temperature	EC	TDS	Salinity	ORP			
Turbidity	1									
pH at 25°C	<b>0.9</b>	1								
Temperature	0.2	0.5	1							
EC	-1.0	-0.9	-0.2	1						
TDS	<b>1.0</b>	<b>0.9</b>	0.0	-1.0	1					
Salinity	<b>1.0</b>	<b>0.9</b>	<b>0.1</b>	-1.0	<b>1.0</b>	1				
Redox (ORP)	<b>1.0</b>	-0.8	-0.1	<b>0.9</b>	-1.0	<b>1.0</b>	1			
Cation & Anion Parameters	Ca <sup>+</sup>	Na <sup>+</sup>	Mg <sup>2+</sup>	K <sup>+</sup>	F <sup>+</sup>	Cl <sup>-</sup>	SO <sub>4</sub> <sup>2-</sup>	NH <sub>3</sub>		
Calcium (Ca)	1									
Sodium (Na)	-0.2	1								
Magnesium (Mg)	-0.4	1.0	1							
Potassium (K)	0.0	<b>0.9</b>	<b>0.9</b>	1						
Fluoride (F <sup>-</sup> )	0.2	-0.8	-0.8	-0.5	1					
Chloride (Cl <sup>-</sup> )	0.1	0.1	0.1	0.5	0.5	1				
Sulfate (SO <sub>4</sub> <sup>2-</sup> )	-0.2	<b>1.0</b>	<b>1.0</b>	<b>0.9</b>	-0.8	0.1	1			
Ammonia (NH <sub>3</sub> )	-0.3	0.1	0.2	-0.3	-0.7	-1.0	0.1	1		
Elemental Parameters	Al	Cd	Cr	Co	Cu	Fe	Mn	Ni	Zn	CN
Aluminium (Al)	1									
Cadium (Cd)	-0.6	1								
Chromium (Cr)	0.3	-0.4	1							
Cobalt (Co)	0.7	-0.1	-0.5	1						
Copper (Cu)	-0.1	0.3	-1.0	0.6	1					
Iron (Fe)	-0.5	0.2	-0.1	0.1	0.8	1				
Manganese (Mn)	<b>0.9</b>	0.1	0.6	0.3	-0.5	-0.6	1			
Nickel (Ni)	<b>1.0</b>	-0.7	0.2	0.7	0.0	-0.3	<b>0.9</b>	1		
Zinc (Zn)	<b>1.0</b>	-0.6	0.4	0.6	-0.2	-0.6	<b>0.9</b>	<b>0.9</b>	1	
Cyanide (CN)	<b>0.9</b>	-0.7	-0.1	0.8	0.2	0.0	0.7	<b>1.0</b>	0.8	1

In the present study, the significant correlations were observed among various metal pairs: Cd-Al, Cr-Al, Cu-Al, Fe-Al, Mn-Al, Zn-Al and CN-Al in the dry season, and between Ni-Al, Zn-Al, Mn-Al, CN-Al, Ni-Mn, Zn-Mn, Zn-Ni, CN-Zn, CN-Ni, C-Co in the wet season. The correlation between metal pairs indicated the existence of a common source of origin for these PTEs, or mutual concentration dependence of the metals (Chabukdhara *et al.*, 2017) in the OPGW. Such relationships of various physical parameters and metallic ions are expected due to several hydrochemical reactions such as ion exchange and oxidation-reduction in a groundwater aquifer system (Chabukdhara *et al.*, 2017).

## 5.6 Summary

This part of the study assessed the seasonal variation of the OPGW quality near a CMM in O’Kiep (South Africa) and to determine its suitability for drinking and irrigation. It was shown that changes in seasons have an influence on the hydrochemical properties of the OPGW as evidenced by the low DO and metallic ion concentration in both seasons showing prevailing anoxic conditions including a deficiency of organic matter in the OPGW. Furthermore, the results also indicated that the groundwater was slightly acidic, with high salinity during both the dry and wet season; albeit SAR during both seasons showed that the OPGW was suitable for irrigation purpose; however, long-term use may cause damage to the soil. This was also further confirmed by a Mg/Ca ratio of less than 1.5, with PHREEQC also suggesting that cation exchanges played a significant role in controlling the OPGW chemistry with chalcocite, CuSe and Cu<sub>3</sub>Se<sub>2</sub> appearing to be the minerals with the greatest chance of precipitation followed by Mn<sub>2</sub>Sb and AlSb, respectively. The results of the present study provides information that can be useful for water resource management in the O’Kiep area, particularly with respect to biodiversity changes due to anthropogenic effects. Based on these results, a water treatment system is recommended as a remedial measure for the contaminated OPGW in O’Kiep. Clearly, the groundwater characteristics indicated possible contamination and the waters’ acidity suggested a potentiality to form ARD in future; an assertion which needed to be evaluated (Chapter 6) as this will directly impact the usability of the groundwater for anthropogenic purposes. The contamination of the groundwater by PTEs from soils in study area also needed to be evaluated.

## CHAPTER 6: RESULTS AND DISCUSSION

---

Published as:

- 1]. **Erdogan, I.G.**, Fosso-Kankeu, E., Ntwampe, S.K., Waanders, F.B., Hoth, N. and Rand, A. 2019. Acid rock drainage prediction of metalliferous soils from O’Kiep, Namaqualand, South Africa: A humidity cell test assessment. In IMWA 2019 Conference – Mine Water: Technological and Ecological Challenges, Perm, Russia.  
Available: [https://www.imwa.info/docs/imwa\\_2019/IMWA2019\\_Erdogan\\_613.pdf](https://www.imwa.info/docs/imwa_2019/IMWA2019_Erdogan_613.pdf)
  
- 2]. **Erdogan, I.G.**, Fosso-Kankeu, E., Ntwampe, S.K., Waanders, F.B., Hoth, N. and Rand, A. 2018. Potential toxic elements contamination of soils in O’Kiep, an arid region of Namaqualand, South Africa. In 10th International Conference on Advances in Science, Engineering, Technology and Healthcare ASETH-18), Nov. 19-20, Cape Town, South Africa.  
Available: <https://doi.org/10.17758/EARES4.EAP1118238>

## **6.1 Acid rock drainage prediction of metalliferous soils from O’Kiep, an arid region of Namaqualand, South Africa: A humidity cell test assessment**

### **6.2 Introduction**

Worldwide, soil contamination has increasingly been studied by various researchers, including in South Africa, with the support of environmental protection organisations (Chen *et al.*, 1997). In South Africa, some studies have been conducted on metal pollution in gold (Naicker *et al.*, 2003), coal (Fosso-Kankeu *et al.*, 2016) and diamond (Bizzi, 2017) mining areas. However, minimal studies have reported on the PTEs of soil in copper mining areas, especially in O’Kiep, South Africa. The area under study is the oldest formally proclaimed copper mining area in South Africa (Yuhara *et al.*, 2001). Soils can be a reservoir of large quantities of PTEs from several sources, including municipal and industrial waste, which includes mining gangue (Rashed, 2010). However, the physicochemical characteristics of the soil is a vital indicator which influences the dispersion of PTEs in contaminated areas (Fosso-Kankeu *et al.*, 2014). Contaminated soils, including arable land, especially in O’Kiep, are no longer suitable for farming, since they are unable to yield healthy crops.

O’Kiep soils have been described as being highly polluted, with the area indicative of significant environmental damage with PTEs in the bound forms (Moncho *et al.*, 2017). Some metal recycling occurs as a result of organic matter decomposition, with soluble minerals being mobilised by interaction of carbonic acid and water. Relatively insoluble minerals such as quartz (SiO<sub>2</sub>) disintegrate as finer particles and the end result of weathering is soil (Sakala *et al.*, 2017). The persistent wind in the area has also been considered a health problem in this town (Rozendaal and Horn, 2013).

In historic metalliferous mining areas, soils are usually enriched with PTEs. These PTEs are from geochemical processes, weathering of mineralised zones and from different mining activities, including disposal of mine wastes (Gałuszka *et al.*, 2015; Nannoni *et al.*, 2011). The mineralogy reported for the O’Kiep mining area are bismuthinite, bornite, chalcocite, chalcopyrite, covellite, galena, ilmenite, magnetite, molybdenite, pentlandite, pyrite, pyrrhotite, quartz, scheelite, sillimanite, sphalerite and thorite (Cairncross, 2004; Raith and Stein, 2000). In some warm-climate areas, including O’Kiep, where chemical weathering dominates, soils tend to be richer in clay – resulting in the localisation entrapment of some PTEs. The closed mining areas are often a source of severe environmental problems caused by the mobility of PTEs and consequently the formation of acid mine drainage (García-Lorenzo *et al.*, 2012), with chemical and biochemical reactions proceeding fastest under warm conditions (Earle, 2016). Before rehabilitation of soils in historic mining areas, it is essential to establish the geochemical characteristics of metals in the soils. The

bioavailability and mobility of PTEs in surface soils were examined in O’Kiep by Moncho *et al.* (2017), with application of sequential extraction analysis. Characterising the factors affecting bioavailability, leaching and toxicity of metals and metalloids in soil to water sources is of paramount importance. This is true although metals and metalloids are significant natural components of all soils, where their presence in the mineral fraction comprises a storage of potentially mobile species that have a negative influence on soil geochemistry and groundwater (Gadd, 2008; Violante *et al.*, 2010).

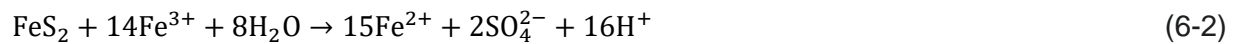
In South Africa, attention has been drawn to the mining industries and their adverse effects on the environment and their posing potential health risks to communities such as those at O’Kiep. Copper contamination of the whole region is the result of processing of copper ores from a CMM. Produced waste material from this mine was stored in the numerous SMW heaps and a TSF. Rehabilitation of the mine, including copper oxide ore dumps and extensive slime dams, remains a challenge and are earmarked for redistribution and reprocessing (Rozendaal and Horn, 2013). This site is well known for copper mining in the past. However, the mining activity ceased in 2007 and the area has been under slow but systematic rehabilitation ever since (Rozendaal and Horn, 2013). The mineralogy and geochemistry of this soil were never examined.

Metalliferous mining usually causes environmental contamination challenges due to MSW impacting on the hydrology, topography and local vegetation. This culminates in the destruction of natural habitats and degradation of soils, essentially resulting in the subsequent collapse of the environment in which the mining is taking place (Moncho *et al.*, 2017; Wahsha *et al.*, 2012). As a result, metalliferous soils are exposed to environmental conditions in these metalliferous mining areas, culminating in a variety of biological, chemical and physical activities which could facilitate the formation of a high concentration of PTEs (Asensio *et al.*, 2013). PTEs such as As, Ba, Cu, Pb, Se and Zn may pose potential human health risks, especially in areas with mining activities (De Souza *et al.*, 2019; Sevilla-Perea *et al.*, 2016; Cheng *et al.*, 2009).

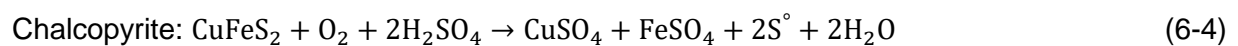
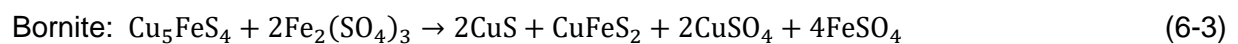
Earlier studies have shown that metalliferous soils from the O’Kiep area have higher concentrations of PTEs, as geochemically characterised by Moncho *et al.* (2017). PTEs are usually present in metalliferous soils, albeit in concentrations that may be higher in mining overburden and tailings than in soils, a risk which has to be investigated to minimise environmental and human health implications (Portales *et al.*, 2015). According to Fey (2010), the soil texture and type in arid regions consist of a different principle of soils with special subsoil characteristics comprising of calcic and silicic constituents.

O’Kiep is a former Cu mine area with ore mineralisation being dominated by Cu-rich sulfide minerals, that is chalcopyrite and bornite, which are the most abundant copper-bearing minerals

in the area (Maier *et al.*, 2012; Maier, 2000). The predominant Cu minerals that occur in the ore body are bornite ( $\text{Cu}_5\text{FeS}_4$ ), chalcopyrite ( $\text{CuFeS}_2$ ), chalcocite ( $\text{Cu}_2\text{S}$ ), malachite ( $\text{Cu}_2\text{CO}_3(\text{OH})_2$ ) and magnetite ( $\text{Fe}_3\text{O}_4$ ), as seen in an unpublished document by the O’Kiep Copper Company. The geology of the O’Kiep region is comprised of granite gneiss and the host rock of the copper ore consists of jotunite, anorthosite, biotite, diorite as well as hypersthene rocks that range from hypersthene to leuconorite (Smuts, 2015; Clifford and Barton, 2012; Reid and Barton, 1983). Cairncross (2004) also describes an ore near the O’Kiep area containing calcite ( $\text{CaCO}_3$ ), chalcocite ( $\text{Cu}_2\text{S}$ ), chalcopyrite ( $\text{CuFeS}_2$ ), fluorite ( $\text{CaF}_2$ ) and gypsum ( $\text{CaSO}_4 \cdot 2\text{H}_2\text{O}$ ). Some of these constituents undergo oxidation that is pyrite oxidation, which initiates ARD, one of the biggest environmental challenges in the mining and mineral industry. ARD enhances the dissolution of rocks and acidifies aquifers, processes which mobilise PTEs (Egiebor and Oni, 2007). The oxidation process of pyrite can be described by the reactions in Eqns. 6-1 and 6-2 (Feng *et al.*, 2019):



Similar to pyrite, bornite and chalcopyrite can undergo oxidation. Although sparingly soluble in water, under ARD, these minerals may produce by-products of different geochemical characteristics. The oxidation of both bornite and chalcopyrite can be signified by Eqns. 6-3 to 6-5 (Watling, 2006).



Since  $\text{SO}_4$  is an abundant and ubiquitous polyatomic constituent available in the earth’s lithosphere and hydrosphere, in higher concentration, it can contaminate water sources (Alpers *et al.*, 2018), particularly as a result of mining. The reactivity of mine tailings and waste can result in the formation of ARD (Elghali *et al.*, 2019), which has been described as an environmental risk matter for mining companies (Blowes *et al.*, 2014; Qian *et al.*, 2019). ARD forms mainly due to the oxidation of pyrite ( $\text{FeS}_2$ ) via a process facilitated by bacteria, water and oxygen and as a result of natural and biochemical weathering processes (Qian *et al.*, 2019; Yu and Hunt, 2018). This occurs particularly when there is an inadequate neutralisation potential (NP) of the rock phase by their carbonate content, that is calcite and dolomite (Elghali *et al.*, 2019). The NP constituents include gypsum, ferric oxyhydroxides and iron sulfates (Quispe *et al.*, 2013), which

create an equilibrium between oxidation and neutralisation reactions, resulting in numerous secondary mineral production and precipitates (Nordstrom *et al.*, 2015).

If the rate of acid generation due to sulfide oxidation is in excess of acid ingesting by neutralising minerals, the progression into the formation of low pH mine water may ensue. In addition to the acidity produced, the consequent mobilisation and solubilisation of rock would result in PTEs, particularly at low pH. This would further lead to ARD, thus severely impacting the receiving environment. The ultimate goal of the research reported herein was to use these tests in conjunction with other relevant data to assist with the development of strategies for the management of mine wastes (Lapakko, 2003), including the metalliferous soils of O’Kiep.

### **6.3 Objectives**

The objectives of this part of the study were:

- to evaluate geochemical and mineralogical studies of the soils;
- to predict ARD potential;
- to assess the environmental impacts of soils in O’Kiep, especially post-mining; and
- to determine weathering rates using the HCTs and the variation in leachate quality.

### **6.4 Materials and methods**

#### **6.4.1 Sample collection**

Sandy-silt-clay metalliferous soil samples with limited agricultural potential were collected from O’Kiep, Namaqualand, South Africa at a geological location of 29° 35’ 45” S, 17° 52’ 51” E (38.63 km<sup>2</sup>) in the Northern Cape. This area is described as arid with a temperature of 37°C with an estimated evaporation rate of 2879 mm per year greatly exceeding the precipitation rate (Smuts, 2015). This high evaporation rate which significantly exceeds the rate of rainfall highlights water scarcity and the dryness of the area. The metalliferous soil samples were collected as per field soil sampling guidelines by means of haphazard, judgement, probability and analysis of soils method described by Gregorich and Carter (2007) and Schoeneberger (2012). The sampling site was cleared of litter, living plants and surface rocks prior to sample collection. The subsoil was sampled from a spolic and transportic soil layer at a subsurface depth of approximately 1 to 1.5 m (Meuser, 2010) using a Draper 24414 steel auger (Schoeneberger *et al.*, 2012; Ferguson *et al.*, 2007). Figure 6-1 enlists the sampling locations (marked using a GPS), namely highland (OCM1, OCM2, OCM3); midland (OCM4, OCM5, OCM6) and lowland (OCM7, OCM8, OCM9, OCM10). All metalliferous soil samples (n = 10, 5 kg each) were collected in August 2017 during the wet season and sampling points were marked using a GPS.

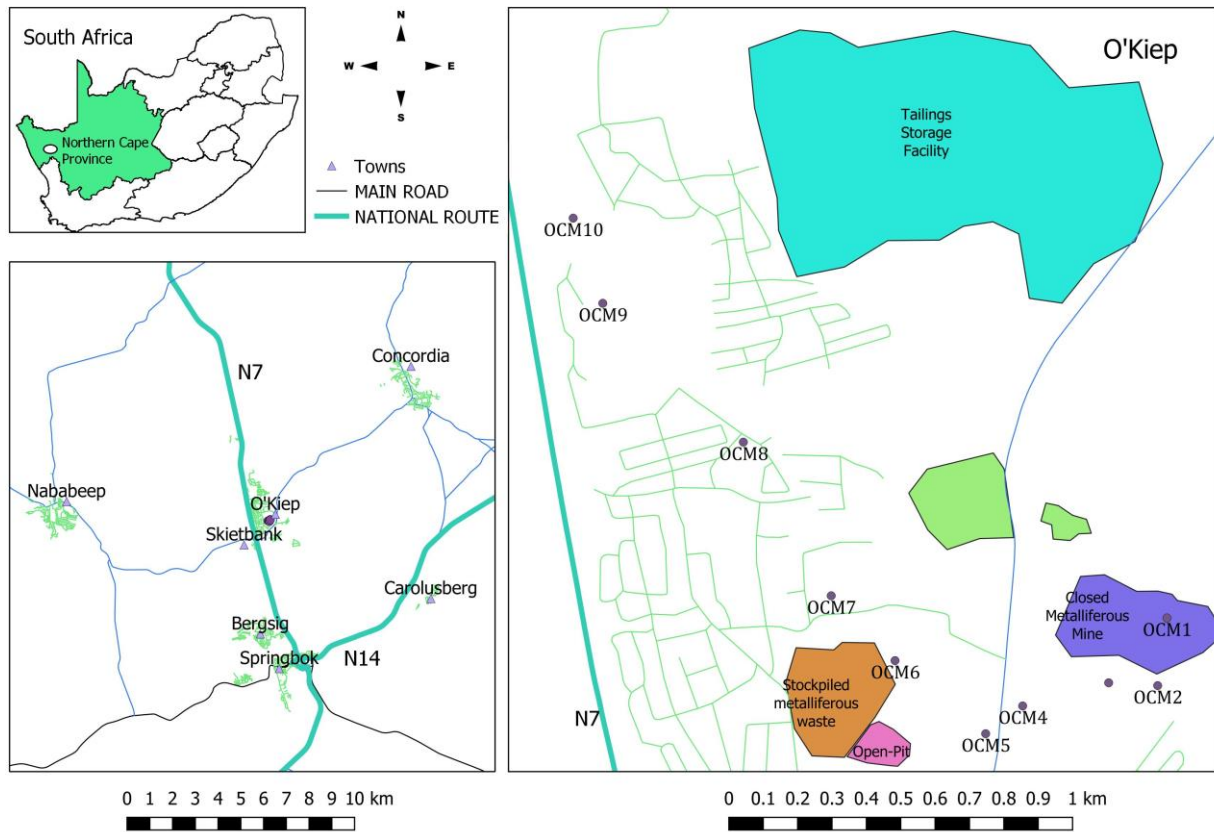


**Figure 6-1: Location of study area and sampling points: Geological maps were generated using Quantum GIS software (v. 2.18.11) and data from National Geo-Spatial Information (NGI), a component of the Department of Rural Development and Land Reform, South Africa**

Each metalliferous soil sample was collected using polypropylene buckets washed with diluted 0.5 M HCL and sterile distilled water to minimise environmental and physical alteration. As mentioned, sampling locations were cleared of litter and surface rocks prior to sample collection. These subsoil samples were collected based on field examination to account for physical weathering and surface conditions. All sample buckets were labelled and transported to the laboratory. All samples were air dried at an ambient temperature, and subsequently screened using a 2 mm sieve prior to further analyses. A portion of each metalliferous soil sample was used for soil mineralogical characterisation, ABA and HCTs. Further analytical analyses were performed, including quantitative mineralogical assessment of the soil using X-ray diffraction (XRD) and X-ray fluorescence (XRF) (Smith *et al.*, 2014).

#### 6.4.2 Acid-generation potential

The potential ARD sources in O'Kiep are the partially rehabilitated metalliferous mine, SMW and MTs (see Figure 6-1). O'Kiep soils also have the potential to generate ARD due to their physico-geochemical characteristics (Moncho *et al.*, 2017). A modified field and laboratory test method for ABA was used for each metalliferous soil sample, as described by Sobek (1978). Additionally, a prediction test was performed using a paste for pH testing to assess individual samples' acid-

forming characteristics, as described by Kwong (1993). Furthermore, the acidity potential (AP) was quantified based on total sulfur content ( $S_{total}$ ). In addition, the NP was determined using a titration experiment, whereby NaOH (0.1 N) and HCl (1 N) were used for each sample. Subsequently, the determination of AP and NP allowed for the computation of the net neutralisation potential (NNP), including the neutralising potential ratio (NPR), as described by Price (2009). This is a criterion used for the determination of the acid rock drainage formation potential (ARDP) of the metalliferous soil samples.

### 6.4.3 Humidity cell tests

The HCTs of each homogenised metalliferous soil sample (1 kg) were performed in a capped Perspex cylindrical chamber (203 mm height x 102 mm diameter), as described in Morin and Hutt (2001) and Lapakko (2003). The metalliferous soil samples were placed at the bottom of the humidity cell, as shown in Figure 6-2.

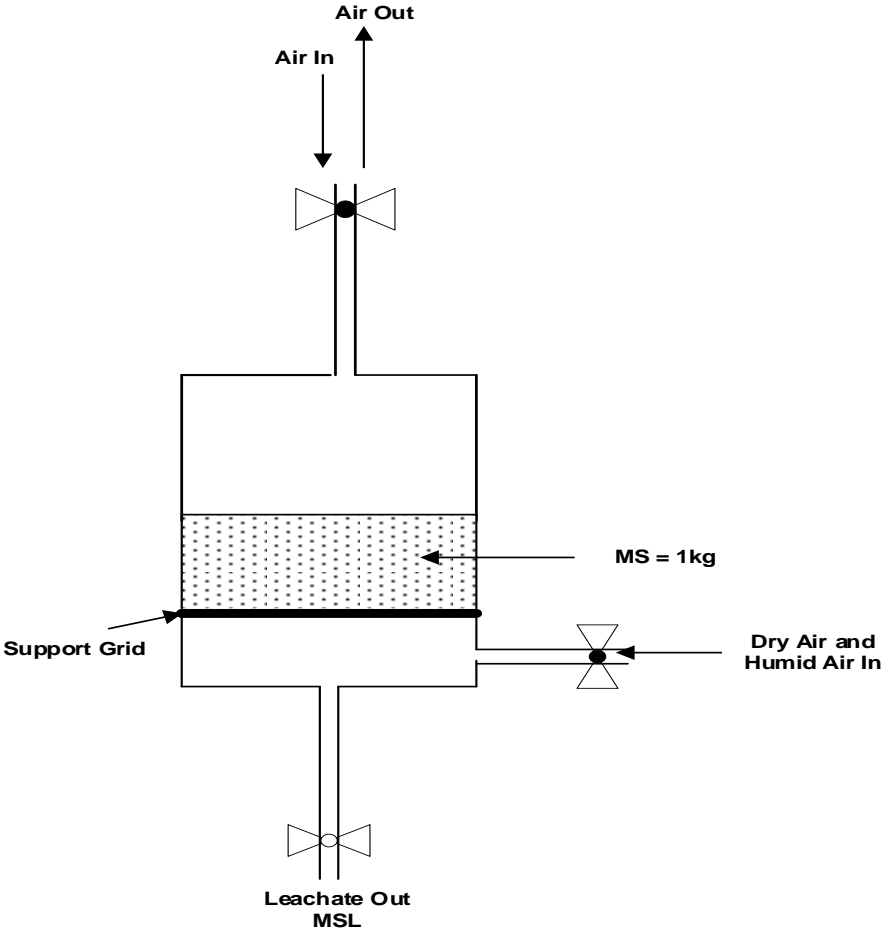


Figure 6-2: Schematic diagram of humidity cell tests

After the metalliferous soil samples had been placed at the bottom of the humidity cell, 750 mL of sterile deionised water was added to each test chamber for the initial immersion of the

metalliferous soil samples. The HCTs were run for 21 weeks, with each week cycle consisting of the following procedure: leach cycle (1 day), dry air cycle (3 days) and moist air cycle (3 days). After each week cycle, metalliferous soil leachates (MSL) of 750 mL were collected into flasks. Subsequent to filtration (45 µm filter into polyethylene bottles of 500 mL capacity), the MSL produced were analysed for quality characterisation to account for alkalinity, EC, pH, TDS, sulfate (SO<sub>4</sub>) and for PTEs using ICP-MS as per the 6020B method described in EPA (2014).

## 6.5 Results and discussion

### 6.5.1 Mineralogical composition of the metalliferous soil samples

In the O’Kiep region, several secondary minerals have been observed at the surface (Gibson *et al.*, 1996). These minerals occur as fine-grained particles described as efflorescent salts (Fosso-Kankeu *et al.*, 2017). The presence of these minerals in large quantities is indicative of rapid acidification potential, particularly if ARD-formation processes are initiated. Therefore, PTEs generated by dissolution and oxidation of the primary minerals may lead to the incorporation of secondary minerals into the local environment by adsorption and/or ion exchange (Hakkou *et al.*, 2008). There was a variation among the metalliferous soil mineralogical composition based on the XRD results obtained. However, the dominant mineralogical constituents (Table 6-1) were quartz and albite.

**Table 6-1: Averaged mineralogical composition of metalliferous soils from the O’Kiep area**

Mineral	Formula	MS (%)
Quartz	SiO <sub>2</sub>	80.1
Albite	NaAlSi <sub>3</sub> O <sub>8</sub>	2.92
Muscovite-1M	KAl <sub>2</sub> Si <sub>3</sub> AlO <sub>10</sub> (OH) <sub>2</sub>	0.19
Halloysite-10A	Al <sub>2</sub> Si <sub>2</sub> O <sub>5</sub> (OH) <sub>4</sub> ·2H <sub>2</sub> O	0.13

Quartz (80.1%) is reported to be less reactive in oxidising conditions and possesses minimal acid-neutralising potential. The presence of albite (2.92%) and muscovite-1M (0.19%) is indicative of an ore body bearing granite and gneisses (Singh, 2005), a characteristic attributed to the geology of the study area. Furthermore, the presence of halloysite-10A (0.13%), also known as kaolinite is indicative of constituents that normally occur in arid soils (Ziegler *et al.*, 2003). During weathering conditions, halloysite-10A is associated with humid climates (Lázaro, 2015) and such conditions are also hypothesised to exist in O’Kiep. Figures 6-3 and 6-4 list both major oxides and PTEs as determined by XRF for the metalliferous soil samples. The samples were characterised by high SiO<sub>2</sub> (67.6%), moderate Al (12.4% as Al<sub>2</sub>O<sub>3</sub>) and Fe (7.3% as Fe<sub>2</sub>O<sub>3</sub>) and K (4.0% as K<sub>2</sub>O), Na (1.9% as Na<sub>2</sub>O) and Ca (1.6% as CaO) (Figure 6-3). The major PTEs (mg/kg) were S (2437) > Cu (57.5) > F (1079) > Ba (674) > Mn (457) > Cl (131) (Figure 6-4).

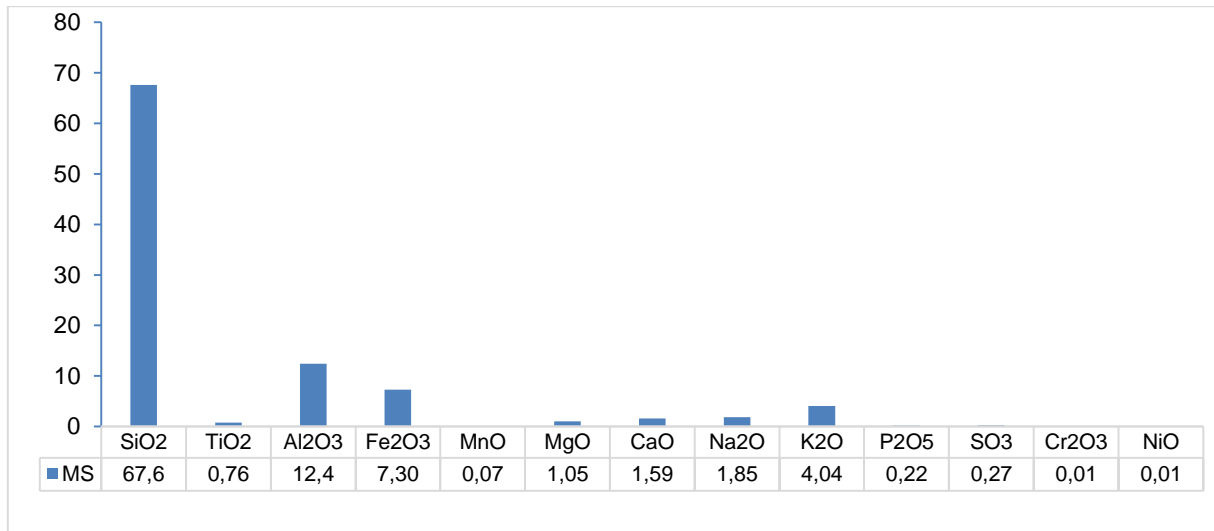


**Figure 6-3: Major oxides of metalliferous soil samples from O'Kiep**

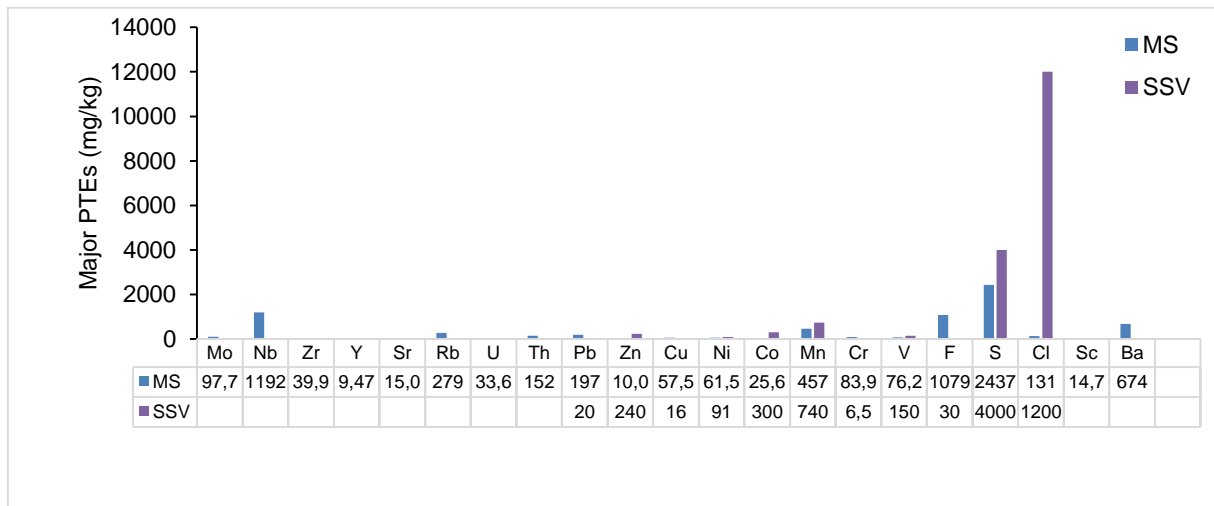


**Figure 6-4: Major potentially toxic element characterisation of metalliferous soil samples compared to soil screening values**

### 6.5.2 Static test-based acid rock drainage formation potential of metalliferous soils

The paste pH of 3.9 indicated that the metalliferous soils of O'Kiep are slightly acidic, which is an indication of the presence of sulfides that could react to form acid, as shown in Table 6-2. This was also confirmed by the total sulfur content of up to 0.89% for the samples tested, with a further low NPR value (0.14). This suggests a considerable percentage of sulfur and a greater potential of ARD production. The total acidity was attributed to dissolve PTEs, which are generally dominant in ARD. The AP was approximated to be high (28 kg CaCO<sub>3</sub>/t), which corresponded to a negative NNP average of -32 kg CaCO<sub>3</sub>/t. By using the criteria as described in Miller *et al.* (1991) in combination with the NP-AP-ratio criteria of Adam *et al.* (1997), the metalliferous soils of O'Kiep can therefore be classified as having a high ARDP.

**Table 6-2: Paste pH and acid-base accounting of metalliferous soils from the O’Kiep area**

	<b>MS</b>
Paste pH	3.9
Sulfur <sub>total</sub> (%) (LECO)	0.89
Acidity Potential (AP) (kg/t)	28
Neutralisation Potential (NP)	-3.91
Net Neutralisation Potential (NNP)	-32
Neutralising Potential Ratio (NPR)	0.141

### 6.5.3 Weathering of metalliferous soils

HCTs are considered to be among the most reliable geochemical characterisation methods for ARDP (Maest and Nordstrom, 2017). Similarly, the ABA test can be used to determine the ARD chemistry, PTE release rates and generic metalliferous soil behaviour when exposed to environmental conditions suited for ARD formation. The geochemical analyses of the MSL using ABA tests exhibited slightly acidic leachate characteristics of AP of 3.9, which were similar to those obtained using the paste pH. There was no clear indication as to the influences of the pH changes, as this parameter can be affected by several environmental mechanisms, including specie retention in the solid phase of the metalliferous soils, thus culminating in MSL characteristic variation during HCTs. As such, the MSL generation and its quality characteristics could be directly associated with factors such as simultaneous oxidation of sulfide species and the dissolution of major oxides and calcite, which would in turn minimise the acidification of the metalliferous soils (Van Zweel, 2015; Strömberg and Banwart, 1999).

The slightly acidic values observed for the metalliferous soil samples of O’Kiep indicated that the generated H<sup>+</sup> ions were to some extent being consumed by the dissolution of the identified aluminosilicate minerals (Romero *et al.*, 2007). This was evidenced by the total alkalinity of the MSL, determined to be <5 mg/kg CaCO<sub>3</sub>. Furthermore, the EC and TDS values of the MSL were initially averaged at 376 mS/m and 5046 mg/kg, respectively, with a sequential steady decline of up to 14 mS/m and 102 mg/kg observed, respectively. Similarly, the SO<sub>4</sub> concentration of the MSL declined from 2682 to 49 mg/kg. Therefore, the variation in EC and TDS profiles was analogous to the observed SO<sub>4</sub> trend. This indicates that the EC and TDS are predominantly associated with SO<sub>4</sub> concentration and metalliferous soil sample decomposition, thus weathering, as shown in Figure 6-5, which was an indication of ARDP (Mäkitalo *et al.*, 2016; Espana *et al.*, 2005).

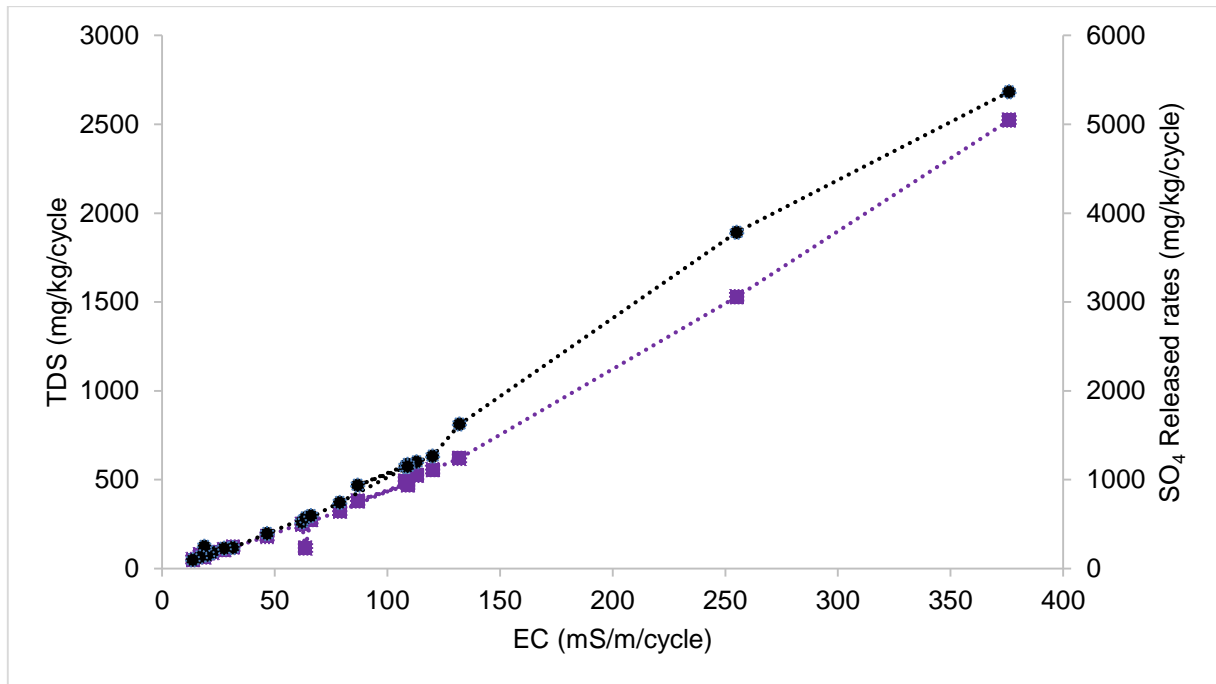


**Figure 6-5: Electrical conductivity correlation to total dissolved solids and sulfate**

Additionally, PTE presence in the MSL indicated dissolution in the liquid phase. This observation is supported by the variation of Si in the MSL, ranging from 4.5 mg/kg to 15.2 mg/kg, albeit with a decrease of Ca from 205.6 to 12.93 mg/kg – a phenomenon associated with complexation of the Ca with other oxide species to form a precipitate. The principal carbonates observed in the metalliferous soils were calcite and quicklime of 1.6%.

As such, the MSL generation and its quality characteristics could be directly associated with factors such as simultaneous oxidation of sulfide species and the dissolution of major oxides and calcite, which would in turn minimise the acidification of the metalliferous soils (Van Zweel, 2015; Strömberg and Banwart, 1999). The slightly acidic values observed for metalliferous soil samples of O’Kiep indicated that the generated H<sup>+</sup> ions were to some extent being consumed by the dissolution of the identified aluminosilicate minerals (Romero *et al.*, 2007). This was evidenced by the total alkalinity of the MSL, determined to be <5 mg/kg CaCO<sub>3</sub>. The rate of PTE release was rapid during the initial stages of the HCTs, with subsequent decreases thereafter. Figure 6-6 shows the concentrations profile of the PTEs in the MSL from the HCTs. The highest average of the major PTEs in the MSL were observed during the HCTs at the following concentrations (mg/kg): Ca (102) > Mg (20.7) > Al (12.28) > Cu (17.5) > Cl (15.3) > Si (8.46) > Na (4.45) > Mn (2.10) > K (0.80) > Zn (0.71) > Ni (0.29) > Fe (0.19). Other PTEs occurred at low concentrations in the MSL, for example F < 2 mg/kg.

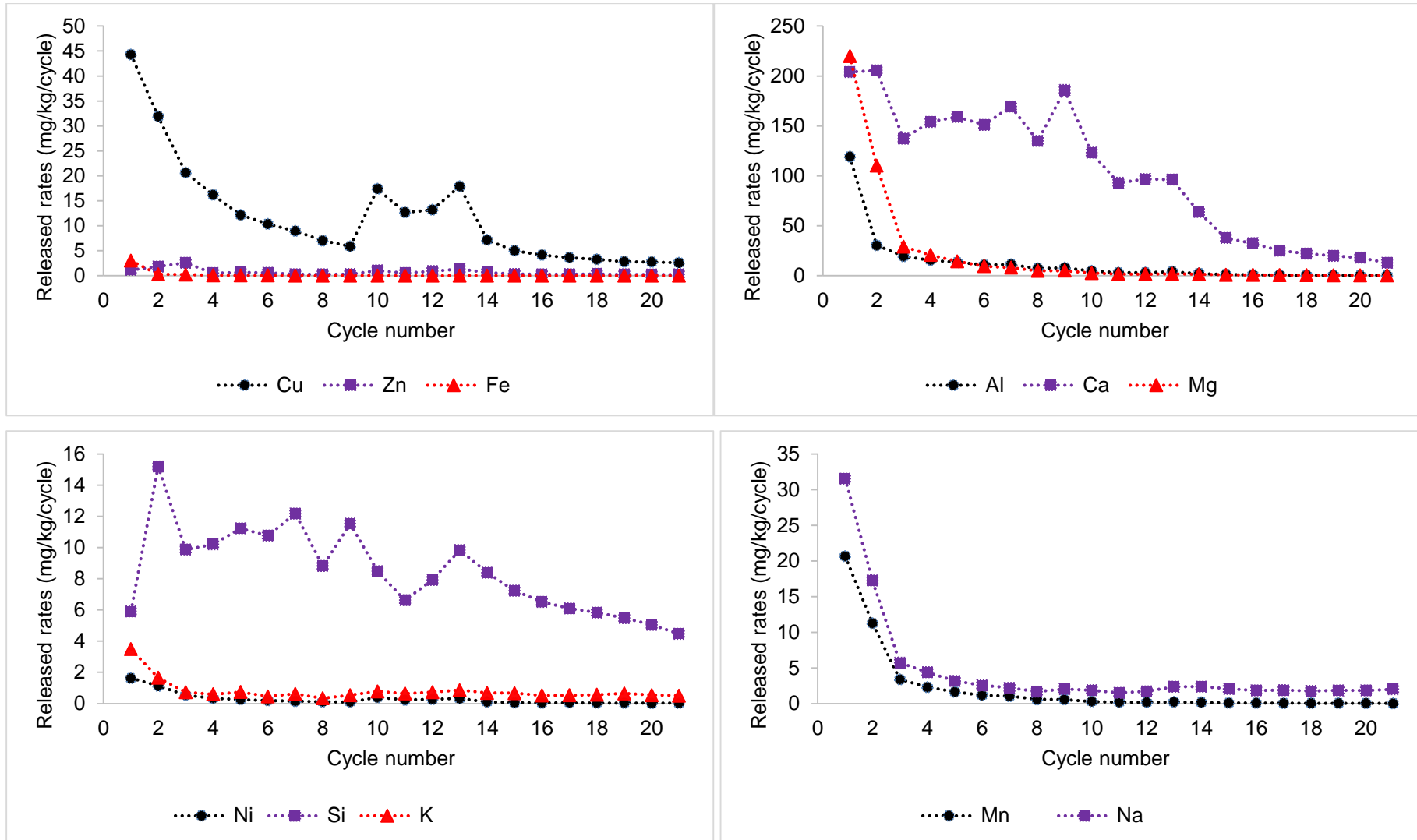
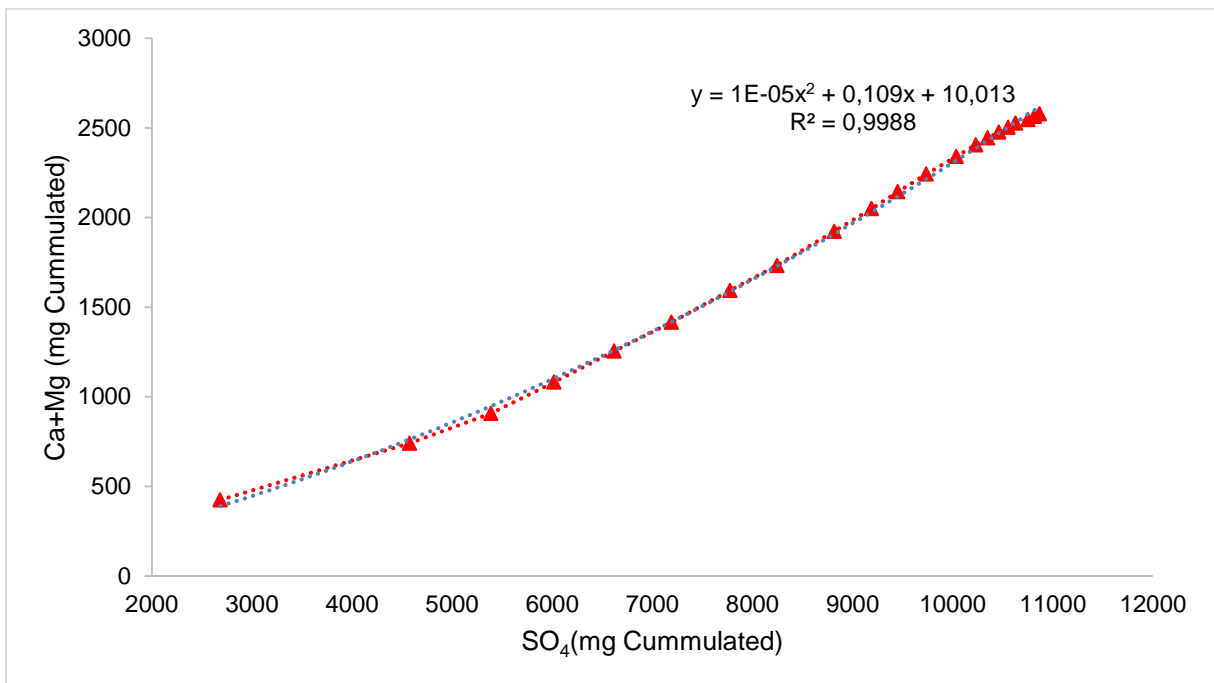
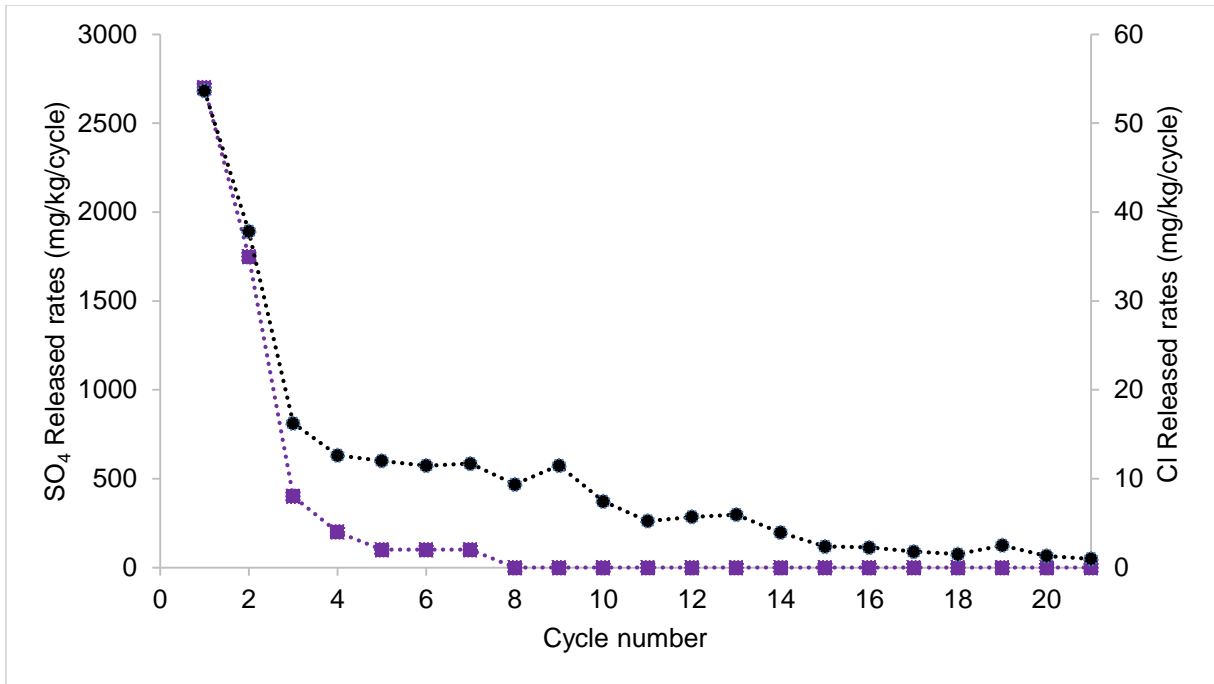


Figure 6-6: Concentrations profile of potentially toxic elements in the metalliferous soil leachates

Although slight variations were observed in the MSL for some PTEs, a steady decline over the period of experimentation (n = 3 cycles) was observed. The MSL contained higher sulfur content and was rich in PTEs. The Na in the MSL is related to albite, whereas K is associated with muscovite in the MSL as the sulfides were assumed to have been partly altered due to oxidation to secondary minerals (i.e. goethite and hematite). Primary minerals, such as chlorite and quartz grains, might be covered in iron sulfate (Mäkitalo *et al.*, 2016), with the Fe leaching being low in the MSL due to reduced oxidation rates. After the first week of the experiment, the concentrations of the Fe in the MSL started to decrease. However, lowly dissolved Fe in the leachate does not indicate the absence of pyrite oxidation (Gleisner and Herbert Jr, 2002). Additionally, Ca, Mg and Mn are likely the products of neutralisation reactions in the metalliferous soils. The oxidation-neutralisation curve represents the geochemical evolution of the HCTs, as presented in Figure 6-7. There was a second-order relationship between Ca and Mg and SO<sub>4</sub>. The discharge of Ca and Mg and SO<sub>4</sub> relationship-content increases were compared for time with variation in pH, indicating changes in acid generation. The Cl and SO<sub>4</sub> from the MSL followed the same trend, indicating various processes, such as dissolution and oxidation (see Figure 6-8).



**Figure 6-7: Oxidative-neutralising curve for the metalliferous soil leachates**



**Figure 6-8: Relationship between anions for the metalliferous soil leachates**

The dissolution and leaching of elements such as Ca, Mg, Al, Cu, Cl, Si, Na, Mn, K, Zn, Ni and Fe, are therefore caused by acid generation related to pyrite oxidation (Mäkitalo *et al.*, 2016). The observed leaching of Al, K and Na is most likely due to aluminosilicate dissolution of metalliferous soil constituents such as albite, which was also identified in the metalliferous soils. Furthermore, the SO<sub>4</sub> production rate of the metalliferous soils was very high at 2682 mg/kg during the first weeks of the HCT experiment. Low concentration values of CaCO<sub>3</sub> were also noticed on the leachates. The MSL was compared to drinking water guidelines, as shown in Table 6-3. The pH, EC, TDS and SO<sub>4</sub> were not within the drinking water limits as prescribed by SANS241-1 (2015) and WHO (2011). Even though most of the PTEs were within the drinking water permissible limits, continuous release will accelerate groundwater contamination.

**Table 6-3: The maximum metalliferous soil leachate quality compared to drinking water guidelines**

Parameters	Unit	MSL	SANS241-1 (2015)	WHO (2011)
Chemical Oxygen Demand (COD)	mg/L	-	-	4
Alkalinity (CaCO <sub>3</sub> )	mg/L	-	-	-
Colour	Pt-Co-true	-	<15	-
Turbidity	NTU	-	≤5	5
pH at 25°C	-	4.3	5-9.7	6.5-8.5
Temperature	°C	-	-	-
Electrical Conductivity (EC)	mS/m	376	≤170	-
Total Dissolved Solids (TDS)	mg/L	5046	≤1200	500
Dissolved Oxygen (DO)	mg/L	-	-	5
Salinity	PPt	-	-	-
Redox (ORP)	mV	-	-	-
Calcium (Ca)	mg/L	-	-	-
Sodium (Na)	mg/L	31.54	≤200	100
Magnesium (Mg)	mg/L	219.9	400	-
Potassium (K)	mg/L	-	-	-
Fluoride (F <sup>-</sup> )	mg/L	0.70	≤1.5	1.5
Chloride (Cl <sup>-</sup> )	mg/L	54.0	≤300	250
Sulfate (SO <sub>4</sub> <sup>2-</sup> )	mg/L	2682	≤500	200
Ammonia (NH <sub>3</sub> )	mg/L	-	≤1.5	-
Nitrate (N)	mg/L	-	≤0.9	45
Ortho-phosphate (P)	mg/L	0.16	-	0.4
Aluminium (Al)	mg/L	0.01	≤300	-
Antimony (Sb)	mg/L	0.00	≤20	-
Arsenic (As)	mg/L	0.00	≤20	0.01
Cadmium (Cd)	mg/L	0.01	≤3	0.003
Chromium (Cr)	mg/L	0.01	≤50	-
Cobalt (Co)	mg/L	0.40	-	-
Copper (Cu)	mg/L	44.3	≤2000	1
Iron (Fe)	mg/L	3.02	≤2000	0.3
Manganese (Mn)	mg/L	219.9	≤400	0.05
Mercury (Hg)	mg/L	0.00	≤6	-
Nickel (Ni)	mg/L	1.63	≤70	70
Selenium (Se)	mg/L	0.00	≤40	40
Vanadium (V)	mg/L	0.00	≤200	-
Zinc (Zn)	mg/L	2.59	≤0.005	2
Cyanide (CN <sup>-</sup> )	mg/L	-	≤200	-

#### 6.5.4 Potentially toxic element mobility from metalliferous soils

The mineralisation of naturally metalliferous sites is essentially made up of copper-sulfide, oxides and PTEs. The lower the pH, the higher the mobility of the PTEs. The mobility of the PTEs followed the following sequence: SO<sub>4</sub> > Ca > Mg > Cl > Al > Cu > Si > Na > Mn > K > Ni > Fe. The extent of soil contamination and its effect on surrounding agro-ecosystems, and all the way to the food chain, have received limited attention in O’Kiep. The bioaccumulation of these PTEs in food crops or even in vegetation has never being explored. As observed in

various literature sources, it can cause long-term cumulative human and environmental health effects, as other maladies related to heavy-metal contamination can ensue especially where these concentrations exceed the soil screening value levels. Currently, the elevated mobility and bioavailability of PTEs in soils of O’Kiep are of great concern in the area. Remedial procedures are required for the adequate protection and restoration of soil ecosystems contaminated by PTEs, especially in O’Kiep, where risk of groundwater contamination is high.

## 6.6 Summary

This part of the study has provided important reference information for the vulnerability of soils with regard to PTE mobility, thus contamination from MSW and mining activity in O’Kiep. The soils in O’Kiep are highly contaminated, with an average pH and Eh of 3.4 and 518 mV, respectively. The mineralogical and geochemical characterisation of the metalliferous soils showed that O’Kiep’s soils are rich in PTEs in the following sequence (mg/kg): S > Cu > F > Mn > Cl > Zn > Cr > V > Pb > Ni > Co. The major oxides are (%): SiO<sub>2</sub> > Al<sub>2</sub>O<sub>3</sub> > FeO<sub>3</sub> > K<sub>2</sub>O > CaO > NaO. ABA tests suggested that the metalliferous soils had a high acid-producing potential, which was confirmed by the results of the HCTs, which revealed signs of ARD formation. Low CaCO<sub>3</sub> of the metalliferous soils therefore contributed to the decline of the neutralising potential. Monitoring of the leachate quality showed that the metalliferous soil sample started producing acid very early in the experiment. Furthermore, the results also demonstrated weathering and production of ARD. The HCT results showed that the soils around the old mining town of O’Kiep are susceptible to ARD generation and can release acid for elongated periods. The concentrations of each dissolved PTE are a function of pH and of the mineralogy of the metalliferous soils. All these results suggest that there is a high risk for ARD formation in the metalliferous soils in O’Kiep under the present conditions. Furthermore, the results of this study also suggest that there is accelerated PTE leaching from the metalliferous soils, resulting in uninhibited PTE contamination in the surrounding groundwater bodies. PTE contamination in metalliferous soils in O’Kiep may pose health and environmental risks. The acidic nature of metalliferous soils in O’Kiep would provide adverse environments for the growth of plants. It was therefore prudent to also evaluate the ARDP of MSW in O’Kiep using a similar test, namely the static test and HCT assessment, to further ascertain whether such waste can also contribute to the contamination of the groundwater. This is discussed in the subsequent chapter (Chapter 7).

## CHAPTER 7: RESULTS AND DISCUSSION

---

Published as:

**Erdogan, I.G.**, Fosso-Kankeu, E., Ntwampe, S.K., Waanders, F.B., Hoth, N. and Rand, A. 2019. Static test-based acid rock drainage formation potential of metalliferous tailings from O’Kiep, South Africa. Nov. 18-19, Johannesburg, South Africa, 17th International Conference on Science, Engineering, Technology and Waste Management (SETWM-19).

Available: <https://doi.org/10.17758/EARES8.EAP1119262>

## **7.1 Acid rock drainage formation potential of metalliferous solid waste from O’Kiep, an arid region of Namaqualand, South Africa: A humidity cell test assessment**

### **7.2 Introduction**

ARD is a predominant environmental challenge in mining industries, especially in low- and middle-income countries, including South Africa, and is associated with several active and closed mine sites (Krampah *et al.*, 2019). The release of ARD from metalliferous mines and metalliferous waste is a worldwide environmental concern. There are two different kinds of mining waste facilities: MTs and SMW. The probability of the movement of PTE constituents from the SMW will be influenced by the particle size and the porosity of the metalliferous waste. Some of these SMW, nonetheless, are inert and therefore less likely to present significant contamination risk to the environment, as indicated by Bäcklund (2009).

The information associated with mineralogical composition and particle size is important for understanding the oxidation of the waste material and the production of ARD. ARDP is interrelated with the surface area of particles exposed to an oxidative environment (Erguler and Erguler, 2015). The environmental hazards of ARD do not rely barely on the physical and mineralogical characteristics of the SMW, but also on the ARD pathways to its receptors such as groundwater (Molson *et al.*, 2012). The protection of groundwater is currently recognised as a decisive constituent of justifiable development. With rising concerns being placed on our limited water resources, effective systems are necessary to protect these resources. One of the significant possible sources of groundwater contamination is from ARD, which is generated from the oxidation of sulfide minerals within the MSW, such as MTs and SMW, which are usually characterised by high dissolved concentrations of PTEs and low pH (Molson *et al.*, 2012; Blowes *et al.*, 2003). The SMW is usually deposited in huge piles, whereas the MTs are stored in TSFs that are heterogeneous in relation to particle size and mineral composition (Elghali *et al.*, 2019). ARD transmitted from SMW and MTs compromises the quality of groundwater, destroying the environment and increasing human health risks (Krampah *et al.*, 2019). The SMW and MTs might contain PTEs which may leach under certain environmental conditions and contaminate the water table (Bäcklund, 2009).

The amount of acidity produced from ARD can be altered by mining activities and exposure of sulfur-bearing SMW and MTs to the atmosphere and bacteria that rather catalyse the mineral oxidation through re-generation of lixivate ( $\text{Fe}^{3+}$ ), which in turn leaches the sulfide minerals (Jennings *et al.*, 2008). ARDP is reliant on local environmental conditions such as climate, degree of distribution of ARD and geomorphology (Plumlee, 1999). The acidified condition further increases the mobility of PTEs (Krampah *et al.*, 2019). The SMW and MTs from which ARDP emanates are characteristically composed of a vastly permeable and porous

undersaturated blend of sand and silt, which might interact with the water table and manifest as percolates along the slopes of the SMW and MTs (Gandy *et al.*, 2009).

The ARD results from oxidation of sulfide minerals and the release of acidity indicate amounts that surpass the amount of aluminosilicates and carbonate, which are the acid-consuming minerals that neutralise the acid (Blowes *et al.*, 2013). ARD with elevated concentrations of PTEs is considered as one of the key challenges associated with the management of mine wastes (Mehta *et al.*, 2019; Dold, 2014a). The European Commission (Bäcklund, 2009) suggested the analysis of some PTEs, including Al, As, Cd, Co, Cr, Cu, Hg, Mo, Ni, Pb, Se, V and Zn, which are poisonous for aquatic life and are often present in water streams affected by ARD. Additionally, through the oxidation and acidification reactions, a substantial quantity of PTEs might be released into the aquatic streams (Lottermoser, 2010). When leached into solution, PTEs can be precipitated and/or adsorbed as secondary minerals, reliant on the solution components, such as pH (Issaad *et al.*, 2019). The SMW in O’Kiep is visually described as a coarse-grained component ranging from fine-grain size to blocks several meters in diameter. The SMW ranges in height up to approximately 8 m and can cover several metres in the area.

Previous studies from this area have shown that there is acid leachate emanating from the SMW, which can potentially contaminate groundwater and soils – as discussed in Chapters 5 and 6 – and often with deleterious effects for environmental systems and human health – as highlighted in Chapter 3. There are minimal published scientific studies on the effect of the MSW on groundwater in the O’Kiep area, specifically for communities within the study area. Since the local community will depend on groundwater resources for their drinking water supply in future, any contamination of these vital resources could therefore have profound consequences on human health and bear an environmental impact in the area.

Metalliferous mining operations generate large volumes of finely crushed rock, commonly referred to as MTs. It is characterised by fine particle sizes (~100 µm) and is stored in TSFs (Perumal *et al.*, 2019). MTs, especially those found in arid or semi-arid environments, pose a long-term health hazard for nearby communities through exposure to PTEs containing dust originating from the MTs, with observed minimal plant growth due to soil toxicity (De-Bashan *et al.*, 2010). The reactivity of MTs can result in acidic and highly charged waters (Elghali *et al.*, 2019). Disposal of MTs is a major concern for many countries as it contaminates the environment, including the atmosphere, water resources and soil (Behera *et al.*, 2019; Rout *et al.*, 2019). The MTs always contain PTEs concentrated during ore processing, which may disperse into the nearby environment and threaten public health (Hu *et al.*, 2017). Elements such as Al, Cd, Cu, Fe, Pb, Zn and Mn are essential for cell growth and metabolism; however,

at high levels, they are toxic for living organisms (Rout *et al.*, 2019) and are thus referred to as PTEs.

The TSF containing copper sulphide MTs in O’Kiep has been exposed to weathering reactions for years. Although the environmental impact, including blowing wind, of MTs on the nearby environments is well known (Rozendaal *et al.*, 2017), only a few comprehensive studies have been carried out in O’Kiep. In general, the primary minerals in the MTs are quartz and pyrite, with secondary minerals such as goethite. ARD from such MTs is generated by the moisture-based weathering and oxidation of sulfide minerals such as pyrite (Khoern *et al.*, 2019). An ARD-management approach is neutralisation by an alkaline reagent such as limestone. This will raise the pH and remove most of the PTEs through precipitation reactions (Khoern *et al.*, 2019; Heviankova *et al.*, 2013). O’Kiep MTs are potentially primary contributors to ARD due to their high sulphide content (Amponsah-Dacosta and Reid, 2014). Under watery acidic conditions, these PTEs will be released from MTs (Liu *et al.*, 2019) as they will undergo chemical alteration under such conditions. The chemical alterations are most often a function of exposure to atmospheric oxidation (Kossoff *et al.*, 2014).

It is crucial to assess the geochemical processes associated with the release of PTEs from the MSW to assess the environmental impact and to establish remediation strategies (Servida *et al.*, 2013). Static-test methods such as ABA tests are usually used for aggressive chemical in the worst-case scenario, not considering other factors which contribute to ARDP, such as mineral composition of the MSW material (Blowes *et al.*, 2013). For any mine sample that has been classified as uncertain and potentially acid-forming, further investigation under kinetic tests such as HCTs will be considered. Current protocols make use of kinetic tests to predict geochemical processes associated with the ARDP from MSW. HCTs are probably the best-known kinetic test techniques or laboratory weathering procedures used in the mining sector to predict the long-term ARDP behaviour of sulfide-bearing MSW (Lapakko, 2003). These tests are useful because they tend to mimic the sites’ environmental conditions and can also accelerate oxidation rates under controlled laboratory settings, thereby providing valuable data for ARD predictive models (Fosso-Kankeu, 2016). Only geochemical parameters (i.e. pH, ORP, EC and SO<sub>4</sub> and PTE department) are often measured in the stockpiled metalliferous waste leachates (SMWL) and in metalliferous tailing leachates (MTL) and are generally used to define the characteristics (Parbhakar-Fox *et al.*, 2013).

Generally, studies on the ARDP of the MSW in O’Kiep are limited. ARD prediction is very important to predict and prevent long-term deleterious environmental contamination. However, the extent of the acid generation as well as the sources and dynamics of PTEs from O’Kiep MSW have not been determined thus far. This part of the study was therefore applicable to establish the environmental risk concomitant with the MSW and to help decision-makers with

effective mitigation strategies in anticipation of possible future effects of the MSW on groundwater resources.

### **7.3 Objectives**

The objectives of this part of the study were:

- to determine the geochemical and mineralogical characterisation of the MSW; and
- to assess the ARDP of the MSW.

### **7.4 Materials and methods**

#### **7.4.1 Study area and sample collection**

The study area is located in O’Kiep, where oxidised MSW, which is greyish-black in colour, has been deposited in the environment. This MSW is subjected to weathering conditions, which promotes the leaching of PTEs into the environment and possible health effects since it is situated within the vicinity of the community of O’Kiep. SMW and MT samples (n = 10) of 5 kg each were collected from the subsurface at depths of 30 cm and 50 cm of the MSW as described by the United States Environmental Protection Agency (USEPA) operating protocol for soil sampling (USEPA, 2014; Moyle and Causey, 2001). Similarly, the MTs were collected from the TSF. All samples were collected using a Draper 24414 steel auger (Schoeneberger *et al.*, 2012) during August 2017 (wet season). The sampling points were marked for the SMW as MW1 to MW10 and for the MTs as MT1 to MT10 using a GPS, as shown in Figure 7-1. All samples were kept in double-sealed Ziploc bags and transported to the laboratory for analysis. The analytical instrumentation analyses and sample preparation were conducted as defined by Beckhoff *et al.* (2007) and Compton *et al.* (2003). At the laboratory, samples were dried at an ambient temperature, mixed and homogenised to form a 10 kg composite sample each of the SMW and MTs. The MSW samples from the study area were analysed in the laboratory to determine the mineralogy, physical properties, and acid-generation potential. Conversely, the static test and HCTs were conducted at a SANAS-accredited commercial laboratory (Parbhakar-Fox and Lottermoser, 2015). A portion of the representative sample was sent to the University of Cape Town Geology Laboratory for X-ray fluorescence (XRF) and X-ray diffraction (XRD) (Smith *et al.*, 2014) to comprehensively determine the mineralogical composition.

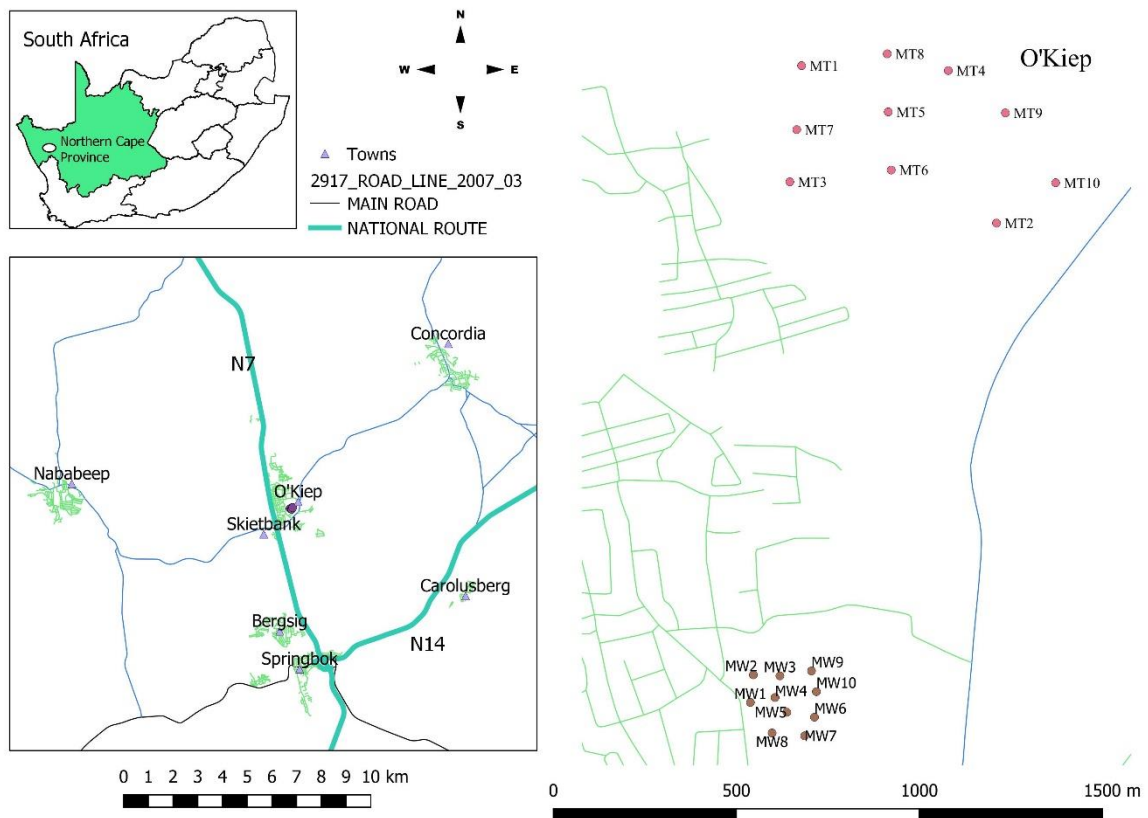


**Figure 7-1: Location of study area and sampling points: Geological maps were generated using Quantum GIS software (v. 2.18.11) and data from National Geo-Spatial Information (NGI), a component of the Department of Rural Development and Land Reform, South Africa**

#### 7.4.2 Particle size distribution and porosity

A dry sieve analysis was used to assess the particle size distribution (PSD) of the MSW composite sample (McGlinchey, 2005), using the procedure for the PSD by the American Society for Testing and Materials (ASTM) C136 (ASTMC136-06, 2006). The porosity of the MSW samples was determined using the method defined by Joardder *et al.* (2015), which is the critical parameters of the microscopic structure of porous material.

#### 7.4.3 Static test predictions

A paste pH assessment was used to determine the acidic class of the MSW and indicated immediate pH characteristics (Weber *et al.*, 2006). pH tests are utilised as screening tools for assessing the ARD from MSW materials (Noble *et al.*, 2017). Additionally, a prediction test was performed using a paste for pH testing, to assess individual samples' acid-forming characteristics. Static tests are empirical techniques usually conducted to predict ARDP. A modified field and laboratory test method for ABA (Sobek, 1978) and test modified by Lawrence and Wang (Lawrence and Wang, 1996) were used in the static tests. The most common static test is ABA (Ferguson and Erickson, 1988), which is based on the determination of three main factors: 1) acid consumption, 2) acid formation and 3) determination of the net acid consumption or production (Lottermoser, 2010). Subsequently, the determination of AP and

NP allowed for the computation of the NNP, including the NPR, a criterion used for the determination of the ARDP of the MSW samples.

#### **7.4.4 Humidity cell tests**

The HCTs of the SMW and MTs were conducted as indicated in Chapter 6: Section 6.4.3. Subsequently, the weekly SMWL and MTL were collected into a shake flask and filtered through a 0.45  $\mu\text{m}$  filter into a polyethylene bottle. EC, TDS and pH were also recorded, and PTE deportment was determined using ICP-MS techniques following the procedure described in ASTM: D2216 (ASTM, 1996). The schematic diagram is shown in Figure 7-2.

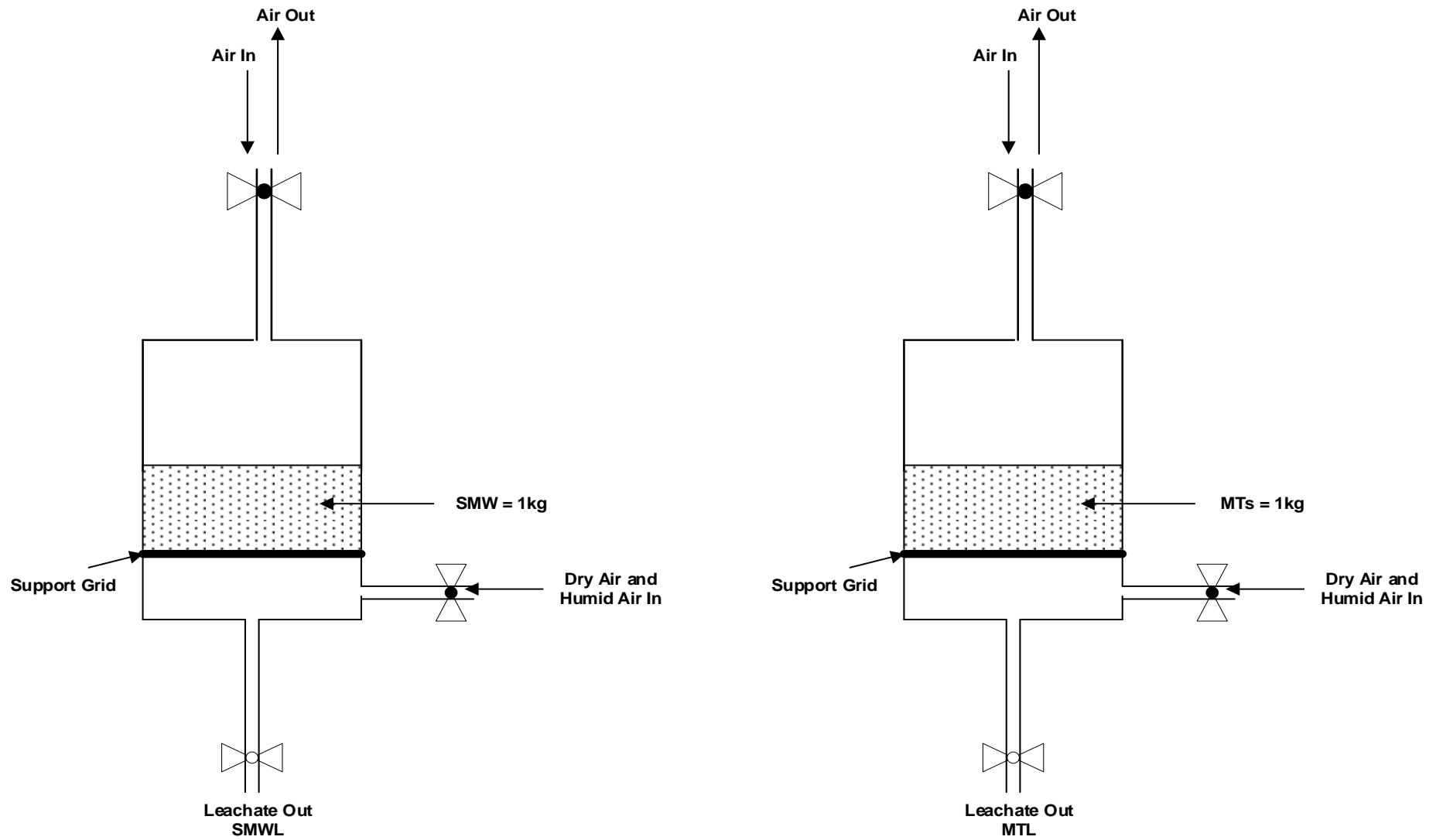


Figure 7-2: Schematic diagram of the humidity cell test assessment of the metalliferous solid waste (Adopted from Morin and Hutt (1999))

## **7.5 Results and discussion**

### **7.6 Results**

#### **7.6.1 Particle size effects**

The samples were not crushed further to avoid excessive fine material and the subsequent twisting of the PSD in favour of finer material. The PSD of the SMW indicated that 25% of the particles were smaller than 2000  $\mu\text{m}$  and 80% of the particles were smaller than 600  $\mu\text{m}$ . The PSD results for the SMW indicated that the particles were fairly small, ranging from 75 to 600  $\mu\text{m}$  in diameter. The MT tailings in the TSF of O’Kiep were greyish course-fine textures of 79 to 98 % of the MTs with a specific gravity of 3.104  $\text{m}^2/\text{g}$  (Amponsah-Dacosta and Reid, 2014). Similar results were obtained from underground copper MTs in southern China (Zheng *et al.*, 2016). The significance of considering the sample PSD when assessing the ARDP has also been suggested in the HCT studies conducted by Elghali *et al.* (2019), Erguler and Erguler (2019) and Guseva *et al.* (2018). The variation in the Fe-sulfide liberation over the size fraction range makes it necessary to re-visit the PSD to assess the size fractions which would control the HCT material behaviour as recommended by Guseva *et al.* (2018). The SMW and MTs are influenced by the material’s PSD, porosity and the dynamics coupled with water retention, evaporation, precipitation, run-off and seepage (Hitch *et al.*, 2010). The calculated porosity of 33% and 42.7% for SMW and MTs, respectively, in the combined structure matches the soil porosity (Gargiulo *et al.*, 2016).

#### **7.6.2 Mineralogy and geochemical characterisation**

Mineralogical analysis showed that the O’Kiep SMW were mainly composed of magnetite > carbon > quartz > hematite and kehoelite, with no sulfide minerals detected. However, the primary minerals in the MTs were quartz, microcline, albite, magnesioferrite, magnetite, gypsum, clinochlore-1MIlb, anorthite, muscovite-1M and halloysite-10A. These were interlinked to the geochemical conditions at the surface of the TSF, which revealed a heterogenic environment that can be divided into an acidic zone and an oxidising zone. The mineralogy characteristics of the MSW samples are presented in Figure 7-3.

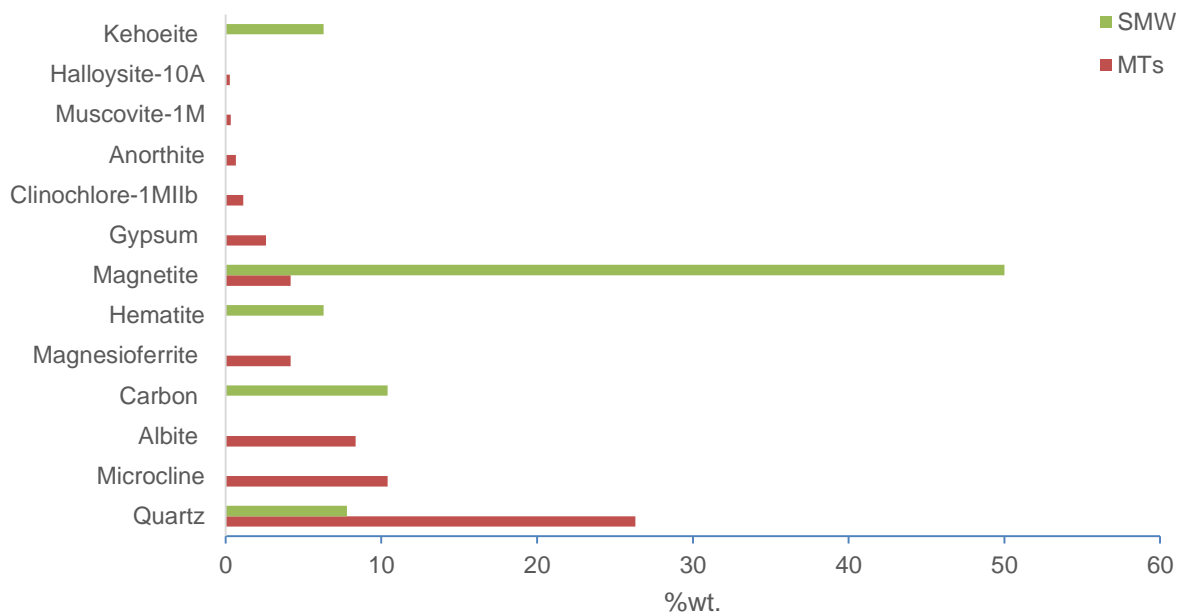


**Figure 7-3: Averaged mineralogical composition of metalliferous solid waste from the O'Kiep area**

The major oxides and PTEs most relevant for the SMW and MT samples are presented in Figures 7-4 and 7-5. Oxides of the SMW are dominated by  $\text{Fe}_2\text{O}_3$  (62.9%) >  $\text{SiO}_2$  (9.82%) >  $\text{Al}_2\text{O}_3$  (3.28%) >  $\text{MgO}$  (1.35%) >  $\text{Na}_2\text{O}$  (1.00%) >  $\text{CaO}$  (0.91%). On the other hand, the major oxides observed in the MTs were  $\text{SiO}_2$  (51.2%) >  $\text{Al}_2\text{O}_3$  (15.6%) >  $\text{Fe}_2\text{O}_3$  (12.6%) >  $\text{CaO}$  (4.61%) >  $\text{MgO}$  (2.19%) >  $\text{K}_2\text{O}$  (1.96%). The MTs exhibited significantly higher concentrations of  $\text{F} > \text{Cu} > \text{Cr} > \text{Mn} > \text{S} > \text{Zr} > \text{Ba} > \text{Sr} > \text{V} > \text{Cl} > \text{Rb} > \text{Ni} > \text{Zn} > \text{Y} > \text{Co}$ . The geochemical characterisation of the SMW revealed a significant PTE content in the following order:  $\text{S} > \text{Cu} > \text{F} > \text{Ni} > \text{Zn} > \text{Co} > \text{Pb} > \text{Mn} > \text{Cr} > \text{Mo} > \text{V} > \text{Cl}$ .

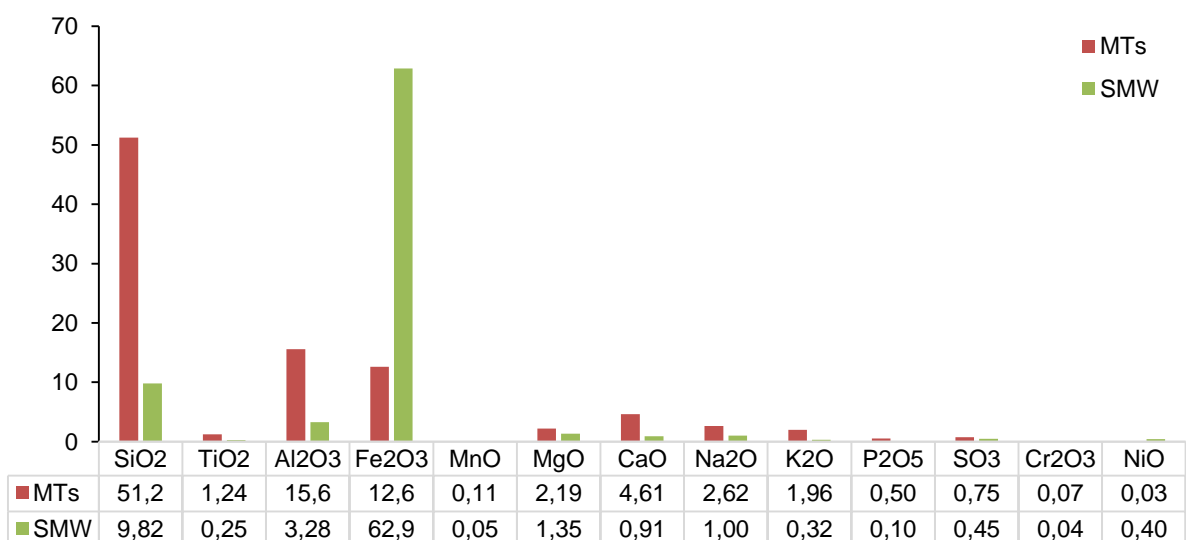


**Figure 7-4: Major oxides of the metalliferous solid waste by X-ray fluorescence**

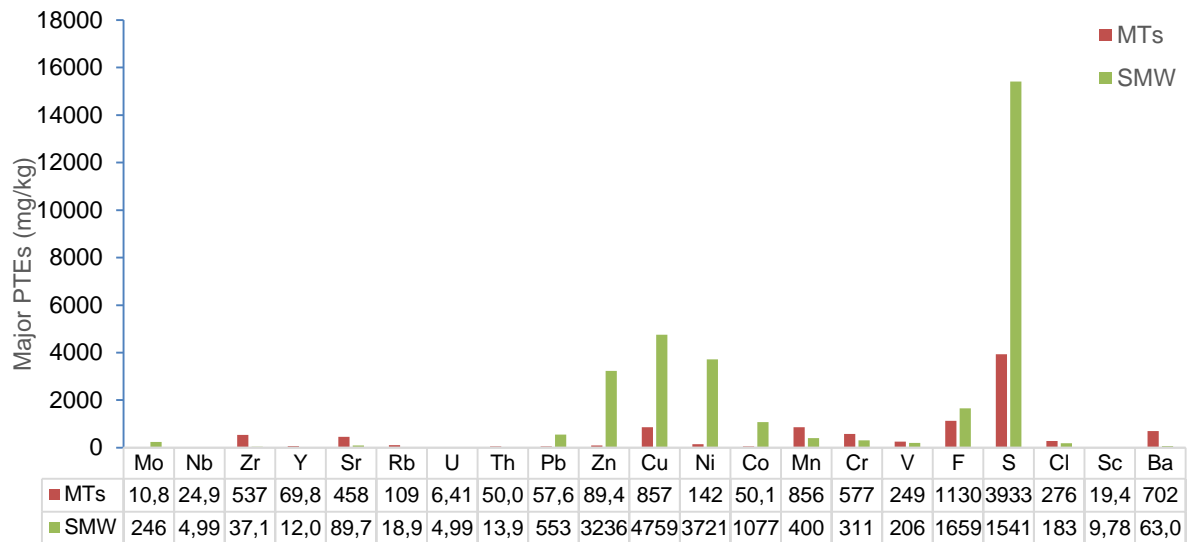


**Figure 7-5: Potentially toxic element characterisation by X-ray fluorescence**

### 7.6.3 Static test predictions

Static tests (Table 7-1) for MSW were conducted to define the potential acidity generated by the MTs disposed of in the TSF in O’Kiep.

**Table 7-1: Static tests for metalliferous solid waste from the O’Kiep area**

	SMW	MTs
Paste pH	5.6	3.1
Total Sulphur (%) (LECO)	0.98	6.09
Acidity Potential (AP) (kg/t)	31	190
Neutralisation Potential (NP)	1.93	-19
Nett Neutralisation Potential (NNP)	-29	-210
Neutralising Potential Ratio (NPR)	0.063	0.102

### 7.6.4 Humidity cell tests

The HCT experiment was also carried out on the MSW due to its uncertain ARDP, and to validate the ABA test results and to determine PTE-deportment release rates and behaviour. The evaluation of pH, EC and TDS for MSW leachates, namely SMWL and MTL, during the HCTs are presented in Figures 7-6a and 7-6b. The average pH of the MTL was near neutral at 5.3 when compared to the acidic pH of 3.2 for the SMWL. The increase of the EC of the SMWL was initially rapid from 86.1mS/m in the first cycle to 1743 mS/m in the second cycle, which could be attributed to the dissolution of fast-weathering minerals such as Ca, and then slowed down to 86 mS/m. Similarly, the sulfate concentration of the SMWL increased from 554 to 1743 mg/kg and dropped after the second cycle to 405 mg/kg. The EC values stabilised after six cycles at values of 147 mS/m for the SMWL and 165 mS/m for the MTL. Similarly, the TDS values followed the same trend, with 1488 mg/kg for the SMWL and 1534 mg/kg for the MTL. Under acidic environments, high amounts of PTEs were released, consequently

increasing the EC and TDS values of the leachates. The EC values for both SMWL and MTL descended, with a subsequent primary high reading of 2254 to 130 mS/m and 1743 to 86.1 mS/m, respectively. A similar profile for the TDS in this study was observed in the SMWL and MTL descending from 39 148 to 602 mg/kg and 27 655 to 1450 mg/kg, respectively.

The oxidation-neutralisation curves representing the geochemical evolution of the HCTs are presented in Figures 7-7a and 7-7b. It was found that a second- (SMWL) and third-order polynomial (MTL) relationship between Ca and Mg and SO<sub>4</sub> exist. The Ca ranged between 93.4 and 294 mg/kg in the SMWL, whereas Ca in the MTL ranged between 249 and 539 mg/kg. Mg ranged between 1.33 and 1159 mg/kg in the SMWL, whereas Mg in the MTL ranged between 1.05 and 1513 mg/kg, as shown in Figure 7-8.

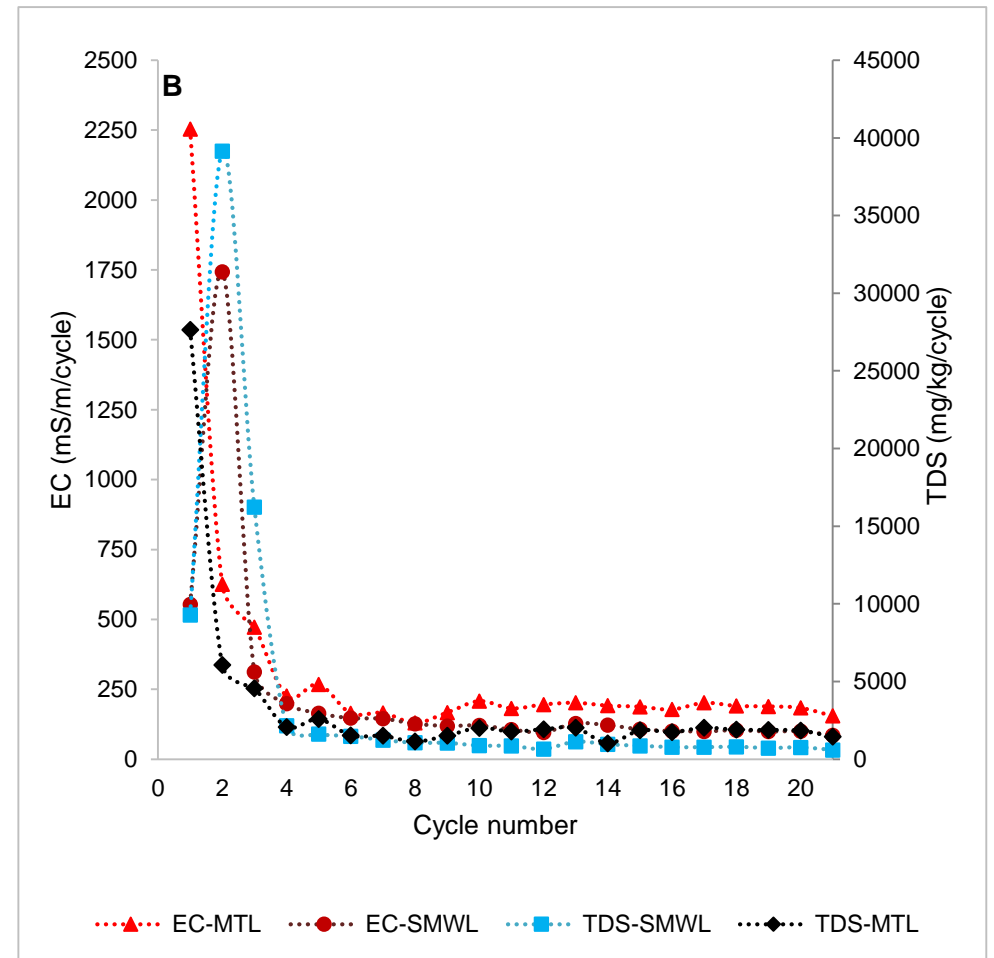
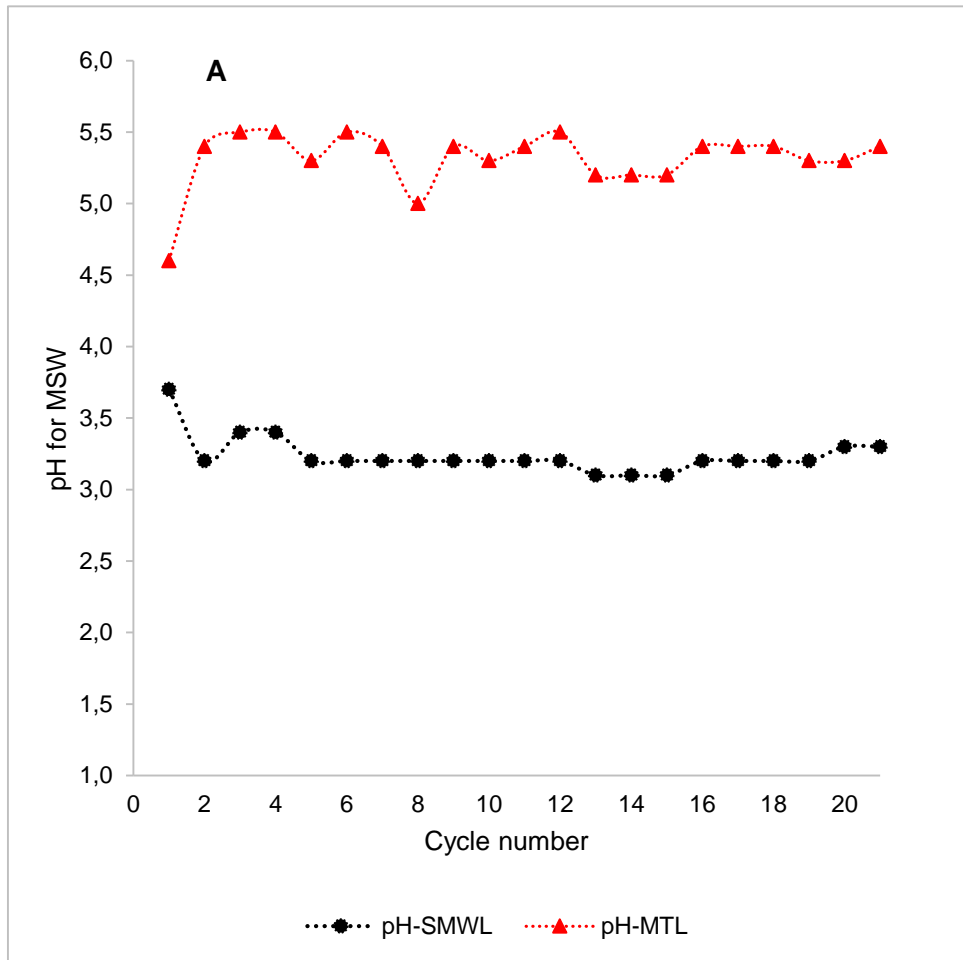


**Figure 7-6: Evaluation of pH, electrical conductivity and total dissolved solids from metalliferous solid waste leachates**

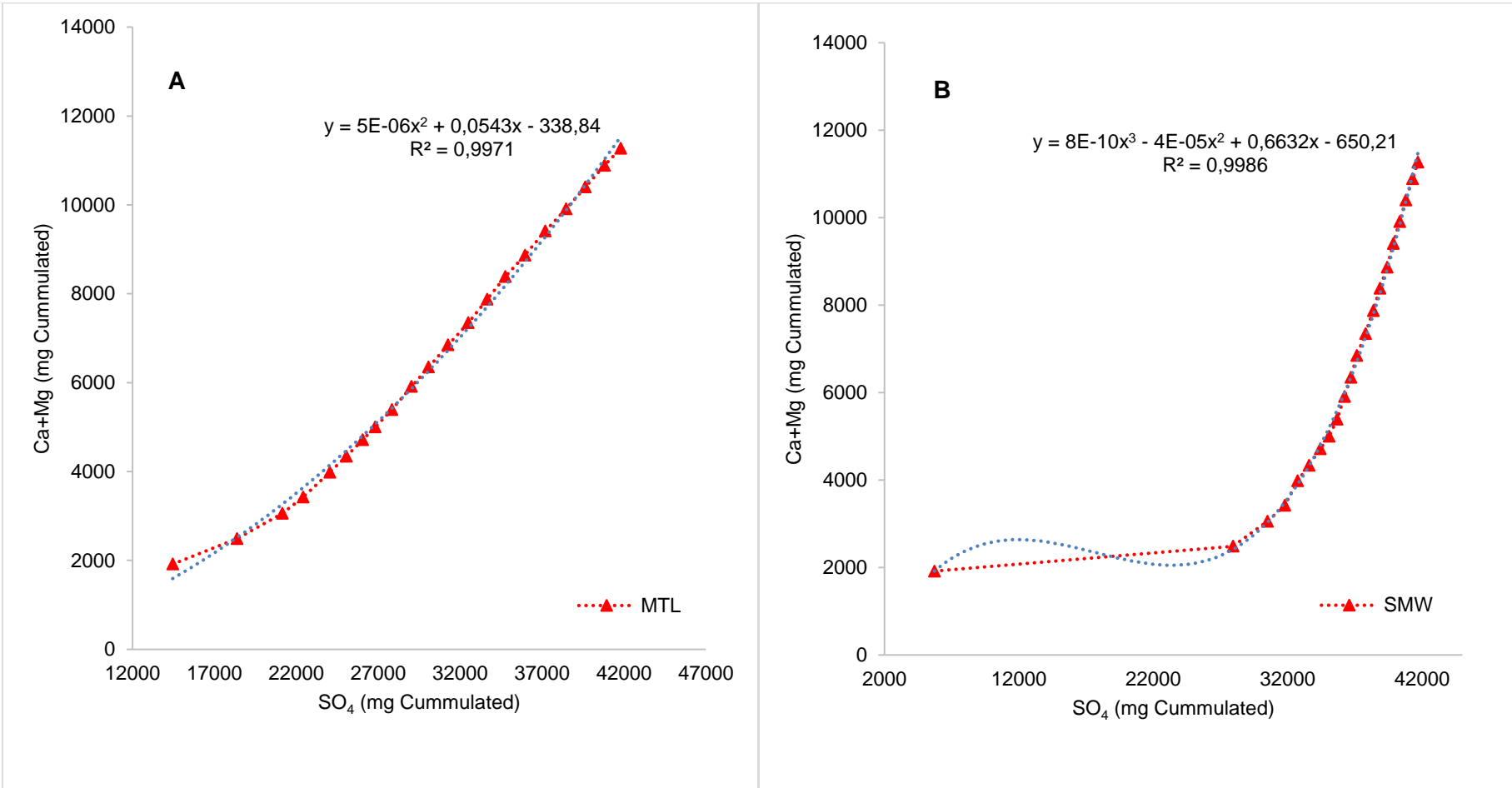


**Figure 7-7: Oxidative-neutralising curve for metalliferous solid waste leachates**

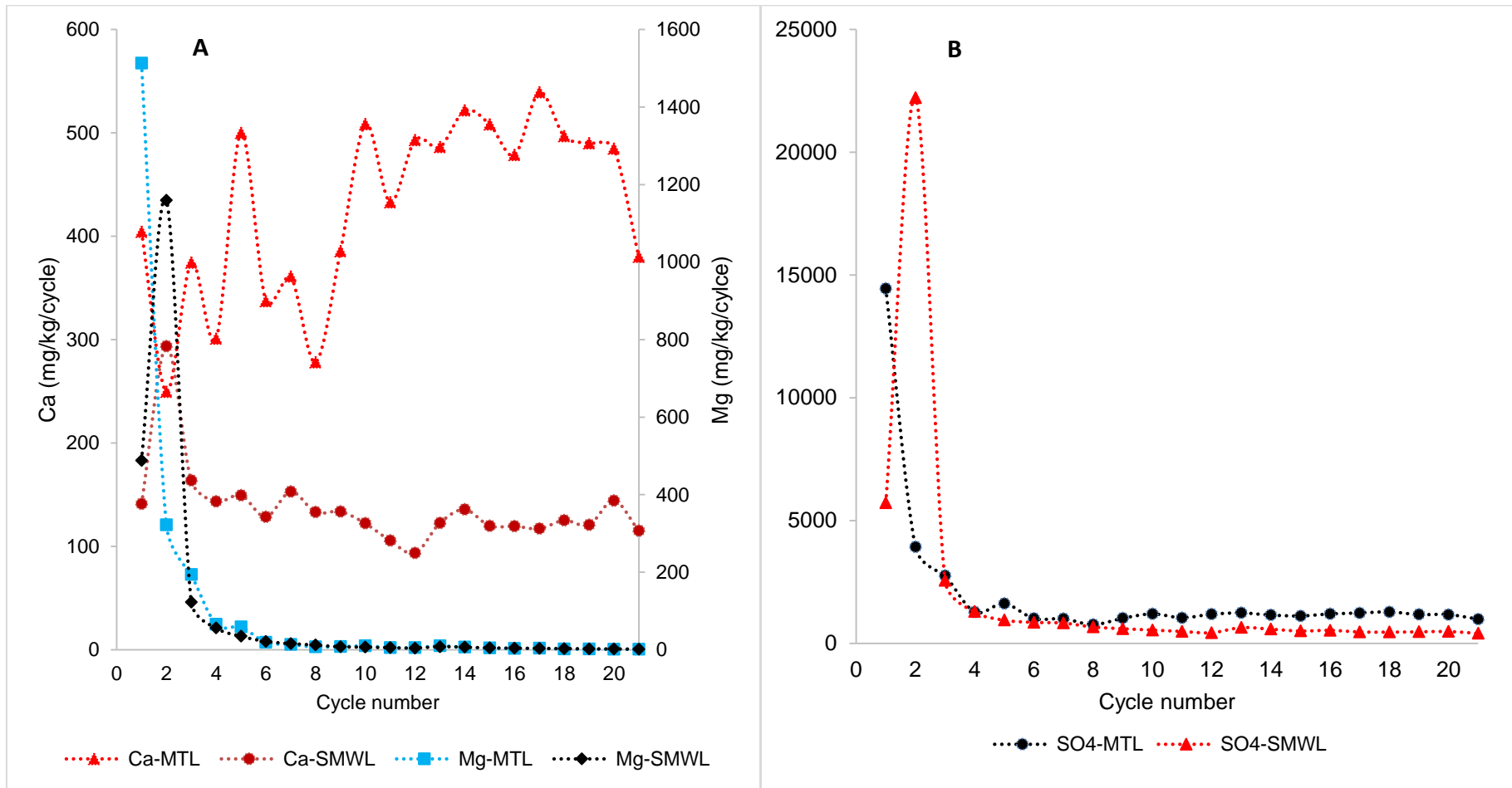


**Figure 7-8: Calcium, magnesium and sulfate release rates of the metalliferous solid waste leachates**

The release rates of PTEs such as Al, Fe, Cu, Zn, Mn, Na, Ni and Si into the SMWL and MTL were plotted against time and are shown in Figure 7 (a-d). All these PTEs displayed a declining production rate with a sharp decline during the first three cycles and gradually until the final cycle. In the HCT and the SMWL, the concentrations of Al and Fe increased from cycle 1 to cycle 2 from 408 to 1274 mg/kg and 30.6 to 129.6 mg/kg, respectively. Subsequently, the Al and Fe concentrations in most of the SMWL decreased rapidly from the second to third cycle and progressively to the 21<sup>st</sup> cycle from 129.1 to 9.01 mg/kg and 26.5 to 2.3 mg/kg, respectively. For Al and Fe in the MTL, the concentrations gradually decreased (from cycle 1 to cycle 21) from 59.5 to 0.2 mg/kg and 4.15 to 0.002 mg/kg, respectively. Similarly, Cu and Zn concentrations in the MTL also showed a reduction from the first cycle to the end of the experiment. The Cu and Zn concentrations in the SMWL varied from 1.93 to 39.3 mg/kg and 0.24 to 14.0 mg/kg, respectively. The Cu-concentration pattern strongly correlated with that of Zn in the SMWL and in the MTL. It is also noted that Al, Cu, Fe, Na, Ni and Zn in the MTL followed a similar pattern. Ni was released in a high concentration in the early stage of the experiment; its concentration varied in the SMWL and MTL from 0.1 to 19.6 mg/kg and from 0.1 to 2.75 mg/kg, respectively. The Si concentration varied in both SMWL and MTL samples from 0.49 to 14.6 mg/kg and 7.8 to 20.4 mg/kg, respectively. Higher concentrations of Na were recorded in the MTL, ranging between 1.77 and 5234 mg/kg, when compared to Na concentrations in the SMWL, ranging between 0.95 and 6.49 mg/kg. Subsequently, after the second cycle of the experiment, despite a slight variation observed in the leachate, the PTE concentrations generally remained relatively stable for most of the experiment (cycles 3 to 21). PTEs with low concentrations in the leachates (i.e. As, Au, B, Ba, Be, Cd, Ce, Co, U and those below the ICP-MS detection limit) are not presented.

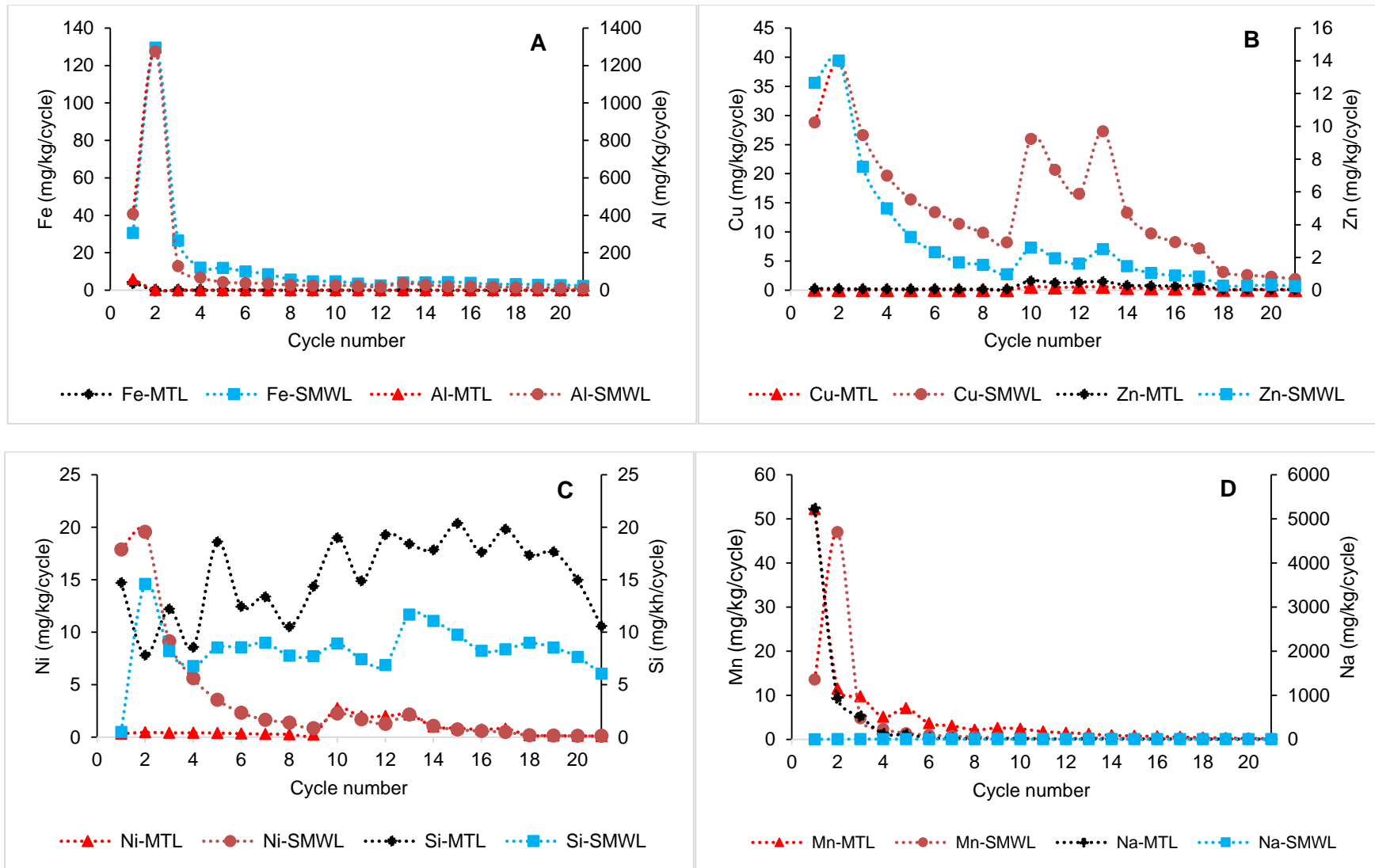


**Figure 7-9: Geochemical parameters of stockpiled metalliferous waste leachates**

An enormous variation was observed in the leachate quality of the MSW leachates (Table 7-2). For example, the EC and TDS were higher than the permissible limit for drinking water quality by SANS241-1 (2015) and WHO (2011). The pH of the SMWL was below the standard as described by SANS241-1 (2015) and WHO (2011), but the MTL pH was within the drinking water standards. The PTE concentrations in the SMWL (i.e. Mg, SO<sub>4</sub>, Al) remained relatively high when compared to SANS241-1 (2015), whereas the PTE concentrations in the MTL, such as for Na, Mg, Cl and SO<sub>4</sub>, were above the drinking water standard as described by SANS241-1 (2015). On the other hand, the Sb, As, Cd, Cr, Ni, Se and V were below the permissible limits of the SANS241-1 (2015) and WHO (2011) drinking water standards.

**Table 7-2: Maximum metalliferous solid waste leachate quality compared to drinking water permissible limits**

Parameters	Unit	SMWL	MTL	SANS241-1 (2015)	WHO (2011)
Chemical Oxygen Demand (COD)	mg/L	-	-	-	4
Alkalinity (CaCO <sub>3</sub> )	mg/L	<0,5	9	-	-
Colour	Pt-Co-true	-	-	<15	-
Turbidity	NTU	-	-	≤5	5
pH at 25°C	-	3.7	5.5	5-9.7	6.5-8.5
Temperature	°C	-	-	-	-
Electrical Conductivity (EC)	mS/m	1743	2254	≤170	-
Total Dissolved Solids (TDS)	mg/L	39 148	27 655	≤1200	500
Dissolved Oxygen (DO)	mg/L	-	-	-	5
Salinity	Ppt	-	-	-	-
Redox (ORP)	mV	-	-	-	-
Calcium (Ca)	mg/L	294	539.4	-	-
Sodium (Na)	mg/L	6.49	5234	≤200	100
Magnesium (Mg)	mg/L	1159	1513	400	-
Potassium (K)	mg/L	0.30	49.1	-	-
Fluoride (F <sup>-</sup> )	mg/L	-	1.40	≤1.5	1.5
Chloride (Cl <sup>-</sup> )	mg/L	111	954	≤300	250
Sulfate (SO <sub>4</sub> <sup>2-</sup> )	mg/L	22 216	14 453	≤500	200
Ammonia (NH <sub>3</sub> )	mg/L	-	-	≤1.5	-
Nitrate (N)	mg/L	-	-	≤0.9	45
Ortho-phosphate (P)	mg/L	0.85	0.03	-	0.4
Aluminium (Al)	mg/L	1274	59.5	≤300	-
Antimony (Sb)	mg/L	0.00	0.001	≤20	-
Arsenic (As)	mg/L	0.00	0.001	≤20	0.01
Cadmium (Cd)	mg/L	0.27	0.018	≤3	0.003
Chromium (Cr)	mg/L	0.07	0.001	≤50	-
Cobalt (Co)	mg/L	2.51	0.68	-	-
Copper (Cu)	mg/L	39.3	0.60	≤2000	1
Iron (Fe)	mg/L	130	4.14	≤2000	0.3
Manganese (Mn)	mg/L	47.0	52.2	≤400	0.05
Mercury (Hg)	mg/L	0.00	0.004	≤6	-
Nickel (Ni)	mg/L	19.6	2.75	≤70	70
Selenium (Se)	mg/L	0.02	0.017	≤40	40
Vanadium (V)	mg/L	0.00	0.002	≤200	-
Zinc (Zn)	mg/L	14.0	0.572	≤0.005	2
Cyanide (CN <sup>-</sup> )	mg/L	-	-	≤200	-

## 7.7 Discussion

### 7.7.1 Particles size distribution and porosity

The sampled SMW can be classified as course-fine, with similar results obtained for SMW of Cyprus-type Cu-pyrite ore by Galanopoulos *et al.* (2019). The SMW particles were relatively small, surging the surface area exposed to the leachate and the possibility of PTEs leaching out of the SMW. The PSD analysis of the SMW of O’Kiep presents an insight of fine-grained material that could be bioaccessible in a given sample through inhalation or ingestion channels (Kim *et al.*, 2011). Eighty-three percent of the MT-sample particles were  $\leq 250 \mu\text{m}$  and can swiftly adhere to surfaces, including those of foodstuff and skin (Plumlee *et al.*, 2006; Plumlee *et al.*, 2003). Additionally, the reasonably higher porosity of 33% and 42.7% of the SMW and MTs, respectively, allows enhanced oxidation and consequently accelerates ARDP (Fosso-Kankeu *et al.*, 2018). Currently, the O’Kiep community, which lives within the surroundings of the SMW and MTs, is exposed to PTEs borne by the wind.

### 7.7.2 Mineralogical and geochemical characteristics

The mineralogy was dominated by iron oxide, hydroxide sulfate minerals, magnetite and hematite minerals due to acid weathering (Dold, 2014b). The reported organic C contents of 10.4% improves the water-holding capacity of the SMW (Arocena *et al.*, 2010; Sollins *et al.*, 2006). On the other hand, the abundant minerals in the MT sample were composed of aluminosilicates such as microcline, albite clinocllore-1MIIb, anorthite, muscovite-1M and halloysite-10A, which is in agreement with the gneiss nature of the granitic host rock in O’Kiep (Potgieter, 1996). Aluminosilicates such as albite, clinocllore-1MIIb, anorthite, muscovite-1M and halloysite-10A may raise the pH, which will result in the release of PTEs during oxidation (Moon *et al.*, 2008). The SMW had a high concentration of Ni (372 mg/kg), indicating that secondary minerals play a significant role in Ni adsorption of the weathered SMW of O’Kiep. Iron secondary minerals are expected to precipitate in neutral drainage environments since magnetite and hematite present in SMW are well-known to play an essential part in governing PTE release in leachates by co-precipitation or sorption (Plante *et al.*, 2011; Heikkinen and Räsänen, 2008).

Oxidation of the SMW was also characterised by the high amount of magnetite ( $\text{Fe}_3\text{O}_4$ ) of 50 wt. %. The presence of kehoeite corroborates with the concentrations of Zn (953 mg/kg) and CaO (1.0 mg/kg) (Barrer, 2012). Secondary Fe minerals can be formed from the reduction and dissolution of Fe(III) in crystalline Fe minerals, that is magnesioferrite and magnetite commonly present in MTs, via transformation processes catalysed by Fe(III)-reducing bacteria (Liu and Huang, 2017). The MT sample also contained magnesioferrite and magnetite, which are initial sources of ARDP. Magnesioferrite and magnetite are the major acid-producing minerals in copper MTs (Behera *et al.*, 2019). The MTs were free of primary sulfide constituents.

Quartz was the most dominant primary mineral and this shows that it is less reactive in oxidising conditions, and has minimal potential to neutralise acid due to its physical characteristics (Rudzani *et al.*, 2018). Furthermore, the presence of halloysite-10A was indicative of constituents that normally occur in arid climates (Ziegler *et al.*, 2003). It can be seen from Figure 7-3 that there were no S-bearing minerals measured in the MSW of O’Kiep. However, the assumption that SO<sub>4</sub> results from sulfide oxidation is reasonable given the absence of S-bearing minerals (Langman *et al.*, 2014). However, the presence of CaO in the MTs can potentially contribute to the neutralisation of the acid being formed (Rudzani *et al.*, 2018).

### 7.7.3 Static test predictions

Static tests were conducted to define the acid-generation potential of SMW and MTs disposed of in the TSF in O’Kiep (Table 7-1). The SMW produced a near-neutral paste pH of 5.6, suggesting some degree of fast-weathering minerals such as calcium with acid-consuming potential. This could be in line with the mineralogy data suggesting dissolution of carbonates. Furthermore, this may imply that the sample is non-acid-forming, though this can be confirmed by the ABA test experiments. The MT samples used in this study were collected in acidic zones of the TSF, which was confirmed by the paste pH of 3.1, revealing the elevated acidity of the MTs. A low paste pH can be related to iron sulphide oxidation and also to soluble mineral dissolution (Yucel and Baba, 2016). However, the paste pH did not provide information about the PTEs released from the SMW material being linked to acid generation (Weber *et al.*, 2006). PTEs such as Co, Ni, Zn and Cu were soluble at near-neutral pH in the SMW and can possibly contaminate mine runoffs, even without acidic surroundings. This is called neutral drainage (Heikkinen *et al.*, 2009; Plante *et al.*, 2011). The NP-AP ratio of 0.06 in the SMW allows the sample to be classified as likely to produce ARD, according to Price *et al.* (1997). Similarly, the NPR ratio of 0.1 and a total sulphur content (S) of >3% indicated a higher chance for MTs to be classified as having ARDP (Cruz *et al.*, 2001).

The NNP value of the SMW was -29 kg CaCO<sub>3</sub>/t, which is less than -20 kg CaCO<sub>3</sub>/t. The sample was therefore considered acid-generating (Benzaazoua *et al.*, 2004). The S present at a high concentration (12 912 mg/kg) is mainly associated with the secondary iron oxide dissolution into magnetite and hematite, which are slow-weathering minerals contributing to the neutralisation of ARDP (Issaad *et al.*, 2019) of the SMW. This shows that SMW may have acid-generating potential, but this does not mean that the S has entirely dissolved. Additionally, if the S<sub>total</sub> content of the SMW is more significant than 0.3%, it oxidises rapidly if exposed to oxygen and water and may result in ARDP (Hutt and Morin, 1999). The MT sample was classified as having a low sulfide (S) content (6.1%) and highly negative values of NNP (-210 kg CaCO<sub>3</sub>/t); this is an indication that the MTs are likely to generate ARD when exposed to atmospheric conditions (Nieva *et al.*, 2018). The value of the NP obtained in the MTs studied was -19, which is in accordance with the low

values of acid-neutralising minerals obtained, such as CaO (3.41 mg/kg) and gypsum (2.6 wt. %). The  $S_{\text{total}}$  content of the SMW samples according to the LECO test was 1% and therefore has a strong capacity for ARDP (Yucel and Baba, 2016). However, this may also depend on the availability of acid-consuming minerals such as carbonate which may contribute to neutralisation.

The ARD-seepage effects can manifest in low pH waters (1.4 to 4), with subsequent precipitates of hydrous ferric oxides, including efflorescent sulfate salts, and blooms of green filamentous biofilms on the TSF (Wierzbicka-Wieczorek *et al.*, 2019) which is the case in O'Kiep. Consequently, the effects of ARD and aggradation by mineralised SMW and MTs would affect nearby communities (Cruz-Hernández *et al.*, 2016). These conditions could enhance PTE leachability and cause an increased environmental risk for the nearby soil and groundwater sources. Furthermore, the chemical and physical dispersion of PTEs might continue from the SMW and MTs for the predictable future unless a mitigation strategy is implemented.

#### **7.7.4 Geochemical evaluation of the metalliferous solid waste leachate using humidity cell tests**

The pH of the SMWL and MTL reached 3.7 and 5.4, respectively, in the first week. At this stage of the experiment, it is expected to see high dissolution of fast-weathering minerals of carbonate which contribute to neutralisation. This is contrary to the ABA test results, which revealed a near-neutral pH for the SMW and acid pH for the MTs. Throughout the HCT experiment, the SMWL exhibited acidic pH values of between 3.1 and 3.7 and the MTL between 4.6 and 5.5, as shown in Figure 7-6. Acid-generation/-neutralisation interactions can be studied through evaluation of  $\text{SO}_4$  oxidation products and acid-neutralisation products such as Ca and Mg (Benzaazoua *et al.*, 2004). The contradictory results of the paste pH of 3.1 for the MTs and 5.6 for the SMW were probably due to the fast reaction of secondary minerals capable of influencing the paste pH (Weber *et al.*, 2006). The acidity produced by the oxidation of the sulfide minerals gradually increased during the first cycle to 3.7 and declined to 3.2. It is hypothesised that the mobility and reactivity of major PTEs increase at low pH. However, the pH of the MTL increased from 4.6 to 5.4 and this may not be indicative of ARD. The ARDP of the sample was probably suppressed by the elevated quantity of neutralising constituents such as carbonates (Méndez-Ortiz *et al.*, 2007). However, the presence of magnesioferrite, magnetite and  $\text{Fe}_2\text{O}_3$  indicates that ARD formation had taken place but was counterbalanced by the existence of neutralising constituents in the MT sample. Subsequently, the pH remained almost steady for 20 weeks and then declined to 3.3, with increasing acid-generating capacity of the SMWL, until it reached a steep decline at week 21, implying progressive oxidation of  $\text{Fe}_2\text{O}_3$  (Parbhakar-Fox *et al.*, 2013). The significant increase in pH between week 1 and week 2 for the MTL sample was indicative of the reduced sulfide quantity and adequate acid neutralisation by carbonate minerals to sustain an acidic condition. However,

high amounts of PTEs were not observed in the SMWL as the mineralogical composition confirmed low contents of secondary minerals (Figure 7-3).

On the other hand, both the SMWL and the MTL alkalinities of the leachates as  $\text{CaCO}_3$  were less than 5 mg/kg throughout the experiment. The pH declined in the SMWL and MTL since the carbonate constituents were insufficient to neutralise the acid generated from sulfide oxidation (Langman *et al.*, 2014). The non-carbonate assemblage in the SMWL and MTL mainly comprises of minerals that exist in the granite (Smith *et al.*, 2014). Following the preliminary release of fine particles and primary weathering products, the maximum concentrations of dissolved solids were detected in the leachates. Acid neutralisation by carbonates was anticipated to be short due to the comparatively higher amount of sulfide in the SMW (Figure 7-4) and its minimum carbonate content. Subsequent to carbonate reduction, the main acid-neutralising mechanisms naturally are the dissolution of Al and Fe hydroxides and reactive aluminosilicate minerals (Langman *et al.*, 2014).

The high EC and TDS values noticed for the SMW and MTs are attributed primarily to the release of large quantities of PTEs. The SMW initial dissolution exhibited a significant release of TDS from 9284 to 39148 mg/kg during the first week of the HCTs because of fine particles and highly reactive mineral surfaces (Langman *et al.*, 2014). Conversely, the MTL initial dissolution exhibited a significant reduction from 27655 to 6080 mg/kg. The EC and TDS profile was quite similar to that of sulfate (see Figures 7a-7b), implying that the EC and TDS of the SMWL and MTL were controlled mainly by sulfate concentration. Similar findings were obtained in the study by Yolcubal *et al.* (2017).

The dissolved sulfate concentration of 3933 mg/kg was primarily the result of the oxidation of sulfide and the dissolution of gypsum (2.6% wt.) in the MTs of 2.6% wt. Moreover, Ca coming from gypsum dissolution had a continual evolution (Benzaazoua *et al.*, 2004). It was observed that for all of the experiments, the amount of cumulative sulfate collected exceeded the amount of sulfate originally found in the SMW and MTs. Acid-generation or acid-neutralisation relationships can be studied through an assessment of sulfide oxidation products such as  $\text{SO}_4$  and acid-neutralisation products such as Ca and Mg (Benzaazoua *et al.*, 2004). The Ca and Mg are contained in carbonate minerals, which dissolve when pyrite and sulfides oxidise. Throughout the test, the pH of the SMWL remained high because of the significant NP of these carbonates in the SMW. However, this NP seems to decline in the acidic MTL following consistent decrease of these carbonates. This can be noted by looking at the evolution of Ca and Mg in the leachates of both samples. This phenomenon is observed in both HCT assessments (see Figure 7-7). The study suggests that Ca and Mg originate from a related source, the dissolution of carbonate minerals (Diehl *et al.*, 2003). Furthermore, these values signify mineral reactivity and

corresponding sulfate concentrations that are dominated by oxidation reactions, with slight influence from neutralisation (Hakkou *et al.*, 2008).

The increase of the discharge of Ca-, Mg- and SO<sub>4</sub>-associated contents was compared at different time intervals for week cycles 0-2 and 2-21 corresponding to the variation in pH or changes in acid-generation potential. The SO<sub>4</sub> of the SMWL increased from 5720 to 22216 mg/kg, while the SO<sub>4</sub> of the MTL decreased from 14453 to 3925 mg/kg in the second cycle of the HCTs. Then there was a significant decrease of SO<sub>4</sub> from cycle 2 to cycle 21 for both experiments. Primarily, the SMW contained existing carbonate minerals to neutralise the quantity of acid produced through the oxidation of the reduced sulfide minerals for cycle 1 to cycle 2, whereas the opposite occurred for the MTL, except for the period from week 2 to 21. No substantial variation in pH for both samples was recorded during this period. The acid-generation/-neutralisation relations for the SMW were dominated by a tendency to acidification, reflected in reduced pH values during the period from 2 to 21 weeks of the HCTs. The oxidation of the sulfide minerals in the SMW and MTs overwhelmed the carbonate acid-neutralisation capability from week 2 to 21 and resulted in a significantly larger release of SO<sub>4</sub> compared to Ca and Mg. Acid neutralisation by carbonates in the SMWL was projected to be short due to the moderately higher sulfide concentration in SMW (15418 mg/kg). It was noticed that the cumulative effect of Ca and Mg in the leachate was more reliant on the Ca amount of the SMW. Acid neutralisation by carbonates in the MTL was minimal since the sulfides in the MTs were low at 3933 mg/kg when compared to that in the SMW. The Mg content was lower and is unlikely to play a part in the neutralisation process of the ARD. Similar results were obtained by Banerjee (2014). Calcite was the primary carbonate and typically found in the granite (Langman *et al.*, 2015; Smith *et al.*, 2014). Such minerals might be produced as secondary minerals in leachates with weathering rates (Blowes *et al.*, 2003). The amount of Ca and Mg in the SMWL and MTL produced a relatively small release of SO<sub>4</sub> at the start of the experiment. The acid generated from sulfide oxidation produced an increase in SO<sub>4</sub> from week 2 to 21. On the other hand, weathering of the SMW resulted in an increase of SO<sub>4</sub> concentrations from week 3 to 21 for both samples. There is no specific reason for the difference in the oxidation-neutralisation curve (see Figures 7a-7b). However, one may take into account alterations and interaction of the PTEs in the MSW. The SMW sample will produce acid if carbonates are depleted while sulfides are still present. If the MTL sample is not acid-producing, it could therefore be suggested that it contains carbonates in sufficient quantities to neutralise all acid produced by sulfide oxidation.

At the beginning of the second cycle of the HCTs, the release rates of Cl and Mg in the SMWL increased to 111 and 1159 mg/kg, respectively. This increase of Cl and Mg was an indication that several acid-consuming reactions had neutralised the acid, that is concerning the leaching of

silicate minerals and carbonate minerals (Wu *et al.*, 2009; Mousavi *et al.*, 2006). The Cl and Mg release rates at the third week varied between 25 and 122.8 mg/kg, with a gradual decline to less than 2 and 3.89 mg/kg, respectively. The gradual decrease of Cl and Mg concentrations in the MTL from 954 to 2 mg/kg and 1513 to 1.05 mg/kg, respectively, provides evidence of a low weathering rate and weak neutralising potential. The non-carbonate accumulation in the SMWL and MTL mainly related to minerals that exist in the granite (Langman *et al.*, 2015; Smith *et al.*, 2014). With a reduction of the acid-neutralisation ability of carbonate minerals, the acid neutralisation was associated with Al-bearing phases which might have stabilised around a near-neutral pH to a pH of 4 to 5 (Price, 2009; Blowes *et al.*, 2003). The relatively stable pH for the SMWL in the HCTs and the increase in dissolved Al concentrations ranging from 9.02 to 1274 mg/kg between week 1 and 2 indicated an overlapping of chemical reactions such as sulfide oxidation and acid neutralisation (Langman *et al.*, 2014). The reverse is true for the MTL, since the Al concentration decreased from 59.5 to 1.28 mg/kg. The Mn in the SMWL ranged between 0.07 to 46.9 mg/kg, whereas Mn in the MTL ranged between 0.14 to 52.2 mg/kg. The Mn-carbonate is a common gangue material of mining areas and it is soluble at low pH (Diehl *et al.*, 2006).

The molar relation of Fe to S in the MSW generated through the entire leaching period was less than 0.5% for the SMW and MT samples, which implies Fe-mineral precipitation (Sapsford *et al.*, 2009). Although Al release rates in SMWL and MTL declined in the second cycle from 1274 to 9.0 mg/kg and 59.5 to 0.2 mg/kg, respectively, in the 21 cycle with PTE reduction in the reacting zone, the rates influenced those of the sluggish dissolving ion (Samson *et al.*, 2005). Fe<sup>2+</sup> to Fe<sup>3+</sup> oxidation is likely to take place in an acidic environment (Murakami *et al.*, 2003). PTEs in the SMWL also displayed similar dissolution behaviour during the HCTs. The rate of PTE release was primarily fast and then declined significantly, whereas the rate of PTE release was slow in the MTL.

Results of the HCTs showed that the PTE and SO<sub>4</sub> release rates from the SMWL and MTL were relatively low as related to that of sulfides. A rapid and subsequently slower PTE release kinetics indicate that various processes, including mineral dissolution and oxidation, played a role in the PTE-dissolution behaviour. Fe was mostly retained in the SMW, whereas Zn showed rather high mobility. These HCTs showed that the SMW is acid-generating with the high release of Al (9.02 to 1274 mg/kg), Ca (93.4 to 294 mg/kg) and Si (0.5 to 14.6 mg/kg) in the SMWL, which elements originate from the acidic dissolution of silicates (Issaad *et al.*, 2019). Fe concentrations in the SMWL ranged from 2.3 to 129.6 mg/kg; this highlights how iron sulfide dissolution is necessary (Issaad *et al.*, 2019). Furthermore, the unlikely dissolution of silicates at acidic pH might result in an insignificant amount of Fe in the SMWL. Cu concentrations were relatively low in the SMWL,

ranging between 1.9 to 39.3 mg/kg and 0.04 to 0.6 mg/kg, respectively. This could be due to a small degree of liberation and amount of Cu-sulfide-bearing minerals within the SMW and MT samples (Issaad *et al.*, 2019). It is advantageous to be acquainted with how sudden acid-producing reactions such as pyrite oxidation are taking place in the SMW and MTs (Sapsford *et al.*, 2009). Therefore, among the studied samples, only the SMW is classified as acid-generating, with the MT sample at the limit of acid-producing.

#### **7.7.5 Mobility of sulfide-bound potentially toxic elements in the metalliferous solid waste**

The mobility of dissolved PTEs within the SMWL and MTL is controlled by a complex series of phenomena such as sorption, desorption, dissolution, oxidation and precipitation reactions. The concentrations of each dissolved PTE are a function of pH and of the mineralogy of the MSW (Romero *et al.*, 2007). The geochemistry of the leachates of the MSW indicates that the mobility of sulfide-bound PTEs observed in the SMW followed the order:  $\text{SO}_4 > \text{Ca} > \text{Al} > \text{Si} > \text{Na} > \text{Fe} > \text{Cu} > \text{Zn} > \text{Mg} > \text{Ni}$ . On the other hand, PTEs in the MTs followed the sequence:  $\text{SO}_4 > \text{Ca} > \text{Si} > \text{K} > \text{Na} > \text{Al} > \text{Sr} > \text{Mg} > \text{Ni} > \text{Cu} > \text{Zn}$ .

#### **7.8 Summary**

The SMW can be classified as gravelly sand with some silt, whereas the MTs can be classified as coarse-fine material. The main mineralogical phases detected were magnetite, carbon, quartz, hematite and kehoite, which contained the highest concentrations of PTEs associated with the secondary minerals (in mg/kg) such as Cu (3266), Zn (953) and Co (568). Some of the secondary minerals may have been less than 5 mg/kg, but their impact can be very significant. Oxides of the SMW were dominated by  $\text{Fe}_2\text{O}_3 > \text{SiO}_2 > \text{Al}_2\text{O}_3 > \text{MgO} > \text{Na}_2\text{O} > \text{CaO}$ . The geochemical characterisation of the SMW revealed relatively high content of the PTEs in concentrations varying according to the following order:  $\text{S} > \text{Cu} > \text{F} > \text{Ni} > \text{Zn} > \text{Co} > \text{Pb} > \text{Mn} > \text{Cr} > \text{Mo} > \text{V} > \text{Cl}$ . On the other hand, the MTs of O’Kiep contain PTEs such as  $\text{F} > \text{Cu} > \text{Cr} > \text{Mn} > \text{S} > \text{Zr} > \text{Ba} > \text{Sr} > \text{V} > \text{Cl} > \text{Rb} > \text{Ni} > \text{Zn} > \text{Y} > \text{Co}$ . The major oxides were  $\text{SiO}_2 > \text{Al}_2\text{O}_3 > \text{Fe}_2\text{O}_3 > \text{CaO} > \text{MgO} > \text{K}_2\text{O} > \text{Na}_2\text{O} > \text{TiO}_2 > \text{P}_2\text{O}_5 > \text{SO}_3 > \text{Cr}_2\text{O}_3 > \text{MnO} > \text{NiO}$ . The ABA and HCTs both allowed the classification of the SMW as acid-generating, whereas the MT sample was at the limit of the acid-producing range. These results are in agreement with the high S contents of 15418 mg/kg for the SMW and 3933 mg/kg for the MTs. O’Kiep SMW and MTs have the potential to generate ARD due to their physico-geochemical composition. The mobility of PTEs was high at low pH and controlled by a sequence of dissolution and precipitation. The PTEs of the SMW were more mobile at acidic pH when compared to the MTs. The findings in this study allow the prediction that SMW and MTs may have significant impacts on soil and groundwater contamination. Additionally, a high precipitation pattern as in the case of the study site may encourage oxidation and cause infiltration of water in the SMW and MTs, leading to a subsequent discharge of ARD harmful to

the environment. Rehabilitation of the SMW and MT site is necessary to limit further environmental impact. After evidenced ARDP of numerous constituents from mining activity, MSW among other constituents, it was therefore required to provide evidence of the historical deterioration of the groundwater over a period of time, as highlighted in Chapter 8. This was done to provide proof of the assertion made, namely that numerous constituents assisted by environmental conditions are hazardous to the groundwater of O’Kiep.

## CHAPTER 8: RESULTS AND DISCUSSION

---

Published as:

- 1]. **Erdogan, I.G.**, Netshiongolwe K., Mosai, A., Fosso-Kankeu, E., Ntwampe, S.K., Waanders, F.B., Hoth, N. 2020. Geochemical modelling data of groundwater in the O’Kiep, Namaqualand region, South Africa – 2013 to 2019: A case of evidenced contamination by historical mining activity. 18th International Conference on Science, Engineering, Technology and Waste Management (SETWM-20), Nov. 16-17, Johannesburg, South Africa.

Available: <https://doi.org/10.17758/EARES10.EAP1120218>

Dataset of the above-mentioned article

- 2]. **Erdogan, I.G.**, Mosai, A., D., Ntwampe, S.K.O., Fosso-Kankeu, E. and Waanders, F.B. 2020. Geochemical modelling of groundwater in the Namaqualand region, South Africa. Cape Peninsula University of Technology. Dataset.  
DOI: 10.25381/cput.12820505.v1 (Supplementary file: S3).

## **8.1 Geochemical modelling data of groundwater in the O’Kiep, Namaqualand region, South Africa – 2013 to 2019: A case of evidenced contamination by historical mining activity**

### **8.2 Introduction**

Surface water is inadequate to meet the accumulative water demand of drinking water in O’Kiep due to the increasing populace and urbanisation. On the other hand, it is unsafe to use the DWSS in O’Kiep due to the possible bacterial contamination and regular interruptions in this area (see Chapter 3). Furthermore, earlier studies suggest that potential ARD formation is recognised as one of the environmental challenges associated with groundwater contamination in this former mining area, as highlighted in Chapter 5. Since groundwater is an essential resource for the community of O’Kiep, and considering that the community might mainly rely upon it in the near future for drinking and irrigation purposes, its monitoring is essential. Subsequently, some studies have been conducted in this area to determine the groundwater quality and its suitability for drinking and irrigation, as discussed in Chapters 4 and 5.

Although soil acts as a natural filter removing and adsorbing PTEs, long-term release of ARD leads to the saturation of PTEs in the soil, with subsequent leachates seeping into the water table. Hence, it can also result in the reduction of filtration and adsorption capability of the soil and subsequently lead to the deterioration of groundwater quality over time. Among many diverse contaminants, the presence of PTEs in groundwater is of major concern. Additionally, it was also shown that there is leaching of ARD into groundwater in O’Kiep. In principle, groundwater quality is influenced by the industrial activities, geology and climate conditions of an area. Furthermore, the groundwater quality could be influenced by geochemical reactions such as dissolution, ion exchange, oxidation and precipitation in the aquifer from where the groundwater is sourced (Ravikumar *et al.*, 2015; Sakram *et al.*, 2013). Some of the tools that are normally used in hydrogeochemistry are the trilinear piper (Piper, 1953) and the Durov diagrams, the former evaluating the groundwater evolution, whereas the latter reveals geochemical processes that could influence the groundwater genesis (Ravikumar *et al.*, 2015). Hence, this part of the study was aimed at determining the hydrogeochemical changes (processes) controlling the hydrogeochemical chemistry of the groundwater in O’Kiep and its evolution over time.

### **8.3 Objectives**

The objectives of this part of the study were:

- to determine if groundwater has deteriorated over time;
- to determine mineral phases and chemical reaction occurring in the groundwater; and

- to assess the deterioration of the groundwater quality due to anthropogenic activities through geochemical modelling.

## 8.4 Materials and methods

### 8.4.1 Hydrogeochemical parameters

To determine the hydrogeochemical parameters of groundwater in O’Kiep, samples were collected from eight boreholes, as highlighted in Chapter 4, whereas historical data were extracted from a study published by Abiye and Leshomo (2013), as shown in Table 8-1. Most of the boreholes in the study area are associated with a fractured basement aquifer in the Namaqualand.

**Table 8-1: Comparison of hydrogeochemical parameters in groundwater (periods 2013 and 2019)**

	Unit	Period 2013	Period 2019	ST. DV.	(SANS241-1, 2015)	(WHO, 2011)
pH @ 25°C	-	7.11	8.1	1.1	5 ≤ 9.7	6.5-9.5
Redox Potential (ORP)	mV	29.2	-57.0	49.3	-	-
Temperature	°C	22.1	15.0	3.6	-	-
Electrical Conductivity (EC)	mS/m	2.04	241	217	≤170	100
Total Dissolved Solids (TDS)	mg/L	911	1793	1561	≤1200	500
Alkalinity (CaCO <sub>3</sub> )	mg/L	179	134	118	-	-
Sodium (Na)	mg/L	224	243	194	≤200	100
Magnesium (Mg)	mg/L	51.5	67.3	54.3	-	-
Potassium (K)	mg/L	5.69	15.3	19.2	-	-
Calcium (Ca)	mg/L	78.5	184	157	-	-
Chloride (Cl)	mg/L	447	470	514	≤300	5
Nitrate (NO <sub>3</sub> )	mg/L	27.3	2.16	12.4	≤11	-
Potassium (PO <sub>4</sub> )	mg/L	1.41	0.50	0.5	-	0.4
Sulfate (SO <sub>4</sub> )	mg/L	121	455	533	≤500	200
Zinc (Zn)	mg/L	0.81	0.00	0.4	≤5	2
Iron (Fe)	mg/L	0.32	0.07	0.1	≤2	0.3
Cadmium (Cd)	mg/L	9.77	0.003	4.9	≤0.003	-
Chromium (Cr)	mg/L	0.16	0.01	0.1	≤0.05	-

The Namaqualand is situated in the south-western region of South Africa, and is an arid region of the Northern Cape (Brenzinger, 2008). The method used for measurement of the hydrogeochemical parameters such as pH, EC, TDS and ions are as described in the studies of Abiye and Leshomo (2013) for the 2013 period and Erdogan *et al.* (2019) for the 2019 period. These hydrogeochemical parameters were compared to the drinking water quality guidelines as described by SANS241-1 (2015) and WHO (2011).

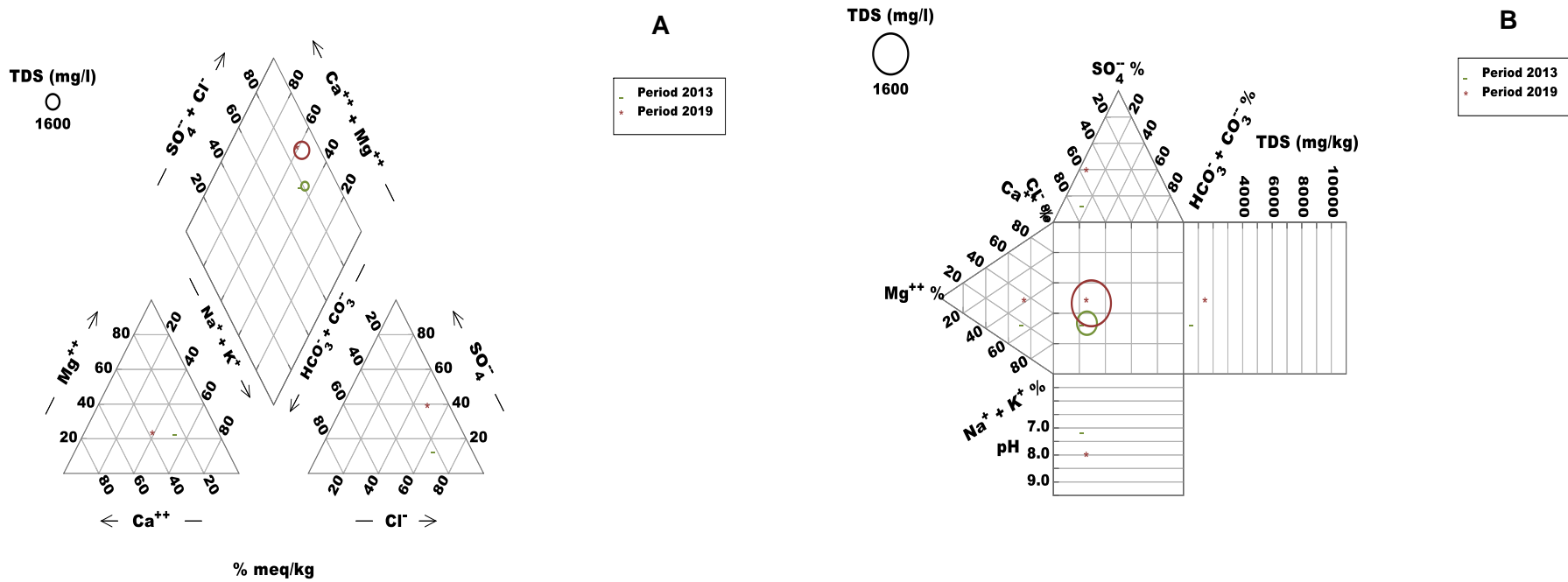
### 8.4.2 Geochemical modelling

PHREEQC v3, a computer programme written in C++ programming and developed by the United States Geological Survey (USGS) agency (<https://www.usgs.gov/software/phreeqc-version-3>), was used to perform an aqueous geochemical modelling that has capabilities to determine a

saturation index (SI) and speciation determinations in a batch-type-reaction system (Parkhurst and Appelo, 2013; Parkhurst and Appelo, 1999). The interaction between the groundwater and rock mineralogy controls the geochemistry of the groundwater in the specified study area (Kumar *et al.*, 2020). As such, such an interaction was accounted for.

#### **8.4.3 Groundwater classification using the trilinear piper and Durov diagrams**

To identify the different groundwater types of the area, the results of the hydrogeochemical analyses were plotted on a trilinear piper diagram, as presented in Figure 8-1a. The major ion concentrations of the groundwater data in the study area for period 2013 and period 2019 were plotted on the confirmatory Durov diagram (Durov, 1948), as presented in Figure 8-1b. The Durov diagram improves the interpretation of the groundwater evolution and provides more information on the hydrogeochemical processes occurring in groundwater schemes such that it is easy to identify mixing of different water types and ion-exchange and reverse ion-exchange processes (Aly *et al.*, 2015).



## 8.5 Results and discussion

### 8.5.1 Hydrogeochemical characteristics

The high values of standard deviation (see Table 8-1) for parameters such as Na, Cl and SO<sub>4</sub> display a high dispersion. This suggests that the groundwater hydrogeochemical characteristics showed a comprehensive spatial variation. The pH varied from 7.11 to 8.1, indicating that the groundwater was slightly alkaline, which was attributed to mineral sources such as carbonates in the groundwater (Liu *et al.*, 2020). The EC and TDS values of the groundwater increased from 2.04 to 241 mS/m and from 911 to 1793 mg/L, respectively. Additionally, the higher values of the standard deviation for EC (217 mS/m) and TDS (1561 mg/L) suggests a great variability in the hydrogeochemical processes, which could be attributed to groundwater residence time, the heterogeneity of the nearby alluvial and crystalline basement of the aquifer (Titus *et al.*, 2002) lithology and former mining activities, especially in O’Kiep. In general, the abundant cations in the groundwater were Ca, Mg and Na (Liu *et al.*, 2020). The concentration of Ca, Mg and Na changed from 78.5 to 184 mg/L, 51.5 to 67.3 mg/L and 224 to 243 mg/L, respectively.

Carbonate dissolution is the key source of Ca and alkalinity in groundwater. With respect to anions, Cl dominated in the groundwater samples and changed from 447 to 470 mg/L, followed by SO<sub>4</sub> from 121 to 455 mg/L. An increase of SO<sub>4</sub> with the increase in Cl could be due to the dissolution of soluble constituents such as halite and gypsum, as reported in Chapter 5. On the other hand, the NO<sub>3</sub> and PO<sub>4</sub> decreased from 27.3 to 2.16 mg/L and from 1.41 to 0.5 mg/L, respectively. It was observed that most of the parameters, including EC, TDS, Na and Cl, were much higher than the recommended values in the guidelines (SANS241-1, 2015; WHO, 2011).

### 8.5.2 Groundwater classification

Data for periods 2013 and 2019 describe the groundwater as chlorine-type water, alkali and strong acid-predominated and saline groundwater (Liu *et al.*, 2020; Ravikumar and Somashekar, 2017). The Namaqualand district is characterised as a Na-Cl region with widespread salt pans. This has a significant role in governing the quality of groundwater salinity, which is relatively high and similar to those obtained by Abiye *et al.* (2018). The trilinear piper diagram presents the hydrogeochemical evolution of the groundwater during the studied period in the Namaqualand and substantiates the alterations amongst the four sets, namely Ca–Mg–HCO<sub>3</sub>; Na–K–HCO<sub>3</sub>; Na–K–Cl–SO<sub>4</sub>; and Ca–Mg–Cl–SO<sub>4</sub>. Types for both periods (2013 and 2019) are shown in Figure 8-1a. The groundwater evolved from being low

mineralised, with EC of 2.04 mS/m in 2013, to a progressive increase in salinity, with EC of 241 mS/m in 2019. Groundwaters rich in Na and K represented 80% for both periods. This was confirmed by the Durov diagram (Figure 8-1b), where the majority of groundwaters were in an ion-exchange zone for periods 2013 and 2019, while Ca was 21% for the period 2013 and 39% for the 2019 period. However, groundwater dominant in Cl-SO<sub>4</sub>, producing a chlorine-type groundwater, represented 80% for the period of 2013 and 90% for the 2019 period. Additionally, the Durov diagram shows that Cl ion is the main ion responsible for the increased salinity, even though the SO<sub>4</sub> ion was also significant in 2019. According to Leshomo (2011) and as highlighted in Chapter 4, the salinity in the groundwater of Namaqualand is derived from halite dissolution and seawater mixing. For alkaline water with predominant Na–K–Cl–SO<sub>4</sub> as strong acids (Cl and SO<sub>4</sub>), facies represented 90% for the 2019 period. In general, the ion-exchange process and weathering of rocks mainly govern the groundwater hydrogeochemistry of Namaqualand. The data plots in the trilinear piper and Durov diagrams reveal that the predominant cations were Na and K followed by Ca and Mg, whereas the most abundant anions were Cl and SO<sub>4</sub> (Figure 8-1b). The increase in SO<sub>4</sub> concentrations in the 2019 period was hypothesised to originate from historical mining-associated activities due to sulfide-mineral oxidation in the SMW and MTs (Miao *et al.*, 2013).

### 8.5.3 Geochemical modelling

In this part of the study, inverse geochemical modelling for the observed variations from period 2013 to period 2019 was performed, given that it is the characteristic of groundwater hydrogeochemical evolution in the Namaqualand. A PHREEQC modelling software approach allows for the simulation and characterisation of the hydrogeochemical processes influencing the groundwater quality. The composition of the groundwater contaminated by various PTEs can be used to predict reactive mineral mechanisms. Any variations observed between different datasets can determine the geological matrix interaction between significant anions and cations (Maoui *et al.*, 2010). PHREEQC determines the SI of various minerals in numerous mixtures and solutions. As such, a positive SI indicates precipitation or supersaturation of secondary minerals and a negative SI indicates the dissolution or undersaturation of minerals, whereas a SI of  $\pm 0.5$  indicates equilibrium conditions (Chidambaram *et al.*, 2012). Figure 8-2 represents the changes of the SI of particular phases.

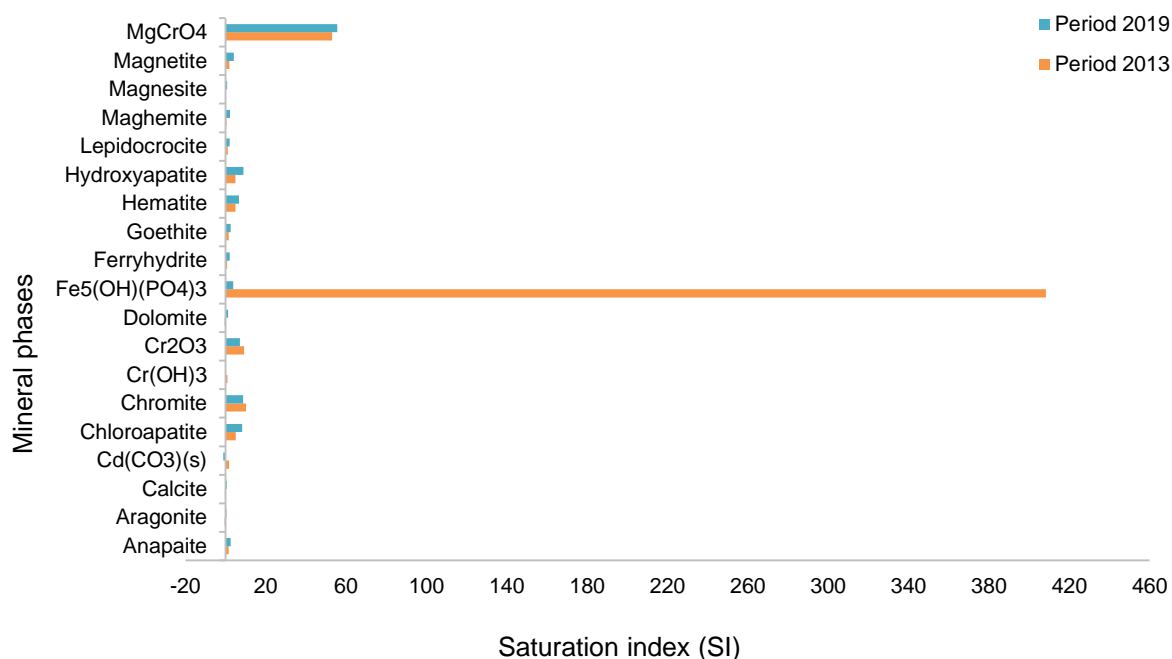


**Figure 8-2: Saturation index of mineral phases in Namaqualand for the 2013 and 2019 periods**

The model output showed phases that are governing the groundwater chemistry in the region, with some geochemical reactions identified as responsible for the evolution of the groundwater chemistry. Regarding dissolution, carbonate minerals such as aragonite,  $\text{Ca}_3(\text{PO}_4)_2$ , calcite, dolomite, ferrihydrite and vaterite were identified as initially undersaturated (2013) to supersaturated (2019), with an undersaturation of  $\text{Cd}(\text{CO}_3)$ ,  $\text{Cr}(\text{OH})_3$  being observed during the same period of 2019. Similarly, the precipitation of anapaite, chloroapatite, chromite,  $\text{Cr}_2\text{O}_3\text{Fe}_5(\text{OH})(\text{PO}_4)_3$ , ferryhydrite, goethite, hematite, hydroxyapatite, lepidocrocite, maghemite and magnetite was observed, with magnesite evolving from being undersaturated to an equilibrium phase. The gypsum, siderite and halite remained undersaturated, indicating that these minerals may be subjected to continuous dissolution as the groundwater hydrogeochemical evolution is mainly controlled by carbonate mineral dissolutions, cation exchange, precipitation and weathering. Several minerals were determined to remain in a dissolution state (see S3: Supplementary data).

## 8.6 Summary

In this research, hydrogeochemical characteristic techniques and geochemical modelling were integrated to identify the significant factors governing groundwater hydrogeochemical evolution in Namaqualand. The pH values of the groundwater were alkaline in nature during the 2013 and 2019 periods. Most of the parameters, including EC, TDS, Na and Cl, exceeded permissible limits of drinking water standards stipulated by SANS241-1 (2015) and WHO

(2011) for drinking water. The groundwater types for both periods (2013 and 2019) was Ca–Mg–HCO<sub>3</sub>, Na–K–HCO<sub>3</sub>, Na–K–Cl–SO<sub>4</sub> and Ca–Mg–Cl–SO<sub>4</sub>. The geochemical model PHREEQC suggested some geochemical reactions and mineral phases being responsible for the evolution of the groundwater chemistry and indicating that the groundwater hydrogeochemical evolution is mainly controlled by carbonate mineral dissolutions, cation exchange, precipitation and weathering. The increase in sulfate concentrations in groundwater during the 2019 period was most likely due to sulfide-mineral oxidation. Anthropogenic sources associated with the CMM, SMW, MTs and ARD were partly responsible for contributing to the increase of PTEs in the groundwater. The accumulation of SO<sub>4</sub> in the groundwater may be due to the arid climate of the area. The typical hypothesis applied at numerous mining locations is that sulfide-mineral oxidation is the main source of sulfate. This information would contribute to risk assessments and evaluation of remediation strategies. It is therefore anticipated that the groundwater contamination will continue to persist at the study area for many years.

## **CHAPTER 9: CONCLUSION AND RECOMMENDATIONS**

---

## 9.1 Conclusion

The study revealed matters associated with the DWSS in O’Kiep and perceptions about surface water and groundwater quality. In addition, some of the contaminants that affect drinking water quality at the POU were quantified and found to be within the required quality guidelines as indicated by SANS241-1 (2015) and WHO (2011). However, some parameters were not within the drinking water quality guidelines, namely DO, DOC, Eh, EC, TDS, Na, Cl<sup>-</sup> and SO<sub>4</sub><sup>2-</sup>. Furthermore, contaminant seepage into the DWSS and an irregular water supply may have contributed to the negative perception about the quality of water supplied to the community. These factors are likely responsible for diarrhoea-like symptoms. As a result, the community has been compelled to boil or add bleach to the drinking water prior to consumption. Although the community has been complaining about the altered taste of water due to high EC, salinity, TDS and SO<sub>4</sub><sup>2-</sup> and diarrhoea-like symptoms, none of the statistical models have confirmed that the physicochemical properties are responsible for any of the health-related symptoms.

MSW heaps are potential sources of PTEs and have been identified as a greater threat to the communities surrounding mining sites, particularly in O’Kiep. The groundwater was classified as being a low to medium alkaline solution as well as having low to high hardness due to the CaCO<sub>3</sub> concentration, indicating that the groundwater is hard. The EC and TDS, which depend on the characteristics of the geological formation in the study area, were high, indicating leaching of salts from the MSW into the aquifer and groundwater, with lower Eh values. According to the GWQI, the groundwater contamination in O’Kiep was classified as of moderate concern. The aquifer in this study area was controlled by weathering reactions, with minimal dilution processes, which reflects a lack of precipitation in the recharge area that feeds the aquifer. Furthermore, the co-occurrence of Mg<sup>2+</sup> and Ca<sup>2+</sup>, an interaction generally observed in arid regions, indicated that the groundwater was an alkalinity hazard. This suggests that excess usage of the water for irrigation purposes may have an undesirable effect on plant growth and have possible human health effects when the community continuously ingests harvested produce. Evidence of further water quality problems arises as a result of the contamination of the groundwater from anthropogenic activities such as mining.

It was shown that changes in seasons do have an influence on the hydrochemical properties of the OPGW, which was slightly acidic with high salinity during both the dry and wet seasons. However, the SAR values recorded during both seasons showed that the OPGW was suitable for irrigation purposes, though it was predicted that its long-term use will cause damage to the arable soil. This was also further confirmed by a Mg-Ca ratio of less than 1.5, with PHREEQC

also suggesting that cation exchanges played a significant role in controlling the OPGW chemistry. The seasonal variation of the OPGW physicochemical parameters provides information that can be useful for water resource management in the O’Kiep area, particularly with respect to biodiversity changes due to the effects of mining activities.

The metalliferous soils in O’Kiep can be classified as fine-grained particles with visible efflorescent salts highly contaminated by PTEs (mg/kg): S > Cu > F > Mn > Cl > Zn > Cr > V > Pb > Ni > Co and major oxides (%) being: SiO<sub>2</sub> > Al<sub>2</sub>O<sub>3</sub> > FeO<sub>3</sub> > K<sub>2</sub>O > CaO > NaO. ABA tests suggested that the metalliferous soils had a high acid-producing potential. This was confirmed by the results of the HCTs, which revealed a predisposition to ARD formation. The low metalliferous soil CaCO<sub>3</sub> content therefore contributed to the decline of its neutralising potential, thus susceptibility to ARD generation for elongated periods and contamination of receiving sources such as the groundwater. Furthermore, the results of this study also suggested that there is accelerated and uninhibited PTE leaching from the metalliferous soils, with the potential to disperse into the surrounding groundwater bodies. PTE contamination in metalliferous soils in O’Kiep may pose health and environmental risks to the community in the form of aerosols due to the aridity of the area. The acidic nature of the metalliferous soils of O’Kiep would provide further adverse environmental challenges for plant growth. Additionally, this study also provided important reference information for the vulnerability of soils with regard to PTE mobility, thus contamination from the MSW and mining activity in O’Kiep.

O’Kiep MSWs comprising of SMW and MTs have the potential to generate ARD due to their physico-geochemical composition. The SMW was classified as gravelly sand with some silt, whereas the MTs were classified as coarse-fine material. The PTEs detected in the SMW were: S > Cu > F > Ni > Zn > Co > Pb > Mn > Cr > Mo > V > Cl, including oxides dominated by Fe<sub>2</sub>O<sub>3</sub> > SiO<sub>2</sub> > Al<sub>2</sub>O<sub>3</sub> > MgO > Na<sub>2</sub>O > CaO. On the other hand, the MTs of O’Kiep contained PTEs such as F > Cu > Cr > Mn > S > Zr > Ba > Sr > V > Cl > Rb > Ni > Zn > Y > Co, with major oxides being SiO<sub>2</sub> > Al<sub>2</sub>O<sub>3</sub> > Fe<sub>2</sub>O<sub>3</sub> > CaO > MgO > K<sub>2</sub>O > Na<sub>2</sub>O > TiO<sub>2</sub> > P<sub>2</sub>O<sub>5</sub> > SO<sub>3</sub> > Cr<sub>2</sub>O<sub>3</sub> > MnO > NiO. The ABA and HCTs both classified the SMW as having an acid-generating potential, with the MTs having limited acid-producing ability. These results are in agreement with observed high S contents (15 418 mg/kg for SMW and 3933 mg/kg for MTs), with the high S content being associated with the oxidation process for acid formation. Therefore, the PTEs from the SMW were more mobile under an acidic pH when compared to those in the MTs. Therefore, the study further suggested that a significant impact on soil and groundwater contamination are attributable to the SMW and MTs in the studied area. Additionally, a high precipitation environment as in the case of the study site may encourage

oxidation and cause infiltration of SMW and MT constituents into water sources, leading to a subsequent discharge of developed pollution streams such as ARD, which is harmful to the environment.

In this research, hydrogeochemical characteristic techniques and geochemical modelling were integrated to identify the significant factors governing groundwater hydrogeochemical changes thus evolution in the study area. The geochemical model PHREEQC suggested some geochemical reactions and mineral phases being responsible for the evolution of the groundwater chemistry, with further indications that the groundwater hydrogeochemical evolution is mainly controlled by carbonate mineral dissolutions, cation exchange, precipitation and weathering. The observed increase in sulfate concentration in the groundwater when comparing 2019 to 2013 is most likely due to sulfide-mineral oxidation, suggesting ARD formation. The various anthropogenic activities associated with the CMM, SMW, MTs and ARD were future-predicted to increase the risk of water contamination, in particular PTE seepage, which will probably increase with time, as evidenced by the accumulation of  $\text{SO}_4$  in the groundwater. Due to this, it is therefore hypothesised that mining locations where sulfide-mineral oxidation is predominant will be the primary source of sulfate. It is therefore anticipated that the groundwater contamination will continue to persist in the study area for many years unless an interventionist rehabilitation programme is implemented.

## **9.2 Recommendations and future work**

To address concerns such as diarrhoea-like symptoms and taste and colour associated to the drinking water supplied to O’Kiep by the local DWSS, it is paramount that effective treatment systems and distribution infrastructure are in place. The long-term water quality supply security at the respective households should be assessed to be able to identify relationships with health indicators and methods for improvement should be studied. This means that it will be required in future to better understand the sources of these elements in the DWSS for the betterment of drinking water quality. The long-term exposure of the community to microcystins must be considered a health risk; therefore, implementing appropriate remedial action is required. Furthermore, biofilm growth and microbially mediated corrosion and the proliferation of cyanobacteria in the DWSS studied need further investigation in O’Kiep.

Moreover, the high percentages of PTEs in the groundwater suggest that strategies and appropriate remediation and rehabilitation protocols are required to improve the current challenges in the study area. This would include the implementation of in-situ groundwater monitoring, remediation and desalination technologies for harvested groundwater to be used

for drinking and agricultural purposes. The hydrochemical characteristics of the OPGW suggest that a water treatment system is essential as a remedial measure for the contaminated groundwater in O’Kiep. Lastly, improved management of groundwater resources in O’Kiep will lead to a more reliable and maintainable resource.

There is a need for further appropriate remedial procedures to remediate areas where mine waste is stockpiled as the generation of metalliferous dust poses a human health risk in O’Kiep. Doing so will warrant the reduction of its negative effects. Further environmental assessments and clinical outcomes must be monitored among vulnerable individuals living in the vicinity of the CMM as the accumulation of high concentrations of PTEs in areas associated with Cu mining can enhance human health comorbidity risks and arable land environmental challenges. It is also essential to determine the firmness of the MSW heaps as well as their potential failure during the wet season which can cause mudslides, although this is considered a low risk at this stage. To reduce the mining footprint and effects as well as to limit population exposure to harmful MSW, limited access to the MSW is advisable while remediation strategies and plans are being developed to resolve the present situation. Such plans may include preventative sulfide-mineral oxidation by air and moisture contact, which has been determined to further result in the release of PTEs into groundwater bodies and their deposition as aerosols in pristine areas further away from the mining site.

Future work should be conducted to improve programmes that integrate the effectiveness of testing drinking water quality and education programmes that encourage the community members of O’Kiep to treat their drinking water when necessary. Furthermore, additional household questionnaires need to be administered to convince the local municipality to incorporate testing of microcystin in the drinking water supplied at the POUs for this community. There is also a need to develop cost-effective water-testing capabilities within the region for daily monitoring of water quality. These should focus on Eh, which must be measured at regular intervals as an indication of the effectiveness of the dose of chlorine used within the O’Kiep DWSS. It is also essential to conduct environmental health and safety assessments of the CMM and MSW. Furthermore, future areas of research must consider to the use of geochemical models to predict chemical reaction and transport models taking place. A rehabilitation study of the MSW and metalliferous soil site is necessary to limit further environmental impact. In addition, the development of suitable treatment methods, such as biological and passive treatments for the OPGW, should be considered such that the technology developed could be used if the groundwater quality deteriorates to the level of the OPGW. This will benefit the community, which has limited access to drinking water resources.

Distribution, fractionation, and contamination assessment of PTEs through vertical profiling of the MSW and metalliferous soils in relation to ARD generation is also required.

## CHAPTER 10: SUPPLEMENTARY FILES

---

Published as:

- 1]. **Erdogan, I.G.**, Mekuto, L., Ntwampe, S.K., Fosso-Kankeu, E. and Waanders, F.B. 2019. Metagenomic profiling dataset of bacterial communities of a drinking water supply system (DWSS) in the arid Namaqualand region, South Africa: Source (lower Orange River) to point-of-use (O'Kiep). *Data in Brief*, 25,104135.  
DOI: 10.1016/j.dib.2019.104135.
  
- 2]. **Erdogan, I.G.**, Bent, D., Ntwampe, S.K.O., Fosso-Kankeu, E. and Waanders, F.B. 2019. Geochemical modelling and seasonal hydrogeochemical processes of the open-pit groundwater at O'Kiep, Namaqualand, South Africa. Dataset.  
DOI: 10.25381/cput.9746537.v1.
  
- 3]. **Erdogan, I.G.**, Mosai, A.D., Ntwampe, S.K.O., Fosso-Kankeu, E. and Waanders, F.B. 2020. Geochemical modelling of groundwater in the Namaqualand region, South Africa. Cape Peninsula University of Technology. Dataset.  
DOI: 10.25381/cput.12820505.v1.

## **10.1 Supplementary files**

### **10.1.1 S1: Supplementary data for Chapter 3**

#### **Metagenomic profiling dataset of bacterial communities of a drinking water supply system in the arid Namaqualand region, South Africa: Source (lower Orange River) to point-of-use (O'Kiep)**

##### **Abstract**

The metagenomic data presented herein contain the bacterial community profile of a drinking water supply system (DWSS) supplying O'Kiep, Namaqualand, South Africa. Representative samples from the source (Orange River) to the point-of-use (O'Kiep), through a 150 km DWSS used for drinking water distribution, were analysed for bacterial content. Polymerase chain reaction (PCR) amplification of the 16S rRNA V1-V3 regions was undertaken using oligonucleotide primers 27F and 518R subsequent to DNA extraction. The PCR amplicons were processed using the illumina® reaction kits as per manufacturer guidelines and sequenced using the illumina® MiSeq-2000 by means of the MiSeq V3 kit. The data obtained were processed using bioinformatics QIIME software with a compatible fast nucleic acid (fna) file. The raw sequences were deposited at the National Centre of Biotechnology Information (NCBI) and the Sequence Read Archive (SRA) database, obtaining accession numbers for each species identified.

**Keywords:** Drinking water supply system (DWSS), Metagenomics, O'Kiep, 16S rRNA gene.

## Specification Table

Subject area	DWSS, biofilms, microbial ecology, metagenomics
More specific subject area	Metagenomics
Type of data	Table
How data were acquired	Sequencing was performed on an illumina®MiSeq-2000, using MiSeq V3 (600 cycle) kits following procedures developed at Inqaba Biotech (Pretoria, South Africa) ( <a href="http://www.inqababiotech.co.za">www.inqababiotech.co.za</a> )
Data format	Raw data
Experimental factors	Metagenomic DNA was extracted from DWSS samples for sequencing
Experimental features	Lower Orange River (source) [-28°90'8617"S, 18°20'7317"E] O'Kiep (POU), South Africa [29°35'45"S, 17°52'51"E]
Data source and location	DWSS, lower Orange River to O'Kiep, Namaqualand, South Africa
Data accessibility	The accession numbers of the sequences is publicly available on a public repository ( <a href="http://hdl.handle.net/11189/6305">http://hdl.handle.net/11189/6305</a> ) and are embedded within the supplementary materials
Related research article	Richards, C.L., Broadaway, S.C., Eggers, M.J., Doyle, J., Pyle, B.H., Camper, A.K. and Ford, T.E. (2018). Detection of pathogenic and non-pathogenic bacteria in drinking water and associated biofilms on the crow reservation, Montana, USA. <i>Microb Ecol</i> , 76:52-63. The research article that is associated with this article is <del>still under construction</del>

## Value of the data

- This data demonstrate the extent of bacterial contamination of a DWSS in an arid region of Namaqualand, South Africa.
- This data can be used to determine the role of the detected bacteria with the observed clinical abnormalities experienced by the O'Kiep community.
- This data can also be used to develop mitigation techniques that will ensure that the drinking water is free of microbial contamination and suitable for drinking purposes.

## Data

The presented data contain the microbial composition of a DWSS for O'Kiep, Namaqualand, South Africa. Table 10-1 represents the bacterial composition of the source point at the lower Orange River, whereas Table 10-2 shows the microbial composition of the treated water, distributed by a state-owned agency responsible for water-management activities in the region.

**Table 10-1: Bacterial community composition of the Orange River as identified by 16S rDNA amplicon gene sequencing**

Organism/HIT	%	Accession
Uncultured bacterium	70.31	gi 507147308 gb KF037310.1
Uncultured sphingomonas	2.39	gi 389547923 gb JQ402851.1
Uncultured pirellula	1.81	gi 192804906 emb FM175708.1
<i>Nocardioides</i> sp.	1.21	gi 119534933 gb CP000509.1
<i>Bacillus</i> sp.	1.18	gi 697883209 gb KM205825.1
Uncultured bosea	0.95	gi 238914939 gb GQ129955.1
Uncultured pseudonocardia	0.79	gi 56547765 gb AY834333.1
Uncultured frankineae	0.78	gi 192805020 emb FM175822.1
Uncultured actinobacterium	0.69	gi 110753753 gb DQ828440.1
<i>Proteobacterium</i>	0.69	gi 451916633 gb KC450497.1
<i>Pimelobacter simplex</i>	0.48	gi 723622094 gb CP009896.1
Uncultured sphingobacterium	0.41	gi 451919518 gb KC453382.1
<i>Proteobacterium</i>	0.40	gi 116687962 gb AF114621.2
Uncultured sphaerobacteraceae	0.26	gi 219906550 emb AM935838.1
Uncultured proteobacterium	0.25	gi 134020863 gb EF019439.1
Uncultured acidobacteria	0.25	gi 330340199 gb JF521694.1
Uncultured rhizobiales	0.18	gi 317448927 emb FR695964.1
Uncultured chloroflexi	0.18	gi 389547105 gb JQ402033.1
Uncultured micrococcaceae	0.16	gi 389547004 gb JQ401932.1
Uncultured anaerolineaceae	0.15	gi 389546919 gb JQ401847.1
Uncultured rubrobacter	0.14	gi 389546452 gb JQ401380.1
<i>Pantoea</i> sp.	0.14	gi 756794783 gb KP326384.1
<i>Variovorax paradoxus</i>	0.13	gi 239804838 gb CP001636.1

**Table 10-2: Bacterial community composition of the treated water board agency reservoir as identified by 16S rDNA amplicon gene sequencing**

Organism/HIT	%	Accession
Uncultured bacterium	64.99	gi 206599296 gb FJ206955.1
Uncultured actinobacterium	6.70	gi 307092119 gb HM480655.1
<i>Actinophytocola xinjiangensis</i>	6.18	gi 636560203 ref NR_116263.1
<i>Myxococcus stipitatus</i>	4.36	gi 441484664 gb CP004025.1
<i>Mycobacterium neoaurum</i>	3.24	gi 674790876 gb CP006936.2
Uncultured anaerolineae	1.72	gi 219932282 emb FM209128.1
<i>Modestobacter marinus</i>	0.78	gi 388483940 emb FO203431.1
<i>Nocardioides</i> sp.	0.58	gi 119534933 gb CP000509.1
Uncultured acidobacteria	0.57	gi 341867197 gb JN205269.1
<i>Pimelobacter simplex</i>	0.54	gi 723622094 gb CP009896.1
<i>Proteobacterium</i>	0.42	gi 323709899 gb HQ857672.1
Uncultured proteobacterium	0.29	gi 110753316 gb DQ828003.1
Uncultured aquificae	0.28	gi 523452696 gb KF183116.1
Uncultured chloroflexi	0.27	gi 781796715 emb LN797050.1
Uncultured acidobacteriaceae	0.25	gi 192805191 emb FM175993.1
<i>Mycobacterium avium</i>	0.23	gi 701188573 gb CP009614.1
Uncultured microorganism	0.21	gi 478859630 gb KC841593.1
<i>Proteobacterium</i>	0.21	gi 825508410 gb KR705964.1
Uncultured planctomycete	0.16	gi 162287674 gb EU299101.1
Uncultured pseudonocardia	0.16	gi 56547765 gb AY834333.1
Uncultured rubrobacter	0.15	gi 389545690 gb JQ400618.1

Table 10-3 represents the microbial composition from a local municipal reservoir at O’Kiep storing the treated water from the water agency, which is further distributed to individual households in O’Kiep.

**Table 10-3: Bacterial community composition of the O'Kiep municipal reservoir as identified by 16S rDNA amplicon gene sequencing**

<b>Organism/HIT</b>	<b>%</b>	<b>Accession</b>
Uncultured bacterium	81.6	gi 399762709 gb JX079102.1
Uncultured verrucomicrobia	4.32	gi 325973802 emb FR749796.1
Uncultured pseudonocardia	1.61	gi 532020985 gb KF150649.1
<i>Nocardioides</i> sp.	0.88	gi 119534933 gb CP000509.1
Uncultured acidobacteria	0.87	gi 31789464 gb AY281356.1
<i>Natronomonas moolapensis</i>	0.67	gi 452081962 emb HF582854.1
Bradyrhizobium sp.	0.61	gi 146189981 emb CU234118.1
Uncultured rhizobiales	0.42	gi 630060146 gb KJ191972.1
<i>Desulfovibrio desulfuricans</i>	0.42	gi 219867585 gb CP001358.1
<i>Pimelobacter simplex</i>	0.36	gi 723622094 gb CP009896.1
<i>Conexibacter woesei</i>	0.35	gi 283945692 gb CP001854.1
<i>Sphingomonas</i> sp.	0.34	gi 918399443 emb HF544321.2
<i>Variovorax paradoxus</i>	0.33	gi 239799596 gb CP001635.1
<i>Modestobacter marinus</i>	0.30	gi 388483940 emb FO203431.1
Uncultured proteobacterium	0.27	gi 155008368 gb EU052121.1
Uncultured actinobacterium	0.25	gi 298231355 emb FN811226.1
<i>Mycobacterium smegmatis</i>	0.22	gi 433294648 gb CP003078.1
<i>Clavibacter michiganensis</i>	0.20	gi 147829108 emb AM711867.1
<i>Leptothrix cholodnii</i>	0.19	gi 170774137 gb CP001013.1
<i>Croceicoccus naphthovorans</i>	0.16	gi 831206920 gb CP011770.1
<i>Limnochorda pilosa</i>	0.15	gi 921142775 dbj AP014924.1
<i>Microvirga</i> sp.	0.14	gi 902761130 dbj LC065182.1
<i>Pandoraea apista</i>	0.13	gi 827413822 gb CP011501.1
Uncultured planctomycete	0.13	gi 197360261 gb EU979049.1

Table 10-4 to Table 10-10 represent microbial composition at the POU that is household taps.

**Table 10-4: Bacterial community composition of the O'Kiep municipal reservoir as identified by 16S rDNA amplicon gene sequencing**

<b>Organism/HIT</b>	<b>%</b>	<b>Accession</b>
Uncultured bacterium	81.6	gi 399762709 gb JX079102.1
Uncultured verrucomicrobia	4.32	gi 325973802 emb FR749796.1
Uncultured pseudonocardia	1.61	gi 532020985 gb KF150649.1
<i>Nocardioides</i> sp.	0.88	gi 119534933 gb CP000509.1
Uncultured acidobacteria	0.87	gi 31789464 gb AY281356.1
<i>Natronomonas moolapensis</i>	0.67	gi 452081962 emb HF582854.1
Bradyrhizobium sp.	0.61	gi 146189981 emb CU234118.1
Uncultured rhizobiales	0.42	gi 630060146 gb KJ191972.1
<i>Desulfovibrio desulfuricans</i>	0.42	gi 219867585 gb CP001358.1
<i>Pimelobacter simplex</i>	0.36	gi 723622094 gb CP009896.1
<i>Conexibacter woesei</i>	0.35	gi 283945692 gb CP001854.1
<i>Sphingomonas</i> sp.	0.34	gi 918399443 emb HF544321.2
<i>Variovorax paradoxus</i>	0.33	gi 239799596 gb CP001635.1
<i>Modestobacter marinus</i>	0.30	gi 388483940 emb FO203431.1
Uncultured proteobacterium	0.27	gi 155008368 gb EU052121.1
Uncultured actinobacterium	0.25	gi 298231355 emb FN811226.1
<i>Mycobacterium smegmatis</i>	0.22	gi 433294648 gb CP003078.1
<i>Clavibacter michiganensis</i>	0.20	gi 147829108 emb AM711867.1
<i>Leptothrix cholodnii</i>	0.19	gi 170774137 gb CP001013.1
<i>Croceicoccus naphthovorans</i>	0.16	gi 831206920 gb CP011770.1
<i>Limnochorda pilosa</i>	0.15	gi 921142775 dbj AP014924.1
<i>Microvirga</i> sp.	0.14	gi 902761130 dbj LC065182.1
<i>Pandoraea apista</i>	0.13	gi 827413822 gb CP011501.1
Uncultured planctomycete	0.13	gi 197360261 gb EU979049.1

## **Experimental Design, Materials and Methods**

### **Sample collection**

The DWSS samples were obtained from a 100-km-long pipe system designed to deliver a flow of 18 ML/day. Freshwater is sourced from the lower Orange River by a regional water supply system to the nearby towns, including O’Kiep which is located in the Northern Cape, Namaqualand region of South Africa [29°35’45”S, 17°52’51”E]. DWSS samples (n = 9) were collected in April 2017 from the source to the POU, that is at numerous household taps, in non-transparent 500 mL sterile polyethylene bottles which were immediately placed on ice prior to transportation to the laboratory. A composite sample (n = 1) was initially collected from the lower Orange River (Table 10-1). The second sample was composed of the treated water prior to distribution (n = 1) at the local water supply agency reservoir (Table 10-2). A similar composite sample (n = 1) from the local municipal reservoir (Table 10-3) and random samples (n = 6) were collected from household taps (Table 10-4 to Table 10-10). All samples were handled according to the guidelines used for drinking water quality standard quantification (WHO, 2011; APHA, 1915).

**Table 10-5: Bacterial community composition of the O'Kiep municipal reservoir as identified by 16S rDNA amplicon gene sequencing**

Organism/HIT	%	Accession
Uncultured bacterium	68.84	gi 385762390 gb JQ427676.1
Uncultured modestobacter	10.87	gi 627529403 gb KJ473576.1
Uncultured pseudonocardia	2.99	gi 56547765 gb AY834333.1
Uncultured acidobacteria	1.82	gi 255669588 gb GQ301073.1
Uncultured micrococci	1.20	gi 192806380 emb FM176888.1
Uncultured actinobacterium	1.11	gi 197360258 gb EU979046.1
<i>Microbacterium</i> sp.	0.81	gi 166197412 dbj AB376081.1
Uncultured niastella	0.73	gi 429999989 gb KC110902.1
<i>Nocardioides</i> sp.	0.62	gi 119534933 gb CP000509.1
Uncultured beta proteobacterium	0.62	gi 451916627 gb KC450491.1
Uncultured actinomycete	0.48	gi 408830686 gb JX507179.1
<i>Pimelobacter simplex</i>	0.34	gi 723622094 gb CP009896.1
Uncultured proteobacterium	0.33	gi 781849781 emb LN808336.1
Uncultured planctomycete	0.31	gi 781829912 emb LN803963.1
<i>Kineococcus radiotolerans</i>	0.29	gi 196121877 gb CP000750.2
<i>Proteobacterium</i>	0.28	gi 238953279 emb FM252918.1
<i>Modestobacter marinus</i>	0.24	gi 388483940 emb FO203431.1
Uncultured streptomyces	0.23	gi 410699491 gb JX576003.1
Uncultured hyphomicrobium	0.23	gi 192805496 emb FM176298.1
Uncultured burkholderiales	0.21	gi 630060167 gb KJ191993.1
<i>Arthrobacter</i> sp.	0.18	gi 723606223 gb CP007595.1
<i>Rhodopseudomonas palustris</i>	0.14	gi 86570155 gb CP000250.1
Uncultured hyphomicrobiaceae	0.14	gi 389547438 gb JQ402366.1
<i>Ralstonia eutropha</i>	0.14	gi 113528459 emb AM260480.1

**Table 10-6: Bacterial community composition of the O'Kiep municipal reservoir as identified by 16S rDNA amplicon gene sequencing**

Organism/HIT	%	Accession
Uncultured bacterium	81.15	gi 330372577 gb JF340965.1
Uncultured actinobacterium	3.87	gi 339646678 gb JN037891.1
Uncultured rhizobiales	2.37	gi 389546865 gb JQ401793.1
Uncultured acidobacteria	1.08	gi 430803015 gb KC011124.1
<i>Proteobacterium</i>	1.04	gi 18874511 gb AF469355.1
Uncultured planctomycete	0.80	gi 146430072 gb EF220888.1
<i>Nocardioides</i> sp.	0.79	gi 119534933 gb CP000509.1
Uncultured gemmatimonadetes	0.58	gi 151352239 gb EF664948.1
Uncultured anaerolineae	0.52	gi 219932282 emb FM209128.1
Uncultured actinomadura	0.48	gi 389546715 gb JQ401643.1
<i>Streptomyces</i> sp.	0.47	gi 822591927 gb CP011492.1
<i>Pimelobacter simplex</i>	0.44	gi 723622094 gb CP009896.1
Uncultured pirellula	0.33	gi 192804504 emb FM175306.1
<i>Proteobacterium</i>	0.29	gi 197360274 gb EU979062.1
Uncultured chloroflexi	0.27	gi 311336157 gb HQ183884.1
<i>Modestobacter marinus</i>	0.26	gi 388483940 emb FO203431.1
<i>Rhizobium</i> sp.	0.24	gi 584450787 emb HG916852.1
<i>Variovorax paradoxus</i>	0.20	gi 239799596 gb CP001635.1
Uncultured sphingomonas	0.20	gi 389547992 gb JQ402920.1
Uncultured frankineae	0.19	gi 192805020 emb FM175822.1
<i>Frankia alni</i>	0.15	gi 111147037 emb CT573213.2
Uncultured xiphinematobacteriaceae	0.14	gi 192806445 emb FM176953.1
Uncultured hyphomicrobiaceae	0.13	gi 166783119 gb EU266779.1
<i>Rhodopseudomonas palustris</i>	0.11	gi 39648490 emb BX572598.1

**Table 10-7: Bacterial community composition of the household as identified by 16S rDNA amplicon gene sequencing**

Organism/HIT	%	Accession
Uncultured bacterium	77.81	gi 558611484 gb KF711530.1
<i>Proteobacterium</i>	1.68	gi 451914712 gb KC448576.1
Uncultured actinobacterium	0.98	gi 347438733 gb JN178920.1
<i>Alicyclobacillus acidocaldarius</i>	0.73	gi 339287872 gb CP002902.1
Proteobacterium	0.67	gi 294828896 gb GU929355.1
<i>Nocardioides</i> sp.	0.65	gi 119534933 gb CP000509.1
Uncultured rubrobacterales	0.58	gi 672229606 emb HE861099.1
Uncultured acidobacteria	0.56	gi 389545490 gb JQ400418.1
Uncultured anaerolineae	0.54	gi 219932282 emb FM209128.1
Uncultured proteobacterium	0.49	gi 110753058 gb DQ827745.1
Uncultured novosphingobium	0.45	gi 375271615 gb JQ649064.1
Uncultured cyanobacterium	0.35	gi 300679387 gb HM439308.1
<i>Pimelobacter simplex</i>	0.33	gi 723622094 gb CP009896.1
<i>Natronomonas moolapensis</i>	0.28	gi 452081962 emb HF582854.1
Uncultured janthinobacterium	0.27	gi 726973695 gb KM391622.1
Uncultured myxococcales	0.18	gi 389545327 gb JQ400255.1
<i>Microbacterium</i> sp.	0.18	gi 590121444 emb HE716934.1
Uncultured hyphomicrobiaceae	0.17	gi 166783147 gb EU266807.1
<i>Variovorax paradoxus</i>	0.17	gi 239799596 gb CP001635.1
Uncultured verrucomicrobia	0.16	gi 523452882 gb KF183302.1
<i>Conexibacter woesei</i>	0.15	gi 283945692 gb CP001854.1
Uncultured prokaryote	0.14	gi 283463150 gb GU208299.1
<i>Modestobacter marinus</i>	0.14	gi 388483940 emb FO203431.1
Uncultured planctomycete	0.12	gi 523452694 gb KF183114.1

**Table 10-8: Bacterial community composition of the household as identified by 16S rDNA amplicon gene sequencing**

Organism/HIT	%	Accession
Uncultured bacterium	73.89	gi 134021494 gb EF020070.1
Uncultured acidobacteria	5.01	gi 325147373 gb HQ597354.1
<i>Pseudonocardia</i> sp.	3.34	gi 124488038 gb EF216352.1
Uncultured singulisphaera	3.25	gi 343787932 gb JN367174.1
Uncultured firmicutes	2.81	gi 392522374 gb JX041802.1
<i>Proteobacterium</i>	1.59	gi 451918460 gb KC452324.1
Uncultured actinobacterium	1.42	gi 110753103 gb DQ827790.1
Uncultured verrucomicrobiales	1.04	gi 192804575 emb FM175377.1
Uncultured balneimonas	1.01	gi 389548038 gb JQ402966.1
<i>Enterococcus hirae</i>	0.72	gi 94467694 gb DQ467841.1
<i>Plasticumulans acidivorans</i>	0.45	gi 645320195 ref NR_117458.1
Uncultured proteobacterium	0.27	gi 781795286 emb LN796725.1
<i>Pseudonocardia dioxanivorans</i>	0.24	gi 444304041 ref NR_074465.1
<i>Frankia alni</i>	0.22	gi 111147037 emb CT573213.2
Uncultured planctomycete	0.19	gi 344050678 gb JN409084.1
<i>Rhodococcus</i> sp.	0.18	gi 909638169 emb LN867321.1
Uncultured earthworm	0.17	gi 25989809 gb AY154543.1
Uncultured carnobacterium	0.16	gi 319659383 gb HM565028.1
<i>Nocardioides</i> sp.	0.13	gi 119534933 gb CP000509.1
<i>Pimelobacter simplex</i>	0.12	gi 723622094 gb CP009896.1
<i>Sphingomonas wittichii</i>	0.12	gi 148498119 gb CP000699.1
Uncultured chloroflexi	0.12	gi 219896099 emb AM934855.1
<i>Microbacterium</i> sp.	0.11	gi 76252801 emb AM051266.1
<i>Actinomycetospora</i> sp.	0.10	gi 557126830 gb KF600710.1

**Table 10-9: Bacterial community composition of the household as identified by 16S rDNA amplicon gene sequencing**

Organism/HIT	%	Accession
Uncultured bacterium	73.91	gi 399762838 gb JX079231.1  gi 781841436 emb LN806491.1
Uncultured actinobacterium	6.32	gi 378781357 emb FO117623.1
<i>Blastococcus saxobidens</i>	3.71	gi 781835702 emb LN805367.1
Uncultured proteobacterium	2.31	gi 384080409 emb HE798551.1
<i>Methylocystis bryophila</i>	1.90	gi 384157059 gb JQ419668.1
<i>Marmoricola</i> sp.	1.29	gi 375271308 gb JQ648757.1
Uncultured acidobacteria	1.02	gi 389546865 gb JQ401793.1
Uncultured rhizobiales	0.94	gi 583826818 emb HG917246.1
<i>Proteobacterium</i>	0.71	gi 166197412 dbj AB376081.1
<i>Microbacterium</i> sp.	0.67	gi 523452566 gb KF182986.1
Uncultured anaerolineae	0.62	gi 545344262 gb KF507494.1
Uncultured pirellula	0.49	gi 380838170 gb JN868141.1
Uncultured planctomycete	0.48	gi 396083910 gb JX114425.1
Uncultured flavisolibacter	0.31	gi 530445182 gb KC914556.1
<i>Pelomonas</i> sp.	0.26	gi 389546277 gb JQ401205.1
Uncultured solirubrobacterales	0.24	gi 389546841 gb JQ401769.1
Uncultured planctomycetaceae	0.23	gi 192806445 emb FM176953.1
Uncultured xiphinematobacteriaceae	0.14	gi 723622094 gb CP009896.1
<i>Pimelobacter simplex</i>	0.14	gi 119534933 gb CP000509.1
<i>Nocardioides</i> sp.	0.14	gi 307564378 gb HM241129.1
Uncultured chloroflexus	0.14	gi 219906527 emb AM935815.1
Uncultured planctomycetes	0.12	gi 389547105 gb JQ402033.1
Uncultured chloroflexi	0.12	gi 630060094 gb KJ191920.1
Uncultured vermiphrobacter	0.10	

**Table 10-10: Bacterial community composition of the household as identified by 16S rDNA amplicon gene sequencing**

Organism/HIT	%	Accession
Uncultured bacterium	76.2	gi 301246918 gb HM710267.1
Uncultured solirubrobacterales	4.04	gi 389545531 gb JQ400459.1
Uncultured alpha proteobacterium	3.25	gi 451914712 gb KC448576.1
Uncultured actinobacterium	2.70	gi 298231355 emb FN811226.1
Uncultured acidobacteria	1.31	gi 396083926 gb JX114441.1
Uncultured rhodospirillaceae	0.60	gi 83999434 emb AM159371.1
Uncultured arthrobacter	0.53	gi 389546219 gb JQ401147.1
<i>Pimelobacter simplex</i>	0.50	gi 723622094 gb CP009896.1
<i>Proteobacterium</i>	0.33	gi 56547781 gb AY834349.1
<i>Nocardioides</i> sp.	0.30	gi 119534933 gb CP000509.1
Uncultured proteobacterium	0.28	gi 134021577 gb EF020153.1
Uncultured acidobacterium	0.28	gi 386649463 gb JQ825225.1
Uncultured bacteroidetes	0.28	gi 149393241 gb EF612369.1
Uncultured sphingomonas	0.24	gi 46812524 gb AY569282.1
Uncultured chloroflexi	0.21	gi 313576414 gb HQ397210.1
Uncultured chitinophaga	0.20	gi 672229257 emb HE860750.1
<i>Novosphingobium pentaromativorans</i>	0.17	gi 698178797 gb CP009291.1
Uncultured microorganism	0.17	gi 529086744 gb KF275220.1
<i>Microbacterium</i> sp.	0.17	gi 914697494 gb CP012299.1
<i>Modestobacter marinus</i>	0.16	gi 388483940 emb FO203431.1
Uncultured planctomycete	0.12	gi 443301414 emb HE613591.1
Uncultured planctomycetaceae	0.11	gi 389547008 gb JQ401936.1
Uncultured xanthomonas	0.11	gi 82792029 gb DQ279336.1
<i>Brachybacterium faecium</i>	0.10	gi 256558041 gb CP001643.1

## DNA extraction and sequencing

The samples were filtered through a 0.22 µm micropore cellulose membrane (Merckmillipore, USA). The membrane was pre-washed with a sterile saline solution followed by the isolation of the genomic DNA using a PowerWater® DNA isolation kit (MO BIO Laboratories, Canada) as per the manufacturer guidelines. The DNA purity and concentration were quantified using microspectrophotometry (NanoDrop™ 2000/2000c Spectrophotometers Technologies, Wilmington, DE) and the DNA concentration ranged from 10.7 to 17.3 ng/µL.

The purified DNA was PCR amplified using the 16S rRNA forward bacterial primers 27F-16S-50-AGAGTTTGATCMTGGCT-CAG-‘3 and reverse primers 518R-16S-50-ATTACCGCGGCTGCTGG-‘3 (Satokari *et al.*, 2001) that targeted the V1 and V3 regions of the 16S rRNA. The PCR amplicons were sent for sequencing at Inqaba Biotechnical Industries (Pretoria, South Africa), a commercial NGS services provider. Briefly, the PCR amplicons were gel purified and end repaired and a illumina® specific adapter sequence was ligated to each amplicon. Following quantification, the samples were individually indexed, followed by a purification step. Amplicons were then sequenced using the illumina® MiSeq-2000, using a MiSeq V3 (600 cycle) kit. Generally, 20 Mb of data (2 x 300 bp long-paired-end reads) (Das and Adhicari, 2017) were produced for each sample. Basic Local Alignment Search Tool (BLAST)-based data analysis was performed using an Inqaba Biotech (Pretoria, South Africa) in-house-developed data analysis system. Overall, sequences were deposited in two databases, namely the National Centre for Biotechnology Information (NCBI) and the Sequence Read Archive (SRA) database, prior to the generation of accession numbers for individual bacterial species.

### **10.1.2 S2: Supplementary data for Chapter 5**

#### **Geochemical modelling and seasonal hydrogeochemical processes of the open-pit groundwater at O’Kiep, Namaqualand, South Africa**

##### **Abstract**

To assess dissolution, precipitation processes and saturation indices (SI's) of some mineral phases, PHREEQC modelling software was used to assess these different geochemical processes and to elucidate reactive minerals of the open-pit groundwater (OPGW) in O’Kiep, Namaqualand, South Africa. Equilibrium constants were not fixed into the coding of the PHREEQC software to accommodate equilibrium constant changes and PHREEQC user-input file manipulation. A SI of less than zero implied that the OPGW was undersaturated and that mineral dissolution was required to reach equilibrium. The data of the hydrogeochemical analysis indicated that the sources delivering ions into the OPGW are largely from the dissolution and leaching of mine waste and tailings, including runoffs during the wet season, with the underlying fracturing of rocks, cation exchanges and other anthropogenic activities making a contribution. Additionally, climatic seasonality significantly influenced the OPGW hydrogeochemistry, indicating that the hydrological processes which control changes were dilution and mobilisation of potentially toxic elements (PTEs). The data set generated showed that the OPGW chemistry was mainly influenced by evaporation, ion exchange, silicate weathering and dissolution of minerals, including precipitation. Overall, this dataset details hydrogeochemical processes that are responsible for seasonal variations in the OPGW chemistry.

**Keywords:** Hydrogeochemical processes, geochemical modelling, open-pit groundwater, PHREEQC, O’Kiep.

## Specification Table

Subject area	Hydrogeochemical modelling, OPGW, PHREEQC
More specific subject area	Hydrogeochemical modelling
Type of data	Table
How data were acquired	PHREEQC Version 3 is a computer programme for speciation, batch-reaction, one-dimensional transport and inverse geochemical computations and modelling, for reactions in water to understand water, sediment and aquifer rock interactions. Equilibrium constants are not fixed into the coding of the software to accommodate changes in the equilibrium constants. PHREEQC and EQ3/6 enable the user to manipulate the database and input files to change equilibrium constants when needed.
Data format	Raw data
Experimental features	O'Kiep (OPGW), South Africa [29°35'55.4"S 17°52'48.2"E]  Sample preparation: Cape Peninsula University of Technology, <i>BioERG</i> laboratory, Cape Town, South Africa [-33°93'0950"S, 18°43'3531"E]
Data source and location	Groundwater from an open pit in O'Kiep, Namaqualand, South Africa [29°35'55.4"S 17°52'48.2"E]
Data accessibility	PHREEQC software was developed by the USGS with speciation and reaction path programme features. The software makes use of a C++ programming language to compute speciation, solubility, reaction pathways and inverse geochemical mass balance modelling. The programme does consider analytical uncertainties. PHREEQC has no licence obligations and permission is not required from the USGS. PHREEQC is downloadable from <a href="https://www.usgs.gov/core-science-systems/ngp/national-hydrography">https://www.usgs.gov/core-science-systems/ngp/national-hydrography</a>  Various mineral phases are available at <a href="https://doi.org/10.25381/cput.9746537.v1">https://doi.org/10.25381/cput.9746537.v1</a> , and are embedded within the supplementary materials.

### **Value of the data**

- Several areas in Namaqualand are affected by elevated levels of PTEs, with their source being attributed to groundwater contamination. Moreover, the processes contributing to changes in the quality of the OPGW in O’Kiep has not been modelled before.
- The hydrochemical characterisation of variations in the OPGW was an essential first step for effective management of groundwater resources in O’Kiep, with PHREEQC modelling being regarded as a vital tool to elucidate geochemical processes involved (Parkhurst and Appelo, 2013; Zhu and Anderson, 2002). PHREEQC software was successfully used to generate hydrogeochemical data of the OPGW to determine factors that control the groundwater chemistry and the hydrogeochemical evolution of the water, a first attempt for the OPGW in O’Kiep. Additionally, future research studies require the use of geochemical modelling to perform speciation, solubility, reaction path and inverse mass balance modelling. Estimation of chemical reactivity in the form of water-rock interactions is needed to understand hydrogeochemical changes in the semi-pocketed aquifer in the region.
- The research data provide crucial simulation-model information for chemically reactive transport processes to optimally characterise the OPGW in O’Kiep.

### **Data**

This study presents the hydrogeochemical analysis of the granite and granitic gneiss OPGW in the arid O’Kiep. OPGW samples were collected in the dry (n = 5) and wet (n = 5) seasons downstream from the CMM. The seasonal variation of species observed was due to changes in the hydrogeochemical quality of the OPGW between the two seasons. The interaction between the OPGW and rock mineralogy controls the geochemistry of the OPGW. The PHREEQC modelling software approach allowed for simulation and characterisation of the primary physical and chemical processes influencing the OPGW quality. The mineral equilibrium calculation predicted the composition of the groundwater contaminated by various minerals, predicting reactive mineral mechanisms. The variations observed between different seasons are attributed to geological-matrix interaction between major cations and anions. Various mineral phases are listed in Table 10-11.

**Table 10-11: Statistical summary of saturation indices of minerals in O’Kiep groundwater using PHREEQC**

Phase	SI	log IAP	log K(291 K)	log K(291 K, 1 atm)
(Co(NH <sub>3</sub> ) <sub>5</sub> Cl)(NO <sub>3</sub> ) <sub>2</sub>	172.61	-166.35	6.26	(Co(NH <sub>3</sub> ) <sub>5</sub> Cl)(NO <sub>3</sub> ) <sub>2</sub>
(Co(NH <sub>3</sub> ) <sub>5</sub> Cl)Cl <sub>2</sub>	-46.17	-41.62	4.55	(Co(NH <sub>3</sub> ) <sub>5</sub> Cl)Cl <sub>2</sub>
(Co(NH <sub>3</sub> ) <sub>5</sub> OH <sub>2</sub> )Cl <sub>3</sub>	-53.47	-41.64	11.83	(Co(NH <sub>3</sub> ) <sub>5</sub> OH <sub>2</sub> )Cl <sub>3</sub>
(Co(NH <sub>3</sub> ) <sub>6</sub> )(NO <sub>3</sub> ) <sub>3</sub>	246.96	-229.03	17.93	(Co(NH <sub>3</sub> ) <sub>6</sub> )(NO <sub>3</sub> ) <sub>3</sub>
(Co(NH <sub>3</sub> ) <sub>6</sub> )Cl <sub>3</sub>	-62.1	-41.94	20.16	(Co(NH <sub>3</sub> ) <sub>6</sub> )Cl <sub>3</sub>
(NH <sub>4</sub> ) <sub>2</sub> CrO <sub>4</sub>	-56.45	-56.08	0.37	(NH <sub>4</sub> ) <sub>2</sub> CrO <sub>4</sub>
(NH <sub>4</sub> ) <sub>2</sub> SeO <sub>4</sub>	-38.51	-38.06	0.45	(NH <sub>4</sub> ) <sub>2</sub> SeO <sub>4</sub>
(VO) <sub>3</sub> (PO <sub>4</sub> ) <sub>2</sub>	-35.27	-60.37	-25.1	(VO) <sub>3</sub> (PO <sub>4</sub> ) <sub>2</sub>
Al(OH) <sub>3</sub> (am)	-6.61	4.62	11.23	Al(OH) <sub>3</sub>
Al <sub>2</sub> O <sub>3</sub>	-11.37	9.28	20.65	Al <sub>2</sub> O <sub>3</sub>
Al <sub>4</sub> (OH) <sub>10</sub> SO <sub>4</sub>	-12.76	9.94	22.7	Al <sub>4</sub> (OH) <sub>10</sub> SO <sub>4</sub>
AlAsO <sub>4</sub> :2H <sub>2</sub> O	-12.65	-7.85	4.8	AlAsO <sub>4</sub> :2H <sub>2</sub> O
AlOHSO <sub>4</sub>	-0.68	-3.91	-3.23	AlOHSO <sub>4</sub>
AlSb	109.2	-43.57	65.62	AlSb
Alunite	-2.56	-3.15	-0.59	KAl <sub>3</sub> (SO <sub>4</sub> ) <sub>2</sub> (OH) <sub>6</sub>
Anhydrite	-0.21	-4.54	-4.33	CaSO <sub>4</sub>
Anilite	2.69	-29.89	-32.58	Cu <sub>0.25</sub> Cu <sub>1.5</sub> S
Antlerite	-7.28	1.51	8.79	Cu <sub>3</sub> (OH) <sub>4</sub> SO <sub>4</sub>
Aragonite	-4.19	-12.44	-8.25	CaCO <sub>3</sub>
Arsenolite	-24.15	-27.15	-2.99	As <sub>4</sub> O <sub>6</sub>
Artinite	-18.14	-8.07	10.07	MgCO <sub>3</sub> :Mg(OH) <sub>2</sub> :3H <sub>2</sub> O
As <sub>2</sub> O <sub>5</sub>	-31.72	-24.92	6.79	As <sub>2</sub> O <sub>5</sub>
Atacamite	-6.26	1.5	7.75	Cu <sub>2</sub> (OH) <sub>3</sub> Cl
Azurite	-6.28	-22.82	-16.54	Cu <sub>3</sub> (OH) <sub>2</sub> (CO <sub>3</sub> ) <sub>2</sub>
Bianchite	-7.83	-9.59	-1.76	ZnSO <sub>4</sub> :6H <sub>2</sub> O
Birnessite	-27.63	-9.54	18.09	MnO <sub>2</sub>
Bixbyite	-32.63	-32.79	-0.16	Mn <sub>2</sub> O <sub>3</sub>
Blaubleil	-2.47	-26.63	-24.16	Cu <sub>0.9</sub> Cu <sub>0.2</sub> S
Blaubleill	-0.85	-28.13	-27.28	Cu <sub>0.6</sub> Cu <sub>0.8</sub> S
Boehmite	-4.4	4.63	9.03	AlOOH
Breithauptite	-20.4	-39.29	-18.89	NiSb
Brochantite	-11.15	4.86	16.01	Cu <sub>4</sub> (OH) <sub>6</sub> SO <sub>4</sub>
Brucite	-13.08	4.2	17.29	Mg(OH) <sub>2</sub>
Bunsenite	-10.77	2.07	12.83	NiO
Ca(VO <sub>3</sub> ) <sub>2</sub>	-26.85	-20.86	5.99	Ca(VO <sub>3</sub> ) <sub>2</sub>
Ca <sub>2</sub> V <sub>2</sub> O <sub>7</sub>	-34.97	-16.86	18.12	Ca <sub>2</sub> V <sub>2</sub> O <sub>7</sub>
Ca <sub>2</sub> V <sub>2</sub> O <sub>7</sub> :2H <sub>2</sub> O	-38.44	-16.89	21.55	Ca <sub>2</sub> V <sub>2</sub> O <sub>7</sub> :2H <sub>2</sub> O
Ca <sub>3</sub> (AsO <sub>4</sub> ) <sub>2</sub> :4H <sub>2</sub> O	-35.27	-12.97	22.3	Ca <sub>3</sub> (AsO <sub>4</sub> ) <sub>2</sub> :4H <sub>2</sub> O
Ca <sub>3</sub> (PO <sub>4</sub> ) <sub>2</sub> (beta)	-13.5	-42.63	-29.13	Ca <sub>3</sub> (PO <sub>4</sub> ) <sub>2</sub>
Ca <sub>3</sub> (VO <sub>4</sub> ) <sub>2</sub>	-52.95	-12.85	40.1	Ca <sub>3</sub> (VO <sub>4</sub> ) <sub>2</sub>
Ca <sub>3</sub> (VO <sub>4</sub> ) <sub>2</sub> :4H <sub>2</sub> O	-52.78	-12.92	39.86	Ca <sub>3</sub> (VO <sub>4</sub> ) <sub>2</sub> :4H <sub>2</sub> O

Phase	SI	log IAP	log K(291 K)	log K(291 K, 1 atm)
Ca <sub>3</sub> Sb <sub>2</sub>	230.23	-84.41	145.81	Ca <sub>3</sub> Sb <sub>2</sub>
Ca <sub>4</sub> H(PO <sub>4</sub> ) <sub>3</sub> ·3H <sub>2</sub> O	-18.92	-66	-47.08	Ca <sub>4</sub> H(PO <sub>4</sub> ) <sub>3</sub> ·3H <sub>2</sub> O
CaCrO <sub>4</sub>	-49.26	-51.42	-2.16	CaCrO <sub>4</sub>
CaHPO <sub>4</sub>	-3.93	-23.32	-19.4	CaHPO <sub>4</sub>
CaHPO <sub>4</sub> ·2H <sub>2</sub> O	-4.27	-23.36	-19.08	CaHPO <sub>4</sub> ·2H <sub>2</sub> O
Calcite	-3.99	-12.44	-8.45	CaCO <sub>3</sub>
Calomel	-1.57	-19.83	-18.27	Hg <sub>2</sub> Cl <sub>2</sub>
CaSeO <sub>3</sub> ·2H <sub>2</sub> O	-12.95	-10.06	2.89	CaSeO <sub>3</sub> ·2H <sub>2</sub> O
CaSeO <sub>4</sub> ·2H <sub>2</sub> O	-30.45	-33.44	-2.99	CaSeO <sub>4</sub> ·2H <sub>2</sub> O
Cd(OH) <sub>2</sub>	-14.91	-0.9	14.01	Cd(OH) <sub>2</sub>
Cd(OH) <sub>2</sub> (am)	-14.96	-0.9	14.07	Cd(OH) <sub>2</sub>
Cd <sub>3</sub> (OH) <sub>2</sub> (SO <sub>4</sub> ) <sub>2</sub>	-26.47	-19.76	6.71	Cd <sub>3</sub> (OH) <sub>2</sub> (SO <sub>4</sub> ) <sub>2</sub>
Cd <sub>3</sub> (OH) <sub>4</sub> SO <sub>4</sub>	-33.78	-11.22	22.56	Cd <sub>3</sub> (OH) <sub>4</sub> SO <sub>4</sub>
Cd <sub>3</sub> (PO <sub>4</sub> ) <sub>2</sub>	-24.69	-57.29	-32.6	Cd <sub>3</sub> (PO <sub>4</sub> ) <sub>2</sub>
Cd <sub>4</sub> (OH) <sub>6</sub> SO <sub>4</sub>	-40.52	-12.12	28.4	Cd <sub>4</sub> (OH) <sub>6</sub> SO <sub>4</sub>
CdCl <sub>2</sub>	-10.71	-11.29	-0.59	CdCl <sub>2</sub>
CdCl <sub>2</sub> ·1H <sub>2</sub> O	-9.64	-11.31	-1.66	CdCl <sub>2</sub> ·1H <sub>2</sub> O
CdCl <sub>2</sub> ·2.5H <sub>2</sub> O	-9.39	-11.33	-1.94	CdCl <sub>2</sub> ·2.5H <sub>2</sub> O
CdF <sub>2</sub>	-18.36	-19.39	-1.03	CdF <sub>2</sub>
Cdmetal(alpha)	-28.4	-14.59	13.81	Cd
Cdmetal(gamma)	-28.5	-14.59	13.91	Cd
CdOHCl	-9.75	-6.1	3.66	CdOHCl
CdSb	-41.81	-42.24	-0.44	CdSb
CdSe	9.32	-11.18	-20.49	CdSe
CdSeO <sub>4</sub> ·2H <sub>2</sub> O	-36.47	-38.32	-1.85	CdSeO <sub>4</sub> ·2H <sub>2</sub> O
CdSO <sub>4</sub>	-9.46	-9.43	0.03	CdSO <sub>4</sub>
CdSO <sub>4</sub> ·1H <sub>2</sub> O	-7.84	-9.45	-1.6	CdSO <sub>4</sub> ·1H <sub>2</sub> O
CdSO <sub>4</sub> ·2.67H <sub>2</sub> O	-7.67	-9.47	-1.8	CdSO <sub>4</sub> ·2.67H <sub>2</sub> O
CH <sub>4</sub> (g)	-29.27	-71.31	-42.04	CH <sub>4</sub>
Chalcanthite	-2.6	-5.27	-2.66	CuSO <sub>4</sub> ·5H <sub>2</sub> O
Chalcocite	4.43	-31.14	-35.57	Cu <sub>2</sub> S
Chalcopyrite	-17.24	-53.09	-35.85	CuFeS <sub>2</sub>
Cinnabar	-2.38	-49.06	-46.68	HgS
Claudetite	-23.86	-27.15	-3.28	As <sub>4</sub> O <sub>6</sub>
Co(OH) <sub>2</sub>	-11.97	1.12	13.09	Co(OH) <sub>2</sub>
Co(OH) <sub>3</sub>	-22.48	-24.43	-1.95	Co(OH) <sub>3</sub>
CO <sub>2</sub> (g)	1.72	-16.45	-18.16	CO <sub>2</sub>
Co <sub>3</sub> (AsO <sub>4</sub> ) <sub>2</sub>	-34.55	-21.51	13.03	Co <sub>3</sub> (AsO <sub>4</sub> ) <sub>2</sub>
Co <sub>3</sub> (PO <sub>4</sub> ) <sub>2</sub>	-16.54	-51.23	-34.69	Co <sub>3</sub> (PO <sub>4</sub> ) <sub>2</sub>
Co <sub>3</sub> O <sub>4</sub>	-37.6	-47.68	-10.08	Co <sub>3</sub> O <sub>4</sub>
CoCl <sub>2</sub>	-17.85	-9.27	8.58	CoCl <sub>2</sub>
CoCl <sub>2</sub> ·6H <sub>2</sub> O	-11.88	-9.37	2.51	CoCl <sub>2</sub> ·6H <sub>2</sub> O
CoCO <sub>3</sub>	-5.38	-15.31	-9.93	CoCO <sub>3</sub>

Phase	SI	log IAP	log K(291 K)	log K(291 K, 1 atm)
CoF <sub>2</sub>	-16	-17.37	-1.37	CoF <sub>2</sub>
CoF <sub>3</sub>	-51.2	-52.18	-0.98	CoF <sub>3</sub>
CoFe <sub>2</sub> O <sub>4</sub>	-3.58	-6.49	-2.91	CoFe <sub>2</sub> O <sub>4</sub>
CoHPO <sub>4</sub>	-7.13	-26.19	-19.06	CoHPO <sub>4</sub>
CoO	-12.86	1.14	14	CoO
CoS(alpha)	-20.91	-28.35	-7.44	CoS
CoS(beta)	-17.28	-28.35	-11.07	CoS
CoSe	7.04	-9.16	-16.2	CoSe
CoSeO <sub>3</sub>	-14.21	-12.89	1.32	CoSeO <sub>3</sub>
CoSeO <sub>4</sub> :6H <sub>2</sub> O	-34.84	-36.37	-1.53	CoSeO <sub>4</sub> :6H <sub>2</sub> O
CoSO <sub>4</sub>	-10.52	-7.41	3.11	CoSO <sub>4</sub>
CoSO <sub>4</sub> :6H <sub>2</sub> O	-5.03	-7.51	-2.48	CoSO <sub>4</sub> :6H <sub>2</sub> O
Covellite	-3.45	-26.13	-22.68	CuS
Cr(OH) <sub>2</sub>	-23.12	-12.16	10.96	Cr(OH) <sub>2</sub>
Cr(OH) <sub>3</sub>	-9.69	-8.24	1.45	Cr(OH) <sub>3</sub>
Cr(OH) <sub>3</sub> (am)	-7.49	-8.24	-0.75	Cr(OH) <sub>3</sub>
Cr <sub>2</sub> O <sub>3</sub>	-14.26	-16.43	-2.16	Cr <sub>2</sub> O <sub>3</sub>
CrCl <sub>2</sub>	-37.08	-22.56	14.52	CrCl <sub>2</sub>
CrCl <sub>3</sub>	-39.41	-23.83	15.58	CrCl <sub>3</sub>
CrF <sub>3</sub>	-24.73	-35.98	-11.25	CrF <sub>3</sub>
Crmetal	-57	-25.85	31.15	Cr
CrO <sub>3</sub>	-52.23	-55.42	-3.19	CrO <sub>3</sub>
Cryolite	-12.46	-46.45	-33.99	Na <sub>3</sub> AlF <sub>6</sub>
Cu(OH) <sub>2</sub>	-5.55	3.35	8.89	Cu(OH) <sub>2</sub>
Cu(SbO <sub>3</sub> ) <sub>2</sub>	-28.61	16.6	45.21	Cu(SbO <sub>3</sub> ) <sub>2</sub>
Cu <sub>2</sub> (OH) <sub>3</sub> NO <sub>3</sub>	-70.4	-60.87	9.53	Cu <sub>2</sub> (OH) <sub>3</sub> NO <sub>3</sub>
Cu <sub>2</sub> Sb:3H <sub>2</sub> O	-9.94	-45.73	-35.79	Cu <sub>2</sub> Sb:3H <sub>2</sub> O
Cu <sub>2</sub> Se(alpha)	34.68	-11.95	-46.63	Cu <sub>2</sub> Se
Cu <sub>2</sub> SO <sub>4</sub>	-8.33	-10.2	-1.88	Cu <sub>2</sub> SO <sub>4</sub>
Cu <sub>3</sub> (AsO <sub>4</sub> ) <sub>2</sub> :2H <sub>2</sub> O	-20.97	-14.87	6.1	Cu <sub>3</sub> (AsO <sub>4</sub> ) <sub>2</sub> :2H <sub>2</sub> O
Cu <sub>3</sub> (PO <sub>4</sub> ) <sub>2</sub>	-7.7	-44.55	-36.85	Cu <sub>3</sub> (PO <sub>4</sub> ) <sub>2</sub>
Cu <sub>3</sub> (PO <sub>4</sub> ) <sub>2</sub> :3H <sub>2</sub> O	-9.48	-44.6	-35.12	Cu <sub>3</sub> (PO <sub>4</sub> ) <sub>2</sub> :3H <sub>2</sub> O
Cu <sub>3</sub> Sb	-6.91	-50.7	-43.79	Cu <sub>3</sub> Sb
Cu <sub>3</sub> Se <sub>2</sub>	45.92	-18.89	-64.81	Cu <sub>3</sub> Se <sub>2</sub>
CuCO <sub>3</sub>	-1.58	-13.08	-11.5	CuCO <sub>3</sub>
CuCrO <sub>4</sub>	-46.62	-52.06	-5.44	CuCrO <sub>4</sub>
CuF	-5.11	-10.08	-4.97	CuF
CuF <sub>2</sub>	-16.52	-15.15	1.37	CuF <sub>2</sub>
CuF <sub>2</sub> :2H <sub>2</sub> O	-10.69	-15.18	-4.49	CuF <sub>2</sub> :2H <sub>2</sub> O
Cumetal	1.35	-7.68	-9.03	Cu
CuOCuSO <sub>4</sub>	-12.66	-1.82	10.84	CuOCuSO <sub>4</sub>
Cupricferrite	-11.07	-4.27	6.8	CuFe <sub>2</sub> O <sub>4</sub>
Cuprite	-0.73	-1.66	-0.93	Cu <sub>2</sub> O

Phase	SI	log IAP	log K(291 K)	log K(291 K, 1 atm)
Cuprousferrite	4.21	-4.64	-8.86	CuFeO <sub>2</sub>
CuSe	26.64	-6.93	-33.57	CuSe
CuSe <sub>2</sub>	30.39	-3.52	-33.91	CuSe <sub>2</sub>
CuSeO <sub>3</sub> :2H <sub>2</sub> O	-11.35	-10.7	0.65	CuSeO <sub>3</sub> :2H <sub>2</sub> O
CuSeO <sub>4</sub> :5H <sub>2</sub> O	-31.69	-34.13	-2.44	CuSeO <sub>4</sub> :5H <sub>2</sub> O
CuSO <sub>4</sub>	-8.41	-5.18	3.22	CuSO <sub>4</sub>
Diaspore	-2.64	4.63	7.27	AlOOH
Djurleite	3.88	-30.81	-34.7	Cu <sub>0.066</sub> Cu <sub>1.868</sub> S
Dolomite(disorder)	-8	-24	.67.16	CaMg(CO <sub>3</sub> ) <sub>2</sub>
Dolomite(ordered)	-7.73	-24.67	-16.94	CaMg(CO <sub>3</sub> ) <sub>2</sub>
Epsomite	-2.27	-4.44	-2.17	MgSO <sub>4</sub> :7H <sub>2</sub> O
FCO <sub>3</sub> Apatite	-20.34	-135.38	115.04	Ca <sub>9.316</sub> Na <sub>0.36</sub> Mg <sub>0.144</sub> (PO <sub>4</sub> ) <sub>4.8</sub> (CO <sub>3</sub> ) <sub>1.2</sub> F <sub>2.4</sub> 8
Fe(OH) <sub>2</sub>	-11.05	2.51	13.56	Fe(OH) <sub>2</sub>
Fe(OH) <sub>2</sub> .7Cl.3	-2.36	-5.4	-3.04	Fe(OH) <sub>2</sub> .7Cl.3
Fe(VO <sub>3</sub> ) <sub>2</sub>	-18.86	-22.34	-3.48	Fe(VO <sub>3</sub> ) <sub>2</sub>
Fe <sub>2</sub> (OH) <sub>4</sub> SeO <sub>3</sub>	-23.25	-21.69	1.55	Fe <sub>2</sub> (OH) <sub>4</sub> SeO <sub>3</sub>
Fe <sub>2</sub> (SeO <sub>3</sub> ) <sub>3</sub> :2H <sub>2</sub> O	-29.13	-49.76	-20.63	Fe <sub>2</sub> (SeO <sub>3</sub> ) <sub>3</sub> :2H <sub>2</sub> O
Fe <sub>2</sub> (SO <sub>4</sub> ) <sub>3</sub>	-30.48	-33.27	-2.8	Fe <sub>2</sub> (SO <sub>4</sub> ) <sub>3</sub>
Fe <sub>3</sub> (OH) <sub>8</sub>	-25.39	-5.17	20.22	Fe <sub>3</sub> (OH) <sub>8</sub>
FeAsO <sub>4</sub> :2H <sub>2</sub> O	-16.71	-16.31	0.4	FeAsO <sub>4</sub> :2H <sub>2</sub> O
FeCr <sub>2</sub> O <sub>4</sub>	-21.64	-13.9	7.74	FeCr <sub>2</sub> O <sub>4</sub>
Ferrihydrite	-7.32	-3.84	3.48	Fe(OH) <sub>3</sub>
Ferroselite	14.42	-4.36	-18.78	FeSe <sub>2</sub>
FeS(ppt)	-24.05	-26.96	-2.91	FeS
FeSe	3.24	-7.77	-11.01	FeSe
Fluorite	-3.97	-14.51	-10.53	CaF <sub>2</sub>
Gibbsite	-4.04	4.62	8.66	Al(OH) <sub>3</sub>
Goethite	-4.55	-3.82	0.73	FeOOH
Goslarite	-7.54	-9.61	-2.07	ZnSO <sub>4</sub> :7H <sub>2</sub> O
Greenockite	-15.8	-30.37	-14.57	CdS
Greigite	-78.02	-123.06	-45.03	Fe <sub>3</sub> S <sub>4</sub>
Gypsum	0.04	-4.57	-4.61	CaSO <sub>4</sub> :2H <sub>2</sub> O
H-Jarosite	-17.41	-28.61	-11.21	(H <sub>3</sub> O)Fe <sub>3</sub> (SO <sub>4</sub> ) <sub>2</sub> (OH) <sub>6</sub>
H <sub>2</sub> S(g)	-21.49	-29.5	-8.01	H <sub>2</sub> S
H <sub>2</sub> Se(g)	-5.41	-10.31	-4.9	H <sub>2</sub> Se
Halite	-5.31	-3.72	1.59	NaCl
Hausmannite	-41.4	21.26	62.66	Mn <sub>3</sub> O <sub>4</sub>
Hematite	-6.71	-7.63	-0.92	Fe <sub>2</sub> O <sub>3</sub>
Hercynite	-12.3	11.81	24.11	FeAl <sub>2</sub> O <sub>4</sub>
Hg(CH <sub>3</sub> ) <sub>2</sub> (g)	-86.61	-162.18	-75.57	Hg(CH <sub>3</sub> ) <sub>2</sub>
Hg(g)	-3.61	-11.56	-7.96	Hg
Hg(OH) <sub>2</sub>	-16.09	-19.59	-3.5	Hg(OH) <sub>2</sub>

Phase	SI	log IAP	log K(291 K)	log K(291 K, 1 atm)
Hg <sub>2</sub> (g)	-7.95	-23.13	-15.18	Hg <sub>2</sub>
Hg <sub>2</sub> (OH) <sub>2</sub>	-14.7	-9.44	5.26	Hg <sub>2</sub> (OH) <sub>2</sub>
Hg <sub>2</sub> CO <sub>3</sub>	-9.64	-25.87	-16.22	Hg <sub>2</sub> CO <sub>3</sub>
Hg <sub>2</sub> CrO <sub>4</sub>	-56.15	-64.85	-8.7	Hg <sub>2</sub> CrO <sub>4</sub>
Hg <sub>2</sub> F <sub>2</sub>	-17.64	-27.93	-10.29	Hg <sub>2</sub> F <sub>2</sub>
Hg <sub>2</sub> HPO <sub>4</sub>	-11.98	-36.75	-24.77	Hg <sub>2</sub> HPO <sub>4</sub>
Hg <sub>2</sub> S	-26.96	-38.91	-11.95	Hg <sub>2</sub> S
Hg <sub>2</sub> SeO <sub>3</sub>	-18.8	-23.45	-4.66	Hg <sub>2</sub> SeO <sub>3</sub>
Hg <sub>2</sub> SO <sub>4</sub>	-11.82	-17.97	-6.15	Hg <sub>2</sub> SO <sub>4</sub>
Hg <sub>3</sub> O <sub>2</sub> CO <sub>3</sub>	-45.48	-75.16	-29.68	Hg <sub>3</sub> O <sub>2</sub> CO <sub>3</sub>
HgCl(g)	-30.04	-9.92	20.12	HgCl
HgCl <sub>2</sub>	-8.3	-29.98	-21.68	HgCl <sub>2</sub>
HgF(g)	-47.63	-13.97	33.66	HgF
HgF <sub>2</sub> (g)	-51.29	-38.08	13.21	HgF <sub>2</sub>
Hgmetal(l)	2.21	-11.56	-13.77	Hg
HgSe	25.83	-29.87	-55.69	HgSe
HgSeO <sub>3</sub>	-21.17	-33.6	-12.43	HgSeO <sub>3</sub>
HgSO <sub>4</sub>	-18.64	-28.12	-9.48	HgSO <sub>4</sub>
Huntite	-19.57	-49.12	-29.55	CaMg <sub>3</sub> (CO <sub>3</sub> ) <sub>4</sub>
Hydromagnesite	-36.85	-44.77	-7.92	Mg <sub>5</sub> (CO <sub>3</sub> ) <sub>4</sub> (OH) <sub>2</sub> ·4H <sub>2</sub> O
Hydroxylapatite	-17.61	-61.94	-44.33	Ca <sub>5</sub> (PO <sub>4</sub> ) <sub>3</sub> OH
K-Alum	-7.29	-12.58	-5.29	KAl(SO <sub>4</sub> ) <sub>2</sub> ·12H <sub>2</sub> O
K-Jarosite	-14.23	-28.52	-14.29	KFe <sub>3</sub> (SO <sub>4</sub> ) <sub>2</sub> (OH) <sub>6</sub>
K <sub>2</sub> Cr <sub>2</sub> O <sub>7</sub>	-93.15	-110.71	-17.56	K <sub>2</sub> Cr <sub>2</sub> O <sub>7</sub>
K <sub>2</sub> CrO <sub>4</sub>	-54.7	-55.28	-0.58	K <sub>2</sub> CrO <sub>4</sub>
K <sub>2</sub> SeO <sub>4</sub>	-36.54	-37.27	-0.73	K <sub>2</sub> SeO <sub>4</sub>
Langite	-13.29	4.84	18.13	Cu <sub>4</sub> (OH) <sub>6</sub> SO <sub>4</sub> ·H <sub>2</sub> O
Lepidocrocite	-5.19	-3.82	1.37	FeOOH
Lime	-29.44	4.01	33.45	CaO
Mackinawite	-23.36	-26.96	-3.6	FeS
Maghemite	-14.02	-7.63	6.39	Fe <sub>2</sub> O <sub>3</sub>
Magnesioferrite	-21.35	-3.41	17.94	Fe <sub>2</sub> MgO <sub>4</sub>
Magnesite	-4.69	-12.23	-7.54	MgCO <sub>3</sub>
Magnetite	-9.31	-5.1	4.21	Fe <sub>3</sub> O <sub>4</sub>
Malachite	-4.13	-9.74	-5.6	Cu <sub>2</sub> (OH) <sub>2</sub> CO <sub>3</sub>
Manganite	-15.98	9.36	25.34	MnOOH
Melanothallite	-13.55	-7.05	6.5	CuCl <sub>2</sub>
Melanterite	-3.85	-6.13	-2.29	FeSO <sub>4</sub> ·7H <sub>2</sub> O
Metacinnabar	-2.98	-49.06	-46.08	HgS
Mg(OH) <sub>2</sub> (active)	-14.59	4.2	18.79	Mg(OH) <sub>2</sub>
Mg(VO <sub>3</sub> ) <sub>2</sub>	-32.46	-20.65	11.81	Mg(VO <sub>3</sub> ) <sub>2</sub>
Mg <sub>2</sub> Sb <sub>3</sub>	176.62	-101.94	74.68	Mg <sub>2</sub> Sb <sub>3</sub>
Mg <sub>2</sub> V <sub>2</sub> O <sub>7</sub>	-43.78	-16.43	27.35	Mg <sub>2</sub> V <sub>2</sub> O <sub>7</sub>

Phase	SI	log IAP	log K(291 K)	log K(291 K, 1 atm)
Mg <sub>3</sub> (PO <sub>4</sub> ) <sub>2</sub>	-18.71	-41.99	-23.28	Mg <sub>3</sub> (PO <sub>4</sub> ) <sub>2</sub>
MgCr <sub>2</sub> O <sub>4</sub>	-29.1	-12.21	16.9	MgCr <sub>2</sub> O <sub>4</sub>
MgCrO <sub>4</sub>	-56.93	-51.21	5.72	MgCrO <sub>4</sub>
MgF <sub>2</sub>	-6.19	-14.29	-8.1	MgF <sub>2</sub>
MgHPO <sub>4</sub> ·3H <sub>2</sub> O	-4.99	-23.16	-18.18	MgHPO <sub>4</sub> ·3H <sub>2</sub> O
MgSeO <sub>3</sub> ·6H <sub>2</sub> O	-12.95	-9.91	3.04	MgSeO <sub>3</sub> ·6H <sub>2</sub> O
MgSeO <sub>4</sub> ·6H <sub>2</sub> O	-32.09	-33.29	-1.2	MgSeO <sub>4</sub> ·6H <sub>2</sub> O
Mirabilite	-4.33	-5.75	-1.42	Na <sub>2</sub> SO <sub>4</sub> ·10H <sub>2</sub> O
Mn(VO <sub>3</sub> ) <sub>2</sub>	-27.61	-22.35	5.26	Mn(VO <sub>3</sub> ) <sub>2</sub>
Mn <sub>2</sub> (SO <sub>4</sub> ) <sub>3</sub>	-53.35	-58.43	-5.08	Mn <sub>2</sub> (SO <sub>4</sub> ) <sub>3</sub>
Mn <sub>2</sub> Sb	111.11	-50.03	61.08	Mn <sub>2</sub> Sb
Mn <sub>3</sub> (AsO <sub>4</sub> ) <sub>2</sub> ·8H <sub>2</sub> O	-30	-17.5	12.5	Mn <sub>3</sub> (AsO <sub>4</sub> ) <sub>2</sub> ·8H <sub>2</sub> O
Mn <sub>3</sub> (PO <sub>4</sub> ) <sub>2</sub>	-23.23	-47.09	-23.86	Mn <sub>3</sub> (PO <sub>4</sub> ) <sub>2</sub>
MnCl <sub>2</sub> ·4H <sub>2</sub> O	-10.71	-7.96	2.76	MnCl <sub>2</sub> ·4H <sub>2</sub> O
MnHPO <sub>4</sub>	0.59	-24.81	-25.4	MnHPO <sub>4</sub>
MnS(grn)	-27.26	-26.97	0.29	MnS
MnS(pnk)	-30.31	-26.97	3.34	MnS
MnSb	-61.62	-64.61	-2.99	MnSb
MnSe	-11.66	-7.78	3.88	MnSe
MnSeO <sub>3</sub>	-12.64	-11.51	1.13	MnSeO <sub>3</sub>
MnSeO <sub>3</sub> ·2H <sub>2</sub> O	-12.49	-11.54	0.95	MnSeO <sub>3</sub> ·2H <sub>2</sub> O
MnSeO <sub>4</sub> ·5H <sub>2</sub> O	-32.92	-34.97	-2.05	MnSeO <sub>4</sub> ·5H <sub>2</sub> O
MnSO <sub>4</sub>	-8.86	-6.03	2.83	MnSO <sub>4</sub>
Monteponite	-16.39	-0.88	15.5	CdO
Montroydite	-16.08	-19.57	-3.49	HgO
Morenosite	-4.4	-6.6	-2.19	NiSO <sub>4</sub> ·7H <sub>2</sub> O
Na-Jarosite	-16.5	-27.11	-10.61	NaFe <sub>3</sub> (SO <sub>4</sub> ) <sub>2</sub> (OH) <sub>6</sub>
Na <sub>2</sub> Cr <sub>2</sub> O <sub>7</sub>	-97.91	-107.89	-9.98	Na <sub>2</sub> Cr <sub>2</sub> O <sub>7</sub>
Na <sub>2</sub> CrO <sub>4</sub>	-55.47	-52.46	3.01	Na <sub>2</sub> CrO <sub>4</sub>
Na <sub>2</sub> SeO <sub>3</sub> ·5H <sub>2</sub> O	-21.45	-11.15	10.3	Na <sub>2</sub> SeO <sub>3</sub> ·5H <sub>2</sub> O
Na <sub>2</sub> SeO <sub>4</sub>	-35.73	-34.45	1.28	Na <sub>2</sub> SeO <sub>4</sub>
Na <sub>3</sub> Sb	139.9	-43.77	96.13	Na <sub>3</sub> Sb
Na <sub>3</sub> VO <sub>4</sub>	-45.39	-7.99	37.4	Na <sub>3</sub> VO <sub>4</sub>
Na <sub>4</sub> V <sub>2</sub> O <sub>7</sub>	-57.12	-18.94	38.18	Na <sub>4</sub> V <sub>2</sub> O <sub>7</sub>
Nantokite	0.86	-6.03	-6.9	CuCl
NaSb	-56.55	-33.03	23.53	NaSb
Natron	-12.08	-13.65	-1.57	Na <sub>2</sub> CO <sub>3</sub> ·10H <sub>2</sub> O
NaVO <sub>3</sub>	-14.93	-10.95	3.98	NaVO <sub>3</sub>
Nesquehonite	-7.7	-12.28	-4.58	MgCO <sub>3</sub> ·3H <sub>2</sub> O
Ni(OH) <sub>2</sub>	-11.12	2.05	13.17	Ni(OH) <sub>2</sub>
Ni <sub>3</sub> (AsO <sub>4</sub> ) <sub>2</sub> ·8H <sub>2</sub> O	-34.56	-18.86	15.7	Ni <sub>3</sub> (AsO <sub>4</sub> ) <sub>2</sub> ·8H <sub>2</sub> O
Ni <sub>3</sub> (PO <sub>4</sub> ) <sub>2</sub>	-17.14	-48.44	-31.3	Ni <sub>3</sub> (PO <sub>4</sub> ) <sub>2</sub>
Ni <sub>4</sub> (OH) <sub>6</sub> SO <sub>4</sub>	-32.33	-0.33	32	Ni <sub>4</sub> (OH) <sub>6</sub> SO <sub>4</sub>

Phase	SI	log IAP	log K(291 K)	log K(291 K, 1 atm)
NiCO <sub>3</sub>	-7.67	-14.38	-6.71	NiCO <sub>3</sub>
NiS(alpha)	-21.82	-27.42	-5.6	NiS
NiS(beta)	-16.32	-27.42	-11.1	NiS
NiS(gamma)	-14.62	-27.42	-12.8	NiS
NiSe	9.47	-8.23	-17.7	NiSe
NiSeO <sub>3</sub> :2H <sub>2</sub> O	-14.93	-12	2.93	NiSeO <sub>3</sub> :2H <sub>2</sub> O
NiSeO <sub>4</sub> :6H <sub>2</sub> O	-33.92	-35.44	-1.52	NiSeO <sub>4</sub> :6H <sub>2</sub> O
Nsutite	-27.04	-9.54	17.5	MnO <sub>2</sub>
O <sub>2</sub> (g)	-57.89	27.42	85.3	O <sub>2</sub>
Orpiment	-39.61	-102.04	-62.42	As <sub>2</sub> S <sub>3</sub>
Otavite	-5.33	-17.33	-12	CdCO <sub>3</sub>
Periclase	-17.95	4.22	22.17	MgO
Portlandite	-19.31	3.99	23.3	Ca(OH) <sub>2</sub>
Pyrite	-24.04	-42.74	-18.7	FeS <sub>2</sub>
Pyrochroite	-13.07	2.5	15.57	Mn(OH) <sub>2</sub>
Pyrolusite	-26.21	16.23	42.43	MnO <sub>2</sub>
Realgar	-22.89	-43.13	-20.24	AsS
Retgersite	-4.52	-6.58	-2.06	NiSO <sub>4</sub> :6H <sub>2</sub> O
Rhodochrosite	-3.36	-13.93	-10.57	MnCO <sub>3</sub>
Sb(OH) <sub>3</sub>	0.11	-7.11	-7.23	Sb(OH) <sub>3</sub>
Sb <sub>2</sub> O <sub>4</sub>	-4.14	-0.47	3.67	Sb <sub>2</sub> O <sub>4</sub>
Sb <sub>2</sub> O <sub>5</sub>	-25.71	-35.38	-9.67	Sb <sub>2</sub> O <sub>5</sub>
Sb <sub>2</sub> Se <sub>3</sub>	24.02	-45.07	-69.09	Sb <sub>2</sub> Se <sub>3</sub>
Sb <sub>4</sub> O <sub>6</sub> (cubic)	-9.86	-28.36	-18.5	Sb <sub>4</sub> O <sub>6</sub>
Sb <sub>4</sub> O <sub>6</sub> (orth)	-10.31	-28.36	-18.05	Sb <sub>4</sub> O <sub>6</sub>
SbCl <sub>3</sub>	-23.41	-22.71	0.71	SbCl <sub>3</sub>
SbF <sub>3</sub>	-24.66	-34.86	-10.2	SbF <sub>3</sub>
Sbmetal	-15.64	-27.65	-12.01	Sb
SbO <sub>2</sub>	3.28	-24.54	-27.82	SbO <sub>2</sub>
Semetal(am)	10.56	3.41	-7.15	Se
Semetal(hex)	11.18	3.41	-7.77	Se
Senarmontite	-1.69	-14.18	-12.48	Sb <sub>2</sub> O <sub>3</sub>
SeO <sub>2</sub>	-14.15	-14.03	0.12	SeO <sub>2</sub>
SeO <sub>3</sub>	-59.02	-37.41	21.61	SeO <sub>3</sub>
Siderite	-3.74	-13.92	-10.18	FeCO <sub>3</sub>
Smithsonite	-7.45	-17.39	-9.94	ZnCO <sub>3</sub>
Sphalerite	-18.87	-30.44	-11.57	ZnS
Spinel	-24.85	13.5	38.35	MgAl <sub>2</sub> O <sub>4</sub>
Stibnite	-51.05	-102.64	-51.6	Sb <sub>2</sub> S <sub>3</sub>
Strengite	-4.81	-31.17	-26.36	FePO <sub>4</sub> :2H <sub>2</sub> O
Sulfur	-13.7	-15.78	-2.08	S
Tenorite	-4.53	3.36	7.9	CuO
Thenardite	-5.94	-5.59	0.36	Na <sub>2</sub> SO <sub>4</sub>

Phase	SI	log IAP	log K(291 K)	log K(291 K, 1 atm)
Thermonatrite	-14.18	-13.5	0.68	Na <sub>2</sub> CO <sub>3</sub> :H <sub>2</sub> O
V(OH) <sub>3</sub>	-10.68	-3.09	7.59	V(OH) <sub>3</sub>
V <sub>2</sub> O <sub>5</sub>	-23.38	-24.87	-1.49	V <sub>2</sub> O <sub>5</sub>
V <sub>3</sub> O <sub>5</sub>	-21.66	-19.44	2.22	V <sub>3</sub> O <sub>5</sub>
V <sub>4</sub> O <sub>7</sub>	-29.17	-21.35	7.82	V <sub>4</sub> O <sub>7</sub>
V <sub>6</sub> O <sub>13</sub>	-40.11	-102.02	-61.91	V <sub>6</sub> O <sub>13</sub>
Valentinite	-5.62	-14.18	-8.55	Sb <sub>2</sub> O <sub>3</sub>
VCl <sub>2</sub>	-39.75	-20.33	19.42	VCl <sub>2</sub>
VCl <sub>3</sub>	-42.81	-18.68	24.13	VCl <sub>3</sub>
VF <sub>4</sub>	-54.63	-38.93	15.7	VF <sub>4</sub>
Vivianite	-11.19	-47.19	-36	Fe <sub>3</sub> (PO <sub>4</sub> ) <sub>2</sub> :8H <sub>2</sub> O
Vmetal	-68.66	-23.63	45.03	V
VO	-25.12	-9.92	15.19	VO
VO(OH) <sub>2</sub>	-7.08	-1.93	5.15	VO(OH) <sub>2</sub>
VO <sub>2</sub> Cl	-20.64	-17.64	3	VO <sub>2</sub> Cl
VOCl	-19.83	-8.27	11.56	VOCl
VOCl <sub>2</sub>	-25.54	-12.32	13.22	VOCl <sub>2</sub>
VOSO <sub>4</sub>	-14.4	-10.46	3.95	VOSO <sub>4</sub>
Wurtzite	-21.4	-30.44	-9.03	ZnS
Zincite	-12.63	-0.95	11.68	ZnO
Zincosite	-13.74	-9.49	4.25	ZnSO <sub>4</sub>
Zn(NO <sub>3</sub> ) <sub>2</sub> :6H <sub>2</sub> O	139.4	-136.18	3.22	Zn(NO <sub>3</sub> ) <sub>2</sub> :6H <sub>2</sub> O
Zn(OH) <sub>2</sub>	-13.16	-0.96	12.2	Zn(OH) <sub>2</sub>
Zn(OH) <sub>2</sub> (am)	-13.75	-0.96	12.79	Zn(OH) <sub>2</sub>
Zn(OH) <sub>2</sub> (beta)	-13.04	-0.96	12.08	Zn(OH) <sub>2</sub>
Zn(OH) <sub>2</sub> (epsilon)	-12.81	-0.96	11.85	Zn(OH) <sub>2</sub>
Zn(OH) <sub>2</sub> (gamma)	-12.7	-0.96	11.73	Zn(OH) <sub>2</sub>
Zn <sub>2</sub> (OH) <sub>2</sub> SO <sub>4</sub>	-17.96	-10.46	7.5	Zn <sub>2</sub> (OH) <sub>2</sub> SO <sub>4</sub>
Zn <sub>2</sub> (OH) <sub>3</sub> Cl	-22.31	-7.12	15.19	Zn <sub>2</sub> (OH) <sub>3</sub> Cl
Zn <sub>3</sub> (AsO <sub>4</sub> ) <sub>2</sub> :2.5H <sub>2</sub> O	-41.46	-27.81	13.65	Zn <sub>3</sub> (AsO <sub>4</sub> ) <sub>2</sub> :2.5H <sub>2</sub> O
Zn <sub>3</sub> (PO <sub>4</sub> ) <sub>2</sub> :4H <sub>2</sub> O	-22.13	-57.55	-35.42	Zn <sub>3</sub> (PO <sub>4</sub> ) <sub>2</sub> :4H <sub>2</sub> O
Zn <sub>3</sub> O(SO <sub>4</sub> ) <sub>2</sub>	-39.85	-19.94	19.91	Zn <sub>3</sub> O(SO <sub>4</sub> ) <sub>2</sub>
Zn <sub>4</sub> (OH) <sub>6</sub> SO <sub>4</sub>	-40.78	-12.38	28.4	Zn <sub>4</sub> (OH) <sub>6</sub> SO <sub>4</sub>
Zn <sub>5</sub> (OH) <sub>8</sub> Cl <sub>2</sub>	-53.71	-15.21	38.5	Zn <sub>5</sub> (OH) <sub>8</sub> Cl <sub>2</sub>
ZnCl <sub>2</sub>	-18.69	-11.36	7.33	ZnCl <sub>2</sub>
ZnCO <sub>3</sub> :1H <sub>2</sub> O	-7.15	-17.41	-10.26	ZnCO <sub>3</sub> :1H <sub>2</sub> O
ZnF <sub>2</sub>	-19.15	-19.46	-0.3	ZnF <sub>2</sub>
Znmetal	-41.04	-14.66	26.38	Zn
ZnO(active)	-12.48	-0.95	11.53	ZnO
ZnS(am)	-21.32	-30.44	-9.11	ZnS
ZnSb	-53.53	-42.31	11.23	ZnSb
ZnSe	3.26	-11.24	-14.5	ZnSe
ZnSeO <sub>4</sub> :6H <sub>2</sub> O	-36.93	-38.45	-1.52	ZnSeO <sub>4</sub> :6H <sub>2</sub> O

<b>Phase</b>	<b>SI</b>	<b>log IAP</b>	<b>log K(291 K)</b>	<b>log K(291 K, 1 atm)</b>
ZnSO <sub>4</sub> :1H <sub>2</sub> O	-9.04	-9.51	-0.47	ZnSO <sub>4</sub> :1H <sub>2</sub> O

### 10.1.3 S3: Supplementary data for Chapter 8

#### Geochemical modelling of groundwater in the Namaqualand region, South Africa

##### Abstract

Namaqualand is one of the most arid areas in South Africa. In recent years, rapid development has created a higher demand for water, which is increasingly fulfilled by groundwater abstraction. Comprehensive information of geochemical evolution of groundwater quality can improve the understanding of hydrochemical characteristics and promote sustainable development and effective management of groundwater resources. The study aims were to use the PHREEQC model to determine the hydrogeochemical characteristics of O'Kiep groundwater, to determine how the groundwater has deteriorated over time and to identify the major phases that control the groundwater in such an arid region. The model output showed phases that are governing the groundwater chemistry in this area. The geochemical reactions responsible for the evolution of groundwater chemistry along the flow path were the dissolution of carbonate minerals such as aragonite,  $\text{Ca}_3(\text{PO}_4)_2$ , calcite, dolomite, ferrihydrite and vaterite. These moved gradually from undersaturated to supersaturated status and vice versa happened for  $\text{Cd}(\text{CO}_3)$  and  $\text{Cr}(\text{OH})_3$ . The following minerals precipitated: anapaite, chloroapatite, chromite,  $\text{Cr}_2\text{O}_3\text{Fe}_5(\text{OH})(\text{PO}_4)_3$ , ferryhydrite, goethite, hematite, hydroxyapatite, lepidocrocite, maghemite and magnetite. In contrast, magnesite changed from undersaturated to equilibrium phase. Gypsum, siderite and halite remained undersaturated, indicating that these minerals may be subject to continuous dissolution. The groundwater hydrogeochemical evolution is thus mainly controlled by carbonate mineral dissolutions, cation exchange, precipitation and weathering.

**Keywords:** Hydrogeochemical processes, geochemical modelling, groundwater quality, PHREEQC, Namaqualand.

## Specification Table

Subject area	Hydrogeochemical modelling, geohydrology, groundwater quality, PHREEQC
More specific subject area	Hydrogeochemical modelling
Type of data	Table
How data were acquired	PHREEQC Version 3 is a computer programme for speciation, batch-reaction, one-dimensional transport, and inverse geochemical computations modelling for reactions in water to understand groundwater and aquifer rock interactions. Equilibrium constants were not fixed into the coding of the software to accommodate variations of the equilibrium constants. PHREEQC and EQ3/6 enable the user to manipulate the database and input files to change equilibrium constants when desired.
Data format	Raw data
Experimental features	Namaqualand, South Africa [30°5'16.0692"S 17°34' 50.4768"E] Sample preparation: Cape Peninsula University of Technology, <i>BioERG</i> laboratory, Cape Town, South Africa [-33°93'0950"S, 18°43'3531"E]
Data source and location	Groundwater from boreholes in Namaqualand, South Africa [30°5'16.0692"S 17°34' 50.4768"E]
Data accessibility	The USGS developed PHREEQC software with speciation and reaction path programme features. The software makes use of a C++ programming language to compute speciation, solubility, reaction pathways and inverse geochemical mass balance modelling. The programme does consider analytical uncertainties. PHREEQC has no licence obligations, and permission is not required from the USGS. PHREEQC is downloadable from <a href="https://www.usgs.gov/core-science-systems/ngp/national-hydrography">https://www.usgs.gov/core-science-systems/ngp/national-hydrography</a>

## **Value of the data**

- Several areas in Namaqualand are affected by elevated levels of PTEs, with their source being attributed to groundwater contamination (Clifford and Barton, 2012).
- In the study of Leshomo (2011), it is reported that the hydrochemistry of any groundwater can indicate whether there is significant groundwater evolution taking place. The processes contributing to changes in the borehole water quality in Namaqualand have not been modelled previously. Therefore, such data can be useful to numerous stakeholders. These include local government in the form of Nama Khoi Municipality, the Department of Environment, Forestry and Fisheries (DEFF) and the Department of Water and Sanitation, and departments of the South African government. Areas such as the south of Peru where the aridity is evidenced with some mining activity can also benefit.
- The hydrochemical characterisation of borehole water is an essential stage for effective management of groundwater resources in Namaqualand, as reported in Chapter 4 and in the study of Abiye and Leshomo (2013). Regarding this, PHREEQC modelling is regarded as a vital tool to elucidate geochemical processes involved in changes in the groundwater. In other words, PHREEQC results are of great significance for understanding the regional hydrochemical evolution of groundwater.
- The research data can assist in determining rock-water interactions and the hydrochemical evolution of groundwater and resolve hydrogeological challenges in the area monitored.
- The data provide critical knowledge on groundwater evolution with the change in environmental conditions. PHREEQC results are thus of great significance for understanding the regional hydrochemical evolution of groundwater.
- The research data will assist in determining rock-water interactions and the hydrochemical evolution of groundwater and resolve hydrogeological challenges in this area.
- The data will provide critical knowledge on groundwater evolution with the change in environmental and societal conditions.

## **Data**

This study presents the hydrogeochemical analysis of the groundwater in the arid Namaqualand, O’Kiep. Groundwater samples were collected from eight boreholes ( $n = 8$ ), as presented in Chapter 5. Other data were obtained from the study published by Abiye and Leshomo (2013), as shown in Table 10-12, with most of the boreholes being an area with fractured basement aquifers. PHREEQC was used to perform an aqueous geochemical modelling that has capabilities to determine the SI and speciation determinations in a batch-reaction system (Parkhurst and Appelo, 2013). The interaction between the groundwater and

rock mineralogy controls the geochemistry of the groundwater in specified areas (Guo *et al.*, 2007). A PHREEQC modelling software approach allows for the simulation and characterisation of the hydrogeochemical processes influencing the groundwater quality. Composition of the groundwater contaminated by various PTEs can be used to predict reactive mineral mechanisms. Any variations observed between different datasets can determine the geological-matrix interaction between significant anions and cations (Mondal *et al.*, 2010). The computed SI of particular phases is presented in Table 10-13.

**Table 10-12: A presentation of major ions from boreholes in the Namaqualand region, O’Kiep**

Parameter	Abiye and Leshomo (2013)	Chapter 4: Table 4-2
pH	7.11	8.1
Redox Potential (Eh)	29.2	-57.0
Temperature	22.1	15.0
Electrical Conductivity (EC)	2.04	241
Total Dissolved Solids (TDS)	911	1793
Alkalinity (CaCO <sub>3</sub> )	179	134
Sodium (Na)	224	243
Magnesium (Mg)	51.5	67.3
Potassium (K)	5.69	15.3
Calcium (Ca)	78.5	184
Chloride (Cl)	447	470
Nitrate (NO <sub>3</sub> )	27.3	2.16
Ortho-phosphate (PO <sub>4</sub> )	1.41	0.50
Sulfate (SO <sub>4</sub> )	121	455
Zinc (Zn)	0.81	0.00
Iron (Fe)	0.32	0.07
Cadmium (Cd)	9.77	0.003
Chromium (Cr)	0.16	0.01

The units are all in mg/L, with the exception of EC (mS/cm), Eh (mV), temperature (°C) and pH

**Table 10-13: Saturation index of minerals in O’Kiep groundwater**

Period 2013					Period 2019				
Phase	SI	log IAP	log K(295 K)	log K(295 K, 1 atm)	Phase	SI	log IAP	log K(288 K)	log K(288 K, 1 atm)
Anapaite	1.64	6.66	5.02	Ca <sub>2</sub> Fe(PO <sub>4</sub> ) <sub>2</sub> :4H <sub>2</sub> O	Anapaite	2.6	7.62	5.02	Ca <sub>2</sub> Fe(PO <sub>4</sub> ) <sub>2</sub> :4H <sub>2</sub> O
Anhydrite	-1.83	-6.24	-4.41	Ca(SO <sub>4</sub> )	Anhydrite	-1.1	-5.43	-4.33	Ca(SO <sub>4</sub> )
Antarcticite	-10.84	-6.93	3.92	CaCl <sub>2</sub> :6H <sub>2</sub> O	Antarcticite	-10.46	-6.61	3.85	CaCl <sub>2</sub> :6H <sub>2</sub> O
Aragonite	-0.49	-8.78	-8.29	CaCO <sub>3</sub>	Aragonite	0.53	-7.71	-8.25	CaCO <sub>3</sub>
Arcanite	-9.15	-11.04	-1.89	K <sub>2</sub> SO <sub>4</sub>	Arcanite	-7.68	-9.68	-2.00	K <sub>2</sub> SO <sub>4</sub>
Artinite	-7.5	2.51	10.01	Mg <sub>2</sub> (CO <sub>3</sub> )(OH) <sub>2</sub> :3H <sub>2</sub> O	Artinite	-5.17	5.36	10.53	Mg <sub>2</sub> (CO <sub>3</sub> )(OH) <sub>2</sub> :3H <sub>2</sub> O
Bassanite	-2.35	-6.24	-3.89	CaSO <sub>4</sub> :0.5H <sub>2</sub> O	Bassanite	-1.62	-5.43	-3.81	CaSO <sub>4</sub> :0.5H <sub>2</sub> O
Bischofite	-11.37	-6.89	4.47	MgCl <sub>2</sub> :6H <sub>2</sub> O	Bischofite	-11.33	-6.81	4.51	MgCl <sub>2</sub> :6H <sub>2</sub> O
Bloedite	-11.24	-13.59	-2.35	Na <sub>2</sub> Mg(SO <sub>4</sub> ) <sub>2</sub> :4H <sub>2</sub> O	Bloedite	-10.11	-12.46	-2.35	Na <sub>2</sub> Mg(SO <sub>4</sub> ) <sub>2</sub> :4H <sub>2</sub> O
Brucite	-6.04	11.26	17.3	Mg(OH) <sub>2</sub>	Brucite	-4.51	13.28	17.79	Mg(OH) <sub>2</sub>
Brushite	-1.54	-0.93	0.61	Ca(HPO <sub>4</sub> ):2H <sub>2</sub> O	Brushite	-1.53	-0.88	0.64	Ca(HPO <sub>4</sub> ):2H <sub>2</sub> O
Burkeite	-23.94	-24.71	-0.77	Na <sub>6</sub> (CO <sub>3</sub> )(SO <sub>4</sub> ) <sub>2</sub>	Burkeite	-21.97	-22.74	-0.77	Na <sub>6</sub> (CO <sub>3</sub> )(SO <sub>4</sub> ) <sub>2</sub>
C <sub>(cr)</sub>	-13.98	40.5	54.48	C	C <sub>(cr)</sub>	-16.35	39.77	56.12	C
C <sub>3</sub> FH <sub>6</sub>	-35.51	37.76	73.27	Ca <sub>3</sub> Fe <sub>2</sub> (OH) <sub>12</sub>	C <sub>3</sub> FH <sub>6</sub>	-28.54	46.95	75.49	Ca <sub>3</sub> Fe <sub>2</sub> (OH) <sub>12</sub>
C <sub>4</sub> FH <sub>13</sub>	-47.16	48.98	96.14	Ca <sub>4</sub> Fe <sub>2</sub> (OH) <sub>14</sub> :6H <sub>2</sub> O	C <sub>4</sub> FH <sub>13</sub>	-38.18	60.44	98.62	Ca <sub>4</sub> Fe <sub>2</sub> (OH) <sub>14</sub> :6H <sub>2</sub> O
Ca(HPO <sub>4</sub> ) <sub>(s)</sub>	-1.27	-0.93	0.34	Ca(HPO <sub>4</sub> )	Ca(HPO <sub>4</sub> ) <sub>(s)</sub>	-1.33	-0.88	0.45	Ca(HPO <sub>4</sub> )
Ca(NO <sub>3</sub> ) <sub>2(s)</sub>	-14.43	-8.54	5.89	Ca(NO <sub>3</sub> ) <sub>2</sub>	Ca(NO <sub>3</sub> ) <sub>2(s)</sub>	-16.36	-10.47	5.89	Ca(NO <sub>3</sub> ) <sub>2</sub>
Ca <sub>(s)</sub>	-99.78	41.47	141.26	Ca	Ca <sub>(s)</sub>	-100.86	43.98	144.84	Ca
Ca <sub>2</sub> Cl <sub>2</sub> (OH) <sub>2</sub> :H <sub>2</sub> O <sub>(s)</sub>	-22.23	4.3	26.53	Ca <sub>2</sub> Cl <sub>2</sub> (OH) <sub>2</sub> :H <sub>2</sub> O	Ca <sub>2</sub> Cl <sub>2</sub> (OH) <sub>2</sub> :H <sub>2</sub> O <sub>(s)</sub>	-19.64	6.89	26.53	Ca <sub>2</sub> Cl <sub>2</sub> (OH) <sub>2</sub> :H <sub>2</sub> O

Period 2013					Period 2019				
Phase	SI	log IAP	log K(295 K)	log K(295 K, 1 atm)	Phase	SI	log IAP	log K(288 K)	log K(288 K, 1 atm)
Ca <sub>2</sub> Fe <sub>2</sub> O <sub>5(s)</sub>	-31.04	26.54	57.58	Ca <sub>2</sub> Fe <sub>2</sub> O <sub>5a</sub>	Ca <sub>2</sub> Fe <sub>2</sub> O <sub>5(s)</sub>	-26.19	33.45	59.64	Ca <sub>2</sub> Fe <sub>2</sub> O <sub>5</sub>
Ca <sub>3</sub> (PO <sub>4</sub> ) <sub>2</sub> (alfa)	-1.07	9.37	10.44	Ca <sub>3</sub> (PO <sub>4</sub> ) <sub>2</sub>	Ca <sub>3</sub> (PO <sub>4</sub> ) <sub>2</sub> (alfa)	0.74	11.73	10.98	Ca <sub>3</sub> (PO <sub>4</sub> ) <sub>2</sub>
Ca <sub>4</sub> Cl <sub>2</sub> (OH) <sub>6</sub> :13H <sub>2</sub> O <sub>(s)</sub>	-42.46	26.74	69.2	Ca <sub>4</sub> Cl <sub>2</sub> (OH) <sub>6</sub> :13H <sub>2</sub> O	Ca <sub>4</sub> Cl <sub>2</sub> (OH) <sub>6</sub> :13H <sub>2</sub> O <sub>(s)</sub>	-36.51	33.87	70.38	Ca <sub>4</sub> Cl <sub>2</sub> (OH) <sub>6</sub> :13H <sub>2</sub> O
Ca <sub>4</sub> H(PO <sub>4</sub> ) <sub>3</sub> :2.5H <sub>2</sub> O <sub>(s)</sub>	-3.37	8.44	11.81	Ca <sub>4</sub> H(PO <sub>4</sub> ) <sub>3</sub> :2.5H <sub>2</sub> O	Ca <sub>4</sub> H(PO <sub>4</sub> ) <sub>3</sub> :2.5H <sub>2</sub> O <sub>(s)</sub>	-0.97	10.84	11.81	Ca <sub>4</sub> H(PO <sub>4</sub> ) <sub>3</sub> :2.5H <sub>2</sub> O
CaCl <sub>2</sub> :2H <sub>2</sub> O <sub>(cr)</sub>	-14.95	-6.93	8.03	CaCl <sub>2</sub> :2H <sub>2</sub> O	CaCl <sub>2</sub> :2H <sub>2</sub> O <sub>(cr)</sub>	-14.83	-6.60	8.22	CaCl <sub>2</sub> :2H <sub>2</sub> O
CaCl <sub>2</sub> :4H <sub>2</sub> O <sub>(cr)</sub>	-12.3	-6.93	5.37	CaCl <sub>2</sub> :4H <sub>2</sub> O	CaCl <sub>2</sub> :4H <sub>2</sub> O <sub>(cr)</sub>	-12.02	-6.60	5.42	CaCl <sub>2</sub> :4H <sub>2</sub> O
CaCl <sub>2</sub> :H <sub>2</sub> O <sub>(s)</sub>	-14.86	-6.93	7.94	CaCl <sub>2</sub> :H <sub>2</sub> O	CaCl <sub>2</sub> :H <sub>2</sub> O <sub>(s)</sub>	-14.77	-6.60	8.17	CaCl <sub>2</sub> :H <sub>2</sub> O
CaCO <sub>3</sub> :H <sub>2</sub> O <sub>(s)</sub>	-1.19	-8.78	-7.59	CaCO <sub>3</sub> :H <sub>2</sub> O	CaCO <sub>3</sub> :H <sub>2</sub> O <sub>(s)</sub>	-0.15	-7.71	-7.56	CaCO <sub>3</sub> :H <sub>2</sub> O
CaCrO <sub>4(s)</sub>	-31.66	-34.77	-3.11	CaCrO <sub>4</sub>	CaCrO <sub>4(s)</sub>	-30.78	-33.80	-3.01	CaCrO <sub>4</sub>
CaFe <sub>2</sub> O <sub>4(s)</sub>	-6.38	15.32	21.69	CaFe <sub>2</sub> O <sub>4</sub>	CaFe <sub>2</sub> O <sub>4(s)</sub>	-2.88	19.96	22.84	CaFe <sub>2</sub> O <sub>4</sub>
Calcite	-0.32	-8.78	-8.46	CaCO <sub>3</sub>	Calcite	0.70	-7.71	-8.42	CaCO <sub>3</sub>
CaMg <sub>3</sub> (CO <sub>3</sub> ) <sub>4(s)</sub>	-4.39	-35.01	-30.62	CaMg <sub>3</sub> (CO <sub>3</sub> ) <sub>4</sub>	CaMg <sub>3</sub> (CO <sub>3</sub> ) <sub>4(s)</sub>	-1.36	-31.48	-30.13	CaMg <sub>3</sub> (CO <sub>3</sub> ) <sub>4</sub>
CaO <sub>(cr)</sub>	-21.81	11.22	33.03	CaO	CaO <sub>(cr)</sub>	-20.39	13.49	33.88	CaO
Carnallite	-17.07	-12.76	4.31	KMgCl <sub>3</sub> :6H <sub>2</sub> O	Carnallite	-16.52	-12.24	4.27	KMgCl <sub>3</sub> :6H <sub>2</sub> O
Cd(CO <sub>3</sub> ) <sub>(s)</sub>	1.68	-10.43	-12.1	Cd(CO <sub>3</sub> )	Cd(CO <sub>3</sub> ) <sub>(s)</sub>	-1.13	-13.24	-12.11	Cd(CO <sub>3</sub> )
Cd <sub>(cr)</sub>	-17.4	39.82	57.22	Cd	Cd <sub>(cr)</sub>	-20.31	38.46	58.77	Cd
Cd(OH) <sub>2(s)</sub>	-4.44	9.57	14.01	Cd(OH) <sub>2</sub>	Cd(OH) <sub>2(s)</sub>	-6.42	7.97	14.39	Cd(OH) <sub>2</sub>
Cd(SO <sub>4</sub> ) <sub>(cr)</sub>	-7.81	-7.88	-0.07	Cd(SO <sub>4</sub> )	Cd(SO <sub>4</sub> ) <sub>(cr)</sub>	-11.11	-10.95	0.16	Cd(SO <sub>4</sub> )
Cd(SO <sub>4</sub> ):2.67H <sub>2</sub> O <sub>(cr)</sub>	-6.37	-7.88	-1.52	Cd(SO <sub>4</sub> ):2.67H <sub>2</sub> O	Cd(SO <sub>4</sub> ):2.67H <sub>2</sub> O <sub>(cr)</sub>	-9.53	-10.95	-1.43	Cd(SO <sub>4</sub> ):2.67H <sub>2</sub> O

Period 2013					Period 2019				
Phase	SI	log IAP	log K(295 K)	log K(295 K, 1 atm)	Phase	SI	log IAP	log K(288 K)	log K(288 K, 1 atm)
Cd <sub>3</sub> (PO <sub>4</sub> ) <sub>2(s)</sub>	-4.9	4.43	9.33	Cd <sub>3</sub> (PO <sub>4</sub> ) <sub>2</sub>	Cd <sub>3</sub> (PO <sub>4</sub> ) <sub>2(s)</sub>	-15.07	-4.84	10.23	Cd <sub>3</sub> (PO <sub>4</sub> ) <sub>2</sub>
Cd <sub>5</sub> (PO <sub>4</sub> ) <sub>3</sub> Cl <sub>(cr)</sub>	-10.32	2.35	12.67	Cd <sub>5</sub> (PO <sub>4</sub> ) <sub>3</sub> Cl	Cd <sub>5</sub> (PO <sub>4</sub> ) <sub>3</sub> Cl <sub>(cr)</sub>	-26.00	-13.33	12.67	Cd <sub>5</sub> (PO <sub>4</sub> ) <sub>3</sub> Cl
Cd <sub>5</sub> (PO <sub>4</sub> ) <sub>3</sub> OH <sub>(cr)</sub>	-8.41	11.43	19.84	Cd <sub>5</sub> (PO <sub>4</sub> ) <sub>3</sub> OH	Cd <sub>5</sub> (PO <sub>4</sub> ) <sub>3</sub> OH <sub>(cr)</sub>	-23.12	-3.28	19.84	Cd <sub>5</sub> (PO <sub>4</sub> ) <sub>3</sub> OH
CdCl <sub>2(s)</sub>	-7.94	-8.57	-0.63	CdCl <sub>2</sub>	CdCl <sub>2(s)</sub>	-11.58	-12.13	-0.55	CdCl <sub>2</sub>
CdCl <sub>2</sub> :2.5H <sub>2</sub> O <sub>(s)</sub>	-6.66	-8.57	-1.91	CdCl <sub>2</sub> :2.5H <sub>2</sub> O	CdCl <sub>2</sub> :2.5H <sub>2</sub> O <sub>(s)</sub>	-10.18	-12.13	-1.94	CdCl <sub>2</sub> :2.5H <sub>2</sub> O
CdCl <sub>2</sub> :H <sub>2</sub> O <sub>(cr)</sub>	-6.89	-8.57	-1.68	CdCl <sub>2</sub> :H <sub>2</sub> O	CdCl <sub>2</sub> :H <sub>2</sub> O <sub>(cr)</sub>	-10.48	-12.13	-1.64	CdCl <sub>2</sub> :H <sub>2</sub> O
CdO <sub>(s)</sub>	-5.7	9.57	15.28	CdO	CdO <sub>(s)</sub>	-7.76	7.97	15.73	CdO
CH <sub>4(g)</sub>	-31.4	101	132.39	CH <sub>4</sub>	CH <sub>4(g)</sub>	-35.40	100.75	136.15	CH <sub>4</sub>
Chloroapatite	5.15	10.59	5.44	Ca <sub>5</sub> Cl(PO <sub>4</sub> ) <sub>3</sub>	Chloroapatite	8.27	14.29	6.02	Ca <sub>5</sub> Cl(PO <sub>4</sub> ) <sub>3</sub>
Chromite	10.27	25.85	15.58	FeCr <sub>2</sub> O <sub>4</sub>	Chromite	8.83	25.59	16.75	FeCr <sub>2</sub> O <sub>4</sub>
Cl <sub>2(g)</sub>	-51.48	-48.4	3.08	Cl <sub>2</sub>	Cl <sub>2(g)</sub>	-53.91	-50.59	3.32	Cl <sub>2</sub>
CO <sub>(g)</sub>	-18.57	10.25	28.82	CO	CO <sub>(g)</sub>	-20.73	9.28	30.01	CO
CO <sub>2(g)</sub>	-1.84	-20	-18.16	CO <sub>2</sub>	CO <sub>2(g)</sub>	-3.03	-21.21	-18.18	CO <sub>2</sub>
Cr(OH) <sub>2(cr)</sub>	-15.62	-4.49	11.13	Cr(OH) <sub>2</sub>	Cr(OH) <sub>2(cr)</sub>	-17.37	-5.91	11.46	Cr(OH) <sub>2</sub>
Cr(OH) <sub>2</sub> (H <sub>2</sub> PO <sub>4</sub> ) <sub>(s)</sub>	-4.38	-3.48	0.9	Cr(OH) <sub>2</sub> (H <sub>2</sub> PO <sub>4</sub> )	Cr(OH) <sub>2</sub> (H <sub>2</sub> PO <sub>4</sub> ) <sub>(s)</sub>	-7.20	-6.28	0.92	Cr(OH) <sub>2</sub> (H <sub>2</sub> PO <sub>4</sub> )
Cr(OH) <sub>3(cr)</sub>	0.99	8.67	7.68	Cr(OH) <sub>3</sub>	Cr(OH) <sub>3(cr)</sub>	-0.04	8.10	8.14	Cr(OH) <sub>3</sub>
Cr <sub>(s)</sub>	-45.89	44.76	90.65	Cr	Cr <sub>(s)</sub>	-48.98	44.18	93.16	Cr
Cr <sub>2</sub> (SO <sub>4</sub> ) <sub>3(s)</sub>	-39.9	-35.04	4.86	Cr <sub>2</sub> (SO <sub>4</sub> ) <sub>3</sub>	Cr <sub>2</sub> (SO <sub>4</sub> ) <sub>3(s)</sub>	-46.64	-40.57	6.07	Cr <sub>2</sub> (SO <sub>4</sub> ) <sub>3</sub>
Cr <sub>2</sub> O <sub>3(cr)</sub>	9.24	17.33	8.09	Cr <sub>2</sub> O <sub>3</sub>	Cr <sub>2</sub> O <sub>3(cr)</sub>	7.24	16.20	8.95	Cr <sub>2</sub> O <sub>3</sub>

Period 2013					Period 2019				
Phase	SI	log IAP	log K(295 K)	log K(295 K, 1 atm)	Phase	SI	log IAP	log K(288 K)	log K(288 K, 1 atm)
CrCl <sub>2(cr)</sub>	-35.54	-22.63	12.91	CrCl <sub>2</sub>	CrCl <sub>2(cr)</sub>	-39.36	-26.00	13.36	CrCl <sub>2</sub>
CrCl <sub>3(cr)</sub>	-39.08	-18.55	20.53	CrCl <sub>3</sub>	CrCl <sub>3(cr)</sub>	-43.44	-22.05	21.39	CrCl <sub>3</sub>
CrO <sub>2(cr)</sub>	-7.03	-15.74	-8.71	CrO <sub>2</sub>	CrO <sub>2(cr)</sub>	-8.04	-16.80	-8.76	CrO <sub>2</sub>
CrO <sub>3(cr)</sub>	-42.99	-45.99	-3.00	CrO <sub>3</sub>	CrO <sub>3(cr)</sub>	44.33	-47.29	-2.96	CrO <sub>3</sub>
CrPO <sub>4(green)</sub>	-0.42	-3.48	-3.06	CrPO <sub>4</sub>	CrPO <sub>4(green)</sub>	-3.22	-6.28	-3.06	CrPO <sub>4</sub>
CrPO <sub>4(purple)</sub>	-6.04	-3.48	2.56	CrPO <sub>4</sub>	CrPO <sub>4(purple)</sub>	-8.84	-6.28	2.56	CrPO <sub>4</sub>
Dolomite	-0.46	-17.52	-17.06	CaMg(CO <sub>3</sub> ) <sub>2</sub>	Dolomite	1.26	-15.64	-16.90	CaMg(CO <sub>3</sub> ) <sub>2</sub>
Epsomite	-4.31	-6.2	-1.9	Mg(SO <sub>4</sub> ):7H <sub>2</sub> O	Epsomite	-3.69	-5.64	-1.95	Mg(SO <sub>4</sub> ):7H <sub>2</sub> O
Ettringite-Fe	-36.1	19.04	55.14	Ca <sub>6</sub> Fe <sub>2</sub> (SO <sub>4</sub> ) <sub>3</sub> (OH) <sub>12</sub> :26H <sub>2</sub> O	Ettringite-Fe	-25.99	30.65	56.64	Ca <sub>6</sub> Fe <sub>2</sub> (SO <sub>4</sub> ) <sub>3</sub> (OH) <sub>12</sub> :26H <sub>2</sub> O
Fe(OH) <sub>2(cr)</sub>	-4.41	8.52	12.93	Fe(OH) <sub>2</sub>	Fe(OH) <sub>2(cr)</sub>	-3.97	9.39	13.36	Fe(OH) <sub>2</sub>
Fe(PO <sub>4</sub> ) <sub>(cr)</sub>	-3.89	-10.1	-6.21	Fe(PO <sub>4</sub> )	Fe(PO <sub>4</sub> ) <sub>(cr)</sub>	-5.02	-11.14	6.13	Fe(PO <sub>4</sub> )
Fe <sub>(s)</sub>	-20.72	38.77	59.49	Fe	Fe <sub>(s)</sub>	-21.22	39.88	61.10	Fe
Fe <sub>5</sub> (OH)(PO <sub>4</sub> ) <sub>3(s)</sub>	408.46	6.14	-402.32	Fe <sub>5</sub> (OH)(PO <sub>4</sub> ) <sub>3</sub>	Fe <sub>5</sub> (OH)(PO <sub>4</sub> ) <sub>3(s)</sub>	3.83	-402.32	406.15	Fe <sub>5</sub> (OH)(PO <sub>4</sub> ) <sub>3</sub>
FeO <sub>(s)</sub>	-5.03	8.52	13.55	FeO	FeO <sub>(s)</sub>	-4.61	9.39	14.00	FeO
Ferrihydrite <sub>(am)</sub>	-0.49	2.05	2.54	Fe(OH) <sub>3</sub>	Ferrihydrite <sub>(am)</sub>	0.69	3.23	2.54	Fe(OH) <sub>3</sub>
Ferryhydrite	0.86	2.05	1.19	Fe(OH) <sub>3</sub>	Ferryhydrite	2.04	3.23	1.19	Fe(OH) <sub>3</sub>
Gaylussite	-9.23	-18.71	-9.48	CaNa <sub>2</sub> (CO <sub>3</sub> ) <sub>2</sub> :5H <sub>2</sub> O	Gaylussite	-7.20	-16.82	-9.62	CaNa <sub>2</sub> (CO <sub>3</sub> ) <sub>2</sub> :5H <sub>2</sub> O
Glaserite	-32.76	-40.51	-7.74	Na <sub>2</sub> K <sub>6</sub> (SO <sub>4</sub> ) <sub>4</sub>	Glaserite	-27.77	-35.86	-8.09	Na <sub>2</sub> K <sub>6</sub> (SO <sub>4</sub> ) <sub>4</sub>
Glauberite	-15.62	-13.63	1.99	Na <sub>2</sub> Ca(SO <sub>4</sub> ) <sub>2</sub>	Glauberite	-14.30	-12.25	2.05	Na <sub>2</sub> Ca(SO <sub>4</sub> ) <sub>2</sub>

Period 2013					Period 2019				
Phase	SI	log IAP	log K(295 K)	log K(295 K, 1 atm)	Phase	SI	log IAP	log K(288 K)	log K(288 K, 1 atm)
Goethite	1.55	2.05	0.5	FeOOH	Goethite	2.47	3.23	0.76	FeOOH
Gypsum	-1.63	-6.24	-4.61	CaSO <sub>4</sub> :2H <sub>2</sub> O	Gypsum	-0.83	-5.43	-4.60	CaSO <sub>4</sub> :2H <sub>2</sub> O
H <sub>2(g)</sub>	-13.22	30.25	43.47	H <sub>2</sub>	H <sub>2(g)</sub>	-14.20	30.49	44.69	H <sub>2</sub>
H <sub>2</sub> O <sub>(g)</sub>	-1.58	0	1.58	H <sub>2</sub> O	H <sub>2</sub> O <sub>(g)</sub>	-1.77	-0.00	1.77	H <sub>2</sub> O
Halite	-5.62	-4.04	1.58	NaCl	Halite	-5.56	-4.00	1.57	NaCl
HCl <sub>(g)</sub>	-15.49	-9.07	6.42	HCl	HCl <sub>(g)</sub>	-16.79	-10.05	6.74	HCl
Hematite	4.9	4.1	-0.81	Fe <sub>2</sub> O <sub>3</sub>	Hematite	6.74	6.47	-0.27	Fe <sub>2</sub> O <sub>3</sub>
Hexahydrate	-4.57	-6.2	-1.63	Mg(SO <sub>4</sub> ):6H <sub>2</sub> O	Hexahydrate	-4.03	-5.64	-1.61	Mg(SO <sub>4</sub> ):6H <sub>2</sub> O
Hydrophilite	-18.83	-6.92	11.91	CaCl <sub>2</sub>	Hydrophilite	-18.87	-6.60	12.26	CaCl <sub>2</sub>
Hydroxyapatite	5	19.66	14.66	Ca <sub>5</sub> (OH)(PO <sub>4</sub> ) <sub>3</sub>	Hydroxyapatite	8.90	24.33	15.44	Ca <sub>5</sub> (OH)(PO <sub>4</sub> ) <sub>3</sub>
K <sub>(cr)</sub>	-53.33	18.33	71.66	K	K <sub>(cr)</sub>	-53.50	19.87	73.37	K
K(NO <sub>3</sub> ) <sub>(s)</sub>	-6.57	-6.67	-0.1	K(NO <sub>3</sub> )	K(NO <sub>3</sub> ) <sub>(s)</sub>	-7.26	-7.36	-0.10	K(NO <sub>3</sub> )
K(OH) <sub>(s)</sub>	-21.39	3.21	24.6	K(OH)	K(OH) <sub>(s)</sub>	-19.98	4.62	24.60	K(OH)
K-carbonate	-16.61	-13.58	3.03	K <sub>2</sub> CO <sub>3</sub> :1.5H <sub>2</sub> O	K-carbonate	-15.00	-11.96	3.04	K <sub>2</sub> CO <sub>3</sub> :1.5H <sub>2</sub> O
K-trona	-19.45	-28.55	-9.1	K <sub>2</sub> NaH(CO <sub>3</sub> ) <sub>2</sub> :2H <sub>2</sub> O	K-trona	-18.02	-27.12	-9.10	K <sub>2</sub> NaH(CO <sub>3</sub> ) <sub>2</sub> :2H <sub>2</sub> O
K <sub>2</sub> CO <sub>3(cr)</sub>	-19.05	-13.58	5.46	K <sub>2</sub> CO <sub>3</sub>	K <sub>2</sub> CO <sub>3(cr)</sub>	-17.57	-11.96	5.60	K <sub>2</sub> CO <sub>3</sub>
K <sub>2</sub> O <sub>(s)</sub>	-78.43	6.42	84.84	K <sub>2</sub> O	K <sub>2</sub> O <sub>(s)</sub>	-77.46	9.24	86.71	K <sub>2</sub> O
Kainite	-11.9	-12.07	-0.17	KMgCl(SO <sub>4</sub> ):3H <sub>2</sub> O	Kainite	-10.96	-11.07	-0.11	KMgCl(SO <sub>4</sub> ):3H <sub>2</sub> O
Kaliginite	-6.67	-16.79	-10.12	KHCO <sub>3</sub>	Kaliginite	-6.31	-16.59	-10.27	KHCO <sub>3</sub>

Period 2013					Period 2019				
Phase	SI	log IAP	log K(295 K)	log K(295 K, 1 atm)	Phase	SI	log IAP	log K(288 K)	log K(288 K, 1 atm)
KFe(CrO <sub>4</sub> ) <sub>2</sub> :2H <sub>2</sub> O <sub>(s)</sub>	-67.28	-86.72	-19.44	KFe(CrO <sub>4</sub> ) <sub>2</sub> :2H <sub>2</sub> O	KFe(CrO <sub>4</sub> ) <sub>2</sub> :2H <sub>2</sub> O <sub>(s)</sub>	-67.17	-86.72	-19.56	KFe(CrO <sub>4</sub> ) <sub>2</sub> :2H <sub>2</sub> O
KFe <sub>3</sub> (CrO <sub>4</sub> ) <sub>2</sub> (OH) <sub>6(cr)</sub>	-64.22	-82.62	-18.4	KFe <sub>3</sub> (CrO <sub>4</sub> ) <sub>2</sub> (OH) <sub>6</sub>	KFe <sub>3</sub> (CrO <sub>4</sub> ) <sub>2</sub> (OH) <sub>6(cr)</sub>	-61.85	-80.25	-18.40	KFe <sub>3</sub> (CrO <sub>4</sub> ) <sub>2</sub> (OH) <sub>6</sub>
KH <sub>2</sub> PO <sub>4(cr)</sub>	-8.54	-8.94	-0.4	KH <sub>2</sub> PO <sub>4</sub>	KH <sub>2</sub> PO <sub>4(cr)</sub>	-9.27	-9.76	-0.49	KH <sub>2</sub> PO <sub>4</sub>
Lansfordite	-3.7	-8.75	-5.04	Mg(CO <sub>3</sub> ):5H <sub>2</sub> O	Lansfordite	-2.87	-7.92	-5.06	Mg(CO <sub>3</sub> ):5H <sub>2</sub> O
Lawrencite	-18.66	-9.63	9.03	FeCl <sub>2</sub>	Lawrencite	-20.10	-10.70	9.39	FeCl <sub>2</sub>
Leonhardtite	-5.35	-6.2	-0.85	MgSO <sub>4</sub> :4H <sub>2</sub> O	Leonhardtite	-4.90	-5.64	-0.74	MgSO <sub>4</sub> :4H <sub>2</sub> O
Leonite	-13.24	-17.24	-4.01	K <sub>2</sub> Mg(SO <sub>4</sub> ) <sub>2</sub> :4H <sub>2</sub> O	Leonite	-11.25	-15.32	-4.07	K <sub>2</sub> Mg(SO <sub>4</sub> ) <sub>2</sub> :4H <sub>2</sub> O
Lepidocrocite	1.19	2.05	0.86	FeOOH	Lepidocrocite	2.09	3.23	1.14	FeOOH
Maghemite <sub>(disord)</sub>	0.53	4.1	3.57	Fe <sub>2</sub> O <sub>3</sub>	Maghemite <sub>(disord)</sub>	2.25	6.47	4.22	Fe <sub>2</sub> O <sub>3</sub>
Maghemite <sub>(ord)</sub>	0.32	4.1	3.78	Fe <sub>2</sub> O <sub>3</sub>	Maghemite <sub>(ord)</sub>	2.04	6.47	4.43	Fe <sub>2</sub> O <sub>3</sub>
Magnesite <sub>(nat)</sub>	0.12	-8.74	-8.87	MgCO <sub>3</sub>	Magnesite <sub>(nat)</sub>	0.84	-7.92	-8.76	MgCO <sub>3</sub>
Magnesite <sub>(syn)</sub>	-0.69	-8.74	-8.05	Mg(CO <sub>3</sub> )	Magnesite <sub>(syn)</sub>	0.00	-7.92	-7.92	Mg(CO <sub>3</sub> )
Magnetite	1.83	12.61	10.78	Fe <sub>3</sub> O <sub>4</sub>	Magnetite	4.14	15.86	11.72	Fe <sub>3</sub> O <sub>4</sub>
Melanterite	-6.7	-8.94	-2.25	FeSO <sub>4</sub> :7H <sub>2</sub> O	Melanterite	-7.20	-9.53	-2.33	FeSO <sub>4</sub> :7H <sub>2</sub> O
Mercallite	-12.85	-14.25	-1.4	KHSO <sub>4</sub>	Mercallite	-12.91	-14.30	-1.40	KHSO <sub>4</sub>
Mg <sub>(cr)</sub>	-82.55	41.51	124.06	Mg	Mg <sub>(cr)</sub>	-83.54	43.77	127.31	Mg
Mg(HPO <sub>4</sub> ):3H <sub>2</sub> O <sub>(s)</sub>	-2.3	-0.89	1.41	Mg(HPO <sub>4</sub> ):3H <sub>2</sub> O	Mg(HPO <sub>4</sub> ):3H <sub>2</sub> O <sub>(s)</sub>	-2.50	-1.09	1.41	Mg(HPO <sub>4</sub> ):3H <sub>2</sub> O
Mg(NO <sub>3</sub> ) <sub>2(s)</sub>	-24.01	-8.51	15.5	Mg(NO <sub>3</sub> ) <sub>2</sub>	Mg(NO <sub>3</sub> ) <sub>2(s)</sub>	-26.18	-10.68	15.50	Mg(NO <sub>3</sub> ) <sub>2</sub>
Mg(NO <sub>3</sub> ) <sub>2</sub> :6H <sub>2</sub> O <sub>(s)</sub>	-11.09	-8.51	2.58	Mg(NO <sub>3</sub> ) <sub>2</sub> :6H <sub>2</sub> O	Mg(NO <sub>3</sub> ) <sub>2</sub> :6H <sub>2</sub> O <sub>(s)</sub>	-13.26	-10.68	2.58	Mg(NO <sub>3</sub> ) <sub>2</sub> :6H <sub>2</sub> O

Period 2013					Period 2019				
Phase	SI	log IAP	log K(295 K)	log K(295 K, 1 atm)	Phase	SI	log IAP	log K(288 K)	log K(288 K, 1 atm)
Mg(SO <sub>4</sub> ) <sub>(s)</sub>	-15.5	-6.2	9.3	Mg(SO <sub>4</sub> )	Mg(SO <sub>4</sub> ) <sub>(s)</sub>	-15.44	-5.64	9.80	Mg(SO <sub>4</sub> )
Mg(SO <sub>4</sub> ):H <sub>2</sub> O <sub>(s)</sub>	-6.17	-6.2	-0.03	Mg(SO <sub>4</sub> ):H <sub>2</sub> O	Mg(SO <sub>4</sub> ):H <sub>2</sub> O <sub>(s)</sub>	-5.83	-5.64	0.19	Mg(SO <sub>4</sub> ):H <sub>2</sub> O
Mg-oxychlorur	-12.86	13.44	26.3	Mg <sub>2</sub> Cl(OH) <sub>3</sub> :4H <sub>2</sub> O	Mg-oxychlorur	-10.45	16.52	26.97	Mg <sub>2</sub> Cl(OH) <sub>3</sub> :4H <sub>2</sub> O
Mg <sub>3</sub> (PO <sub>4</sub> ) <sub>2(cr)</sub>	-6.72	9.47	16.19	Mg <sub>3</sub> (PO <sub>4</sub> ) <sub>2</sub>	Mg <sub>3</sub> (PO <sub>4</sub> ) <sub>2(cr)</sub>	-6.02	11.10	17.12	Mg <sub>3</sub> (PO <sub>4</sub> ) <sub>2</sub>
Mg <sub>3</sub> (PO <sub>4</sub> ) <sub>2</sub> :22H <sub>2</sub> O <sub>(s)</sub>	-6.54	9.46	16	Mg <sub>3</sub> (PO <sub>4</sub> ) <sub>2</sub> :22H <sub>2</sub> O	Mg <sub>3</sub> (PO <sub>4</sub> ) <sub>2</sub> :22H <sub>2</sub> O <sub>(s)</sub>	-4.91	11.09	16.00	Mg <sub>3</sub> (PO <sub>4</sub> ) <sub>2</sub> :22H <sub>2</sub> O
Mg <sub>3</sub> (PO <sub>4</sub> ) <sub>2</sub> :8H <sub>2</sub> O <sub>(s)</sub>	-4.43	9.47	13.9	Mg <sub>3</sub> (PO <sub>4</sub> ) <sub>2</sub> :8H <sub>2</sub> O	Mg <sub>3</sub> (PO <sub>4</sub> ) <sub>2</sub> :8H <sub>2</sub> O <sub>(s)</sub>	-2.81	11.09	13.90	Mg <sub>3</sub> (PO <sub>4</sub> ) <sub>2</sub> :8H <sub>2</sub> O
Mg <sub>5</sub> (CO <sub>3</sub> ) <sub>4</sub> (OH) <sub>2</sub> :4H <sub>2</sub> O <sub>(s)</sub>	-13.82	-23.72	-9.91	Mg <sub>5</sub> (CO <sub>3</sub> ) <sub>4</sub> (OH) <sub>2</sub> :4H <sub>2</sub> O	Mg <sub>5</sub> (CO <sub>3</sub> ) <sub>4</sub> (OH) <sub>2</sub> :4H <sub>2</sub> O <sub>(s)</sub>	-9.53	-18.41	-8.88	Mg <sub>5</sub> (CO <sub>3</sub> ) <sub>4</sub> (OH) <sub>2</sub> :4H <sub>2</sub> O
MgCl <sub>2(s)</sub>	-29.19	-6.89	22.3	MgCl <sub>2</sub>	MgCl <sub>2(s)</sub>	-29.81	-6.81	23.00	MgCl <sub>2</sub>
MgCl <sub>2</sub> :2H <sub>2</sub> O <sub>(s)</sub>	-19.79	-6.89	12.9	MgCl <sub>2</sub> :2H <sub>2</sub> O	MgCl <sub>2</sub> :2H <sub>2</sub> O <sub>(s)</sub>	-19.71	-6.81	12.90	MgCl <sub>2</sub> :2H <sub>2</sub> O
MgCl <sub>2</sub> :4H <sub>2</sub> O <sub>(s)</sub>	-14.33	-6.89	7.44	MgCl <sub>2</sub> :4H <sub>2</sub> O	MgCl <sub>2</sub> :4H <sub>2</sub> O <sub>(s)</sub>	-14.25	-6.81	7.44	MgCl <sub>2</sub> :4H <sub>2</sub> O
MgCl <sub>2</sub> :H <sub>2</sub> O <sub>(s)</sub>	-23.11	-6.89	16.22	MgCl <sub>2</sub> :H <sub>2</sub> O	MgCl <sub>2</sub> :H <sub>2</sub> O <sub>(s)</sub>	-23.03	-6.81	16.22	MgCl <sub>2</sub> :H <sub>2</sub> O
MgCrO <sub>4(s)</sub>	53.01	-34.73	-87.74	MgCrO <sub>4</sub>	MgCrO <sub>4(s)</sub>	55.65	-34.01	-89.65	MgCrO <sub>4</sub>
Mirabilite	-6.02	-7.39	-1.37	Na <sub>2</sub> SO <sub>4</sub> :10H <sub>2</sub> O	Mirabilite	-5.11	-6.82	-1.71	Na <sub>2</sub> SO <sub>4</sub> :10H <sub>2</sub> O
Monosulfate-Fe	-35.35	31.52	66.87	Ca <sub>4</sub> Fe <sub>2</sub> (SO <sub>4</sub> )(OH) <sub>12</sub> :6H <sub>2</sub> O	Monosulfate-Fe	-27.44	41.51	68.95	Ca <sub>4</sub> Fe <sub>2</sub> (SO <sub>4</sub> )(OH) <sub>12</sub> :6H <sub>2</sub> O
Na <sub>(cr)</sub>	-47.88	20.16	68.04	Na	Na <sub>(cr)</sub>	-48.40	21.30	69.70	Na
Na(NO <sub>3</sub> ) <sub>(s)</sub>	-5.94	-4.85	1.09	Na(NO <sub>3</sub> )	Na(NO <sub>3</sub> ) <sub>(s)</sub>	-7.02	-5.93	1.09	Na(NO <sub>3</sub> )
Na <sub>2</sub> (CO <sub>3</sub> ) <sub>(cr)</sub>	-11.1	-9.93	1.17	Na <sub>2</sub> (CO <sub>3</sub> )	Na <sub>2</sub> (CO <sub>3</sub> ) <sub>(cr)</sub>	-10.38	-9.10	1.28	Na <sub>2</sub> (CO <sub>3</sub> )
Na <sub>2</sub> CO <sub>3</sub> :7H <sub>2</sub> O <sub>(s)</sub>	-9.4	-9.93	-0.53	Na <sub>2</sub> CO <sub>3</sub> :7H <sub>2</sub> O	Na <sub>2</sub> CO <sub>3</sub> :7H <sub>2</sub> O <sub>(s)</sub>	-8.38	-9.10	-0.72	Na <sub>2</sub> CO <sub>3</sub> :7H <sub>2</sub> O
Na <sub>2</sub> HPO <sub>4(cr)</sub>	-11.38	-2.08	9.3	Na <sub>2</sub> HPO <sub>4</sub>	Na <sub>2</sub> HPO <sub>4(cr)</sub>	-11.73	-2.27	9.45	Na <sub>2</sub> HPO <sub>4</sub>

Period 2013					Period 2019				
Phase	SI	log IAP	log K(295 K)	log K(295 K, 1 atm)	Phase	SI	log IAP	log K(288 K)	log K(288 K, 1 atm)
Na <sub>2</sub> O <sub>(cr)</sub>	-58	10.07	68.07	Na <sub>2</sub> O	Na <sub>2</sub> O <sub>(cr)</sub>	-57.49	12.10	69.60	Na <sub>2</sub> O
Na <sub>3</sub> PO <sub>4(cr)</sub>	-20.75	2.96	23.7	Na <sub>3</sub> PO <sub>4</sub>	Na <sub>3</sub> PO <sub>4(cr)</sub>	-20.39	3.78	24.17	Na <sub>3</sub> PO <sub>4</sub>
NaH <sub>2</sub> PO <sub>4(cr)</sub>	-9.43	-7.11	2.31	NaH <sub>2</sub> PO <sub>4</sub>	NaH <sub>2</sub> PO <sub>4(cr)</sub>	-10.66	-8.32	2.34	NaH <sub>2</sub> PO <sub>4</sub>
Nahcolite	-4.17	-14.97	-10.8	Na(HCO <sub>3</sub> )	Nahcolite	-4.21	-15.15	-10.94	Na(HCO <sub>3</sub> )
Natron	-8.99	-9.93	-0.94	Na <sub>2</sub> (CO <sub>3</sub> ):10H <sub>2</sub> O	Natron	-7.88	-9.10	-1.22	Na <sub>2</sub> (CO <sub>3</sub> ):10H <sub>2</sub> O
Nesquehonite	-3.68	-8.74	-5.06	Mg(CO <sub>3</sub> ):3H <sub>2</sub> O	Nesquehonite	-2.96	-7.92	-4.96	Mg(CO <sub>3</sub> ):3H <sub>2</sub> O
O <sub>2(g)</sub>	-57.62	-60.5	-2.88	O <sub>2</sub>	O <sub>2(g)</sub>	-58.15	-60.98	-2.83	O <sub>2</sub>
P <sub>(cr)</sub>	-78.52	63.47	141.99	P	P <sub>(cr)</sub>	-83.89	61.85	145.74	P
Pentahydrate	-4.95	-6.2	-1.26	MgSO <sub>4</sub> :5H <sub>2</sub> O	Pentahydrate	-4.45	-5.64	-1.19	MgSO <sub>4</sub> :5H <sub>2</sub> O
Periclase	-10.58	11.26	21.84	MgO	Periclase	-9.22	13.28	22.50	MgO
Picromerite	-12.86	-17.24	-4.39	K <sub>2</sub> Mg(SO <sub>4</sub> ) <sub>2</sub> :6H <sub>2</sub> O	Picromerite	-10.79	-15.32	-4.53	K <sub>2</sub> Mg(SO <sub>4</sub> ) <sub>2</sub> :6H <sub>2</sub> O
Pirssonite	-9.78	-18.71	-8.93	Na <sub>2</sub> Ca(CO <sub>3</sub> ) <sub>2</sub> :2H <sub>2</sub> O	Pirssonite	-7.85	-16.82	-8.97	Na <sub>2</sub> Ca(CO <sub>3</sub> ) <sub>2</sub> :2H <sub>2</sub> O
Polyhalite	-15.98	-29.72	-13.74	K <sub>2</sub> MgCa <sub>2</sub> (SO <sub>4</sub> ) <sub>4</sub> :2H <sub>2</sub> O	Polyhalite	-12.44	-26.18	-13.74	K <sub>2</sub> MgCa <sub>2</sub> (SO <sub>4</sub> ) <sub>4</sub> :2H <sub>2</sub> O
Portlandite	-11.81	11.22	23.03	Ca(OH) <sub>2</sub>	Portlandite	-10.11	13.49	23.60	Ca(OH) <sub>2</sub>
Siderite	-0.7	-11.48	-10.78	Fe(CO <sub>3</sub> )	Siderite	-1.09	-11.81	-10.73	Fe(CO <sub>3</sub> )
Sylvite	-6.7	-5.86	0.84	KCl	Sylvite	-6.19	-5.43	0.76	KCl
Syngenite	-9.83	-17.28	-7.45	K <sub>2</sub> Ca(SO <sub>4</sub> ) <sub>2</sub> :6H <sub>2</sub> O	Syngenite	-7.66	-15.11	-7.45	K <sub>2</sub> Ca(SO <sub>4</sub> ) <sub>2</sub> :6H <sub>2</sub> O
Tachyhydrite	-38.09	-20.71	17.38	Mg <sub>2</sub> CaCl <sub>6</sub> :12H <sub>2</sub> O	Tachyhydrite	-37.61	17.38	-20.23	Mg <sub>2</sub> CaCl <sub>6</sub> :12H <sub>2</sub> O
Thermonatrite	-10.43	-9.93	0.5	Na <sub>2</sub> (CO <sub>3</sub> ):H <sub>2</sub> O	Thermonatrite	-9.66	-9.10	0.5	Na <sub>2</sub> (CO <sub>3</sub> ):H <sub>2</sub> O

Period 2013					Period 2019				
Phase	SI	log IAP	log K(295 K)	log K(295 K, 1 atm)	Phase	SI	log IAP	log K(288 K)	log K(288 K, 1 atm)
Thernardite	-7.03	-7.39	-0.36	Na <sub>2</sub> SO <sub>4</sub>	Thernardite	-6.47	-6.82	-0.35	Na <sub>2</sub> SO <sub>4</sub>
Trona	-13.45	-24.9	-11.45	Na <sub>3</sub> H(CO <sub>3</sub> ) <sub>2</sub> ·2H <sub>2</sub> O	Trona	-12.64	-24.26	-11.62	Na <sub>3</sub> H(CO <sub>3</sub> ) <sub>2</sub> ·2H <sub>2</sub> O
Vaterite	-0.9	-8.78	-7.87	CaCO <sub>3</sub>	Vaterite	0.10	-7.71	-7.81	CaCO <sub>3</sub>

## CHAPTER 11: BIBLIOGRAPHY

---

## 11.1 Bibliography

- Abadom, C. and Nwankwoala, H. 2018. Interpretation of groundwater quality using statistical techniques in Federal University, Otuoke and Environs, Bayelsa State, Nigeria. *World Scientific News*, 95: 124-48.
- Abboud, I. A. 2018. Geochemistry and quality of groundwater of the Yarmouk basin aquifer, north Jordan. *Environmental Geochemistry and Health*, 40(4): 1405-1435.
- Abdelgawad, A., 2015, March. Mineralogical and morphological features of fractured granitic rock tested under water-rock interaction. *Eighteenth International Water Technology Conference (IWTC18)*, 6(4): 12-14.
- Abdi, H. 2010. Coefficient of variation. In: Salkind, N. J. (ed.) *Encyclopedia of research design*. United Kingdom: Sage Publications Ltd.
- Abiye, T., Bybee, G. and Leshomo, J. 2018. Fluoride concentrations in the arid Namaqualand and the Waterberg groundwater, South Africa: Understanding the controls of mobilization through hydrogeochemical and environmental isotopic approaches. *Groundwater for Sustainable Development*, 6: 112-120.
- Abiye, T. A. and Leshomo, J. T. 2013. Groundwater flow and radioactivity in Namaqualand, South Africa. *Environmental Earth Sciences*, 70(1): 281-293.
- Abreu, M., Matias, M., Magalhães, M. C. F. and Basto, M. 2008. Impacts on water, soil and plants from the abandoned Miguel Vacas copper mine, Portugal. *Journal of Geochemical Exploration*, 96(2-3): 161-170.
- Accuweather, 2017. Available: <http://www.accuweather.com/en/za/okiep/299938/month/299938?monyr=4/01/2017> [Accessed 30 April 2017].
- Accuweather, 2018. Available: <http://www.accuweather.com/en/za/okiep/299938/month/299938?monyr=4/01/2017> [Accessed 30 September 2018].
- Adam, K., Kourtis, A., Gazea, B. and Kontopoulos, A. 1997. Evaluation of static tests used to predict the potential for acid drainage generation at sulphide mine sites. *Mineral Processing and Extractive Metallurgy*, 106: A1.
- Adams, S., Titus, R. and Xu, Y. 2004. Groundwater recharge assessment of the basement aquifers of central Namaqualand. Doctoral Dissertation. University of the Western Cape. Bellville.
- Adeleke, R. A. and Bezuidenhout, C. C. 2011. Integrated water resources management (IWRM) in South Africa-challenges of microbiology quality of water resources. *African Journal of Science, Technology, Innovation and Development*, 3(4): 55-64.
- Adimalla, N. and Venkatayogi, S. 2018. Geochemical characterization and evaluation of groundwater suitability for domestic and agricultural utility in semi-arid region of Basara, Telangana State, South India. *Applied Water Science*, 8(1): 44.
- Adler, R. and Rascher, J. 2007. A strategy for the management of acid mine drainage from gold mines in Gauteng. *Contract Report for Thutuka (Pty) Ltd*. Submitted by the Water

Resource Governance Systems Research Group. Pretoria: CSIR. Report No. CSIR/NRE/PW/ER/2007/0053/C.

Adler, R. A., Claassen, M., Godfrey, L. and Turton, A. R. 2007. Water, mining, and waste: an historical and economic perspective on conflict management in South Africa. *The Economics of Peace and Security Journal*, 2(2): 33-41.

Afolabi Olubukola, O., Olutomilola Olabode, O. and Ishaki Jamil, D. 2018. Assessment of groundwater system characteristics in Ilorin Metropolis, South-Western Nigeria. *American Journal of Water Science and Engineering*, 4(1): 1-8.

Ahmad, R., Begum, S., Zhang, C. C., Karanfil, T., Genceli, E. A., Yadav, A. and Ahmed, S. 2005. Physico-chemical processes. *Water Environment Research*, 77(6): 982-1156.

Al-Mashakbeh, H. M. 2017. The influence of lithostratigraphy on the type and quality of stored water in Mujib Reservoir-Jordan. *Journal of Environmental Protection*, 8(04): 568.

Ali, A., Wahid, F. and Guo, D. 2019. Bio-processing of mining solid waste and resource recovery. *Biological Processing of Solid Waste*, 169.

Alpers, C. N., Jambor, J. L. and Nordstrom, D. 2018. Sulfate minerals: crystallography, geochemistry, and environmental significance, Washington, DC: Walter de Gruyter GmbH and Co KG.

Aly, A. A., Al-Omran, A. M. and Alharby, M. M. 2015. The water quality index and hydrochemical characterization of groundwater resources in Hafar Albatin, Saudi Arabia. *Arabian Journal of Geosciences*, 8(6): 4177-4190.

Amponsah-Dacosta, M. and Reid, D. L. 2014. Mineralogical characterization of selected South African mine tailings for the purpose of mineral carbonation. *Annual International Mine Water Association Conference-An Interdisciplinary Response to Mine Water Challenges*, Xuzhou, China.

Antivachis, D. N., Chatzitheodoridis, E., Skarpelis, N. and Komnitsas, K. 2017. Secondary sulphate minerals in a Cyprus-type ore deposit, Apliki, Cyprus: Mineralogy and its implications regarding the chemistry of pit lake waters. *Mine Water and the Environment*, 36(2): 226-238.

Antonijević, M., Dimitrijević, M., Stevanović, Z., Serbula, S. M. and Bogdanovic, G. D. 2008. Investigation of the possibility of copper recovery from the flotation tailings by acid leaching. *Journal of Hazardous Materials*, 158(1): 23 - 34.

APHA 1915. American Public Health Association: Standard methods for the examination of water and wastewater (Vol. 2). Washington DC, USA.

APHA 2005. American Public Health Association: Standard methods for the examination of water and wastewater. Washington DC, USA.

Appelo, C. A. J. and Postma, D. 2004. Geochemistry, groundwater and pollution, Netherlands: CRC press.

- ArcGIS, 2017. Average household size in South Africa <https://www.arcgis.com/home/item.html?id=582208ecec2424ab6e387d9cdcf01e3> [Accessed 11 November 2018].
- Arocena, J. M., Van Mourik, J. M., Schilder, M. L. and Faz Cano, A. 2010. Initial soil development under pioneer plant species in metal mine waste deposits. *Restoration Ecology*, 18: 244- 252.
- Asensio, V., Vega, F. A., Singh, B. R. and Covelo, E. F. 2013. Effects of tree vegetation and waste amendments on the fractionation of Cr, Cu, Ni, Pb and Zn in polluted mine soils. *Science of the Total Environment*, 443: 446-453.
- Aslam, R. A., Shrestha, S. and Pandey, V. P. 2018. Groundwater vulnerability to climate change: a review of the assessment methodology. *Science of the Total Environment*, 612: 853- 875.
- ASTM, 1996. American Society for Testing and Materials: D5744-96 standard test method for accelerated weathering of solid materials using modified humidity cell. West Conshohocken, Pennsylvania.
- ASTM, 2006. American Society for Testing and Materials: C136-06 standard test method for sieve analysis of fine and coarse aggregates. West Conshohocken, Pennsylvania.
- ASTM, 2013. American Society for Testing and Materials: D5744-13, Standard test method for laboratory weathering of solid materials using a humidity cell. West Conshohocken, Pennsylvania.
- Avigliano, E. and Schenone, N. F. 2015. Human health risk assessment and environmental distribution of trace elements, glyphosate, fecal coliform and total coliform in Atlantic rainforest mountain rivers (South America). *Microchemical Journal*, 122: 149-158.
- Awadh, S. M., Abdulhusein, F. M. and Al-Kilabi, J. A. 2016. Hydrogeochemical processes and water-rock interaction of groundwater in Al-Dammam aquifer at Bahr Al-Najaf, Central Iraq. *Iraqi Bulletin of Geology and Mining*, 12(1): 1-15.
- Ayob, S. and Gupta, A. K. 2006. Fluoride in drinking water: a review on the status and stress effects. *Critical Reviews in Environmental Science and Technology*, 36(6): 433-487.
- Back, W. 1960. Hydrochemical facies and ground-water flow patterns in Northern Atlantic Coastal Plain. *AAPG Bulletin*, 44(7): 1244-1245.
- Bäcklund, A.K. 2009. Impact assessment in the European Commission-a system with multiple objectives. *Environmental Science and Policy*, 12: 1077-1087.
- Ball, J.W., Nordstrom, D.K., McCleskey, R.B. and To, T.B. 1999, March. A new method for the direct determination of dissolved Fe (III) concentration in acid mine waters. *US Geological Survey Toxic Substances Hydrology Program-Proceedings of the Technical Meeting, Charleston*, 297-304.
- Banerjee, D. 2014. Acid drainage potential from coal mine wastes: Environmental assessment through static and kinetic tests. *International Journal of Environmental Science and Technology*, 11(5): 1365-1378.

- Barnes, S. J., Cruden, A. R., Arndt, N. and Saumur, B. M. 2016. The mineral system approach applied to magmatic Ni-Cu-PGE sulphide deposits. *Ore Geology Reviews*, 76: 296- 316.
- Barney, G.O., 1980. The global 2000 report to the President--entering the twenty-first century: a report (Vol. 2). US Government Printing Office.
- Barrer, R. M. 2012. South Kensington, London SW7 2AY. Surface Organometallic Chemistry: Molecular Approaches to Surface Catalysis. Boston, London: Kluwer Academic Publishers.
- Basset, J.M., Gates, B.C., Candy, J.P., Choplin, A., Leconte, M., Quignard, F. and Santini, C. eds. 2012. Surface Organometallic Chemistry: Molecular Approaches to Surface Catalysis (Vol. 231). Springer Science and Business Media.
- Beale, C. 1985. Copper in South Africa-Part 1. *Journal of the Southern African Institute of Mining and Metallurgy*, 85(3): 73 - 80.
- Beauford, R. 2012. *Rare earth element minerals and ores*. Available: [http://rareearthelements.us/mineral\\_ores](http://rareearthelements.us/mineral_ores) [Accessed 13 August 2019].
- Beckhoff, B., Kanngießler, B., Langhoff, N., Wedell, R. and Wolff, H. 2007. Handbook of practical X-ray fluorescence analysis, Heidelberg: Springer Science and Business Media.
- Beech, I. B. and Sunner, J. 2004. Biocorrosion: towards understanding interactions between biofilms and metals. *Current Opinion in Biotechnology*, 15(3): 181-186.
- Behera, S. K., Mishra, D. P., Ghosh, C. N., Prashant, Mandal, P. K., Singh, K. M. P., Buragohain, J. and Singh, P. K. 2019. Characterization of lead-zinc mill tailings, fly ash and their mixtures for paste backfilling in underground metalliferous mines. *Environmental Earth Sciences*, 78(14): 394.
- Bell, F., De Bruyn, I. and Stacey, T. 2002. Some examples of the impact of metalliferous mining on the environment: A South African perspective. *Bulletin of Engineering Geology and the Environment*, 61(1): 1-20.
- Benzaazoua, M., Bussière, B., Dagenais, A.-M. and Archambault, M. 2004. Kinetic tests comparison and interpretation for prediction of the Joutel tailings acid generation potential. *Environmental Geology*, 46(8): 1086 - 1101.
- Berry, D., Xi, C. and Raskin, L. 2006. Microbial ecology of drinking water distribution systems. *Current Opinion in Biotechnology*, 17(3): 297-302.
- Bini, C., Wahsha, M. and Spiandorello, M. 2014. Land contamination and soil evolution in abandoned mine areas (Italy). EGUGA, 2379.
- Bizzi, L. A. 2017. Diamond exploration: Fundamentals and opportunities in South America. *Revista Brasileira de Geociências*, 31(4): 631-634.
- Blowes, D., Ptacek, C., Jambor, J. and Weisener, C. 2003. The geochemistry of acid mine drainage. *Environmental Geochemistry*, 9:149-204.

- Blowes, D.W., Ptacek, C.J., Jambor, J.L., Weisener, C.G., Paktunc, D., Gould, W.D. and Johnson, D.B. 2014. 11.5-the geochemistry of acid mine drainage. *Treatise on Geochemistry*, 131-190. Oxford: Elsevier
- Blowes, D. W., Ptacek, C. J., Jambor, J. L., Vaughan, D. and Wogelius, R. 2013. Mineralogy of mine wastes and strategies for remediation, Jena, Germany: European Mineralogical Union.
- Blowes, D.W., Ptacek, C.J. and Jambor, J.O.H.N.L. 2013. Mineralogy of mine wastes and strategies for remediation. *Environmental Mineralogy; Vaughan, DJ, Wogelius, RA, Eds.; European Mineralogical Union: Jena, Germany*, 13: 295-338.
- Bosire, G.O., Ngila, J.C. and Nkambule, T.T. 2018. Geochemical scaling potential simulations of natural organic matter complexation with metal ions in cooling water at Eskom power generation plants in South Africa. *Water SA*, 44(4): 706-718.
- Braune, E. and Xu, Y. 2010. The role of ground water in Sub-Saharan Africa. *Groundwater*, 48(2): 229-238.
- Bredenhann, L. and Braune, E. 2000. Department of Water Affairs and Forestry. Policy and strategy for groundwater quality management in South Africa, Pretoria.
- Brenzinger, M. 2008. The twelve modern Khoisan languages. Khoisan languages and linguistics. *Proceedings of the 3rd International Symposium, Riezlern/Kleinwalsertal*.
- Brindha, K., Pavelic, P., Sotoukee, T., Douangsavanh, S. and Elango, L. 2017. Geochemical characteristics and groundwater quality in the Vientiane Plain, Laos. *Exposure and Health*, 9(2): 89-104.
- Bruneel, O., Mghazli, N., Sbabou, L., Héry, M., Casiot, C. and Filali-Maltouf, A. 2019. Role of microorganisms in rehabilitation of mining sites, focus on Sub-Saharan African countries. *Journal of Geochemical Exploration*, 205: 06327.
- Cairncross, B. 2004. History of the O'Kiep copper district Namaqualand, Northern Cape Province South Africa. *Mineralogical Record*, 35(4): 289.
- Campbell, I. C. and Beardall, J. 2019. Ok Tedi copper mine, Papua New Guinea, stimulates algal growth in the Fly River. *Sustainable Water Resources Management*, 5(2): 425-437.
- Camper, A. K. 2004. Involvement of humic substances in regrowth. *International Journal of Food Microbiology*, 92(3): 355-364.
- Chabukdhara, M., Gupta, S. K., Kotecha, Y. and Nema, A. K. 2017. Groundwater quality in Ghaziabad district, Uttar Pradesh, India: Multivariate and health risk assessment. *Chemosphere*, 179: 167-178.
- Chakraborti, D., Rahman, M. M., Ahamed, S., Dutta, R. N., Pati, S. and Mukherjee, S. C. 2016. Arsenic contamination of groundwater and its induced health effects in Shahpur block, Bhojpur district, Bihar state, India: risk evaluation. *Environmental Science and Pollution Research*, 23(10): 9492-9504.

- Chandrawat, M., Sunita, K. and Yadav, R. 2005. A fluorosis survey and defluoridation of drinking water by calcium oxide. *Fluoride*, 38(3): 258.
- Chaturvedi, N., Dhal, N. and Reddy, P. S. R. 2012. Comparative phytoremediation potential of *Calophyllum inophyllum* L., *Bixa orellana* L. and *Schleichera oleosa* (Lour.) Oken on iron ore tailings. *International Journal of Mining, Reclamation and Environment*, 26(2): 104- 118.
- Chen, T., Wong, J., Zhou, H. and Wong, M. 1997. Assessment of trace metal distribution and contamination in surface soils of Hong Kong. *Environmental Pollution*, 96(1): 61-68.
- Cheng, H., Hu, Y., Luo, J., Xu, B. and Zhao, J. 2009. Geochemical processes controlling fate and transport of arsenic in acid mine drainage (AMD) and natural systems. *Journal of Hazardous Materials*, 165(1-3): 3-26.
- Chidambaram, S., Anandhan, P., Prasanna, M., Ramanathan, A., Srinivasamoorthy, K. and Kumar, G. S. 2012. Hydrogeochemical modelling for groundwater in Neyveli aquifer, Tamil Nadu, India, using PHREEQC: a case study. *Natural Resources Research*, 21(3): 11-324.
- Cho, B. W. and Choo, C. O. 2019. Geochemical behavior of uranium and radon in groundwater of Jurassic granite area, Icheon, Middle Korea. *Water*, 11(6): 1278.
- Clarke, C. E., le Roux, S. G. and Roychoudhury, A. N. 2014. The role of evaporation on the formation of secondary Cu-hydroxy minerals in the arid Namaqualand soil system of South Africa. *Applied Geochemistry*, 47: 52-60.
- Claveria, R. J. R., Perez, T. R., Perez, R. E. C., Algo, J. L. C. and Robles, P. Q. 2019. The identification of indigenous Cu and As metallophytes in the Lepanto Cu-Au Mine, Luzon, Philippines. *Environmental Monitoring and Assessment*, 191(3): 185.
- Clifford, T. N. and Barton, E. S. 2012. The O'okiep Copper District, Namaqualand, South Africa: a review of the geology with emphasis on the petrogenesis of the cupriferous Koperberg Suite. *Mineralium Deposita*, 47(8): 837-857.
- Cobbing, J. 2008. Institutional linkages and acid mine drainage: the case of the Western Basin in South Africa. *Water Resources Development*, 24(3): 451-462.
- Coetzee, H., Hobbs, P.J., Burgess, J.E., Thomas, A., Keet, M., Yibas, B., Van Tonder, D., Netili, F., Rust, V., Wade, P. and Maree, J. 2010. Mine water management in the Witwatersrand Gold Fields with special emphasis on acid mine drainage. Report to the inter-ministerial committee on acid mine drainage, 1-128.
- Compton, J.S., White, R.A. and Smith, M. 2003. Rare earth element behavior in soils and salt pan sediments of a semi-arid granitic terrain in the Western Cape, South Africa. *Chemical Geology*, 201(3-4): 239-255.
- Constantine, K., Massoud, M., Alameddine, I. and El-Fadel, M. 2017. The role of the water tankers market in water stressed semi-arid urban areas: Implications on water quality and economic burden. *Journal of Environmental Management*, 188: 85-94.
- Constitution of the Republic of South Africa, 1996. Constitution of the Republic of South Africa, no. 108 of 1996. Government Printer, South Africa.

- Cowling, R. 2015. Namaqualand: a succulent desert. Penguin Random House, South Africa.
- Cox, D. R. and Snell, E. J. 1989. Analysis of binary data, London: CRC Press.
- Cruz-Hernández, P., Pérez-López, R., Parviainen, A., Lindsay, M. B. and Nieto, J. M. 2016. Trace element-mineral associations in modern and ancient iron terraces in acid drainage environments. *Catena*, 147: 386-393.
- Cruz, R., Bertrand, V., Monroy, M. and González, I. 2001. Effect of sulfide impurities on the reactivity of pyrite and pyritic concentrates: a multi-tool approach. *Applied Geochemistry*, 16(7-8): 803-819.
- Das, N., Pattanaik, P. and Das, R. 2005. Defluoridation of drinking water using activated titanium rich bauxite. *Journal of Colloid and Interface Science*, 292(1): 1-10.
- Das, S. and Adhicari, P. 2017. Lichen striatus in children: A clinical study of ten cases with review of literature. *Indian Journal of Paediatric Dermatology*, 18(2): 89.
- De-Bashan, L. E., Hernandez, J.-P., Nelson, K. N., Bashan, Y. and Maier, R. M. 2010. Growth of quailbush in acidic, metalliferous desert mine tailings: Effect of *Azospirillum brasilense* Sp6 on biomass production and rhizosphere community structure. *Microbial ecology*, 60(4): 915-927.
- de Miranda, F. S., da Silva, J. d. J. B., Mota, L. H. S., da Silva Santos, R., Issa, Amor, A. L., Moreno, U. and da Silva, I. d. M. M. 2018. Quality of water for human consumption in a rural area community from Brazil. *African Journal of Microbiology Research*, 12(29): 688- 696.
- de Souza, E. S., Dias, Y. N., da Costa, H. S. C., Pinto, D. A., de Oliveira, D. M., de Souza Falção, N. P., Teixeira, R. A. and Fernandes, A. R. 2019. Organic residues and biochar to immobilize potentially toxic elements in soil from a gold mine in the Amazon. *Ecotoxicology and Environmental Safety*, 169: 425-434.
- Delpla, I., Jung, A.-V., Baures, E., Clement, M. and Thomas, O. 2009. Impacts of climate change on surface water quality in relation to drinking water production. *Environment International*, 35(8): 1225-1233.
- Derkics, D. 1985. Report to congress: wastes from the extraction and beneficiation of metallic ores, phosphate rock, asbestos, overburden from uranium mining, and oil shale. Report No. PB-88-162631/XAB; EPA-530/SW-85/033. Environmental Protection Agency, Washington, DC (USA): Office of Solid Waste.
- Dickschat, J. S., Nawrath, T., Thiel, V., Kunze, B., Müller, R. and Schulz, S. 2007. Biosynthesis of the Off-Flavor 2-Methylisoborneol by the Myxobacterium *Nannocystis exedens*. *Angewandte Chemie International Edition*, 46(43): 8287-8290.
- Diehl, S.F., Hageman, P.L. and Smith, K.S. 2006. What's weathering? Mineralogy and field leach studies in mine waste, Leadville and Montezuma mining districts, Colorado. *Proceedings of the Seventh International Conference on Acid Rock Drainage (ICARD 7)*. St. Louis, Missouri.
- Diehl, S.F., Smith, K.S., Desborough, G.A., Goldhaber, M.B. and Fey, D.L. 2003. Trace-metal sources and their release from mine wastes: examples from humidity cell tests of hard-

rock mine waste and from Warrior Basin coal. In *Working Together for Innovative Reclamation: Proceedings of a Joint Conference of the 9th Billings Land Reclamation Symposium and the 20th Annual Meetings of the American Society of Mining and Reclamation*. Lexington, KY.

Dold, B. 2014a. Evolution of acid mine drainage formation in sulphidic mine tailings. *Minerals*, 4(3): 621-641.

Dold, B. 2014b. Mineralogical and geochemical controls in biomining and bioremediation. *Geomicrobiology and Biogeochemistry*. Berlin, Heidelberg: Springer

Domenico, P.A. and Schwartz, F.W., 1998. Physical and chemical hydrogeology (Vol. 506). New York: Wiley.

Dudka, S. and Adriano, D. C. 1997. Environmental impacts of metal ore mining and processing: a review. *Journal of Environmental Quality*, 26(3): 590-602.

Durov, S. 1948. Natural waters and graphic representation of their composition. *Dokl Akad Nauk SSSR*, 59(3): 87-90.

DWA, 2004. Department of Water Affairs: Integrated water resource management strategies, guidelines and pilot implementation in three water management areas. Government Gazzette, Pretoria.

DWA, 2009. Department of Water and Environmental Affairs: Development of an integrated water quality management strategy for the upper and lower Orange water management areas, Desktop Catchment Assessment Study: Lower Orange Water Management Area (WMA 14). Report No. 2.2 (P RSA D000/00/7909/3). Available t: [http://www.dwaf.gov.za/dir\\_wqm/docs/desktopcatchmentassessmentlowerorangereport2\\_2.pdf](http://www.dwaf.gov.za/dir_wqm/docs/desktopcatchmentassessmentlowerorangereport2_2.pdf) [Accessed 01 June 2017].

DWA, 2010. Department of Water Affairs: Mine Water Management in the Witwatersrand Gold Fields with Special Emphasis on Acid Mine Drainage. Report to the Inter-Ministerial Committee on Acid Mine Drainage. Available: <http://www.dwaf.gov.za/Documents/ACIDReport.pdf> [Accessed 19 August 2019].

DWA 2012. Department of Water Affairs: The annual national state of water resources report 2011/12. <http://www.dwa.gov.za/groundwater/documents/201112%20Annual%20National%20State%20of%20Water%20Resources%20report.pdf> [Accessed on 10 August 2019].

DWAF, 1996. Department of Water Affairs and Forestry: South African Water Quality Guidelines. Volume 7: Aquatic Ecosystems. *Domestic Water Use*, 1: 86-87. Pretoria, South Africa.

DWAF 2008. Department of Water Affairs and Forestry: A Guideline for the assessment, planning and management of groundwater resources in South Africa. Pretoria.

DWAF, 2009a. Department of Water Affairs and Forestry: South Africa Blue Drop Report, Pretoria, South Africa. Available at: <http://www.dwa.gov.za/Documents/BD2012/Intro.pdf> [Accessed 15 November 2018].

DWAF, 2009b. South Africa Green Drop Report, Department of Water Affairs, Pretoria, South Africa, 2009. Available : <http://www.dwa.gov.za/Documents/GDR2009/Intro.pdf>

- [dwa.gov.za/Documents/Executive%20Summary%20for%20the%202013%20Green%20Drop%20Report.pdf](http://dwa.gov.za/Documents/Executive%20Summary%20for%20the%202013%20Green%20Drop%20Report.pdf) [Accessed 15 November 2018].
- Earle, S. 2016. Physical geology, Campus Manitoba. Campus Manitoba. Available: <https://openlibrary-repo.ecampusontario.ca/jspui/handle/123456789/402> [Accessed 21 October 2019].
- Earthworks. 2004. Dirty Metals: Mining Communities and the Environment. Washington DC,: Oxfam America. Available: <https://www.miningresettlement.org/elibrary/dirty-metals-mining-communities-and-the-environment> [Accessed 15 August 2019].
- Edet, A. and Okereke, C. 2002. Delineation of shallow groundwater aquifers in the coastal plain sands of Calabar area (Southern Nigeria) using surface resistivity and hydrogeological data. *Journal of African Earth Sciences*, 35(3): 433-443.
- Edmunds, W. M. and Shand, P. 2009. Natural groundwater quality, United Kingdom, John Wiley and Sons.
- Edokpayi, J. N., Enitan, A. M., Mutileni, N. and Odiyo, J. O. 2018. Evaluation of water quality and human risk assessment due to heavy metals in groundwater around Muledane area of Vhembe District, Limpopo Province, South Africa. *Chemistry Central Journal*, 12(1): 2.
- Egiebor, N. O. and Oni, B. 2007. Acid rock drainage formation and treatment: A review. *Asia-Pacific Journal of Chemical Engineering*, 2(1): 47-62.
- Eglington, B. 2006. Evolution of the Namaqua-Natal Belt, Southern Africa: A geochronological and isotope geochemical review. *Journal of African Earth Sciences*, 46(1-2): 93-111.
- Elghali, A., Benzaazoua, M., Bussière, B. and Genty, T. 2019. Spatial mapping of acidity and geochemical properties of oxidized tailings within the former Fagle/Telbel mine site. *Minerals*, 9(3):180.
- Entwistle, J. A., Hursthouse, A. S., Marinho Reis, P. A. and Stewart, A. G. 2019. Metalliferous mine dust: Human health impacts and the potential determinants of disease in mining communities. *Current Pollution Reports*, 5(3): 67-83.
- EPA, 1985. Environmental Protection Agency: Office of Solid Waste: Wastes from the extraction and beneficiation of metallic ores, phosphate rock, asbestos, overburden from uranium mining, and oil shale, U.S. Environmental Protection Agency Office of Solid Waste, Washington, DC. Available: <https://www.epa.gov/sites/production/files/2016-03/documents/epa-530-sw-85-033.pdf> [Accessed 26 September 2019].
- EPA, 2003. Environmental Protection Agency. Contaminant Candidate List Regulatory Determination Support Document for Sulfate. Washington, DC. Available: [https://www.epa.gov/sites/production/files/201409/documents/support\\_cc1\\_sulfate\\_dwreport.pdf](https://www.epa.gov/sites/production/files/201409/documents/support_cc1_sulfate_dwreport.pdf) [Accessed 27 September 2019].
- EPA 2014 Method 6020B, Rev. 2. Inductively coupled plasma-mass spectrometry. In test methods for evaluating solid waste, physical/chemical methods (SW-846). *Method 6020B* Washington, DC. Available: <https://www.epa.gov/sites/production/files/2015-12/documents/6020b.pdf> [Accessed 12 April 2017].

- Erasmus 2004. *On Route in South Africa*, Jeppestown, Jonathan Ball Publishers. Available: <https://www.namibiana.de/namibia-information/literaturauszuege/titel/on-route-in-south-africa-bpj-erasmus-9781868420254.html> [Accessed 04 April 2017].
- Erdogan, I.G., Fosso-Kankeu, E., Ntwampe, S.K.O., Waanders, F.B., Hoth, N. and Rand, A., 2019. Groundwater as an alternative source to irregular surface water in the O'Kiep area, Namaqualand, South Africa. *Physics and Chemistry of the Earth, Parts A/B/C* (114):102801.
- Erguler, G. K. and Erguler, Z. A. 2019. Hydro-geochemical behavior of acid formation of sulfide bearing rocks based on kinetic column tests. *Recent Advances in Geo-Environmental Engineering, Geomechanics and Geotechnics, and Geohazards*, 21-23. Springer.
- Erguler, Z. A. and Erguler, G. K. 2015. The effect of particle size on acid mine drainage generation: Kinetic column tests. *Minerals Engineering*, 76: 154-167.
- Espana, J. S., Pamo, E. L., Santofimia, E., Aduvire, O., Reyes, J. and Baretino, D. 2005. Acid mine drainage in the Iberian Pyrite Belt (Odiel river watershed, Huelva, SW Spain): geochemistry, mineralogy and environmental implications. *Applied Geochemistry*, 20(7): 1320-1356.
- European Commission, 2009. Commission Decision 2009/337/EC of 20 April 2009 on the Definition of the Criteria for the Classification of Waste Facilities in Accordance with Annex III of Directive 2006/21/EC of the European Parliament and of the Council Concerning the Management of Waste from Extractive Industries. OJ L102.
- Faris, N., Ram, R., Chen, M., Tardio, J., Pownceby, M. I., Jones, L. A., McMaster, S., Webster, N. A. and Bhargava, S. 2017. The effect of thermal pre-treatment on the dissolution of chalcopyrite (CuFeS<sub>2</sub>) in sulfuric acid media. *Hydrometallurgy*, 169: 68-78.
- Farjana, S. H., Huda, N., Mahmud, M. P. and Saidur, R. 2019. A review on impact of mining and mineral processing Industries through Life cycle assessment. *Journal of Cleaner Production*. 231: 1200-1217.
- Feng, J., Tian, H., Huang, Y., Ding, Z. and Yin, Z. 2019. Pyrite oxidation mechanism in aqueous medium. *Journal of the Chinese Chemical Society*, 66(4): 345-354.
- Ferguson, K. and Erickson, P. 1988. Pre-mine prediction of acid mine drainage. Environmental Management of Solid Waste. Berlin, Heidelberg: Springer.
- Ferguson, R.B., Hergert, G.W., Shapiro, C.A. and Wortmann, C.S. 2007. Guidelines for soil sampling. *NebGuide G1740*, University of Nebraska–Lincoln, USA.
- Feris, L. and Kotzé, L. J. 2014. The regulation of acid mine drainage in South Africa: Law and governance perspectives. *Potchefstroom Electronic Law Journal*, 17(5): 2105-2163.
- Ferreira, S., Meyer, S. and Vivier., J. 2015. Department of Environmental Affairs: Environmental impact assessment RVM 1 Hydroelectric Power (Pty) Ltd. Riemvasmaak Hydropower Project, DEA Reference Number: 14/12/16/3/3/2/600 Orange River, Northern Cape Province, Pretoria, South Africa.

- Festin, E. S., Tigabu, M., Chileshe, M. N., Syampungani, S. and Odén, P. C. 2019. Progresses in restoration of post-mining landscape in Africa. *Journal of Forestry Research*, 30(2): 381-396.
- Fey, M.V. 2010, August. A short guide to the soils of South Africa, their distribution and correlation with World Reference Base soil groups. *Proceedings* 19: 32-35.
- Fisher, R.S. and Mullican III, W.F., 1997. Hydrochemical evolution of sodium-sulfate and sodium-chloride groundwater beneath the northern Chihuahuan Desert, Trans-Pecos, Texas, USA. *Hydrogeology Journal*, 5(2): 4-16.
- Fitzpatrick, R. and Shand, P. 2008. Inland acid sulfate soils: Overview and conceptual models. Inland acid sulfate soil systems across Australia. Perth, Australia: CRC LEME.
- Fosso-Kankeu, E. 2016. Investigation of the oxidation rate of sediments from AMD using humidity cell test. In *International Conference on Advances in Science, Engineering, Technology and Natural Resources (ICASETNR-16)*, Parys, South Africa.
- Fosso-Kankeu, E., Waanders, F. and Botes, W. 2015. Recovery of base metals from mine tailings dumps collected in the vicinity of Potchefstroom: leaching assisted by complexing agent. *7th International Conference on Latest Trends in Engineering and Technology (ICLTET'2015)*. Pretoria, South Africa.
- Fosso-Kankeu, E., Manyatshe, A. and Waanders, F. 2017. Mobility potential of metals in acid mine drainage occurring in the Highveld area of Mpumalanga Province in South Africa: Implication of sediments and efflorescent crusts. *International Biodeterioration and Biodegradation*, 119: 661-670.
- Fosso-Kankeu, E., Kaitano, R., Waanders, F. and Mulaba-Bafubiandi, A. 2014. Soil quality in the basin of mine effluents and the potential of alleviation of metal dispersion. *An Interdisciplinary Response to Mine Water Challenges*. University of Mining and Technology Press, Xuzhou. China.
- Fosso-Kankeu, E., Manyatshe, A., Munyai, A. and Waanders, F. 2016. AMD formation and dispersion of inorganic pollutants along the main stream in a mining area. *Mining Meets Water- Conflicts and Solutions, (IMWA2016)*. Freiberg/Germany.
- Fosso-Kankeu, E., Olivier, C., Moyakhe, D., Barlow, B., Campbell, Q. and Waanders, F. 2018. Effect of Fine Coal Tailing Porosity on the Mobility and Speciation of Heavy Metals in the Leachates *10th Int'l Conference on Advances in Science, Engineering, Technology and Healthcare (ASETH-18)*. Cape Town, South Africa.
- Funke, N. and Jacobs, I. 2011. Integration challenges of water and land reform: A critical review of South Africa. *Current issues of water management*, 81-106. Croatia: InTech.
- Gadd, G. 2008. Transformation and mobilization of metals, metalloids, and radionuclides by microorganisms. *Biophysico-chemical processes of heavy metals and metalloids in soil environments*, 1: 53-96. Hoboken, New Jersey: Wiley-Jupac Series.
- Galaitzi, S., Russell, R., Bishara, A., Durant, J. L., Bogle, J. and Huber-Lee, A. 2016. Intermittent domestic water supply: A critical review and analysis of causal-consequential pathways. *Water*, 8(7): 274.

- Galanopoulos, E., Skarpelis, N. and Argyraki, A. 2019. Supergene alteration, environmental impact and laboratory scale acid water treatment of Cyprus-type ore deposits: case study of Mathiatis and Sha abandoned mines. *Geochemistry: Exploration, Environment, Analysis*, 19(4): 299-315.
- Gałuszka, A., Migaszewski, Z. M., Dołęgowska, S., Michalik, A. and Duczmal-Czernikiewicz, A. 2015. Geochemical background of potentially toxic trace elements in soils of the historic copper mining area: a case study from Miedzianka Mt., Holy Cross Mountains, south-central Poland. *Environmental Earth Sciences*, 74(6): 4589-4605.
- Gandy, C., Younger, P. and Lindsay, P. 2009. Modelling waste rock leaching at an opencast coal mine in New Zealand: The effects of mineral grain size on long-term contamination. *Journal of Environmental Geology*.
- García-Giménez, R. and Jiménez-Ballesta, R. 2017. Mine tailings influencing soil contamination by potentially toxic elements. *Environmental Earth Sciences*, 76(1): 51.
- García-Lorenzo, M., Pérez-Sirvent, C., Martínez-Sánchez, M. and Molina-Ruiz, J. 2012. Trace elements contamination in an abandoned mining site in a semiarid zone. *Journal of Geochemical Exploration*, 113: 23-35.
- Gargiulo, L., Mele, G. and Terribile, F. 2016. Effect of rock fragments on soil porosity: a laboratory experiment with two physically degraded soils. *European Journal of Soil Science*, 67(5): 597-604.
- Gibbs, R. J. 1970. Mechanisms controlling world water chemistry. *Science*, 170(3962): 1088- 1090.
- Gibs, J. and Wilde, F. D. 2007. Use of multiparameter instruments for routine field measurements (ver. 1.0). *U.S. Geological Survey Techniques of Water-Resources Investigations*. Washington, DC: U.S. Geological Survey.
- Gibs, J. and Wilde, F. D. 2020. Use of Multiparameter 6.8 instrument for routine field measurements. Washington, DC: U.S. Geological Survey.
- Gibson, R., Robb, L., Kisters, A. and Cawthorn, R. 1996. Regional setting and geological evolution of the Okiep Copper District, Namaqualand, South Africa. *South African Journal of Geology*, 99(2), 107-120.
- Giri, S., Singh, A. K. and Mahato, M. K. 2017. Metal contamination of agricultural soils in the copper mining areas of Singhbhum shear zone in India. *Journal of Earth System Science*, 126(4): 1-13.
- Gitari, M., Akinyemi, S., Ramugondo, L., Matidza, M. and Mhlongo, S. 2018. Geochemical fractionation of metals and metalloids in tailings and appraisal of environmental pollution in the abandoned Musina Copper Mine, South Africa. *Environmental Geochemistry and Health*, 40(6): 2421-2439.
- Gleisner, M. and Herbert Jr, R. B. 2002. Sulfide mineral oxidation in freshly processed tailings: Batch experiments. *Journal of Geochemical Exploration*, 76(3): 139-153.
- Godfrey, L. K., Oelofse, S. H., Phiri, A., Nahman, A. and Hall, J. 2007. Mineral waste: The required governance environment to enable re-use. Pretoria: CSIR.

- Goncharuk, V., Bagrii, V., Mel'nik, L., Chebotareva, R. and Bashtan, S. Y. 2010. The use of redox potential in water treatment processes. *Journal of Water Chemistry and Technology*, 32(1): 1-9.
- Govett, G. J. S. 2013. *Rock Geochemistry in Mineral Exploration*. Amsterdam: Elsevier.
- Gregorich, E. G. and Carter, M. R. 2007. *Soil sampling and methods of analysis*, Washington, DC: CRC Press.
- Güler, C., Thyne, G. D., McCray, J. E. and Turner, K. A. 2002. Evaluation of graphical and multivariate statistical methods for classification of water chemistry data. *Hydrogeology Journal*, 10(4): 455-474.
- Guo, Q., Wang, Y., Ma, T. and Ma, R. 2007. Geochemical processes controlling the elevated fluoride concentrations in groundwaters of the Taiyuan Basin, Northern China. *Journal of Geochemical Exploration*, 93(1): 1-12.
- Guseva, O., Opitz, A. K., Broadhurst, J. L., Harrison, S. T., Bradshaw, D. J. and Becker, M. 2018. Fe-sulfide liberation and association as a proxy for the Interpretation of acid rock drainage (ARD) test results. *11th ICARD, IMWA, MWD Conference - "Risk to Opportunity"*. Pretoria, South Africa.
- Hakkou, R., Benzaazoua, M. and Bussière, B. 2008. Acid mine drainage at the abandoned Kettara mine (Morocco): Environmental characterization. *Mine Water and the Environment*, 27(3): 145-159.
- Hangone, G., Bradshaw, D. and Ekmekci, Z. 2005. Flotation of a copper sulphide ore from Okiep using thiol collectors and their mixtures. *Journal of the South African Institute of Mining and Metallurgy*, 105(3): 199-206.
- Harilal, C., Hashim, A., Arun, P. and Baji, S. 2004. Hydrogeochemistry of two rivers of Kerala with special reference to drinking water quality. *Ecology Environment and Conversation*, 10: 187-192.
- Hattingh, J. and Van Deventer, P. W. 2004. *The Effect of the Chemical Properties of Tailings and Water Application on the Establishment of a Vegetative Cover on Gold Tailings Dams*: Pretoria: Water Research Commission. Report No. 899/1/04.
- Heikkinen, P., Räisänen, M. and Johnson, R. 2009. Geochemical characterisation of seepage and drainage water quality from two sulphide mine tailings impoundments: acid mine drainage versus neutral mine drainage. *Mine Water the Environment*, 28(1): 30-49.
- Heikkinen, P. M. and Räisänen, M. L. 2008. Mineralogical and geochemical alteration of Hitura sulphide mine tailings with emphasis on nickel mobility and retention. *Journal of Geochemical Exploration*, 97(1): 1-20.
- Helsen, S., Rommens, T., De Ridder, A., Panayiotou, C. and Colpaert, J. 2009. Remediation and rehabilitation of abandoned mining sites in Cyprus. *EGU General Assembly Conference Abstracts*. Vienna, Austria.
- Heviankova, S., Bestova, I., Kyncl, M., Simková, L. and Zechner, M. 2013. Calcium carbonate as an agent in acid mine water neutralization. *Inżynieria Mineralna*, 14.

- Hitch, M., Ballantyne, S. M. and Hindle, S. R. 2010. Revaluing mine waste rock for carbon capture and storage. *International Journal of Mining, Reclamation and Environment*, 24(1): 64-79.
- Hobbs, P.J. and Cobbing, J.E., 2007. The hydrogeology of the Krugersdorp Game Reserve area and implications for the management of mine water decant. *Proceedings of the Groundwater Conference*. Bloemfontein, South Africa.
- Hohne, S. and Hansen, R. 2008. Preliminary conceptual geo-environmental model of the abandoned copper mines of the Okiep Copper District, Namaqualand, Northern Cape. Council for Geoscience.
- Holmes, S. 1995. South African water quality guidelines. Department of Water Affairs and Forestry. Pretoria.
- Hu, L., Wu, H., Zhang, L., Zhang, P. and Wen, Q. 2017. Geotechnical properties of mine tailings. *Journal of Materials in Civil Engineering*, 29(2): 04016220.
- Huang, X., Deng, H., Zheng, C. and Cao, G. 2016. Hydrogeochemical signatures and evolution of groundwater impacted by the Bayan Obo tailing pond in northwest China. *Science of the Total Environment*, 543: 357-372.
- Hudson-Edwards, K. and Dold, B. 2015. Mine waste characterization, management and remediation. *Minerals*, 5: 82-85.
- Hutt, N. M. and Morin, K. A. 1999. The international static database (ISD). *Proceedings of Mining and the Environment II, Sudbury'99 Conference*. Ontario, Canada.
- Imran, S. A., Dietz, J. D., Mutoti, G., Xiao, W., Taylor, J. S. and Desai, V. 2006. Optimizing source water blends for corrosion and residual control in distribution systems. *Journal of American Water Works Association*, 98(5): 107-115.
- Indelicato, S., Orecchio, S., Avellone, G., Bellomo, S., Ceraulo, L., Di Leonardo, R., Di Stefano, V., Favara, R., Candela, E. G. and La Pica, L. 2017. Effect of solid waste landfill organic pollutants on groundwater in three areas of Sicily (Italy) characterized by different vulnerability. *Environmental Science and Pollution Research*, 24(20): 16869-16882.
- Ippolito, J. A., Cui, L., Novak, J. and Johnson, M. G. 2019. Biochar for Mine-land Reclamation. *Biochar from Biomass and Waste*. Amsterdam, Netherlands: Elsevier.
- Issaad, M., Boutaleb, A., Kolli, O., Edahbi, M., Benzaazoua, M. and Hakkou, R. 2019. Environmental characterization of mine waste at the Pb–Zn Sidi Kamber abandoned mine (NE Algeria). *Rendiconti Lincei. Scienze Fisiche e Naturali*, 30(2): 427-441.
- Iwatsuki, T., Furue, R., Mie, H., Ioka, S. and Mizuno, T. 2005. Hydrochemical baseline condition of groundwater at the Mizunami underground research laboratory (MIU). *Applied Geochemistry*, 20(12): 2283-2302.
- James, C. N., Copeland, R. C. and Lytle, D. 2004. Relationships between oxidation-reduction potential, oxidant, and pH in drinking water. *Proceedings AWWA Water Quality Technology Conference*. San Antonio, Texas.

- Jayalakshmi, V., Lakshmi, N. and Singara Charya, M. 2011. Assessment of physico-chemical parameters of water and waste waters in and around Vijayawada. *International journal of research in Pharmaceutical and Biomedical Sciences*, 2: 1040-1046.
- Jeevanandam, M., Kannan, R., Srinivasalu, S. and Rammohan, V. 2007. Hydrogeochemistry and groundwater quality assessment of lower part of the Ponnaiyar River Basin, Cuddalore district, South India. *Environmental Monitoring and Assessment*, 132(1-3): 263-274.
- Jennings, S. R., Blicher, P. S. and Neuman, D. R. 2008. Acid mine drainage and effects on fish health and ecology: A review, Bozeman, Montana: Reclamation Research Group.
- Joardder, M. U., Kumar, C., Brown, R. J. and Karim, M. 2015. A micro-level investigation of the solid displacement method for porosity determination of dried food. *Journal of Food Engineering*, 166: 156-164.
- Jonch-Clausen, T. 2004. "Integrated water resources management (IWRM) and water efficiency plans by 2005": Why, What and How?, 5-4. Sweden: Global Water Partnership Stockholm.
- Jurinak, J. and Tanji, K. 1993. Geochemical factors affecting trace element mobility. *Journal of Irrigation and Drainage Engineering*, 119(5): 848-867.
- Khoeurn, K., Sasaki, A., Tomiyama, S. and Igarashi, T. 2019. Distribution of Zinc, Copper, and Iron in the Tailings Dam of an Abandoned Mine in Shimokawa, Hokkaido, Japan. *Mine Water and the Environment*, 38(1): 119-129.
- Kim, C., Wilson, K. and Rytuba, J. 2011. Particle-size dependence on metal (loid) distributions in mine wastes: Implications for water contamination and human exposure. *Applied Geochemistry*, 26(4): 484-495.
- Kimball, B. E., Rimstidt, J. D. and Brantley, S. L. 2010. Chalcopyrite dissolution rate laws. *Applied Geochemistry*, 25(7): 972-983.
- Kirillov, M. V., Bortnikova, S. B. and Gaskova, O. L. 2016. Authigenic gold formation in the cyanidation tailings of gold–arsenopyrite–quartz ore of Komsomolsk deposit (Kuznetski Alatau, Russia). *Environmental Earth Sciences*, 75: 1-11. Berlin Heidelberg: Springer-Verlag.
- Kogel, J. E., Trivedi, N. C., Barker, J. M. and Krukowski, S. T. 2006. Industrial minerals and rocks: commodities, markets, and uses, Littleton, Colorado: Society for Mining and Exploration Inc.
- Komnitsas, K., Xenidis, A. and Adam, K. 1995. Oxidation of pyrite and arsenopyrite in sulphidic spoils in Lavrion. *Minerals Engineering*, 8(12):1443-1454.
- Komnitsas, K., Kontopoulos, A., Lazar, I. and Cambridge, M. 1998. Risk assessment and proposed remedial actions in coastal tailings disposal sites in Romania. *Minerals Engineering*, 11(12): 1179-1190.
- Konikow, L.F. and Glynn, P.D., 2013. Modeling Groundwater Flow and Quality. In: Selinus O. (eds) *Essentials of Medical Geology*. Dordrecht: Springer.

- Kontopoulos, A., Komnitsas, K., Xenidis, A. and Papassiopi, N. 1995. Environmental characterisation of the sulphidic tailings in Lavrion. *Minerals Engineering*, 8(10): 1209- 1219.
- Koski, R. A. and Munk, L. 2007. Chemical data for rock, sediment, biological, precipitate, and water samples from abandoned copper mines in Prince William Sound, Alaska: US Geological Survey.
- Kossoff, D., Dubbin, W., Alfredsson, M., Edwards, S., Macklin, M. and Hudson-Edwards, K. A. 2014. Mine tailings dams: characteristics, failure, environmental impacts, and remediation. *Applied Geochemistry*, 51: 229-245.
- Krampah, F., Lartey-Young, G., Sanful, P. O., Dawohoso, O. and Asare, A. 2019. Hydrochemistry of surface and groundwater in the vicinity of a mine waste rock dump: Assessing impact of acid rock drainage (ARD). *Journal of Geoscience and Environment Protection*, 7(1): 52- 67.
- Křibek, B., Nyambe, I., Majer, V., Knésl, I., Mihaljevič, M., Ettler, V., Vaněk, A., Penížek, V. and Sracek, O. 2019. Soil contamination near the Kabwe Pb-Zn smelter in Zambia: Environmental impacts and remediation measures proposal. *Journal of Geochemical Exploration*, 197: 159-173.
- Kuhn, K. and Meima, J. A. 2019. Characterization and economic potential of historic tailings from gravity separation: Implications from a mine waste dump (Pb-Ag) in the Harz Mountains Mining District, Germany. *Minerals*, 9(5): 303.
- Kumar, A., Roy, S. S. and Singh, C. K. 2020. Geochemistry and associated human health risk through potential harmful elements (PHEs) in groundwater of the Indus basin, India. *Environmental Earth Sciences*, 79(4): 86.
- Kumar, M., Ramanathan, A., Rao, M. S. and Kumar, B. 2006. Identification and evaluation of hydrogeochemical processes in the groundwater environment of Delhi, India. *Environmental Geology*, 50(7): 1025-1039.
- Kwon, M. J., Yang, J.-S., Lee, S., Lee, G., Ham, B., Boyanov, M. I., Kemner, K. M. and O'Loughlin, E. J. 2015. Geochemical characteristics and microbial community composition in toxic metal-rich sediments contaminated with Au-Ag mine tailings. *Journal of Hazardous Materials*, 296: 147-157.
- Kwong, Y.-T. J. 1993. Prediction and prevention of acid rock drainage from a geological and mineralogical perspective. Canada: MEND Project 1.32.1.
- Langman, J., Moore, M., Ptacek, C., Smith, L., Segó, D. and Blowes, D. 2014. Diavik waste rock project: Evolution of mineral weathering, element release, and acid generation and neutralization during a five-year humidity cell experiment. *Minerals*, 4(2): 257-278.
- Langman, J. B., Blowes, D. W., Veeramani, H., Wilson, D., Smith, L., Segó, D. C. and Paktunc, D. 2015. The mineral and aqueous phase evolution of sulfur and nickel with weathering of pyrrhotite in a low sulfide, granitic waste rock. *Chemical Geology*, 401: 169-179.
- Lapakko, K. A. 2003. Developments in humidity-cell tests and their application. Environmental Aspects of Mine Wastes: Mineralogical Association of Canada Short Course Series, Economic Geology Publishing Company, 147-164.

- Larkins, C., Turunen, K., Mänttari, I., Lahaye, Y., Hendriksson, N., Forsman, P. and Backnäs, S. 2018. Characterization of selected conservative and non-conservative isotopes in mine effluent and impacted surface waters: Implications for tracer applications at the mine-site scale. *Applied Geochemistry*, 91: 1-13.
- Lawrence, R. and Wang, Y. 1996. Determination of neutralization potential for acid rock drainage prediction. *MEND project*, 1(3): 38.
- Lázaro, B. B. 2015. Halloysite and kaolinite: two clay minerals with geological and technological importance. *Revista de la Academia de Ciencias Exactas, Físicas, Químicas y Naturales de Zaragoza* 70: 7-38.
- Lee, E., Ha, K., Ngoc, N. T. M., Surinkum, A., Jayakumar, R., Kim, Y. and Hassan, K. B. 2017. Groundwater status and associated issues in the Mekong-Lancang River Basin: international collaborations to achieve sustainable groundwater resources. *Journal of Groundwater Science and Engineering*, 5(1): 1-13.
- Lee, H., Choi, Y., Suh, J. and Lee, S.-H. 2016. Mapping copper and lead concentrations at abandoned mine areas using element analysis data from ICP–AES and portable XRF instruments: a comparative study. *International Journal of Environmental Research and Public Health*, 13(4): 384.
- Lee, H., Kabir, M., Kwon, P. S., Kim, J. M., Kim, J. G., Hyun, S. H., Rim, Y. T., Bae, M. S., Ryu, E. R. and Jung, M. S. 2009. Contamination assessment of abandoned mines by integrated pollution index in the Han River watershed. *The Open Environmental Pollution and Toxicology Journal*, 1(1).
- Lee, J. Y., Choi, J. C., Yi, M. J., Kim, J. W., Cheon, J. Y., Choi, Y. K., Choi, M. J. and Lee, K. K. 2005. Potential groundwater contamination with toxic metals in and around an abandoned Zn mine, Korea. *Water, Air, and Soil Pollution*, 165(1-4): 67-185.
- Leshomo, J. 2011. Investigation of hydrochemistry and uranium radioactivity in the groundwater of Namaqualand, Northern Cape, South Africa. Master of Science. University of Witwatersrand. Johannesburg.
- Li, Y. and Migliaccio, K. 2010. Water quality concepts, sampling, and analyses, New York: CRC Press.
- Likus-Cieślak, J., Pietrzykowski, M., Szostak, M. and Szulczewski, M. 2017. Spatial distribution and concentration of sulfur in relation to vegetation cover and soil properties on a reclaimed sulfur mine site (Southern Poland). *Environmental Monitoring and Assessment*, 189(2): 87.
- Liu, F., Wang, S., Yeh, T. C. J., Zhen, P., Wang, L. and Shi, L. 2020. Using multivariate statistical techniques and geochemical modelling to identify factors controlling the evolution of groundwater chemistry in a typical transitional area between Taihang Mountains and North China Plain. *Hydrological Processes*, 34(8): 1888-1905.
- Liu, J.-l., Yao, J., Wang, F., Min, N., Gu, J.-h., Li, Z.-f., Sunahara, G., Duran, R., Sölevic-Knudsen, T. and Hudson-Edwards, K. A. 2019. Bacterial diversity in typical abandoned multi-contaminated nonferrous metal (loid) tailings during natural attenuation. *Environmental Pollution*, 247: 98-107.

- Liu, Y. and Huang, L. 2017. Magnetite recovery from copper tailings increases arsenic distribution in solution phase and uptake in native grass. *Journal of Environmental Management*, 186: 175-182.
- Lombaard, A., Günzel, A., Innes, J. and Krüger, T. 1986. The Tsumeb lead-copper-zinc-silver deposit, south west Africa/Namibia. *Mineral Deposits of Southern Africa*, 2: 1761-1787.
- Lothrop, N., Bright, K. R., Sexton, J., Pearce-Walker, J., Reynolds, K. A. and Verhougstraete, M. P. 2018. Optimal strategies for monitoring irrigation water quality. *Agricultural Water Management*, 199: 86-92.
- Lottermoser, B. 2016. Environmental Indicators in Metal Mining, Switzerland: Springer.
- Lottermoser, B. G. 2010. Tailings. Mine wastes. Switzerland: Springer.
- Luby, S. P., Rahman, M., Arnold, B. F., Unicomb, L., Ashraf, S., Winch, P. J., Stewart, C. P., Begum, F., Hussain, F. and Benjamin-Chung, J. 2018. Effects of water quality, sanitation, handwashing, and nutritional interventions on diarrhoea and child growth in rural Bangladesh: a cluster randomised controlled trial. *The Lancet Global Health*, 6: e302- e315.
- Ma, X., Chen, Y., Zhu, C. and Li, W. 2011. The variation in soil moisture and the appropriate groundwater table for desert riparian forest along the Lower Tarim River. *Journal of Geographical Sciences*, 21(1): 150-162.
- Maest, A. S. and Nordstrom, D. K. 2017. A geochemical examination of humidity cell tests. *Applied Geochemistry*, 81: 109-131.
- Maier, W. D. 2000. Platinum-group elements in Cu-sulphide ores at Carolusberg and East Okiep, Namaqualand, South Africa. *Mineralium Deposita*, 35(5): 422-429.
- Maier, W. D. and Barnes, S.-J. 1999. The origin of Cu sulfide deposits in the Curaca Valley, Bahia, Brazil; evidence from Cu, Ni, Se, and platinum-group element concentrations. *Economic Geology*, 94(2): 165-183.
- Maier, W. D., Andreoli, M. A., Groves, D. and Barnes, S.-J. 2012. Petrogenesis of Cu-Ni sulphide ores from O'okiep and kliprand, Namaqualand, South Africa: constraints from chalcophile metal contents. *South African Journal of Geology*, 115(4): 499-514.
- Makgae, M. 2011. Key areas in waste management: a South African perspective. Integrated Waste Management-Volume II 2: 1169. Croatia: Intech.
- Mäkitalo, M., Stenman, D., Ikumapayi, F., Maurice, C. and Öhlander, B. 2016. An evaluation of using various admixtures of green liquor dregs, a residual product, as a sealing layer on reactive mine tailings. *Mine Water and the Environment*, 35(3): 283-293.
- Manoj, S., Thirumurugan, M. and Elango, L. 2017. An integrated approach for assessment of groundwater quality in and around uranium mineralized zone, Gogi region, Karnataka, India. *Arabian Journal of Geosciences*, 10(24): 557.
- Maoui, A., Kherici, N. and Derradji, F. 2010. Hydrochemistry of an Albian sandstone aquifer in a semi arid region, Ain oussera, Algeria. *Environmental Earth Sciences*, 60(4): 689-701.

- Marandi, A. and Shand, P. 2018. Groundwater chemistry and the Gibbs Diagram. *Applied Geochemistry*, 97: 209-212.
- Maret, W. 2016. The metals in the biological periodic system of the elements: Concepts and conjectures. *International Journal of Molecular Sciences*, 17(1): 66.
- Mark, R., 2006. Closure of tailings facilities: Current practice review and guidelines for success. Master of Science in Engineering (Civil). University of the Witwatersrand, Johannesburg.
- Martín-Moreno, C., Martín Duque, J. F., Nicolau Ibarra, J. M., Hernando Rodríguez, N., Sanz Santos, M. Á. and Sánchez Castillo, L. 2016. Effects of topography and surface soil cover on erosion for mining reclamation: the experimental spoil heap at El Machorro Mine (Central Spain). *Land Degradation and Development*, 27(2): 145-159.
- Mativenga, P. T. and Marnewick, A. 2018. Water quality in a mining and water-stressed region. *Journal of Cleaner Production*, 171: 446-456.
- McCarthy, T. S. 2011. The impact of acid mine drainage in South Africa. *South African Journal of Science*, 107(5-6): 01-07.
- McGlinchey, D. 2005. *Characterisation of bulk solids*. New York: John Wiley and Sons.
- McNeill, L. S. and Edwards, M. 2002. The importance of temperature in assessing iron pipe corrosion in water distribution systems. *Environmental Monitoring and Assessment*, 77(3): 229-242.
- Mehta, N., Cocerva, T., Cipullo, S., Padoan, E., Dino, G. A., Ajmone-Marsan, F., Cox, S. F., Coulon, F. and De Luca, D. A. 2019. Linking oral bioaccessibility and solid phase distribution of potentially toxic elements in extractive waste and soil from an abandoned mine site: Case study in Campello Monti, NW Italy. *Science of The Total Environment*, 651: 2799-2810.
- Méndez-Ortiz, B. A., Carrillo-Chávez, A. and Monroy-Fernández, M. G. 2007. Acid rock drainage and metal leaching from mine waste material (tailings) of a Pb-Zn-Ag skarn deposit: Environmental assessment through static and kinetic laboratory tests. *Revista Mexicana de Ciencias Geológicas*, 24(2): 161-169.
- Meuser, H. 2010. Contaminated urban soils, (Vol. 18). New York: Springer Science and Business Media.
- Miao, Z., Carroll, K. C. and Brusseau, M. L. 2013. Characterization and quantification of groundwater sulfate sources at a mining site in an arid climate: The Monument Valley site in Arizona, USA. *Journal of Hydrology*, 504: 207-215.
- Miller, S., Jeffery, J. and Wong, J. 1991. Use and misuse of the acid base account for "AMD" prediction. *Proceedings of the 2nd International Conference on the Abatement of Acidic Drainage*. Montréal, Que.
- Mladenov, N., Wolski, P., Hettiarachchi, G. M., Murray-Hudson, M., Enriquez, H., Damaraju, S., Galkaduwa, M. B., McKnight, D. M. and Masamba, W. 2014. Abiotic and biotic factors influencing the mobility of arsenic in groundwater of a through-flow island in the Okavango Delta, Botswana. *Journal of Hydrology*, 518: 326-341.

- Molson, J., Aubertin, M. and Bussière, B. 2012. Reactive transport modelling of acid mine drainage within discretely fractured porous media: Plume evolution from a surface source zone. *Environmental Modelling and Software*, 38: 259-270.
- Moncho, T., Erdogan, I., Emandien, M., Ntwampe, S., Fosso-Kankeu, E., Waanders, F., Rand, A. and Fourie, B. 2017. Prediction of metals bioavailability in the soils of O'kiep, South Africa. *9th Int'l Conference on Advances in Science, Engineering, Technology and Waste Management (ASETWM-17)*. Parys, South Africa.
- Mondal, N., Singh, V., Singh, V. and Saxena, V. 2010. Determining the interaction between groundwater and saline water through groundwater major ions chemistry. *Journal of Hydrology*, 388(1-2): 100-111.
- Moon, Y., Song, Y. and Moon, H.-S. 2008. The potential acid-producing capacity and factors controlling oxidation tailings in the Guryong mine, Korea. *Environmental Geology*, 53(8): 1787-1797.
- Morin, K.A. and Hutt, N.M. 1999. Geochemical characterization of molybdenum leaching from rock and tailings at the Brenda minesite, British Columbia. *In Proceedings of the 1999 Workshop on Molybdenum Issues in Reclamation*. Kamloops, British Columbia.
- Morin, K. A. and Hutt, N. M. 2001. *Environmental geochemistry of minesite drainage: Practical theory and case studies, Digital Edition*. Vancouver, British Columbia: MDAG Publishing.
- Morrel, I., Pulido-Bosch, A. and Fernandez, R. 1986. Rubio, hydro geochemical analysis of salinization processes in the coastal aquifers of Oropesa, Spain. *Environmental Geology*, 29: 118-131.
- Mousavi, S., Jafari, A., Yaghmaei, S., Vossoughi, M. and Roostaazad, R. 2006. Bioleaching of low-grade sphalerite using a column reactor. *Hydrometallurgy*, 82(1-2): 75-82.
- Moyle, P. R. and Causey, J. D. 2001. Chemical Composition of Samples Collected from Waste Rock Dumps and Other Mining-Related Features at Selected Phosphate Mines in Southeastern Idaho, Western Wyoming, and Northern Utah: U.S Geological Survey Open-File Report No. 01-411, 46. Available: <https://pubs.usgs.gov/of/2001/0411/>. [Accessed 16 October November 2019].
- Nama Khoi Municipality Draft Integrated Development Plan, 2018/2019. Available: [Nama-Khoi-Draft-IDP-2018-19.pdf](#) [Accessed 11 November 2018].
- Munyai, A., Fosso-Kankeu, E. and Waanders, F. 2016. Mobility of metals from mine tailings using different types of organic acids: Batch leaching experiment. *International Journal of Science and Research*, 5(11): 520-527.
- Murakami, T., Utsunomiya, S., Yokoyama, T. and Kasama, T. 2003. Biotite dissolution processes and mechanisms in the laboratory and in nature: Early stage weathering environment and vermiculitization. *American Mineralogist*, 88(2-3): 377-386.
- Musekiwa, C. and Majola, K. 2013. Groundwater vulnerability map for South Africa. *South African Journal of Geomatics*, 2(2): 152-162.

- Naicker, K., Cukrowska, E. and McCarthy, T. 2003. Acid mine drainage arising from gold mining activity in Johannesburg, South Africa and environs. *Environmental Pollution*, 122(1): 29- 40.
- Naidoo, D. 2014. The National Water and Sanitation Summit. *The Star*, 29 July 2014. South Africa.
- Naidoo, S. 2015. An assessment of the impacts of acid mine drainage on socio-economic development in the Witwatersrand: South Africa. *Environment, Development and Sustainability*, 17(5): 1045-1063.
- Naidoo, S. 2017. The Global Context of AMD. Acid Mine Drainage in South Africa. *SpringerBriefs in Environmental Science* , 9-17. Springer, Cham.
- Nakwafila, A. N. 2015. Salinisation source (s) and mechanism (s) in shallow alluvial aquifers along the Buffels River, Northern Cape Province, South Africa. Doctoral Dissertation, Stellenbosch University, Stellenbosch.
- Nannoni, F., Protano, G. and Riccobono, F. 2011. Fractionation and geochemical mobility of heavy elements in soils of a mining area in northern Kosovo. *Geoderma*, 161(1-2): 63-73.
- Naseem, S., Hamza, S. and Bashir, E. 2010. Groundwater geochemistry of Winder agricultural farms, Balochistan, Pakistan and assessment for irrigation water quality. *European Water*, 31: 21-32.
- Navarro, M., Pérez-Sirvent, C., Martínez-Sánchez, M., Vidal, J., Tovar, P. and Bech, J. 2008. Abandoned mine sites as a source of contamination by heavy metals: A case study in a semi-arid zone. *Journal of Geochemical Exploration*, 96(2-3): 183-193.
- Négre, P., Lemièrre, B., Machard de Grammont, H., Billaud, P. and Sengupta, B. 2007. Hydrogeochemical processes, mixing and isotope tracing in hard rock aquifers and surface waters from the Subarnarekha River Basin, (East Singhbhum District, Jharkhand State, India). *Hydrogeology Journal*, 15(8): 1535-1552.
- Nell, J. P. and Van Huyssteen, C. W. 2014. Geology and groundwater regions to quantify primary salinity, sodicity and alkalinity in South African soils. *South African Journal of Plant and Soil*, 31(3): 127-135.
- Nielsen, D. M. and Nielsen, G. 2006. The essential handbook of ground-water sampling. New York: CRC Press.
- Nieva, N. E., Borgnino, L. and García, M. G. 2018. Long term metal release and acid generation in abandoned mine wastes containing metal-sulphides. *Environmental Pollution*, 242: 264- 276.
- Nikolov, H. and Borisova, D. 2012. Long term monitoring of water basin of an abandoned copper open pit mine. *European Geosciences Union General Assembly Conference*. Vienna, Austria.
- Niquette, P., Servais, P. and Savoie, R. 2001. Bacterial dynamics in the drinking water distribution system of Brussels. *Water Research*, 35(3): 675-682.

- Niu, Q., Xia, M., Ludsin, S. A., Chu, P. Y., Mason, D. M. and Rutherford, E. S. 2018. High-turbidity events in Western Lake Erie during ice-free cycles: Contributions of river-loaded vs. resuspended sediments. *Limnology and Oceanography*, 63(6): 2545-2562.
- Nkosi, V., Wichmann, J. and Voyi, K. 2015. Chronic respiratory disease among the elderly in South Africa: any association with proximity to mine dumps? *Environmental Health*, 14(1): 33.
- Noble, T. L., Lottermoser, B. and Parbhakar-Fox, A. 2017. pH Testing Methods for Sulfidic Mine Wastes. *Environmental Indicators in Metal Mining*, 199-210. Switzerland: Springer, Cham.
- Nordstrom, D. K., Blowes, D. W. and Ptacek, C. J. 2015. Hydrogeochemistry and microbiology of mine drainage: an update. *Applied Geochemistry*, 57: 3-16.
- Nordstrom, D.K., and Wilde, F.D., 2005. Reduction-oxidation potential (electrode method) (ver. 1.2, September 2005): U.S. Geological Survey Techniques of Water-Resources Investigations, (Electrode Method) (No. 09-A6. 5). Available: <https://doi.org/10.3133/twri09A6.5>. [Accessed 12 November 2018].
- Northern Cape Department of Environmental Affairs and Nature Conservation, 2018. Available: <https://www.northern-cape.gov.za/denc/index.php/nature-reserves/goegap>. [Accessed 02 Dec 2019].
- Nuclear, 2006. Available: [https://www.eskom.co.za/OurCompany/SustainableDevelopment/EnvironmentalImpactAssessments/Documents/Nuclear1FSR\\_Ch\\_6\\_pgs\\_89-1071.pdf](https://www.eskom.co.za/OurCompany/SustainableDevelopment/EnvironmentalImpactAssessments/Documents/Nuclear1FSR_Ch_6_pgs_89-1071.pdf). [Accessed 10 August 2017].
- Nwankwoala, H. and Udom, G. 2011. Hydrochemical facies and ionic ratios of groundwater in Port Harcourt, Southern Nigeria. *Research Journal of Chemical Sciences*, 1(3): 87-101.
- Nwankwoala, H. and Ememu, A. 2018. Hydrogeochemical signatures and estimates of underground water quality in Okpoko and neighborhoods, South-East Nigeria. *Author Journal*, 3(3): 49-54.
- Ochieng, G. M., Seanego, E. S. and Nkwonta, O. I. 2010. Impacts of mining on water resources in South Africa: A review. *Scientific Research and Essays*, 5(22): 3351-3357.
- Olalde, M., 2016. What's Left in the Wake of South Africa's Abandoned Gold Mines. Available in: <https://www.greenbiz.com/article/whats-left-wake-south-africas-abandoned-gold-mines>. [Accessed 07 July 2020].
- Osborne, M. R., Champlain, D., Garrett, C., Hall, R., Hengst, G., McCarty, P., Miller, J., Moreau, C., Pedri, J. and Poole, C. 2009. *Biological Wastewater Treatment and reactive nitrogen*. Master of Chemical and Life Sciences, University of Maryland: USA.
- Ouyang, Y., Zhang, J. E. and Cui, L. 2014. Estimating impacts of land use on groundwater quality using trilinear analysis. *Environmental Monitoring and Assessment*, 186(9): 5353-5362.
- Oyourou, J., McCrindle, R., Combrinck, S. and Fourie, C. 2019. Investigation of zinc and lead contamination of soil at the abandoned Edendale mine, Mamelodi (Pretoria, South Africa) using a field-portable spectrometer. *Journal of the Southern African Institute of Mining and Metallurgy*, 119(1): 55-62.

- Pacheco Castro, R., Pacheco Ávila, J., Ye, M. and Cabrera Sansores, A. 2018. Groundwater quality: analysis of its temporal and spatial variability in a karst aquifer. *Groundwater*, 56(1): 62-72.
- Palumbo-Roe, B. and Colman, T. 2010. The nature of waste associated with closed mines in England and Wales. The nature of waste associated with closed mines in England and Wales. Nottingham, UK, British Geological Survey, 82. Report No. OR/10/014.
- Parbhakar-Fox, A. and Lottermoser, B. G. 2015. A critical review of acid rock drainage prediction methods and practices. *Minerals Engineering*, 82: 107-124.
- Parbhakar-Fox, A., Lottermoser, B. and Bradshaw, D. 2013. Evaluating waste rock mineralogy and microtexture during kinetic testing for improved acid rock drainage prediction. *Minerals Engineering*, 52: 111-124.
- Paredes, J. M. 2016. Measuring the Effects of Mining on Peru's Health: Is the Apurimac Region Prepared to Assess Heavy Metal Exposure? Doctoral Dissertation, Duke University. North Carolina.
- Parkhurst, D.L. and Appelo, C.A.J. 1999. User's guide to PHREEQC (Version 2): A computer program for speciation, batch-reaction, one-dimensional transport, and inverse geochemical calculations. Water-resources investigations report, 99(4259): 312.
- Parkhurst, D.L. and Appelo, C.A.J. 2013. Description of input and examples for PHREEQC version 3: A computer program for speciation, batch-reaction, one-dimensional transport, and inverse geochemical calculations (No. 6-A43). US Geological Survey.
- Pehoiu, G., Radulescu, C., Murarescu, O., Dulama, I. D., Bucurica, I. A., Teodorescu, S. and Stirbescu, R. M. 2019. Health risk assessment associated with abandoned copper and uranium mine tailings. *Bulletin of Environmental Contamination and Toxicology*, 102(4): 504-510.
- Perumal, P., Piekkari, K., Sreenivasan, H., Kinnunen, P. and Illikainen, M. 2019. One-part geopolymers from mining residues—effect of thermal treatment on three different tailings. *Minerals Engineering*, 144: 106026.
- Petrisor, I. G., Dobrota, S., Komnitsas, K., Lazar, I., Kuperberg, J. M. and Serban, M. 2004. Artificial inoculation-perspectives in tailings phytostabilization. *International Journal of Phytoremediation*, 6(1): 1-15.
- Pietersen, K., Titus, R. and Cobbing, J. 2009. Effective groundwater management in Namaqualand. Sustaining supplies. Pretoria: Water Research Commission. Report No. 419/09. Available: <http://www.wrc.org.za/wp-content/uploads/mdocs/TT%20418%20-09%20Ground%20water.pdf> [Accessed 08 September 2018].
- Piper, A. 1953. A graphic representation in the geochemical interpretation of groundwater analyses. *Transactions of the American Geophysical Union*, 25: 914-923.
- Pirajno, F. 2012. *Hydrothermal mineral deposits: principles and fundamental concepts for the exploration geologist*. Berlin, Springer Science and Business Media.

- Plante, B., Benzaazoua, M. and Bussière, B. 2011. Predicting geochemical behaviour of waste rock with low acid generating potential using laboratory kinetic tests. *Mine Water the Environment*, 30(1): 2-21.
- Plumlee, G.S., Ziegler, T.L., Lamothe, P., Meeker, G.P. and Sutley, S. 2003. The Toxicological Geochemistry of Dusts, Soils, and Other Earth Materials: Insights from in vitro physiologically-based geochemical leach tests. AGUFM, V51D-0316.
- Plumlee, G.S. 1999. The environmental geology of mineral deposits. The environmental geochemistry of mineral deposits. *Society of Economic Geologists, Part A*: 71-116.
- Plumlee, G.S., Morman, S.A. and Ziegler, T.L. 2006. The toxicological geochemistry of earth materials: an overview of processes and the interdisciplinary methods used to understand them. *Reviews in Mineralogy and Geochemistry*, 64(1): 5-57.
- Portales, R. L., Jiménez, G. C., Michel, H. C., Amador, D. O. R., Mikuš, K. V., Kump, P. and de la Rosa, G. 2015. Understanding copper speciation and mobilization in soils and mine tailings from “Mineral La Aurora” in central Mexico: contributions from Synchrotron techniques. *Boletín de la Sociedad Geológica Mexicana*, 67(3): 447-456.
- Potgieter, J. 1996. Exploration in the Okiep Copper District, Northern Cape Province, South Africa: An overview. *South African Journal of Geology*, 99(2): 209-220.
- Prasad, M. N. V. and Shih, K. 2016. Environmental materials and waste: Resource recovery and pollution prevention. Oxford: Elsevier.
- Prasanth, S. S., Magesh, N., Jitheshlal, K., Chandrasekar, N. and Gangadhar, K. 2012. Evaluation of groundwater quality and its suitability for drinking and agricultural use in the coastal stretch of Alappuzha District, Kerala, India. *Applied Water Science*, 2(3): 165-175.
- Praveena, S. M., Abdullah, M. H., Bidin, K. and Aris, A. Z. 2011. Understanding of groundwater salinity using statistical modeling in a small tropical island, East Malaysia. *The Environmentalist*, 31(3): 279.
- Preite, V., Sailer, C., Syllwasschy, L., Bray, S., Ahmadi, H., Krämer, U. and Yant, L. 2019. Convergent evolution in *Arabidopsis halleri* and *Arabidopsis arenosa* on calamine metalliferous soils. *Philosophical Transactions of the Royal Society*, 374(1777): 20180243.
- Pretorius, J., Usher, B. and Gebrekristos, R. 2008. Groundwater monitoring guidelines for DNAPLs in South African aquifers. Pretoria: Water Research Commission. , Report No. 1501/3/08. Available: <http://citeseerx.ist.psu.edu/viewdoc/download?doi=10.1.1.607.7833&rep=rep1&type=pdf> [Accessed 09 October 2018].
- Price, W.A., 2009. Prediction Manual for Drainage Chemistry from Sulphidic Geologic Materials. MEND Report 1.20. 1. CANMET-Mining and Mineral Sciences Laboratories. Smithers. British Columbia. V0J2N0.
- Price, W.A., Morin, K. and Hutt, N., 1997, May. Guidelines for the prediction of acid rock drainage and metal leaching for mines in British Columbia: Part II. Recommended procedures for static and kinetic testing. *In Proceedings of the Fourth International Conference on Acid Rock Drainage*. British Columbia.

- Priya, R. and Kumar, G. K. 2018. Geotechnical aspects of overburden materials for stowing in underground coal mines. *International Journal of Engineering Research and Technology*, 4.
- Purandara, B.K., Varadarajan, N. and Jayashree, K. 2003. Impact of sewage on ground water quality: A case study. *Pollution Research*, 22(2): 189-197.
- Qian, G., Fan, R., Short, M. D., Schumann, R. C., Li, J., Li, Y., Smart, R. S. C. and Gerson, A. R. 2019. Evaluation of the rate of dissolution of secondary sulfate minerals for effective acid and metalliferous drainage mitigation. *Chemical Geology*, 504: 14-27.
- Qin, W., Han, D., Song, X. and Engesgaard, P. 2019. Effects of an abandoned Pb-Zn mine on a karstic groundwater reservoir. *Journal of Geochemical Exploration*, 200: 221-233.
- Quevauviller, P., Fouillac, A. M., Grath, J. and Ward, R. 2009. Groundwater monitoring, Chichester, Wiley-Blackwell.
- Quispe, D., Pérez-López, R., Acero, P., Ayora, C., Nieto, J. M. and Tucoulou, R. 2013. Formation of a hardpan in the co-disposal of fly ash and sulfide mine tailings and its influence on the generation of acid mine drainage. *Chemical Geology*, 355: 45-55.
- Rabbani, M., Rahman, A. and Islam, N. 2010. Climate change and sea level rise: issues and challenges for coastal communities in the Indian Ocean region. *Coastal Zones and Climate Change*, 17-29.
- Rademeyer, J. 2013. *Laim that 94% in SA have access to safe drinking water... doesn't hold water* Available:<https://africacheck.org/reports/false-claim-that-sa-one-of-only-twelve-countries-with-safe-tap-water/> [Accessed 16 May 2017].
- Raith, J. and Stein, H. 2000. Re–Os dating and sulfur isotope composition of molybdenite from tungsten deposits in western Namaqualand, South Africa: implications for ore genesis and the timing of metamorphism. *Mineralium Deposita*, 35(8): 741-753.
- Raith, J. and Meisel, T. 2001. Metabasites along the amphibolite-granulite facies transition in the Okiep Copper District, South Africa. *South African Journal of Geology*, 104(1): 77-100.
- Raith, J. G., Cornell, D. H., Frimmel, H. E. and De Beer, C. H. 2003. New insights into the geology of the Namaqua tectonic province, South Africa, from ion probe dating of detrital and metamorphic zircon. *The Journal of Geology*, 111(3): 347-366.
- Rajendran, R., Emerenshiya, C.A. and Dheenadayalan, M.S. 2019. Investigations on groundwater quality in Tiruchirappalli city, Tamilnadu, India. *Sustainable Water Resources Management*, 5(2): 599-609.
- Ramakrishnaiah, C., Sadashivaiah, C. and Ranganna, G. 2009. Assessment of water quality index for the groundwater in Tumkur Taluk, Karnataka State, India. *Journal of Chemistry*, 6: 523-530.
- Ramontja, T., Coetzee, H., Hobbs, P., Burgess, J., Thomas, A., Keet, M., Yibas, B., van Tonder, D., Netili, F. and Rust, U. 2011. *Mine water management in the Witwatersrand Gold Fields with special emphasis on acid mine drainage Inter-Ministerial-Committee on acid mine drainage*, 146. Pretoria.

- Rao, N. S. 2006. Seasonal variation of groundwater quality in a part of Guntur District, Andhra Pradesh, India. *Environmental Geology*, 49(3): 413-429.
- Rao, N. S., Subrahmanyam, A., Kumar, S. R., Srinivasulu, N., Rao, G. B., Rao, P. S. and Reddy, G. V. 2012. Geochemistry and quality of groundwater of Gummanampadu sub-basin, Guntur District, Andhra Pradesh, India. *Environmental Earth Sciences*, 67(5): 1451-1471.
- Rashed, M. 2010. Monitoring of contaminated toxic and heavy metals, from mine tailings through age accumulation, in soil and some wild plants at Southeast Egypt. *Journal of Hazardous Materials*, 178(1-3): 739-746.
- Ravikumar, P. and Somashekar, R. 2017. Principal component analysis and hydrochemical facies characterization to evaluate groundwater quality in Varahi river basin, Karnataka state, India. *Applied Water Science*, 7(2): 745-755.
- Ravikumar, P., Somashekar, R. and Prakash, K. 2015. A comparative study on usage of Durov and Piper diagrams to interpret hydrochemical processes in groundwater from SRLIS river basin, Karnataka, India. *Elixir International Journal*, 80: 31073-31077.
- Reddy, D., Nagabhushanam, P., Sukhija, B., Reddy, A. and Smedley, P. 2010. Fluoride dynamics in the granitic aquifer of the Wailapally watershed, Nalgonda District, India. *Chemical Geology*, 269(3-4): 278-289.
- Regan, J. M., Harrington, G. W., Baribeau, H., De Leon, R. and Noguera, D. R. 2003. Diversity of nitrifying bacteria in full-scale chloraminated distribution systems. *Water Research*, 37(1): 197-205.
- Reid, D. and Barton, E. S. (Ed.). 1983. Geochemical characterization of granitoids in the Namaqualand geotraverse. *Namaqualand Metamorphic Complex*, 16(19): 67-82. South Africa: The Geological Society of South Africa.
- Richards, C. L., Broadaway, S. C., Eggers, M. J., Doyle, J., Pyle, B. H., Camper, A. K. and Ford, T. E. 2018. Detection of pathogenic and non-pathogenic bacteria in drinking water and associated biofilms on the Crow reservation, Montana, USA. *Microbial Ecology*, 76(1): 52- 63.
- Richards, L. 1954. Diagnosis and improvement of saline and alkali soils. Handbook, 60. Plant Soil. Washington, DC US Department of Agriculture.
- Rickwood, C. and Carr, G.M. 2007. Global drinking water quality index development and sensitivity analysis report. *United Nations Environment Programme (UNEP) and Global Environment Monitoring System (GEMS)/Water Programme*, 1203: 1196-1204.
- Riedel, T. and Kübeck, C. 2018. Uranium in groundwater: A synopsis based on a large hydrogeochemical data set. *Water Research*, 129: 29-38.
- Rietveld, L. C., Haarhoff, J. and Jagals, P. 2009. A tool for technical assessment of rural water supply systems in South Africa. *Physics and Chemistry of the Earth*, 34(1): 43-49.
- Rijal, M. L., Appel, E., Petrovský, E. and Blaha, U. 2010. Change of magnetic properties due to fluctuations of hydrocarbon contaminated groundwater in unconsolidated sediments. *Environmental Pollution*, 158(5): 756-1762.

- Rivett, U., Champanis, M. and Wilson-Jones, T. 2013. Monitoring drinking water quality in South Africa: Designing information systems for local needs. *Water SA*, 39(3): 409-414.
- Roets, W., 2008. Groundwater dependence of aquatic ecosystems associated with the table mountain group aquifer. Doctoral Dissertation. University of the Western Cape. Bellville.
- Romero, F., Armienta, M. and González-Hernández, G. 2007. Solid-phase control on the mobility of potentially toxic elements in an abandoned lead/zinc mine tailings impoundment, Taxco, Mexico. *Applied Geochemistry*, 22(1): 109-127.
- Root, R. A., Hayes, S. M., Hammond, C. M., Maier, R. M. and Chorover, J. 2015. Toxic metal (loid) speciation during weathering of iron sulfide mine tailings under semi-arid climate. *Applied Geochemistry*, 62: 131-149.
- Rotiroti, M., McArthur, J., Fumagalli, L., Stefania, G. A., Sacchi, E. and Bonomi, T. 2017. Pollutant sources in an arsenic-affected multilayer aquifer in the Po Plain of Italy: Implications for drinking-water supply. *Science of the Total Environment*, 578: 502-512.
- Rout, G. R., Swain, D. and Deo, B. 2019. Restoration of metalliferous mine waste through genetically modified crops. *Transgenic Plant Technology for Remediation of Toxic Metals and Metalloids*. Oxford: Elsevier.
- Rozendaal, A. and Horn, R. 2013. Textural, mineralogical and chemical characteristics of copper reverb furnace smelter slag of the Okiep Copper District, South Africa. *Minerals Engineering*, 52: 184-190.
- Rozendaal, A., Rudnick, T. and Heyn, R. 2017. Mesoproterozoic base metal sulphide deposits in the Namaqua sector of the Namaqua-Natal Metamorphic Province, South Africa: A review. *South African Journal of Geology*, 120(1): 153-186.
- Rudzani, L., Gumbo, J. R., Yibas, B. and Novhe, O. 2018. Acid Base Accounting (ABA) of mine tailings for the Potential of Acid Mine Drainage in the Sabie-Pilgrim's Rest Goldfields, (11th ICARD, IMWA2018). Pretoria. South Africa. Available: [http://www.mwen.info/docs/imwa\\_2018/IMWA2018\\_Lusunzi\\_392.pdf](http://www.mwen.info/docs/imwa_2018/IMWA2018_Lusunzi_392.pdf) [Accessed 09 July 2019].
- Saha, S. and Sinha, A. 2016. A Review on Different Active Treatment Methods for Acid Mine Drainage. *Journal of Basic and Applied Engineering Research*, 3(8): 676-680.
- Sahraei Parizi, H. and Samani, N. 2013. Geochemical evolution and quality assessment of water resources in the Sarcheshmeh copper mine area (Iran) using multivariate statistical techniques. *Environmental Earth Sciences*, 69(5): 1699-1718.
- Sakala, E., Fourie, F., Gomo, M. and Coetzee, H. 2017. Hydrogeological investigation of the Witbank, Ermelo and Highveld Coalfields: Implications for the subsurface transport and attenuation of acid mine drainage. 13th International Mine Water Association Congress - "Mine Water and Circular Economy - A Green Congress" (IMWA2017). Lappeenranta, Finland. Available: [http://www.imwa.info/docs/imwa\\_2017/IMWA2017\\_Sakala\\_564.pdf](http://www.imwa.info/docs/imwa_2017/IMWA2017_Sakala_564.pdf) [Accessed 09 March 2019].
- Sakram, G., Sundaraiah, R. and Vishnu Bhoopathi, P. R. S. 2013. The impact of agricultural activity on the chemical quality of groundwater, Karanja Vagu Watershed, Medak District,

- Andhra Pradesh. *International Journal of Advanced Technology and Science Research*, 6(3): 769-786.
- Saladi, J. A. and Salehe, F. S. 2017. Assessment of water supply and its implications on household income in Kabuku Ndani Ward, Handeni District, Tanzania. *Asian Journal of Environment and Ecology*, 2(1): 1-26.
- Salomons, W. and Forstner, U. 2012. Chemistry and biology of solid wastes, dredge materials and mine tailings. Berlin, Heidelberg: Springer Science and Business Media.
- Samson, S. D., Nagy, K. L. and Cotton III, W. B. 2005. Transient and quasi-steady-state dissolution of biotite at 22–25° C in high pH, sodium, nitrate, and aluminate solutions. *Geochimica et Cosmochimica Acta*, 69(2): 399-413.
- SANS241-1 2015. South African National Standard: Drinking water. Part 1. Microbial, physical, aesthetic and chemical determinants. 2 ed. Pretoria: SABS.
- Sany, S. M. K. 2016. *Chalcopyrite (Bio) leaching in sulphate solutions: An investigation into hindered dissolution with a focus on solution redox potential*. Doctoral Dissertation. Luleå University of Technology. Sweden.
- Sapsford, D. J., Bowell, R., Dey, M. and Williams, K. P. J. M. E. 2009. Humidity cell tests for the prediction of acid rock drainage 22(1): 25-36.
- Sarin, P., Snoeyink, V., Bebee, J., Jim, K., Beckett, M., Kriven, W. and Clement, J. 2004. Iron release from corroded iron pipes in drinking water distribution systems: effect of dissolved oxygen. *Water Research*, 38(5): 1259-1269.
- Satokari, R. M., Vaughan, E. E., Akkermans, A. D., Saarela, M. and de Vos, W. M. 2001. Bifidobacterial diversity in human feces detected by genus-specific PCR and denaturing gradient gel electrophoresis. *Applied and Environmental Microbiology*, 67(2): 504-513.
- Sawyer, C. N. and McCarty, P. L. 1967. Chemistry for sanitary engineers. Washington, DC: McGraw-Hill.
- Schoch, A. E. and Conradie, J. A. 1990. Petrochemical and mineralogical relationships in the Koperberg Suite, Namaqualand, South Africa. *American Mineralogist*, 75(1-2): 27-36.
- Schoeneberger, P.J., Wysocki, D.A. and Benham, E.C. eds. 2012. Field book for describing and sampling soils. USA, National Soil Survey Center. Government Printing Office.
- Schutte, C.F. 2001. Quality of Domestic Water Supplies, Vol. 3: Analysis Guide. Pretoria: Water Research Commission. Report No. TT129/00.
- Selvakumar, S., Chandrasekar, N. and Kumar, G. 2017. Hydrogeochemical characteristics and groundwater contamination in the rapid urban development areas of Coimbatore, India. *Water Resources and Industry*, 17: 26-33.
- Servida, D., Comero, S., Dal Santo, M., de Capitani, L., Grieco, G., Marescotti, P., Porro, S., Forray, F. L., Gál, A. and Szakács, A. 2013. Waste rock dump investigation at Roşia Montană gold mine (Romania): a geostatistical approach. *Environmental Earth Sciences*, 70(1): 13-31.

- Sevilla-Perea, A., Romero-Puertas, M. and Mingorance, M. 2016. Optimizing the combined application of amendments to allow plant growth in a multielement-contaminated soil. *Chemosphere*, 148: 220-226.
- Shah, D. and Mjalli, F. S. 2014. Effect of water on the thermo-physical properties of Reline: An experimental and molecular simulation based approach. *Physical Chemistry Chemical Physics*, 16(43): 23900-23907.
- Shanmuga, P.R., Kumar, K.G. 2015. Geotechnical Aspects of Overburden Materials for Stowing in Underground Coal Mines. *International Journal of Engineering, Science and Technology*, 4: 03.
- Shen, S., Ma, T., Du, Y., Luo, K., Deng, Y. and Lu, Z. 2019. Temporal variations in groundwater nitrogen under intensive groundwater/surface-water interaction. *Hydrogeology Journal*, 27(5): 1753-1766.
- Sheoran, A. and Sheoran, V. 2006. Heavy metal removal mechanism of acid mine drainage in wetlands: a critical review. *Minerals Engineering*, 19(2): 105-116.
- Shorieh, A., Porel, G. and Razack, M. 2015. Assessment of Groundwater Quality in the Dogger Aquifer of Poitiers, Poitou-Charentes Region, France. *Journal of Water Resource and Protection*, 7(03): 171.
- Sima, M., Dold, B., Frei, L., Senila, M., Balteanu, D. and Zobrist, J. 2011. Sulfide oxidation and acid mine drainage formation within two active tailings impoundments in the Golden Quadrangle of the Apuseni Mountains, Romania. *Journal of Hazardous Materials*, 189(3): 624-639.
- Singh, G. and Kamal, R.K. 2015. Assessment of groundwater quality in the mining areas of Goa, India. *Indian Journal of Science and Technology*, 8(6): 588.
- Singh, K. P., Malik, A. and Sinha, S. 2005. Water quality assessment and apportionment of pollution sources of Gomti river (India) using multivariate statistical techniques: A case study. *Analytica Chimica Acta*, 538(1-2): 355-374
- Singh, N. T. 2005. Irrigation and soil salinity in the Indian subcontinent: past and present. Bethlehem: Lehigh University Press.
- Singh, U. K., Ramanathan, A. L. and Subramanian, V. 2018. Groundwater chemistry and human health risk assessment in the mining region of East Singhbhum, Jharkhand, India. *Chemosphere*, 204: 501-513.
- Smith, D.B.C., Woodruff, W.F., Solano, L.G., Ellefsen, F. and Karl, J. 2014. Geochemical and mineralogical maps for soils of the conterminous United States.
- Smuts, I. H. 2015. *Influence of acid mine drainage on the soils of Nababeep, Namaqualand with reference to soil chemistry, minerals and metal mobility*. Master of Science (Agriculture). Stellenbosch University. Stellenbosch.
- Sobek, A. A. 1978. Field and laboratory methods applicable to overburdens and minesoils, Ohio, Industrial Environmental Research Laboratory, United States Environmental Protection Agency.

- Soldatova, E., Guseva, N. and Bychinsky, V. 2017. Modelling of redox conditions in the shallow groundwater: a case study of agricultural areas in the Poyang Lake basin, China. *Procedia Earth and Planetary Science*, 17: 197-200.
- Sollins, P., Swanston, C., Kleber, M., Filley, T., Kramer, M., Crow, S., Caldwell, B. A., Lajtha, K. and Bowden, R. 2006. Organic C and N stabilization in a forest soil: Evidence from sequential density fractionation. *Soil Biology and Biochemistry*, 38(11): 3313-3324.
- Srinivas, Y., Aghil, T.B., Oliver, D.H., Nair, C.N. and Chandrasekar, N. 2017. Hydrochemical characteristics and quality assessment of groundwater along the Manavalakurichi coast, Tamil Nadu, India. *Applied Water Science*, 7(3): 1429-1438.
- Stanković, S., Morić, I., Pavić, A., Vojnović, S., Vasiljević, B. and Cvetković, V. 2015. Bioleaching of copper from old flotation tailings samples (Copper Mine Bor, Serbia). *Journal of the Serbian Chemical Society*, 80(3): 391-405.
- Strömberg, B. and Banwart, S. 1999. Weathering kinetics of waste rock from the Aitik copper mine, Sweden: scale dependent rate factors and pH controls in large column experiments. *Journal of Contaminant Hydrology*, 39(1-2): 59-89.
- Strydom, W., Hill, L. and Hobbs, P. 2010. Water state of the environment: Issue summary Pretoria: CSIR, Available: <http://hdl.handle.net/10204/4220> [Accessed 12 March 2019].
- Stumpfl, E.F., Clifford, T.N., Burger, A.J. and Van Zyl, D. 1976. The copper deposits of the O'okiep district, South Africa: New data and concepts. *Mineralium Deposita*, 11(1): 46-70.
- Sun, Z., Soldatova, E.A., Guseva, N.V. and Shvartsev, S.L. 2014. Impact of human activity on the groundwater chemical composition of the south part of the Poyang Lake Basin. *Ieri Procedia*, 8: 113-118.
- Sundaram, B., Feitz, A., de Caritat, P., Plazinska, A., Brodie, R., Coram, J. and Ransley, T. 2009. Groundwater sampling and analysis-a field guide. *Geoscience Australia, Record*, 27(95): 104.
- Swanepoel, A., du Preez, H., Schoeman, C., Janse van Vuuren, S. and Sundram, A. 2008. Condensed laboratory methods for monitoring phytoplankton, including cyanobacteria, in South African freshwaters. Report to the Water Research Commission by Rand Water, 117. Available: <http://www.wrc.org.za/wp-content/uploads/mdocs/TT323-08.pdf> [Accessed 22 February 2018].
- Swartz, C. 2009. A planning framework to position rural water treatment in South Africa for the future. Pretoria: Water Research Commission. Report No. TT 419/09.
- Szczepańska, J. and Twardowska, I. 2004. Mining waste. Waste Management Series, 4: 319- 385. Elsevier.
- Tabelin, C., Sasaki, A., Igarashi, T., Tomiyama, S., Villacorte-Tabelin, M., Ito, M. and Hiroyoshi, N. 2019. Prediction of acid mine drainage formation and zinc migration in the tailings dam of a closed mine, and possible countermeasures. *The 25<sup>th</sup> Regional Symposium on Chemical Engineering (RSCE 2018) In MATEC Web of Conferences*. EDP Sciences. Available: [https://www.mateconferences.org/articles/mateconf/pdf/2019/17/mateconf\\_rsce18\\_06003.pdf](https://www.mateconferences.org/articles/mateconf/pdf/2019/17/mateconf_rsce18_06003.pdf) [Accessed 22 March 2019].

- Tayebi-Khorami, M., Edraki, M., Corder, G. and Golev, A. 2019. Re-thinking mining waste through an integrative approach led by circular economy aspirations. *Minerals*, 9(5): 286.
- Tessema, A., Nzotta, U. and Chirenje, E. 2014. Assessment of Groundwater Potential in Fractured Hard Rocks Around Vryburg, North West Province, South Africa. Pretoria: Water Research Commission. Report No. (2055/1),13. <http://www.wrc.org.za/wp-content/uploads/mdocs/2055-1-13.pdf> [Accessed 12 August 2019].
- Thurston, R.S., Mandernack, K.W. and Shanks III, W.C. 2010. Laboratory chalcopyrite oxidation by *Acidithiobacillus ferrooxidans*: oxygen and sulfur isotope fractionation. *Chemical Geology*, 269(3-4): 252-261.
- Tikhomirov, V. V. 2016. Hydrogeochemistry Fundamentals and Advances, Mass Transfer and Mass Transport. Hoboken: John Wiley and Sons.
- Titshall, L.W., Hughes, J.C. and Bester, H.C. 2013. Characterisation of alkaline tailings from a lead/zinc mine in South Africa and evaluation of their revegetation potential using five indigenous grass species. *South African Journal of Plant and Soil*, 30(2): 97-105.
- Titus, R. 2002. Groundwater Assessment and Strategies for Sustainable Resource Supply in Arid Zones: The Namaqualand Case Study. Pretoria: Water Research Commission.
- Titus, R., Adams, S. and Xu, Y. 2002. Groundwater Situation Assessment in Olifants Doorn Water Management Area (Version 1). Final draft report prepared for Danced Project of Department of Water Affairs and Forestry. Groundwater Group, Department of Earth Sciences at the University of the Western Cape. Bellville.
- Tomlinson, D. W., Rivett, M. O., Wealthall, G. P. and Sweeney, R. E. 2017. Understanding complex LNAPL sites: Illustrated handbook of LNAPL transport and fate in the subsurface. *Journal of Environmental Management*, 204: 748-756.
- Tordoff, G., Baker, A. and Willis, A. 2000. Current approaches to the revegetation and reclamation of metalliferous mine wastes. *Chemosphere*, 41(1-2): 219-228.
- Trick, J. K., Stuart, M. and Reeder, S. 2008. Contaminated groundwater sampling and quality control of water analyses. *Environmental geochemistry: site characterization, data analysis and case histories*, 29-57. Amsterdam: Elsevier.
- Tyagi, S., Sharma, B., Singh, P. and Dobhal, R. 2013. Water quality assessment in terms of water quality index. *American Journal of Water Resources*, 1(3): 34-38.
- Ukpong, E., Ekanem, E.N.U.E.A., Ikpe, E. and Nyoyoko, I., 2017. Assessment of Water Quality from Bore Holes in Ikot Akpaden and Some Surrounding Villages of Mkpato Enin Local Government Area of Akwa Ibom State, Nigeria. *Assessment*, 9(2).
- USEPA, 2014. United States Environmental Protection Agency: Operating protocol for soil sampling. Science and Ecosystem Support Division operating procedure. Athens, Georgia
- Vallero, D.A. and Blight, G. 2019. Mine Waste: A Brief Overview of Origins, Quantities, and Methods of Storage. *In Waste*, 129-151. United Kingdom: Academic Press.
- Van der Ent, A. and Edraki, M. 2018. Environmental geochemistry of the abandoned Mamut copper mine (Sabah) Malaysia. *Environmental Geochemistry and Health*, 40(1): 189-207.

- Van Dyk, G.S., Makheta, J., Potgiter, D., Zikali, T., Leeme, V., Moletsane, F. and Vonya, T. 2008. Groundwater resource in the Northern Cape Province, Kimberly.
- Van Wyk, I., Roychoudhury, A.N., Maherry, A. and Genthe, B. 2012. Hydrogeochemical characterisation and evaluation of groundwater resources and review of groundwater management schemes in Kamiesberg, Northern Cape.
- Van Zweel, K. N. 2015. Development of a geochemical model to predict leachate water quality associated with coal mining practices. Doctoral Dissertation. North West University. Potchefstroom.
- Van Zwieten, A.J.M., McCarthy, T.S. and Cawthorn, R.G. 1996. A petrogenetic model for the Koperberg Suite: evidence from the Jubilee Mine, Namaqualand, South Africa. *South African Journal of Geology*, 99(2): 121-134.
- Vandenberg, J., McCullough, C. and Castendyk, D. 2015, April. Key issues in mine closure planning related to pit lakes. In Agreeing on solutions for more sustainable mine water management. *Proceedings of the 10th ICARD and IMWA Annual Conference*. Santiago, Chile (GECAMIN).
- Vearrier, D., Curtis, J.A. and Greenberg, M.I. 2009. Technologically enhanced naturally occurring radioactive materials. *Clinical Toxicology*, 47(5): 393-406.
- Venkateswarlu, K., Nirola, R., Kuppusamy, S., Thavamani, P., Naidu, R. and Megharaj, M. 2016. Abandoned metalliferous mines: ecological impacts and potential approaches for reclamation. *Reviews in Environmental Science and Bio/Technology*, 15(2): 327-354.
- Villain, L., Sundström, N., Perttu, N., Alakangas, L. and Öhlander, B. 2015. Evaluation of the effectiveness of backfilling and sealing at an open-pit mine using ground penetrating radar and geoelectrical surveys, Kimheden, northern Sweden. *Environmental Earth Sciences*, 73(8): 4495-4509.
- Violante, A., Cozzolino, V., Perelomov, L., Caporale, A.G. and Pigna, M. 2010. Mobility and bioavailability of heavy metals and metalloids in soil environments. *Journal of Soil Science and Plant Nutrition*, 10(3): 268-292.
- Wahsha, M., Bini, C., Argese, E., Minello, F., Fontana, S. and Wahsheh, H. 2012. Heavy metals accumulation in willows growing on Spolic Technosols from the abandoned Imperina Valley mine in Italy. *Journal of Geochemical Exploration*, 123: 19-24.
- Walls, J. T., Wyatt, K. H., Doll, J. C., Rubenstein, E. M. and Rober, A. R. 2018. Hot and toxic: Temperature regulates microcystin release from cyanobacteria. *Science of The Total Environment*, 610: 786-795.
- Wapwera, S. D., Egbu, C., Parsa, A. and Ayanbinpe, G. 2015. Abandoned mines, homes for the people: case study of Jos Tin-mining region. *International Journal of Housing Markets and Analysis*, 8: 239-264.
- Watling, H. 2006. The bioleaching of sulphide minerals with emphasis on copper sulphides: A review. *Hydrometallurgy*, 84(1-2): 81-108.

- Weaver, J. M., Cave, L. and Talma, A. S. 2007. Groundwater Sampling. Pretoria: Water Research Commission Report No. TT 303-07. Available: <http://www.wrc.org.za/wp-content/uploads/mdocs/TT303-07.pdf> [Accessed 13 June 2018].
- Weaver, M.J.T., O’Keeffe, J., Hamer, N. and Palmer, C.G. 2017. Water service delivery challenges in a small South African municipality: Identifying and exploring key elements and relationships in a complex social-ecological system. *Water SA*, 43(3): 398-408.
- Weber, P.A., Hughes, J.B., Conner, L.B., Lindsay, P. and Smart, R. 2006. Short-term acid rock drainage characteristics determined by paste pH and kinetic NAG testing: cypress, Prospect, New Zealand. Available: [http://www.imwa.info/docs/imwa\\_2006/2289-Weber-NZ.pdf](http://www.imwa.info/docs/imwa_2006/2289-Weber-NZ.pdf) [Accessed 19 May 2019].
- Whitworth, K.L., Silvester, E. and Baldwin, D.S. 2014. Alkalinity capture during microbial sulfate reduction and implications for the acidification of inland aquatic ecosystems. *Geochimica et Cosmochimica Acta*, 130: 113-125.
- WHO, 1998. Cyanobacterial Toxins: Microcystin-LR in Drinking-Water. WHO Guidelines for Drinking Water Quality. 2nd edn. Addendum to Vol. 2. Health Criteria and Other Supporting Information. Geneva: World Health Organisation.
- WHO, 2004. World Health Organisation: Guidelines for drinking-water quality. (Vol. 1). Geneva: World Health Organisation.
- WHO, 2011. Guidelines for drinking-water quality. Geneva: World Health Organisation.
- WHO and UNICEF, 2015. Joint Water Supply, Sanitation Monitoring Programme and World Health Organisation. Progress on sanitation and drinking water: 2015 update and MDG assessment. Geneva: World Health Organisation.
- WHO and UNICEF, 2006. Core questions on drinking water and sanitation for household surveys. Available: [http://www.who.int/water\\_sanitation\\_health/monitoring/household\\_surveys/en/](http://www.who.int/water_sanitation_health/monitoring/household_surveys/en/) [Accessed 15 April 2017 ].
- Wierzbicka-Wieczorek, M., Lottermoser, B.G., Kiefer, S., Sindern, S., Gronen, L. and Hensler, A.S., 2019. Indium distribution in metalliferous mine wastes of the Iberian Pyrite Belt, Spain–Portugal. *Environmental Earth Sciences*, 78(8): 253.
- Wilde, F.D. and Radtke, D.B. eds., 1998. Handbooks for Water-resources Investigations: National field manual for the collection of water-quality data. Field measurements. US Department of the Interior, US Geological Survey.
- Wu, A., Yin, S., Qin, W., Liu, J. and Qiu, G., 2009. The effect of preferential flow on extraction and surface morphology of copper sulphides during heap leaching. *Hydrometallurgy*, 95(1- 2): 76-81.
- Wulfse, A.D. and Holdsworth, R. 1994. Application of regional geochemical surveys to environmental studies; a case study from the Namaqualand copper district. *Journal of African Earth Sciences*, 18(4): 343-346.
- Xtract, Resources and Plc. 2015. Acquisition of sulphide copper tailings project. Available: <http://www.xtractresources.com/rns/Acquisition%20of%20Sulphide%20Copper%20Tailings%20Project.pdf> [Accessed 06 October 2019].

- Xu, Y. and Braune, E. 2009. Sustainable groundwater resources in Africa: water supply and sanitation environment. London: CRC Press.
- Xu, Y. and Beekman, H.E. 2019. Groundwater recharge estimation in arid and semi-arid southern Africa. *Hydrogeology Journal*, 27(3): 929-943.
- Yan, S.F., Yu, S.E., Wu, Y.B., Pan, D.F., She, D.L. and Ji, J. 2015. Seasonal variations in groundwater level and salinity in coastal plain of eastern China influenced by climate. *Journal of Chemistry*, 2015.
- Yang, F., Shi, B., Bai, Y., Sun, H., Lytle, D. A. and Wang, D. 2014. Effect of sulfate on the transformation of corrosion scale composition and bacterial community in cast iron water distribution pipes. *Water Research*, 59: 46-57.
- Yolcubal, I., Demiray, A.D. and Çiftçi, E. 2017. Assessment of acid mine drainage potential of flotation slurry from a tailing dam in a copper mine, Murgul, Northeastern Turkey. *Environmental Earth Sciences*, 76(3): 100.
- You, M., Huang, Y., Lu, J. and Li, C. 2015. Characterization of heavy metals in soil near coal mines and a power plant in Huainan, China. *Analytical Letters*, 48(4): 726-737.
- Younger, P.L. and Robins, N.S. 2002. Challenges in the characterization and prediction of the hydrogeology and geochemistry of mined ground. *Geological Society*, London, Special Publications, 198(1): 1-16.
- Yu, F. and Hunt, A.G. 2018. Predicting soil formation on the basis of transport-limited chemical weathering. *Geomorphology*, 301: 21-27.
- Yucel, D.S. and Baba, A., 2016. Prediction of acid mine drainage generation potential of various lithologies using static tests: Etili coal mine (NW Turkey) as a case study. *Environmental Monitoring and Assessment*, 188(8): 473.
- Yuhara, M., Kagami, H. and Tsuchiya, N. 2001. Rb-Sr and Sm-Nd systematics of granitic and metamorphic rocks in the Namaqualand Metamorphic Complex, South Africa: Implications for evolution of marginal part of Kaapvaal craton. *Memoirs of National Institute of Polar Research*, 55: 127-144.
- Zawadzki, J., Przędziecki, K. and Miatkowski, Z. 2016. Determining the area of influence of depression cone in the vicinity of lignite mine by means of triangle method and LANDSAT TM/ETM+ satellite images. *Journal of Environmental Management*, 166: 605-614.
- Zhang, Y., Wu, J. and Xu, B. 2018. Human health risk assessment of groundwater nitrogen pollution in Jinghui canal irrigation area of the loess region, northwest China. *Environmental Earth Sciences*, 77(7): 273.
- Zheng, J., Zhu, Y. and Zhao, Z. 2016. Utilization of limestone powder and water-reducing admixture in cemented paste backfill of coarse copper mine tailings. *Construction and Building Materials*, 124: 31-36.
- Zheng, Y., Stute, M., Van Geen, A., Gavrieli, I., Dhar, R., Simpson, H., Schlosser, P. and Ahmed, K. 2004. Redox control of arsenic mobilization in Bangladesh groundwater. *Applied Geochemistry*, 19(2): 201-214.

- Zhou, X., Zhang, K., Zhang, T., Li, C. and Mao, X. 2017. An ignored and potential source of taste and odor (T&O) issues biofilms in drinking water distribution system (DWDS). *Applied Microbiology and Biotechnology*, 101(9): 3537-3550.
- Zhu, C. and Anderson, G. 2002. Environmental applications of geochemical modeling. United Kingdom: Cambridge University Press.
- Ziegler, K., Hsieh, J. C., Chadwick, O. A., Kelly, E. F., Hendricks, D. M. and Savin, S. M. 2003. Halloysite as a kinetically controlled end product of arid-zone basalt weathering. *Chemical Geology*, 202(3-4): 461-478.

## **CHAPTER 12: ANNEXURES**

---

## Annexures for Chapter 3

### 12.1.1 Annexure A: Letter of consent (English language and Afrikaans language).

#### Request for access for potable water testing (English Language)

18 March 2017

Dear O’Kiep Resident,

The purpose of this letter is to kindly invite you to partake in the research being conducted jointly by the University of North-West and Cape Peninsula University of Technology. This research is part of an effort to learn about the quality of potable water in your community. The outcomes of this research will help investigators with a sound understand about the health and environmental risks associated with water.

We request your cooperation in obtaining access to your property to collect the potable water sample. You will not be requested to provide your name and under no circumstances you will be connected to your answer in any way. The information you provide will only be used for statistical reporting, and your name will not be used in any way. Your contribution in this research is voluntary and the water sampling will be conducted at no cost to you. However, you can help us by taking a few minutes to shares your thoughts about the environmental and health risks associated water quality.

Together with this is a small token of our thankfulness for your assistance. If you have any queries or remarks about this study, please feel free to ask. Once you are entirely certified with this explanation and freely choose to participate in this study, you may indicate your willingness to do so by ticking the box below Thank you very much for helping with this important study. If needed, any additional information can be obtained from Prof Frans Waanders, Director of the School of Chemical and Minerals Engineering, NWU. Thank you very much for helping with this important study.

Accept       Decline

Yours Sincerely.

Innocentia Erdogan (Researcher)

Student No.: 29645204

Email:innocentia.erdogan@gmail.com

## **Verseok rakende toegang vir drink water ontleding (Afrikaanse Taal)**

18 Maart 2017

Geagte Inwoners van O'Kiep

U word vriendelik verseok om deel te neem aan 'n navorsings projek wat gesamentlik deur die Universiteit van Noordwes en die Kaapse Skiereiland Universiteit van Tegnologie gedoen word. Hierdie navorsings projek dien as deel van 'n poging om te leer oor die gehalte van drinkwater in u gemeenskap. Die uitkomste van hierdie navorsings projek sal help dat die ondersoekbeamptes 'n beter begrip rakende die gesondheids- en omgewing risiko's wat verband hou met water.

Ons vra u samewerking dat u ons sal toegang tot u eiendom sal verleen om die nodige water monsters te versamel. Hierdie proses is anoniem en u sal geensins verbind word met enige van die resultate en antwoorde wat u sal gee, indien u toegang sal verleen tot u eiendom en die vrae in die opname beantwoord. Die inligting wat u verskaf sal slegs gebruik word vir statistiek doeleindes. U bydrae tot hierdie navorsing is vrywillig en die monsterneming van die water sal gedoen word teen geen onkoste vir u. U kan ons help deur 'n paar minute van u tyd met ons te deel deur 'n opnamete voltooi; rakende u gedagtes oor die omgewing en die gesondheidsrisiko's wat verband hou met die kwaliteit van die water in u omgewing.

Indien u enige navrae of kommentaar het oor hierdie studie voel vry om ons te kontak by die kontak nommers wat verskaf is. As u tevrede is met die inligting wat verskaf is of addisionele inligting wat u kan bekom deur ons te kontak, kan u, u bereidwilligheid aandui om deel te wees van die navorsings projek deur 'n regmerk in een van die onderstaande blokkies te maak. Indien u enige verder navrae het, kan u ook Prof Frans Waanders by die Skool vir Chemiese en Mineraalingenieurswese, NWU, kontak.

Baie dankie vir die hulp met hierdie belangrike studie.

Baie dankie vir die hulp met hierdie belangrike studie.

Aanvaar     Weier

Byvoorbaat dank.

Innocentia Erdogan (Navorsers)

Student No.: 29645204

Email:innocentia.erdogan@gmail.com

## 12.1.2 Annexure B: O’Kiep water supply and hygiene household questionnaires.

(April 2018)

### SECTION A

**Q1: WOULD YOU AGREE TO PARTICIPATE IN THE INTERVIEW?**

yes

no

**Q2: GENDER**

Male

Female

**Q3: YOUR AGE IS**

under 18

between 18 and 40

over 40

### SECTION B: WATER SUPPLY

**Q4: WHAT IS THE MAIN SOURCE OF DRINKING WATER FOR MEMBERS OF YOUR HOUSEHOLD?**

*Interviewer: Mark with an “x”.*

<b>a)</b> Piped municipal water into house	<b>b)</b> Rainwater collection in closed containers
<b>c)</b> Piped water to yard	<b>d)</b> Rainwater collection in open containers
<b>e)</b> Public tap	<b>f)</b> Bottled water
<b>g)</b> Borehole	<b>h)</b> Small-scale vendor
<b>i)</b> Protected dug well	<b>j)</b> Tanker-truck
<b>k)</b> Unprotected dug well	<b>l)</b> Protected spring
<b>m)</b> Unprotected spring	<b>n) Other:</b>
<b>o)</b> Surface water (river dam, lake, pond, stream, canal, irrigation channels).	

**Q5: WHERE, DO YOU THINK, WATER OF THE HIGHEST QUALITY IS FOUND?**

*Interviewer: Mark with an “x”.*

<b>a)</b> Piped municipal water into house	<b>b)</b> Rainwater collection in closed containers
<b>c)</b> Piped water to yard	<b>d)</b> Rainwater collection in open containers
<b>e)</b> Public tap	<b>f)</b> Bottled water
<b>g)</b> Borehole	<b>h)</b> Small-scale vendor
<b>i)</b> Protected dug well	<b>j)</b> Tanker-truck
<b>k)</b> Unprotected dug well	<b>l)</b> Protected spring
<b>m)</b> Unprotected spring	<b>n) Other:</b>
<b>o)</b> Surface water (river dam, lake, pond, stream, canal, irrigation channels).	

**Q6: WOULD YOU PREFER BOREHOLE AS AN ALTERNATIVE SOURCE OF DRINKING WATER**

- Yes
- No
- Don't know

**Q7: HOW FREQUENTLY WAS THE DRINKING WATER FROM THE MAIN SOURCE AVAILABLE TO YOUR HOUSEHOLD DURING THE LAST TWO WEEKS?**

- Daily, 24 hours a day
- One - two days a week
- Daily, at certain hours
- Less frequent than once a week
- Three - five days a week

**Q8: BETWEEN WHAT HOURS IS DRINKING WATER FROM THE BOREHOLE AVAILABLE TO YOUR HOUSEHOLD?**

*Interviewer: Use the second line only when applicable, i.e. if water is available in two intervals each day*

From..... To.....

From..... To.....

**Q9: DID YOUR HOUSEHOLD EXPERIENCE INTERRUPTIONS/BREAKDOWNS IN THE DRINKING WATER SUPPLY FROM THE MAIN SOURCE DURING THE LAST SIX MONTHS?**

*Interviewer: If the source was not used the entire period due to e.g. seasonality, ask for irregular interruptions since they last started using the main source.*

- Yes
- No
- Don't know

**Q10: DURING THESE INTERRUPTIONS/BREAKDOWN, HOW MANY DAYS WAS DRINKING WATER NOT AVAILABLE FROM THE BOREHOLE?**

*Interviewer: Instruct the respondent to add up from all irregular interruptions in the period.*

Total number of days: .....

**Q11: DOES YOUR HOUSEHOLD USE OTHER SOURCES OF WATER FOR DRINKING AND OTHER PURPOSES?**

- Yes
- No
- Don't know

**Q12: WHAT IS THE COLOUR OF THE BOREHOLE WATER?**

- Brown
- Yellow
- White
- Clear

**Q13: WHAT IS THE TASTE OF THE BOREHOLE WATER ?**

- salty,
- muddy,
- Not sure

**Q14: HAS ANY MEMBER OF THE FAMILY GOT SICK FROM THE BOREHOLE WATER THEY DRANK?**

- Yes
- No
- Don't know

**Q15: HAS ANY MEMBER OF THE FAMILY NOTICED THE DISCOLOURATION OF TEETH?**

- Yes
- No
- Don't know

**Q16: IS THIS WATER SUITABLE FOR WASHING OF CLOTHES?**

- Yes
- No
- Don't know

**Q17: PLEASE STATE THE MAIN SOURCE AND OTHER SOURCES FOR EACH USE OF WATER.**

*Interviewer: Write in the category number as above, write "0" for none and use Q 4 for other category.*

	Main	Other	Other
a) Drinking			
b) Cooking			
c) Washing clothes			
d) House cleaning			
e) Bathing/washing your bodies			
f) Domestic agriculture			

**SECTION B: WATER TREATMENT**

**Q18: ARE YOU SATISFIED WITH THE COLOUR OF THE MAIN WATER SOURCE?**

- Yes
- No
- Don't know

**Q19: WHAT ARE YOU DOING TO IMPROVE DRINKING WATER QUALITY?**

What did your household do to make the water safer to drink?

*Interviewer: Mark with an "x" for all mentioned*

a) Boil the water	e) Sieve it through cloth
b) Add bleach	f) Water filter (ceramic, sand, composite, etc.)
c) Let it stand and settle	g) Don't know
g) Other (please write down)	

**Q20: WHEN WAS THE LAST TIME YOUR HOUSEHOLD TREATED THE WATER USING THIS METHOD?**

*Interviewer: Mark with an "x" for all mentioned*

- |                       |                        |
|-----------------------|------------------------|
| a) Today              | b) Less than one month |
| c) Yesterday          | d) More than one month |
| e) Less than one week | f) Less than one week  |

**SECTION C: OTHER METHOD OF WATER SOURCE**

**Q21: DO YOU USE TAP WATER**

- Yes  
 No

**Q22: WHAT IS THE SIZE OF THE CONTAINER(S) YOU ARE USING TO STORE THE WATER?**

*Interviewer: If Q19 is yes note the size.*

- Size of container, type 1.....litres  
 Size of container, type 2.....litres  
 Size of container, type 3 .....litres

**Q23: HOW MANY CONTAINERS DOES YOUR HOUSEHOLD USUALLY USE PER DAY (FOR ALL PURPOSES AND SOURCES)?**

- Number of containers per day, type 1.....  
 Number of containers per day, type 2.....  
 Number of containers per day, type 3.....

**Q25: HOW OFTEN DO YOU CLEAN YOUR CONTAINERS?**

- everyday  
 weekly  
 once a month  
 yearly  
 never

**Q26: DO YOU BUY DRINKING WATER IN A STORE?**

- yes  
 no  
 sometimes

**Q27: ARE YOU CONFIDENT THAT THE DRINKING WATER WHICH YOU BUY IN A STORE IS SUITABLE FOR DRINKING?**

- yes  
 no  
 never thought about it  
 I don't know

**Q28: HAVE YOU ANALYSED YOUR BOREHOLE WATER IN A LABORATORY?**

- yes
- no, I don't need it because I'm satisfied with the quality of my drinking water
- no, I can't afford it.

**SECTION D: ATTITUDE TOWARDS THE WATER QUALITY**

**Q29: HOW WOULD YOU RATE THE QUALITY OF YOUR DRINKING WATER COMING FROM THE BOREHOLE?.**

*Interviewer: Mark one with an "x" only.*

	Poor	Acceptable	Good	Not applicable
a) Clarity (no sediments in the water)				
b) Colour				
c) Smell				
d) Taste				
e) Healthiness				
f) Stability of service				

**Q30: ARE THERE SOME MONTHS WHERE YOUR HOUSEHOLD CANNOT USE THE BOREHOLE WATER?**

- yes
- no
- not sure

**Q31: WHICH MONTHS?**

*Interviewer: Mark with "x" for all mentioned*

January	February
March	April
May	June
July	August
September	October
November	December

**Q32: WHAT IS THE MAIN SOURCE OF DRINKING WATER FOR MEMBERS OF YOUR HOUSEHOLD DURING MONTHS MENTIONED ABOVE?**

*Interviewer: Mark one with an "x" only.*

<b>a)</b> Piped municipal water into house	<b>b)</b> Rainwater collection in closed containers
<b>c)</b> Piped water to yard	<b>d)</b> Rainwater collection in open containers
<b>e)</b> Public tap	<b>f)</b> Bottled water
<b>g)</b> Borehole	<b>h)</b> Small-scale vendor
<b>i)</b> Protected dug well	<b>j)</b> Tanker-truck
<b>k)</b> Unprotected dug well	<b>l)</b> Protected spring
<b>m)</b> Unprotected spring	<b>n) Other:</b>
<b>o)</b> Surface water (river dam, lake, pond, stream, canal, irrigation channels).	

**Q33: DURING THIS PERIOD, HOW FREQUENTLY IS THE WATER YOU FETCH FROM THAT SOURCE AVAILABLE TO YOUR HOUSEHOLD?**

*Interviewer: Mark with "x" for all mentioned.*

Daily	Less frequent than once a week
Two days a week	Three to five days a week
Daily at certain hours	

**Q34: BETWEEN WHAT HOURS IS DRINKING WATER FROM THE MAIN SOURCE AVAILABLE TO YOUR HOUSEHOLD?**

*Interviewer: Use the second line only when applicable, i.e. if water is available in two intervals each day*

From..... To.....

From..... To.....

**Q36: HOW MUCH IS THE COST OF YOUR WATER?**

R 100 - 500

R500 – R1000

R 1000 – 1500

R1500 – 2000

**Q37 ADDITIONAL COMMENTS:** *Interviewer: To take notes*

### 12.1.3 Annexure C: Frequencies from questionnaires.

<b>Section A: Drinking water Source and Quality</b>	
<b>Variable</b>	<b>Frequency (%)</b>
<b>Where do you get your water?</b>	
Water Tap	90
Water Tap + Purchase	10
<b>Where do you think water of the highest quality is found?</b>	
Bottle purchased water	100
<b>What are you doing to improve the water quality?</b>	
Boil	64
Boil + Bleach	36
<b>Are you satisfied with the quality of drinking water?</b>	
Could be better	12
No	88
<b>What is the colour of the drinking water from your tap?</b>	
Brownish	28
Greenish + Brownish	14
Greenish	28
Whitish	26
Whitish + Brownish	4
<b>Section B: Possible health risks</b>	
<b>Variable</b>	<b>Frequency (%)</b>
<b>Does anyone in the family suffer from pain or tiredness?</b>	
Yes	54
N/A	18
No	28
<b>Have you been sick from the water you drank?</b>	
Yes	88
No	12
<b>If yes, you got sick from?</b>	88
Diarrhoea	12
N/A	
<b>How does the water smell?</b>	
No smell	14
Unpleasant smell	86
<b>Does the water have a taste?</b>	
Salty taste	100
<b>Have you noticed decolouration of your teeth?</b>	
Yes	72
Dentures	8
No	20
<b>Section C: Drinking water Supply</b>	
<b>Variable</b>	<b>Frequency (%)</b>
<b>Who supply you with your drinking water?</b>	
Municipality	90
Municipality + Store	10

<b>Does your household experience any interruptions of the drinking water supply?</b>	
Yes	100
<b>What is the frequency of interruptions of the drinking water supply?</b>	
Once a week	42
One to two days per week	20
Three to four days	38
<b>If there are interruptions of drinking water supply, how do you access water?</b>	
Tanker-truck	48
Tanker-truck + Bottle purchased water	22
Bottle purchased water + Stored water from containers	10
Stored water from containers	20
<b>What type of storage container you use for your drinking water?</b>	
Bucket	88
Jojo Tank	12
<b>Are you satisfied with your drinking water service?</b>	
No	100
<b>In your view, who should be accountable for the drinking water quality and supply?</b>	
Government	12
Government + Municipality	22
Municipality	66